Distribution Agreement

In presenting this thesis or dissertation as a partial fulfillment of the requirements for an advanced degree from Emory University, I hereby grant to Emory University and its agents the non-exclusive license to archive, make accessible, and display my thesis or dissertation in whole or in part in all forms of media, now or hereafter known, including display on the world wide web. I understand that I may select some access restrictions as part of the online submission of this thesis or dissertation. I retain all ownership rights to the copyright of the thesis or dissertation. I also retain the right to use in future works (such as articles or books) all or part of this thesis or dissertation.

Signature:

_____ _____

Janise N. Kuehner Date

A Profiling of DNA Modifications in Neurodegenerative and Neuropsychiatric Disorders

By

Janise N. Kuehner

Doctor of Philosophy

Graduate Division of Biological and Biomedical Sciences

Genetics and Molecular Biology

Bing Yao, Ph.D.

Advisor

Anita H. Corbett, Ph.D.

Committee Member

Karen Conneely, Ph.D.

Committee Member

Jingjing Yang, Ph.D.

Committee Member

Zhexing Wen, Ph.D.

Committee Member

Accepted:

Kimberly J. Arriola, Ph.D.

Dean of the James T. Laney School of Graduate Studies

Date

A Profiling of DNA Modifications in Neurodegenerative and Neuropsychiatric Disorders

By

Janise N. Kuehner
B.S., Purdue University, 2016

Advisor: Bing Yao, Ph.D.

An abstract of
A dissertation submitted to the Faculty of the
James T. Laney School of Graduate Studies of Emory University
in partial fulfillment of the requirements for the degree of
Doctor of Philosophy
in Graduate Division of Biological and Biomedical Science
Genetics and Molecular Biology
2023

Abstract

Epigenetics refers to heritable changes in gene expression without altering the DNA sequence through mechanisms such as DNA and histone modifications and non-coding RNAs. Mounting evidence implicates critical roles for DNA modifications, specifically 5-methylcytosine (5mC) and 5-hydroxymethylcytosine (5hmC), in regulating brain development and disease. 5mC is one of the best characterized epigenetic marks and is regarded as a highly stable mark in differentiated cells typically at CpG dinucleotides. On the other hand, 5hmC has emerged as a key DNA modification in the nervous system due to its significant enrichment in the brain and its ability to regulate neuronal-specific gene expression during neural progenitor cell differentiation. Both nervous system development and function can be affected by epigenetic spatiotemporal regulation of gene expression. In the mammalian central nervous system, epigenetic dysregulation is associated with neurodegenerative diseases such as Alzheimer Disease and neuropsychiatric diseases such as major depressive disorder (MDD).

Towards this end, this thesis investigates the roles of 5mC and 5hmC in neurodegenerative and neuropsychiatric diseases. First, using a forebrain organoid model system, we investigated the dynamic changes of 5hmC during mammalian brain development and in Alzheimer's Disease (AD). 5hmC and transcriptome profiles encompassing several developmental time points of healthy forebrain organoids and organoids derived from several familial AD patients were developed. We observed that stage-specific differentially hydroxymethylated regions (DhMRs) display an acquisition or depletion of 5hmC modifications across development stages. Importantly, our AD organoids corroborate cellular and molecular phenotypes previously observed in human AD brains. These data suggest a highly coordinated molecular system that may be dysregulated in these early developing AD organoids. In the second half of this thesis, we explored the contribution of 5mC and 5hmC underlying the individual differences in stress susceptibility and resilience. Genome-wide 5mC, 5hmC and transcriptome profiles from animals that underwent various durations of social defeat were generated. We characterized the epigenetic impact of chronic stress in young and mature animals to determine if DNA modifications were responsible for increased stress susceptibility with age. Moreover, we observed that 5mC and 5hmC work in parallel in young animals, while in mature animals they function in distinct biological process. Acute stress responses may epigenetically "prime" the animals to either increase or decrease their predisposition to depression susceptibility. Re-exposure studies reveal that the enduring effects of social defeat affect differential biological process between susceptible and resilient animals. Stress-induced 5mC and 5hmC fluctuations across the acute-chronic-longitudinal time course demonstrate that the negative outcomes of chronic stress do not discriminate between susceptible and resilient animals. Finally, 5mC appears to be responsible for acute stress response, whereas 5hmC may function as a persistent and stable modification in response to stress. This study broadened the scope of previous research and offers a comprehensive analysis of the role of DNA modifications in stress-induced depression.

A Profiling of DNA Modifications in Neurodegenerative and Neuropsychiatric Disorders

By

Janise N. Kuehner

B.S., Purdue University, 2016

Advisor: Bing Yao, Ph.D.

A dissertation submitted to the Faculty of the
James T. Laney School of Graduate Studies of Emory University
in partial fulfillment of the requirements for the degree of
Doctor of Philosophy
in Graduate Division of Biological and Biomedical Science
Genetics and Molecular Biology
2023

Acknowledgements

I would first like to thank my advisor, Dr. Bing Yao for adopting me into his lab and guiding my graduate school experience. Bing has been an outstanding mentor – he has supported me every step of the way, he always has my best interests in mind and has played an immense role in helping me to become the scientist that I am today. For all his efforts and support, I could not be more grateful. I would also like to sincerely thank my committee members: Drs. Anita Corbett, Karen Conneely, Jingjing Yang and Zhexing Wen. Anita always made herself available (even when on a bus in Germany!) for conversations and expanding my career network. Both Karen and Jingjing contributed greatly to my growth in computation and Zhexing in my neuroscience background. They have been an absolutely incredible team of individuals to have had the privilege to collaborate with and learn from. Each one of them are truly wonderful and inspirational people who I will always look up to greatly. They have all made a huge impact on my experience at Emory and have left a lasting impression.

Next, I would like to thank my lab mates: Feng, Yangping, Paula, Kat, Yingzi and Huifeng. You have each contributed to the fantastic lab dynamic making science that much more enjoyable. I will forever treasure our dinner and game nights, smooth play offs when the boss walks in and we were all clearly chatting and the endless supply in the snack drawer (except the durian candy). To my undergraduates Nevin and Rachel, thank you, thank you, thank you, from the bottom of my heart for putting up with me and showing up every day ready to science. It has been an absolute joy to see you both grow in confidence and celebrate your success and achievements with you. I also want to thank Emily. Your mentorship, advice, guidance and friendship over the past 6 years have been invaluable and have made the highs and lows of grad school manageable. Without this group of people, I truly could not have accomplished all of my research goals. Whether it be experiments, coding, experimental design, IACUC protocols, dissections, scoring mouse videos or cell culture, you were all always there for me. You listened when I needed an ear, answered questions when I was lost and most importantly you made me laugh. You are an amazing group that I will treasure for a lifetime.

Outside of lab I am lucky to have made life-long friends with Beverly and Hunter Robinson. They have always and continue to be right there to celebrate my success and remind me to drink wine… I mean rest… even all the way from California now. I know they both will be a part of my family forever and I thank them for their unwavering support.

Most importantly, I thank my family and incredibly supportive husband, Chris. Without their love and support, I wouldn't be where I am today. I am incredibly fortunate to have parents whom have supported me through what seems like my never-ending academic career, siblings to call up when I leave work past mom and dad's bed time and in-laws who are always willing to supply the chocolate and RV for quick get-aways. My sweet kitties Cloe and Niko, who listened to every practice seminar and gave the best snugs after rough days. And words cannot begin to describe the gratitude and love I have for my husband. You gave me a bottomless supply of support, encouragement when I was overwhelmed, level headedness when I was groundless, courage when I was unsure and your love at all times. Together we have walked this journey and overcame the challenges of us both being in grad school. Thank you and love you always.

Table Of Contents

List of Figures:

List of Tables:

Abbreviations:

+/- Reg.	positive/negative regulation
5caC	5-carboxylcytosine
5fC	5-formylcytosine
5hmC or hmC	5-hydroxymethylcytosine
5hmC-seq	5-hydroxymethylcytosine sequencing
5mC or mC	5-methylcytosine
5mC-seq	5-methylcytosine sequencing
6mA	N6-methyladenine
Aβ	amyloid-beta
ACTH	adrenocorticotrophic hormone
AD	Alzheimer's Disease
AID	activation-induced cytidine deaminase
APP	amyloid beta precursor
APOBEC	apolipoprotein B mRNA-editing catalytic polypeptides
APOE	apolipoprotein-E
ASDS	acute social defeat stress
AVP	arginine vasopressin
BDNF	brain-derived neurotrophic factor
BER	base excision repair
CAF-1	chromatin assembly factor
CNS	central nervous system
CORT	corticosterone
C_R	chronic resilient specific
CRH	corticotrophin-releasing hormone
C_s	chronic susceptible specific
CSDS	chronic social defeat stress
CSF	cerebral spinal fluid
Ctrl.	control
Dev.	development
DhMRs	differentially hydroxymethylated regions
Diff.	differentiation
DMRs	differentially methylated regions
DNMT	DNA methyltransferase
EB	embryoid body
esBAF	ESC specific BAF
ESC	embryonic stem cell
Esc/EED	extra sex combs
EWAS	epigenome-wide association study
E(z)/EZH	enhancer of zeste
fAD	familial AD
FDR	false discovery rate
FMRP	Fragile X mental retardation protein
GABA	gamma-aminobutyric acid
GO	gene ontology
GREAT	Genomic Regions Enrichment of Annotations Tool
GWAS	genome-wide association study
HAT	histone acetyltransferase
HDAC	histone deacetylase
HPA	hypothalamic-pituitary-adrenal axis
HPI	heterochromatin protein 1

ICE	imprint control element
ICV	intracerebroventricular
ILPFC	infralimbic prefrontal cortex
KO	knock-out
LFC	log fold change
LINE 1	long interspersed nuclear element-1
lncRNA	long non-coding RNA
LSDS	longitudinal social defeat sress
MBD	methyl-CpG-binding domain
MDD	major depressive disorder
Med.	medium
miRNA	microRNA
Morph.	morphogenesis
NAc	nucleus accumbens
nBAF	mature neuron BAF
No.	number
Norm.	normalized
npBAF	neural progenitor BAF
NPC	neuronal progenitor cells
n.s.	not significant
NURD	nucleosome remodeling and histone deacetylation
OGT	O-GlcNAc transferase
Org.	organization
PAK	p21-active kinase
Pc	polycomb
PCA	principal component analysis
Pcdhs	protocadherins
PcG	polycomb group
PCNA	proliferating cell nuclear antigen
Ph	polyhomeotic
POA	preoptic area
PRC	polycomb repressive complex
Psc	posterior sex combs
PSEN1/2	presenilin 1/2
RBAP48/46	histone binding protein p55
RE 1	repressor element 1
Reg.	regulation
Res.	resilient
REST/NRSF	RE1-silencing transcription factor
RPKM	reads per kilobase-per-million
RR or L_{RR}	resilient remained resilient
RS	resilient turned susceptible
RTqPCR	real time quantitative polymerase chain reaction
Sce/dRing1	sex combs extra
SERT	serotonin transporter
shRNA	small hairpin RNA
SI	social interaction
Sig.	signaling
SIR	social interaction ratio
SNRI	serotonin-norepinephrine reuptake inhibitor
SS or L_{SS}	susceptible remained susceptible
SSRI	serotonin reuptake inhibitors

Str	stress
Sus.	susceptible
Su(z)/SU(Z)	suppressor of zeste
TDG	thymine-DNA glycosylase
TES	transcription end site
TET	Ten-Eleven Translocation
$Tet2^{KO}$	Ten-Eleven Translocation knock-out
TGF-β	transforming growth factor-β
TRK	tyrosine receptor kinase
TrxG	trithorax
TSS	transcription start site
TTS	transcription termination site
UTR	untranslated region
VEG	vascular endothelial growth signaling
VTA	ventral tegmental area
WT	wild type

Chapter 1: Introduction to Dissertation

Portions of this chapter are published as either:

Kuehner, J.N., et al., *Epigenetic Regulations in Neuropsychiatric Disorders*. Frontiers in genetics, 2019. 10.

Kuehner, J.N. and B. Yao, *The Dynamic Partnership of Polycomb and Trithorax in Brain Development and Diseases*. Epigenomes, 2019. 3(3): p. 17.

Introduction

The concept of epigenetics was first proposed in 1939 by Conrad Waddington to describe early embryonic development [1]. He proposed that development originates from the interactions of the starting material in the fertilized egg, and that the interactions give rise to something new. He further postulated that this process cycles, leading to the formation of a whole organism. Today, the accepted definition of epigenetics is the study of modifications that directly affect the expression of a gene, but do not change the underlying DNA sequence [2-4]. There are several major epigenetic mechanisms that are extensively studied including DNA modifications **(Figure 1.1:**), histone modifications (**Figure 1.4:**), chromosome remodeling (**Figure 1.5:**) and RNA regulation via non-coding RNAs such as microRNA (miRNA) and long non-coding RNA (lncRNA) (**Figure 1.6:**). Modifications can be added, removed and interpreted by various classes of proteins collectively known as 'writers,' 'erasers' and 'readers,' respectively. Disruption of these epigenetic mechanisms and their molecular machinery can have catastrophic consequences in the mammalian central nervous system (CNS).

Both nervous system development and function can be affected by epigenetic spatiotemporal regulation of gene expression. In the mammalian CNS, epigenetic dysregulation is associated with neurodegenerative diseases such as Alzheimer Disease and neuropsychiatric diseases such as major depressive disorder (MDD) and stress. Epigenetic studies are actively trying to identify biomarkers that could be associated with diseases to aid in our development of novel therapeutics. This information is critical, as the prevalence of neurological diseases is on the rise [5]. Here, we review the current understanding of epigenetic regulation in brain development and functions, with a focus on DNA methylation, as well as their implications in neurological diseases.

1.1. DNA Methylation

1.1.1. Functional Roles of DNA Methylation

DNA methylation is one of the best characterized epigenetic marks studied and has been regarded as a highly stable mark found in differentiated cells [6, 7]. It involves the covalent methylation of the fifth position in the cytosine ring, generating 5-methylcytosine (5mC) (**Figure 1.1:**). DNA methylation largely occurs at CpG dinucleotides [8]. Accumulation of short, unmethylated CpG-rich clusters known as CpG islands occurs in the promoter regions of most genes [9]. Genome-wide studies have implicated that the distribution of 5mC in

transcripts could have differential roles in gene expression. For example, methylation status of the CpG islands helps to determine whether the corresponding gene will be expressed, whereas gene body methylation has been proposed to promote transcriptional elongation [10] and affect splicing [11]. In addition, the methylation status of CpG islands can be influenced spatially based on tissue and cell type [12]. For instance, the gene *HTR2A,* which has been implicated in many neuropsychiatric disorders [13], shows differential expression in the cerebellum and the cortex and is regulated by DNA methylation [14]. Strikingly, the methylated CpG loci regulating *HTR2A* expression is over 1Kb upstream of the promoter rather than being in the promoter region, illustrating that methylation can regulate genes across long distances. Thus, DNA methylation has important roles for brain region-specific transcriptome profiles.

Not only can DNA methylation regulate protein coding genes, it can also regulate non-protein coding RNA like lncRNAs. Random X-inactivation, an essential embryonic event, is triggered by the production of *Xist*, a lncRNA that coats the X chromosome destined to be inactivated [15, 16]. The promoter of the *Xist* gene contains a CpG island whose methylation status ultimately dictates whether the X chromosome is active [17]. How DNA methylation regulates lncRNA in the brain is still unclear. One study compared the DNA methylation patterns around the transcription start sites (TSSs) of protein coding genes and lncRNA loci [18]. Surprisingly, a sharp increase in DNA methylation immediately downstream of the TSS was associated with lncRNA loci, but did not correlate with expression of the lncRNA. While this finding suggests that DNA methylation may not play an essential role in lncRNA expression, it would be interesting to investigate if blocking methylation at these sites influenced lncRNA expression.

In addition to its roles in gene regulation, DNA methylation also maintains genomic stability by controlling the expression of highly repetitive regions in the genome such as retrotransposons and satellite DNA [19-21]. In general, long interspersed nuclear element-1 (LINE 1) is only active in the germline and during early development [22]. During somatic cell differentiation, DNA methylation silences LINE 1. Interestingly, studies have suggested that LINE 1 may be active during human and rodent neuronal differentiation and influence neuronal gene expression to create cell heterogeneity in the adult brain [23-25]. Indeed, LINE 1 has been shown to be more active in the brain compared to other tissues [25].

Finally, DNA methylation has important roles in early developmental processes such as gene imprinting. Often, the "imprint" is methylation of a long-range control element called an imprint control element (ICE) (also referred to as imprint control region, ICR, or imprint center, IC) [26, 27]. Parental specific methylation of the ICE is established by the DNA methyltransferase (DNMT) complex DNMT3A/3L during gamete development [28, 29]. Of the approximately 100 imprinted genes currently known, the majority of them are expressed in brain tissues, though not always exclusively, and have been reviewed previously [30]. One of the more extensively studied imprinted genes, specifically in the CNS of mammals, is the paternally expressed gene *Necdin* (*Ndn*) [31]. *Ndn* regulates neuronal differentiation and axonal outgrowth. Also, *Ndn* is most highly expressed during mouse neuronal generation and between postnatal days 1–4.

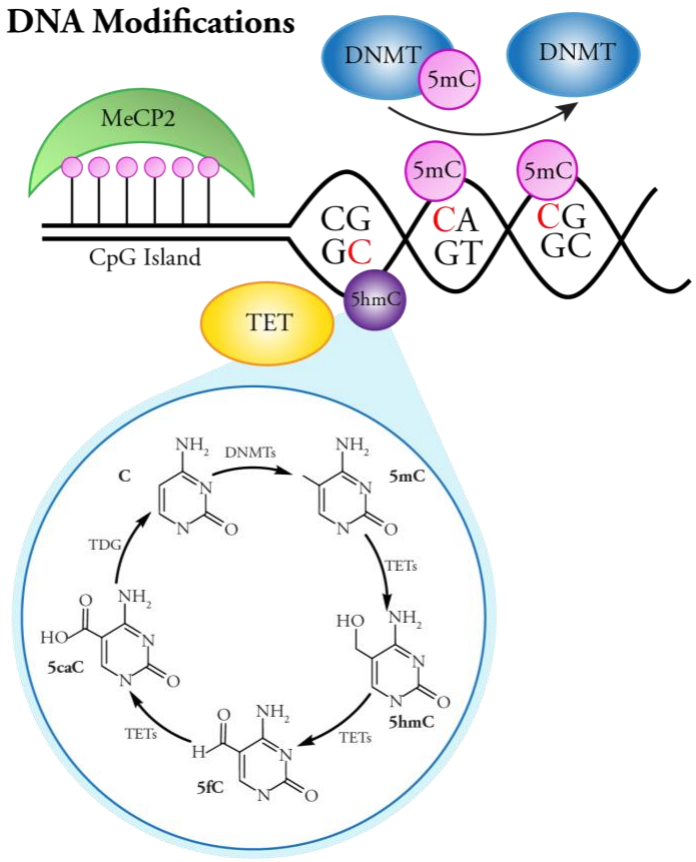

Figure 1.1: Epigenetic Regulation in the CNS: DNA Modifications
A. DNA modifying proteins can methylate CG of CH dinucleotides. Methylated cytosines can be further modified to 5hmC, 5fC, or 5caC to be replaced with an unmodified cytosine through thymine DNA glycosylase, TDG.

1.1.2. DNA Methylation in the Brain

DNA methylation in the brain is required for brain development and function throughout all stages in life. Dynamic regulation of DNA methylation is critical for cellular differentiation. One study compared the changes in DNA methylation patterns between two differentiation phases: the transition of embryonic stem cells (ESCs) to neuronal progenitor cells (NPCs), and the transition of NPCs to differentiated neurons [32]. The most dynamic changes in DNA methylation patterns were found when ESCs lost their pluripotency and became NPCs. In fact, ESCs were nearly devoid of DNA methylation marks except at the promoters of genes that were germline specific. In contrast, during the differentiation of NPCs to mature neurons, only 2.3% of the analyzed promoters gained *de novo* methylation and only 0.1% of promoters were demethylated, suggesting that the majority of DNA methylation dynamics do not occur in this phase. Similar to neurogenesis, astrocytogenesis is tightly controlled by DNA methylation. In mouse, astrocyte differentiation from neuroepithelial cells requires that the promoter of the *GFAP* gene be demethylated on embryonic day 14.5, allowing for the transcription factor STAT3 to bind and activate *GFAP* expression [33, 34].

Very few studies have focused on how DNA methylation regulates other brain developmental features, such as neural migration and axonal/dendritic outgrowth. Two recent studies have demonstrated that the DNA methyltransferase, DNMT1, as having putative regulatory roles in immature GABAergic interneuron migration [35, 36]. They found that Dnmt1 promotes the migration and survival of immature migratory GABAergic interneurons that derive from the embryonic preoptic area (POA) by repressing *Pak6* expression [35]. p21-active kinases (PAKs) are known for their roles in cytoskeletal organization [37], and *Pak6* has previously been shown to stimulate neurite outgrowth in post-migratory neurons derived from POA [35, 38]. *De novo* methylation by Dnmt3b in early embryonic neurodevelopmental processes has been shown to be critical in regulating the clustered protocadherins (*Pcdhs*) genes [39]. Protocadherins are cell-surface adhesion proteins that are predominantly expressed in the nervous system [40], and have critical functions in neurite self-avoidance [41], neuronal survival [42], and dendritic patterning [43]. In mammals, they are found in three closely linked gene clusters call a (*Pcdha*), b (*Pcdhb*), and g (*Pcdhg*) [44, 45]. Interestingly, the *Pcdhs* are stochastically expressed by alternative promoters in individual neurons generating single cell diversity of isoforms in the brain

[42]. This stochastic expression is regulated by methylation of variable exons and this has been thoroughly reviewed elsewhere [46].

DNA methylation also has roles in brain function such as memory processing. In the mammalian brain, the hippocampus and the cortex are largely responsible for memory formation and storage [47-49]. In the hippocampus, contextual fear conditioning induced changes in DNA methylation during memory formation in rats. When DNMTs were inhibited by either zebularine or 5-aza-20-deoxycytidine, neuronal plasticity-promoting genes *Bdnf* and *Reelin* demonstrated altered methylation patterns [50]. After contextual fear conditioning, *Dnmt3a* and *Dnmt3b* mRNA were highly upregulated in the brain; however, when DNMT inhibitors, zebularine or 5-aza-20-deoxycytidine, were injected into the hippocampus immediately after contextual fear conditioning, the fear response was eliminated, suggesting that DNA methylation is required for memory formation [51]. Importantly, when the memory suppressor gene *Pp1* was examined after fear conditioning, there was an increase in methylation at the CpG island upstream of the *Pp1* transcriptional start site. It was postulated that the increase in *de novo* Dnmts may be necessary to transcriptionally silence memory suppressor genes after fear conditioning training to allow for memory formation and consolidation. In addition to the formation of memories, DNA methylation also has putative roles in long-term memory storage. Contextual fear conditioning was found to disrupt DNA methylation at three genes associated with memory, *Egr1*, *reelin*, and *calcineurin*, which also happen to have large promoter CpG islands [49]. Both *reelin* and *calcineurin* were hypermethylated; however, only *calcineurin* maintained this hypermethylated state for 30 days, suggesting that DNA methylation might be required for long term memory storage.

Worth noting is that DNA methylation patterns in the brain can be affected by external stimuli in one's environment. Interestingly, a study found that in mature neuronal cells, CpGs in low density regions compared to CpG islands undergo dynamic DNA methylation changes in response to electroconvulsive stimulation [52]. Numerous studies have shown that maternal care during childhood [53], early life stressors including abuse [54], parental separation and social defeat stressors can alter DNA methylation patterns in the brain and have been reviewed elsewhere [55].

1.1.3. DNA Methyltransferases

DNA methylation is generated by a group of DNMTs, also regarded as 5mC enzymatic "writers" (**Figure 1.1:**). Each Dnmt (Dnmt1, 3a, 3b, 2, and 3L) has evolved to have its own specialized regulatory functions. These specialized functions could be attributed to the lack of sequence homology seen in the N-terminal regulatory domains of the Dnmts [56]. All of the Dnmts contain some version of a cysteine rich domain that further define their functions. The most conserved region between the DNMTs is the C-terminal catalytic domain, which is characteristic of all enzymes that modify pyrimidines at the fifth position (**Figure 1.2:).**

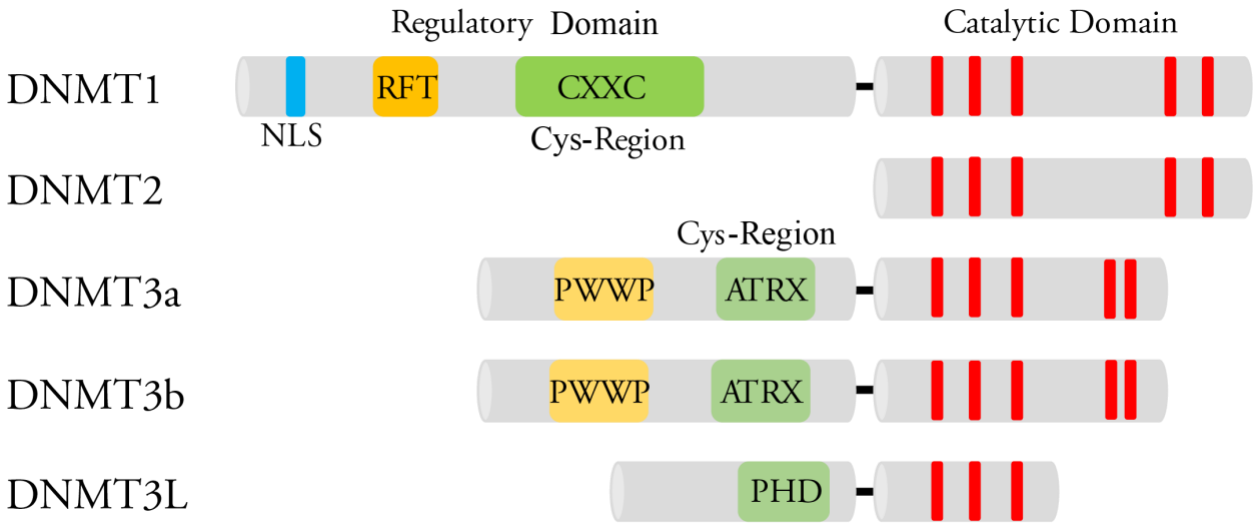

Figure 1.2: Domains of DNMTs
The N-terminal and C-terminal domains of DNMTs. In the N-terminus of each Dnmt is a cysteine rich region. In Dnmt1 this region contains a CXXC zinc finger which is thought to aid in DNA binding [57]. Dnmt3a and 3b both contain a PWWP domain that specifically recognizes the repressive histone 3 lysine 36 trimethylation mark (H3K36me3) found in heterochromatin [58]. Dnmt3L contains a PHD-like cysteine rich domain that closely resembles the PHD domain encoded in Dnmt3a and 3b's ATRX domain [59]. All the DNMTs have a conserved C-terminal catalytic domain (I, IV, VI, IX, and X are the most conserved motifs in cytosine methyltransferases) responsible for modifying pyrimidines. NLS, nuclear localization signal; RFT, replication foci-targeting domain.

The first Dnmt purified was Dnmt1 back in 1983, and was found to be responsible for maintaining methylated CpG sites during DNA replication [60]. Dnmt1 interacts with replication machinery, such as proliferating cell nuclear antigen (PCNA). Maintenance of the genomic methylation pattern requires that

unmethylated regions also be maintained during replication. During the S phase, the transcription factor p21 blocks Dnmt1 from interacting with PCNA, which ensures that unmethylated regions maintain their original state [61]. This regulation of Dnmt1 plays an important role in asynchronous replication, specifically at replication origins that include CpG islands [62]. Mutation and loss-of-function studies have demonstrated the necessity of Dnmt1 during embryonic development. By gestational day 9.5, *Dnmt1*-null mouse embryos failed to develop and died by gestational day 11 [63]. In addition, overall global methylation levels decreased by threefold in the *Dnmt1*-null embryos.

Nearly 15 years later, two additional Dnmts were discovered, Dnmt3a and Dnmt3b. Both Dnmt3a and Dnmt3b are responsible for *de novo* methylation, which is also critical during early embryogenesis [64]. When either *Dnmt3a* or *Dnmt3b* are deleted during embryogenesis, severe developmental defects or embryonic lethality are observed, respectively [65]. Mouse embryos with *Dnmt3a* depletion appear normal at birth, but die around 4 weeks of age. In contrast, embryos null for *Dnmt3b* were not viable and had growth retardation and neural tube defects. In addition to embryonic development, the *de novo* methyltransferases work in conjunction with Dnmt1 to regulate genome stability and imprinted genes. At a global level, deletion of *Dnmt3a* and/or *Dnmt3b* results in slight demethylation at repetitive sequences, but not to the same extent observed in *Dnmt1* gene deletion. This indicates that Dnmt1 is more important for the maintenance of methylation at repetitive sequences. At a loci-specific level, deletion of *Dnmt3a* and/or *Dnmt3b* has varied effects. For example, at several imprinted gene loci, *Igf2r* and *H19*, neither single nor dual gene disruption of *Dnmt3a* or *Dnmt3b* resulted in the demethylation pattern observed in *Dnmt1* gene disruption. However, at another imprinted loci, *Igf2*, dual deletion of *Dnmt3a*/*Dnmt3b* showed demethylation levels comparable to *Dnmt1* loss, whereas single gene disruption had no effect on demethylation. This indicates that there is some overlap in the roles of the Dnmts at certain gene sites.

Lesser-known methyltransferases include Dnmt2 and Dnmt3L that were identified by sequence homology studies. Dnmt2 contains all of the C-terminal catalytic domains necessary to act as a methyltransferase; however, it was found to be non-essential for maintenance or *de novo* methylation [66], but rather responsible for tRNA methylation [67, 68]. Dnmt3L demonstrates homology with Dnmt3a and Dnmt3b,

but lacks the enzymatic activity required to generate *de novo* methylation [28, 59]. Instead, Dnmt3L is essential in the establishment of maternal imprints and co-localizes with Dnmt3a/3b to regulate imprinting. Furthermore, in the male germ line, loss of Dnmt3L resulted in the reactivation of retrotransposons and meiotic failure in spermatocytes [69], suggesting a role in genomic stability.

1.1.4. DNA Methyltransferases in the CNS

As writers of DNA methylation, Dnmts play critical roles in the mammalian CNS. Studies conducted on embryonic and adult mice revealed that Dnmts are highly expressed in neural progenitor cells, but are maintained at substantially lower levels in most differentiated neurons [70]. Furthermore, mouse studies revealed that in the CNS, Dnmt3a is detected as early as embryonic day (E) E10.5 in the ventricular and subventricular zones, but its expression is predominantly in adult post-mitotic neurons [71]. In contrast, Dnmt3b could only be detected during early neurogenesis. These specific time points of expression suggest that Dnmt3b may be important during the early stages of brain development, whereas Dnmt3a is more crucial to mature neurons. Further supporting different spatiotemporal roles for the *de novo* methyltransferases, it was shown that *Dnmt3b* is required for methylation at centromeric minor satellite repeats during embryonic brain development, whereas *Dnmt3a* is not [65].

Targeted mutagenesis studies revealed how critical the Dnmts are in the CNS. Conditional deletion of *Dnmt1* in CNS precursor cells, but not post-mitotic neurons, caused daughter cells to be severely hypomethylated [72]. Interestingly, mice that had 30% of their CNS cells mutated showed selective pressure against the *Dnmt*-knockout cells in their brain. Three weeks after birth, all *Dnmt*-knockout cells were abolished. In adult forebrain neurons, double knockout of both *Dnmt1* and *Dnmt3a* (but neither gene by itself) resulted in significantly smaller hippocampi and dentate gyrus brain regions, due to smaller neurons [73]. These mice also showed impairments in learning and memory as well as inappropriate upregulation of immune genes associated with demethylation. These results suggest that Dnmt1 and Dnmt3a may have redundant roles in post-mitotic neurons.

To further enhance the elaborate network of DNA methylation in the mammalian CNS, non-CpG dinucleotide methylation (CpH) has surfaced and shown to be highly enriched and have critical roles in the

brain (**Figure 1.1:**). CpG dinucleotides make up around 75% of total cytosine methylation, whereas CpH dinucleotides ('H' could be adenosine, thymine or cytosine) make up the remaining 25% [74]. Interestingly, CpH methylation is enriched in low CpG dense regions, and associated with repressed gene expression, but is unassociated with protein–DNA interaction sites. As previously mentioned, Dnmt1 preferentially associates with CpG dinucleotides, and maintains symmetric CpG methylation on both strands of DNA during replication. This symmetric balance is further facilitated by the complimentary base pairing (GpC). CpH methylation does not maintain the sequence symmetry and consequently during replication, CpH methylation is not conserved. This requires the re-establishment of CpH methylations after each cell division [75]. Re-establishment of CpH methylation has been linked to *Dnmt3a* gene expression [75-77]. In knockdown experiments, loss of *Dnmt3a*, but not *Dnmt1* or *Dnmt3b*, resulted in reduced CpH methylation with no effect on CpG methylation [74].

Like CpG methylation dynamics in early development, CpH methylation levels change during development. CpH methylation has been shown in relatively high abundance in stem cells [78, 79] and found to be enriched in both adult mouse and human brain tissues [76, 77, 80]. A recent study showed that CpH methylation accumulates in the frontal cortex of the brain early after birth through adolescence and then slightly diminishes during aging [80]. Different subclasses of neurons have unique CpH and CpG methylomes and CpH methylation may correlate more robustly with gene expression as compared to CpG methylation [81].

1.1.5. Methyl-Binding Proteins

After the establishment of DNA methylation marks by "writers,' a subset of proteins with methyl binding abilities known as "readers" can bind, protect and interpret these marks and facilitate function (**Figure 1.1:)**. There are two main classes of methyl-CpG-binding proteins that have been thoroughly reviewed elsewhere [82], so this review will briefly discuss methyl-CpG-binding domain (MBD) proteins and MeCP2. Both protein families, for the most part, selectively bind to methylated DNA and aid in transcriptional repression [83]. MeCP2 can facilitate gene repression by recruiting histone deacetylase (HDAC) machinery that further remodel the chromatin environment, facilitating a repressed state [84-86]. Later it was found that MeCP2 could also bind to non-CpG methylation modifications [74, 87, 88]. Methyl-binding proteins are

ubiquitously expressed in somatic cells, but are particularly enriched in the mammalian CNS [83, 86, 89-91]. Several studies have found that MeCP2 is involved in the regulation of brain-derived neurotrophic factor (*BDNF*), which promotes neuronal maturation [92, 93]. Additionally, MeCP2 was found to regulate a maternally imprinted gene called *Dlx5* that is part of the gamma-aminobutyric acid (GABA) pathway for inhibitory GABAergic neurons [94]. Importantly, mutations in the MBD of MeCP2 have been implicated in the X-linked, neurodevelopment disorder known as Rett syndrome [95].

In addition to MeCP2, there are four other mammalian MBD proteins. MBD1-3 are known for their roles in transcriptional repression, whereas MBD4 functions as a thymine glycosylase in the mismatch repair pathway [96]. The MBD proteins can repress gene expression in several ways. One is through the recruitment of the H3K9 methyltransferase Suv39h1 and heterochromatin protein 1 (HP1). Both Suv39h1 and HP1 interact with MBD1 and aid in the establishment and maintenance of a repressive chromatin state which is further facilitated by the recruitment of both HDAC1 and HDAC2 [97]. During the S phase of DNA replication, regions of the chromosome that are repressed by DNA methylation, or histone modifications must be maintained. MBD1 forms an S phase specific complex with the H3K9 methyltransferase SETDB1, and then associates with chromatin assembly factor (CAF-1) to help maintain a repressed chromatin state [98]. MBD2 and 3 were found to be in the nucleosome remodeling and histone deacetylation (NURD) complex, further associating the cross-talk of DNA methylation with histone modifications and chromatin remodeling enzymes [99]. Although MBD3 cannot bind methylated DNA, it was found to mediate the association between metastasis-associated protein 2 (MTA2), a MBD-containing protein, and the HDAC core of the NuRD complex. MBD2 is thought to direct the NuRD complex to methylated DNA and aid in the maintenance of a repressed environment.

Very little work has been done to identify functions of MBD1-3 in the CNS. Mice with a loss-of-function *MBD1* gene showed normal development, but as adults exhibited deficits in neurogenesis, impaired spatial learning and reduced long-term potentiation in the dentate gyrus [100]. Additionally, MBD1 was most enriched in the hippocampus. During early embryogenesis, MBD3 was found to be highly expressed in the developing brain compared to MBD2 expression [101]. In addition, in the adult brain, MBD3 is highly

expressed in hippocampal and cortex neurons, but has very little expression in the outer cortical layer. Based on overall brain region enrichment patterning, it appears that the MBD proteins have some role in adult neurogenesis, but to what extent is unknown.

1.2. DNA Demethylation

1.2.1. Mechanism of DNA Demethylation

The mammalian genome undergoes genome-wide passive and active DNA demethylation processes during early embryogenesis and in the germline [102-104]. During passive demethylation, there is either a lack of, or inhibition of Dnmt1 preventing the replacement of methyl marks [105-108]. Furthermore, Dnmt1 is unable to recognize and bind to unmethylated DNA [109], rather it prefers to bind to hemi-methylated DNA. The precise molecular events of active DNA demethylation were not elucidated until 2009 when two seminal studies identified the presence of 5-hydroxymethylcytosine (5hmC) in the mammalian genome [110, 111]. Tahiliani et al. discovered that Ten-Eleven Translocation 1 (TET1) could oxidize the methyl group on 5mC to generate 5hmC (**Figure 1.1:**). Subsequent studies further identified TET2 and TET3 proteins as additional "erasers" of 5mC [112]. 5hmC can be furthered catalyzed by all TETs to form 5-formylcytosine (5fC) and 5-carboxylcytosine (5caC) [113, 114]. In addition, 5hmC can be converted to 5-hydroxymethyluracil (5hmU) via the activation-induced cytidine deaminase (AID) and apolipoprotein B mRNA-editing catalytic polypeptides (APOBEC) enzymes [115]. All three of these derivatives (5fC, 5caC, and 5hmU) can be cleaved by thymine-DNA glycosylase (TDG), which excises the modified cytosine base allowing for the base excision repair (BER) pathway to return it to an unmodified cytosine base [114, 115]. Contrary to previous belief that the accumulation of 5hmC was solely dependent on TET activity on 5mC, recent work has suggested that Dnmt1 and Dnmt3a, drive the initial accumulation of 5hmC in the early mouse zygote stage [116]. Knockout models and small molecule inhibitor studies were able to uncouple the formation of 5hmC from 5mC in the paternal pronucleus. This suggests that 5hmC could itself be an independent epigenetic modification.

1.2.2. TET enzymes

TET enzymes catalytically oxidize the methyl group on 5mC to form 5hmC. The TET protein family is made up of three members: TET1, 2 and 3 (**Figure 1.3:**). Each contains a core catalytic domain structured as a double-stranded b-helix (DSBH) fold [111, 117]. Distinguishing the TET proteins from other related TET

J-binding proteins (TET- JBP) families is the presence of a Cys domain located in the N-terminus of the DSBH domain that is thought to be essential for the catalytic activity. Also contained in TET1 and TET3 is a CXXC domain allowing the TET proteins to associate with chromatin through its binding to methylated cytosines. During development, the TET proteins can elect both an activating and repressive response from the genes they control based on what cofactors associate with them. In ES cells, TET1 has a repressive role when bound to the promoter region because it recruits MBD3-NURD [118] and SIN3A [119]. On the other hand, TET2 is not able to recruit either repressive component and has been associated with active cofactors such as Nanog and OGT (O-GlcNAc transferase) [120, 121]. In the male pronucleus, TET3 is responsible for the complete loss of 5mC and the accumulation of 5hmC, as shown by antibody staining and TET3 knockdown studies [122-124].

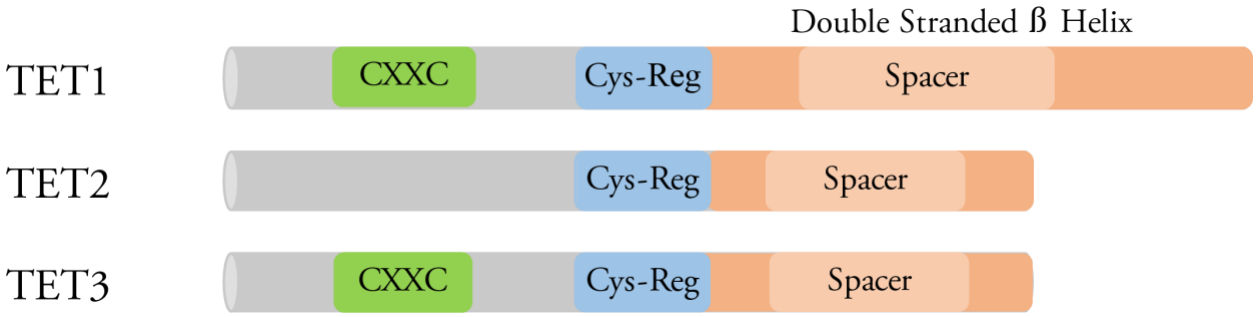

Figure 1.3: Domains of TETs.
Domains of TET1, TET2, and TET3. Each TET protein has a core catalytic domain structured as a double stranded beta helix and a cys-regulatory region. Only TET1 and TET3 contain a CXXC domain to facilitate chromatin binding.

1.2.3. TET Enzymes in the CNS

Once it was discovered that TET enzymes were the long sought- after DNA demethylases, extensive efforts were made to understand the dynamics of the global demethylation events observed in early embryogenesis. The catalytic function of the TET enzyme family and their putative novel roles were yet to be discovered. Even after all the advancements made in the past decade, very little is known about the function of TET enzymes in the mammalian CNS. Although all three TET proteins are expressed in the brain, Tet2 and Tet3 have higher expression compared to Tet1 [110, 125, 126]. When Tet2 and Tet3 are overexpressed, premature neuronal differentiation was observed, whereas knockdown caused defects in differentiation

progression [126]. *Tet1* knockout studies have identified several neural activity-regulated genes that are downregulated. Animals with this knockout display abnormal hippocampal synaptic plasticity and impaired memory extinction [127]. Intriguingly, *Tet1* deletion did not appear to affect anxiety or depression related behaviors. Due to the embryonic lethality of *Tet3* deletion in mice, determining its function in the adult brain has been challenging. Instead of knockout studies, several groups have utilized small hairpin RNAs (shRNAs) to conditionally inhibit Tet3 expression. A recent study demonstrated that deletion of *Tet3*, and not *Tet1*, in mouse infralimbic prefrontal cortex (ILPFC), a region of the brain associated with fear extinction learning, impaired their ability to reverse a previously learned fear response [128]. Importantly, it was found that Tet3 mediates the drastic genome-wide redistribution of 5hmC in the ILPFC in response to extinction learning. Furthermore, posttraumatic stress disorders and phobias have been associated with impairments in fear extinction learning [129].

1.2.4. Roles of 5hmC, 5fC, and 5caC in the CNS

As previously discussed, 5hmC is the immediate product of TET enzymes in the demethylation of 5mC. Relative to other tissue types, 5hmC is found to be approximately 10 times higher in the brain compared to ESCs [111, 130, 131]. Genome-wide analysis studies have demonstrated that 5hmC is dynamically regulated in human [132] and mouse brains during neurodevelopment and aging [125]. Dot blot analysis on cerebellum DNA showed 5hmC increased roughly 42% from fetal to adult brains. Furthermore, human 5hmC modifications were enriched at CpG islands and shores, exons and untranslated regions, consistent with 5hmC being associated with active genes. In addition to brain regions, some neurons have been found to contain high levels of 5hmC. For example, Purkinje neurons in the cerebellum were found to have roughly 40% more 5hmC relative to 5mC [110]. The enrichment of 5hmC in Purkinje neurons could account for its active biological functions as motor neurons that require an active transcriptome. Locus specific demethylation has been observed at the *Bdnf* loci. *Bdnf* is involved in adult neural plasticity and learning and memory [133]. When cortical and hippocampal neurons experience a depolarization event, the *Bdnf* promoter is activated, enhancing its transcription [134, 135]. The depolarization was also found to correlate with a decrease in CpG methylation in the *Bdnf* regulatory region [93, 136].

Very little is known about the functional roles of 5fC and 5caC other than their roles in active demethylation and conversion back to an unmodified cytosine. Genome-wide profiling studies found an enrichment of 5fC at poised and active enhancers, but with a clear preference for poised enhancers [137]. A recent study examined the dynamics of 5fC and 5caC in embryonic day 11.5 mice through 15-week-old adult mice [138]. They found that 5fC could be detected throughout all of the developmental time points, while 5caC could not be detected. Interestingly, both 5fC and 5caC were found to induce pausing of RNA Pol II during elongation, where this effect was not observed at C, 5mC nor 5hmC bases [139]. It is possible that TDG could be recruited to sites of paused RNA Pol II to initiate the BER mechanism. Interestingly, TDG is the only glycosylase that is required for embryonic development [140, 141]. Even more intriguing is that in ESCs, both 5fC and 5caC recruit more proteins than either 5mC or 5hmC [142]. The recruited proteins mostly had functional roles in DNA damage response (such as Tdg and p53), and proteins involved in chromatin remodeling (such as BAF170) were also found to interact with them.

1.3. Histone Modifications

DNA is wrapped around a core histone octamer containing two copies each of the histone variants H2A, H2B, H3 and H4 forming a chromatin structure [143]. The amino acids that make up the amino-terminal 'histone tails,' mainly lysines and arginines, are subject to modifications, such as methylation and acetylation, that can affect transcription (**Figure 1.4:**). Unlike DNA methylation which only has three major methyltransferases, there have been numerous histone methyltransferases and demethylases identified for histones [144]. The potential crosstalk between histone methylations and DNA modifications and chromatin remodelers and regulatory RNAs add another layer of complexity. These crosstalk events are thought to establish and maintain the local chromatin environment as well as help cells "remember" their differentiated state [145, 146]. Several mechanisms facilitate this crosstalk such as DNMT3L and methyl-binding proteins like MeCP2 and MBD2, but we will focus in detail on the Polycomb (PcG) repressive proteins and the Trithorax (TrxG) activating proteins (**Figure 1.4:**). These two groups of proteins antagonistically regulate genes that are critical for development and cell differentiation pathways [147]. The proteins encoded by PcG and TrxG form

large complexes to maintain the local chromatin environment in either a repressed or active state, respectively [148, 149].

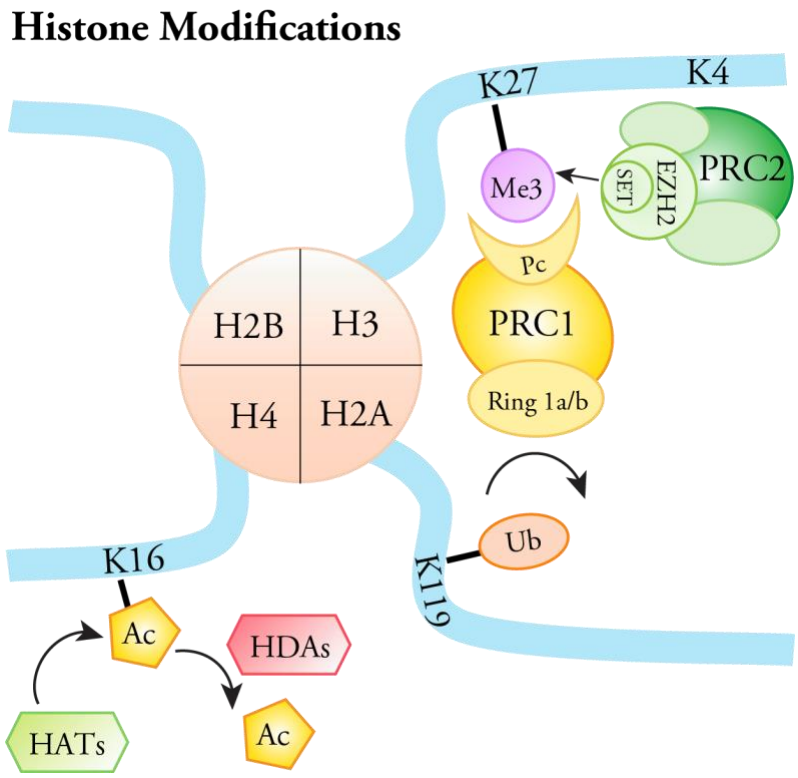

Figure 1.4: Epigenetic Regulation in the CNS: Histone Modifications
Histone modifiers can add various groups to the tails of the histone proteins that can affect the expressivity of a gene's transcript.

1.3.2. Polycomb Group Proteins

The PcG proteins are divided into two major multiprotein complexes: polycomb repressive complexes 1 and 2 (PRC1 and PRC2) [150]. Both complexes contain a core set of proteins critical for their basic function and can incorporate accessory proteins, permitting the complex to act in a spatiotemporal manner. There are four core proteins that are present in all PRC2 complexes: the SET domain contained in the enhancer of zeste [E(z), EZH1, and EZH2] protein, extra sex combs (Esc, EED) proteins, suppressor of zeste 12 [Su(z)12, SU(Z)12] and the histone binding protein p55 (RBAP48 and RBAP46) [151-153]. The SET domain within E(Z) is responsible for the lysine methyltransferase activity specifically occurring on histone 3 at lysine 27 (H3K27) [154]. PRC1 is also composed of a set of four major core proteins including polycomb (Pc),

polyhomeotic (Ph), posterior sex combs (Psc) and Sex combs extra (Sce/dRing 1) [150]. The chromodomain in Pc is responsible for recognizing and binding trimethylated H3K27 (H3K27me3) and upon binding will induce structural changes in the chromatin [155, 156]. In addition, PRC1 is also responsible for the monoubiquitination of lysines on histone H2A via the proteins Ring1A/B [157].

1.3.3. Trithorax Group Proteins

Antagonistic to the PcG proteins, the TrxG proteins are recognized for their activating mechanisms and addition of histone 3 lysine 4 trimethylation (H3K4me3). TrxG proteins are also evolutionarily conserved and are categorized into three groups based on their function. Group one is composed of the SET-domain-containing proteins that methylate histone tails, group two contains ATP-dependent chromatin remodeling proteins and finally group three contains the TrxG proteins that can bind DNA in a sequence specific manner. Each of these groups are thoroughly reviewed elsewhere [158]. One of the first SET-domain-containing histone modifying complexes identified that could catalyze mono-, di-, and trimethylation on H3K4 was a complex called COMPASS in yeast [159, 160]. Mammals have six COMPASS-like complexes that have been shown to facilitate most H3K4me3 present, indicating that they are likely involved in global gene activation [161].

1.3.4. PcG and TrxG Proteins in CNS

In the mammalian CNS, both PcG and TrxG proteins help to regulate the differentiation process of neuronal cells. In ESCs, polycomb proteins prevent neuronal differentiation by adding H3K27me3 repressive marks at neuronal specific genes such as *Ngns, Pax6, Sox1* [162, 163]. However, these genes simultaneously contain the active trithorax H3K4me3 mark, making these promoters bivalent. As ESCs differentiate into NPCs, the H3K27me3 polycomb mark is removed specifically by the histone demethylase Jmjd3 to further commit them to a neural lineage [164]. In addition to histone demethylation, activation of the TrxG COMPASS-like complex proteins RBBP5 and DBY30 are essential for the differentiation of ESCs into NPCs [165]. In NPCs, the PRC2 subunit Ezh2 is initially highly expressed, but declines during cortical neuron differentiation [166]. The loss of Ezh2 was shown to augment neurogenesis and neuronal differentiation. PcG complexes have also been associated with differentiation of NPCs to astrocytes [167] and oligodendrocytes [168]. As the brain develops, NPCs can travel up and outward to form the outer layers of the brain. A study demonstrated that

Ezh2 silences genes associated with neuron migration, such as *Netrin1*, to maintain correct migration patterns throughout the brain [169].

Furthermore, several studies have demonstrated the importance of cross-talk between DNA methylation and histone modifications during mammalian brain development [126, 170]. As previously described, during neurogenesis as NPCs begin to differentiate, there is an increase in 5hmC specifically in gene bodies of developmentally active genes with little change in 5mC. Accompanying this increase, there is also a decrease in Polycomb-mediated repression and H3K27me3 formation [126]. Overexpression of *Tet2* and *Tet3*, both of which are highly expressed in the embryonic cortex, prompted early differentiation of NPCs. An analogous and more obvious transition was seen when *Ezh2* was also depleted. Moreover, when Tet proteins were inhibited and *Ezh2* overexpressed, NPCs failed to differentiate. This suggests that Polycomb may regulate the transition of NPCs differentiation, and Tet proteins putatively maintain the differentiated state. Additionally, it has been demonstrated that there is an inverse association of Dnmt3a *de novo* methylation on non-promoter CpGs and H3K27me3 formation in the mouse brain [170]. Mice deficient for *Dnmt3a* had an increase of H3K27me3 as well as increases of PRC2 components Suz12 and Ezh2 at Dnmt3a targets. As previously discussed, Dnmt3a has more of a role in DNA methylation maintenance in postnatal development. The proposed cross-talk suggests that in addition to methylating promoters of self-renewal genes in NPCs, Dnmt3a also has an activating function by inducing transcription of mature neural genes by down regulating H3K27me3 and antagonizing PRC2 binding.

1.3.5. Histone Acetylation

Methylation is just one type of modification that can be present on histone tails; acetylation is a second type of modification that also regulates chromatin dynamics. Histone acetyltransferases (HATs) and HDACs are enzymatic proteins that either add or remove acetylation residues on lysines, respectively [171, 172] (**Figure 1.4:).** Core histones are acetylated by transcriptional coactivators like CBP/p300 that are ubiquitously expressed and involved in cell cycle control, differentiation and apoptosis [173]. HATs can be divided into three families based on the structure of their catalytic domains: GNAT, MYST and CBP/p300 which are reviewed elsewhere [174, 175]. Supportive of their activating role, HATs will interact with various transcription factors to promote

many signaling cascades [176]. Similar to methylation, acetylation is reversible and removed by HDACs that silence gene expression. HDACs can also be categorized into four distinct classes where class 1 and class 2 HDACs seem to have important roles in the nervous system [177, 178]. Inhibitors of HDACs have shown promising effects in treating both neurodegenerative and neuropsychiatric diseases. It has been demonstrated that HDAC inhibitors could re-establish histone acetylation that is potentially lost due to dysregulation of the HAT, Tip60 [179]. Furthermore, inhibition of HDACs restored learning and memory in a mouse model of neurodegeneration [180]. In the mouse brain, *Hdac3* deletion provoked abnormal locomotor coordination, sociability and cognition [181]. Interestingly, a cross-talk between HDAC3 and MeCP2 was shown to positively regulate neuronal genes by deacetylating FOXO, a transcription factor that is highly expressed in the hippocampus.

1.4. Chromatin Remodeling

The total length of DNA in one mammalian cell is on average 2 meters, yet the size of the nucleus is only 6μm. In order to fit the entire genome into such a limited space, DNA molecules have to undergo extraordinary consolidation by a process termed chromatin remodeling. In addition to histones, a major contributor to chromatin compaction is a family of ATP-dependent remodeling proteins. The BAF (mammalian SWI/SNF) complex is a chromatin remodeling multiplex that uses ATP-dependent energy to modify the chromatin landscape to promote cell differentiation [182] (**Figure 1.5:**). BAF complexes exist in a very spatiotemporal specific fashion. For example, in the mammalian CNS, there are developmental stage-specific BAF complexes in ESCs [183], NPCs and in post-mitotic neurons [184]. A unique feature to BAF complexes is that the alternative subunits that make up the various stage-specific complexes are not interchangeable, indicating their functions are non-overlapping [185, 186].

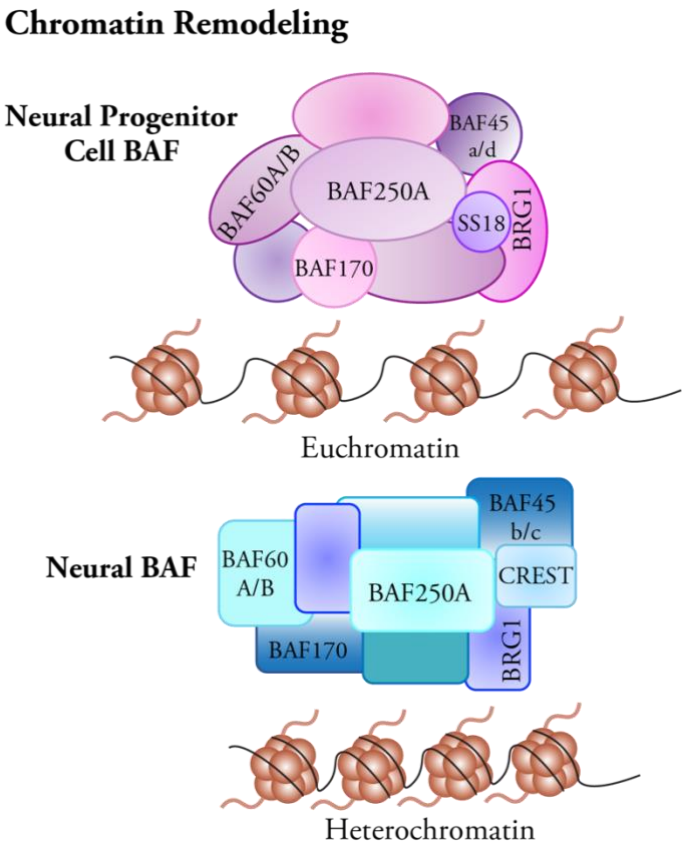

Figure 1.5: Epigenetic Regulation in the CNS: Chromatin Remodeling
Chromatin remodeling proteins can remodel the chromatin environment by affecting how tightly and loosely packed histones are and ultimately contribute to the gene's expression.

1.4.2. BAF Chromatin Remodelers

The ESC specific BAF (esBAF) contains the ATPase BRG1, BAF250a, BAF60a/b and BAF155 [183]. Deletion of any of the core subunits results in a lethal phenotype [187]. For example, shRNA depletion of *Brg1* impairs self-renewal properties of ESCs and results in loss of key ESC markers such as *Oct4*, *Sox2* and *Nanog* [188]. In addition, deletion of *Brg1* also resulted in an increase of the PRC2 recruitment and subsequently, H3K27me3 repression at active ESC genes [189]. All this evidence suggests that esBAF maintains a euchromatic environment that is required to maintain the pluripotency of ESCs.

The transition from esBAF to neural progenitor BAF (npBAF) is associated with the replacement of esBAF155 with npBAF170 [188, 190]. npBAF is composed of a combination of either ATPase BRG1 or BRM along with several other BAF subunits. Similar to esBAF, npBAF are critical for the self-renewal properties of NPCs and loss of *Brg1* shows similar phenotypes as those seen in esBAF. Interestingly, BAF170 was shown to

interact with the transcription factor Pax6 whose primary function is to regulate neural progenitor division during early cortical development [191]. Upon BAF170 binding to Pax6, the transcriptional repressor REST (RE1- silencing transcription factor, also known as NRSF) is recruited, and represses Pax6 in non-neuronal radial glia cells [190]. A conserved, 23 base pair sequence known as RE1 (repressor element 1, also known as NRSE) acts as the binding site for REST [192-194]. Two corepressors are required for REST mediated silencing, Sin3-HDAC and the CoREST protein complex that contains HDACs [195, 196]. Additionally, it was shown that CoREST interacts with BAF57, a subunit present in all stage-specific complexes, to induce long term silencing [197]. BAF170 is present in the subset of radial glia cells that are destined to be non-neuronal, and absent in radial glia cells destined to become intermediate progenitors that migrate outward to form the outer cortex layer [190, 195, 196].

The substitutions of BAF53a for BAF53b, SS18 for CREST and BAF45a/d for BAF45b/c marks the transition from npBAF to the mature neuron (nBAF) complex [198]. Importantly, the nBAF subunits are exclusive to neuronal cells and maintain the chromatin environment of post-mitotic neurons [198, 199]. nBAF, in complex with CREST, is essential in regulating dendritic outgrowth [200]. Normal brain function depends on the correct wiring and synaptic function controlled by adequate dendritic outgrowth. Calcium regulation in the CNS can activate calcium mediated transcription factors, such as CREST, to promote the activation of genes required for dendrite growth [201].

1.5. Regulatory RNA

An emerging field in epigenetics is focusing on debunking the large amount of non-protein coding DNA contained in the mammalian genome. Over the past 20 years, scientists have begun to discover that non-coding is not equivalent to non- functional. When transcribed, these regions generate non-coding RNA (ncRNA) that can range in size from just ~21 nucleotides to 100,000 nucleotides and can post-transcriptionally regulate mRNA. Many flavors of ncRNAs have been identified [202]; however, this review will briefly cover miRNA and lncRNA and the putative functions they may serve in the mammalian CNS.

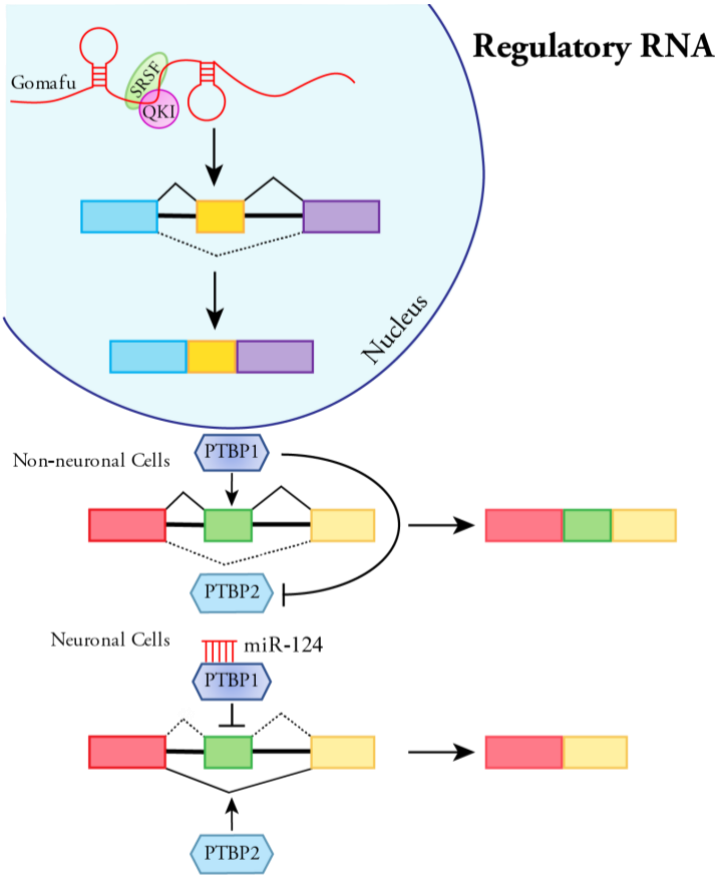

Figure 1.6: Epigenetic Regulation in the CNS: Regulatory RNA
Regulatory RNAs, such as long non-coding RNAs and microRNAs, can affect alternative splicing and protein expression.

1.5.2. microRNAs

MicroRNAs are roughly 22 nucleotides in length and have major roles in post-transcriptionally regulating gene expression by destabilizing their target mRNA [203]. Partial sequence complementarity to the 3' untranslated region (3'-UTR) of the target is adequate for gene downregulation [204]. Perfect complementarity is required at what is called the "seed sequence" in the 5'-UTR of the miRNA. Interestingly, a single miRNA can target hundreds of different mRNA and that a single mRNA can be targeted by more than one miRNA [205]. Determining functional roles for the hundreds of miRNAs discovered has eluded scientists for years. Early studies proposed that miRNA had extensive roles during mammalian brain development and several of these studies identified neural- specific miRNA [206-209]. Of the neural-specific miRNA identified, one in particular stands out, miR-124. miR-124 is the most abundant and highly conserved miRNA found in the mammalian brain [210]. Accounting for nearly 25–48% of all the miRNA in the brain, miR-124 has been

implicated as a major contributor in neuronal differentiation and maturation [207, 211]. For example, the direct targeting and repression of the RNA binding protein, PTBP1 by miR-124 has critical roles in non-neuronal cell development [211] (**Figure 1.6:**). PTBP1 is highly expressed in non-neuronal cells and inhibits alternative splicing of neuron-specific genes [212, 213]. In cells destined to become neurons, miR-124 binds and represses PTBP1, resulting in an increase of PTBP1's neuronal homolog, PTBP2 protein expression, inducing neuron-specific alternative splicing.

Another brain enriched miRNA, miR-137, is thought to have roles in both adult neurogenesis and neuronal maturation. During adult neurogenesis, miR-137 regulation of proliferation versus differentiation is coupled with its ability to cross-talk with MeCP2 and Ezh2 [131]. Roughly 2–4Kb upstream of miR-137, methylated CpGs were found as well as a threefold enrichment of MeCP2 binding. Subsequently, it was found that Sox2 also binds upstream of miR-137, and concurrent binding of Sox2 with MeCP2 inhibited miR-137. When miR-137 expression is reduced, there is an increase in neuronal differentiation and a decrease in adult neural stem cell proliferation. This is concurrent with a previous observation that miR-137 expression increases during neuronal differentiation [214]. The polycomb protein Ezh2, was found to be a direct target of miR-137 *in vitro* [131]. MiR-137 reduces the expression of *Ezh2* and consequently there is also a decrease in H3K27me3. Loss of H3K27me3 encourages adult stem cells to begin to differentiate rather than proliferate.

1.5.3. Long non-coding RNAs

Long non-coding RNAs are classified as having at least 200 nucleotides and non-protein coding abilities [215]. They are also one of the least well understood class of ncNRAs because of the difficulty in distinguishing them from transcription by-products. Compositionally, lncRNA do not appear to be very well conserved between mouse and human [216]. In the mouse genome, the vast majority of lncRNAs do not contain an open reading frame [217]. In addition, compared to protein coding transcripts, lncRNA tend to be shorter and contain fewer introns. Unusually, some lncRNA such as the paternally imprinted lncRNA *H19*, are polyadenylated, spliced and exported to the cytoplasm just like protein coding transcripts [218]. Functional roles of lncRNA may depend on where in the genome they are located. Those that are transcribed near expressed genes have the potential to regulate the expression of that gene in *cis*. One of the most well studied

lncRNAs is *Xist*, which functions in *cis* and is critical for inactivating one of the X chromosomes in mammalian females [219]. As *Xist* coats the X chromosome, other repressive factors are recruited, such as Polycomb repressive complexes PRC1 and PRC2 and other histone modifying enzymes [157, 220, 221]. lncRNAs have also been demonstrated to regulate transcriptional repressors and activators from a distance (in *trans*). The *HOTAIR* lncRNA is 2.2 Kb in length, and was shown to repress the transcription of 40Kb of the *HOXD* locus [222]. It is proposed that *HOTAIR* interacts with PRC2 to facilitate H3K27me3 of the *HOXD* locus because siRNA mediated knockdown of *HOTAIR* resulted in the loss of H3K27me3 marks specifically at *HOXD*. Beyond chromatin remodeling, other putative functions for lncRNAs have been suggested, such as transcriptional control and post-transcriptional processing, which are reviewed in detail elsewhere [223, 224].

The role of lncRNAs in chromatin remodeling has been extensively studied and the scientific community is just starting to make strides in investigating their roles in the brain [225]. lncRNAs have been found in many tissues [226], but are strikingly enriched in the mammalian brain. One study identified over 800 lncRNAs in the mouse brain, and found that most were associated with specific brain regions, cell types or subcellular compartments, suggesting some putative function [227]. One of the better studied lncRNAs in the brain is *Malat1* (also known as *NEAT2*), which is particularly enriched in neurons [228, 229]. *Malat1* localizes to nuclear speckles which are storage/assembly sites for processing factors involved in pre-mRNA splicing [230-232]. Studies demonstrated that *Malat1* recruits SR splicing factors in the nuclear spectacle and can regulate genes involved in neural processes and synaptic function [228]. Importantly, *Malat1* was shown to have 90% conservation between human and mouse, suggesting maintenance of a critical function. A recent computational study utilized RNA-seq data from mouse embryonic brains to identify temporally regulated lncRNAs in brain development. Interestingly, lncRNAs specifically expressed in embryonic brains were no longer expressed in adult brains [233]. Another study employed RNA-seq on human iPSCs to investigate the expression of lncRNAs during their differentiation into mature neurons [234]. Much research is being conducted on identifying and determining functional roles of the ever-growing list of lncRNAs; however, more work remains to be done.

To add another layer of complexity, different groups of non- coding RNAs have been found to cross-talk with each other and form regulatory networks in the brain [235]. A recent study found that in mouse brain, the lncRNA *Cyrano* destabilizes miR-7 through its highly complementary site for miR-7. Degradation of miR-7 promoted the accumulation of a circular RNA Cdr1as, which is known to dampen neuronal activity [236, 237]. Interestingly, Cdr1as contains an inherent destruction mechanism where binding of miR-671 induces its slicing [235]. It has been proposed that because the binding sites for miR-7 and miR-671 are so close on Cdr1as, cooperative binding could recruit a silencing complex and control the accumulation of Cdr1as in the brain [238, 239].

Proper epigenetic regulations are critical for normal brain development and functions. Numerous evidences suggest that their dysregulation could serve as causal roles in the onset of neurological, neurodegenerative and neuropsychiatric disorders. In the following sections, we will focus on several neurological disorders with known roles of epigenetic regulation in their etiology and progression.

1.6. Alzheimer's Disease

Alzheimer's disease (AD) is considered one of the most common neurodegenerative diseases worldwide, and is characterized by memory loss and impairments in cognitive function [240]. These phenotypes are accompanied by β-amyloid plaques, phosphorylated Tau and neurofibrillary tangles that accumulate in the brain [241]. Typically, sporadic onset does not occur until 60 years of age and is strongly associated with the risk gene apolipoprotein-E (APOE) ε4 [242]. However, there is a relatively rare early onset form known as familial AD that is linked to genetic mutations in the key AD risk genes amyloid beta precursor (APP), presenilin 1 (PSEN1) or presenilin 2 (PSEN2) [243]. These key risk genetic mutations provided opportunity for establishing both AD mouse models and human patient-derived Induced Pluripotent Stem Cells (iPSCs) to model AD progression. Research has mainly focused on risk gene discovery, cognitive function, neurodegeneration pathologies and epigenetic modifications in the later stages of AD. In chapter 2, we discuss how epigenetic changes that occur in the early stages of AD, before disease onset, could advance our understanding and provide alternative approaches to studying AD.

1.6.1. The Roles of DNA Methylation and Demethylation in AD

DNA methylation has been highly correlated with aging [244], making it an attractive research area for age-related diseases. During brain development and aging, global CpG methylation is maintained at abundant levels in the human frontal cortex, whereas non-CpG methylated cites increased in abundance with age [80]. Furthermore, several studies have demonstrated the importance of more localized hyper- and hypomethylation changes of CpG islands in various brain regions with respect to aging [245-247]. Because of this robust predictive relationship between aging and DNA methylation, studies are now utilizing a subset of methylated CpGs spread across the genome as biomarkers to connect chronological age with ones' epigenetic age to predict potential health outcomes [244, 248], such as earlier onset of age-related diseases [249, 250]. For example, a study conducted by Jager et al., identified 71 differentially methylated CpG cites whose altered methylation status occurred in the early, pre-symptomatic stages of the AD neurodegenerative process [251].

With respect to specific brain regions, immunohistochemical methods have been used to demonstrate a global reduction of 5mC in the hippocampus of AD individuals [252]. However, several other studies examining specific subregions of the cortex known to be highly susceptible to AD pathologies have revealed conflicting evidence in their global 5mC levels [253-255]. These discrepancies could likely be influenced by unknown underlying comorbidities, environment, postmortem delay in tissue preservation or different experimental approaches for detecting 5mC alterations. Although global alterations to the 5mC landscape with respect to AD has provided critical contributions to the field, a more targeted analysis of differentially methylated genes or cell type specific 5mC shifts could provide more direct evidence supporting the role of DNA methylation in AD. Subsequently, there has been an exponential rise in the number of epigenome-wide association study (EWAS) studies being used to investigate differentially methylated regions (DMRs) between control and AD brain samples. Most DNA methylation meta-analyses have been performed on single AD cohorts that can be under powered due to limited sample size making it difficult to identify truly significant DMRs associated with AD. A recent study by Smith et al., performed a meta-analysis combining six independent AD cohorts where in addition to confirming numerous previously reported genes identified in single cohort analysis, such as *HOXA3*, *ANK1*, *RHBDF2*, *SLC44A2*, *BIN1* and *MAMSTR* [251, 256-258],

they also discovered 84 novel genes with significant scores [259]. A major challenge for bulk tissue meta-analysis arises from cell type heterogeneity which affects decerning signal from background noise. Another consideration to take into account is the shift in cell type proportions, particularly for age-related and degenerative diseases [260]. To address this, Gasparoni et al. first purified neuronal and non-neuronal (glial) cell populations from healthy and AD patients prior to preforming an EWAS study [261]. Not only was this study able to confirm previously reported DMRs found in larger AD EWAS, they identified cell type specific DMRs and DMRs in the two AD risk genes *APP* and *ADAM17,* which were previously unreported.

The roles for the DNA epigenetic writers (DNMTs) and erasers (TETs) have not been thoroughly investigated with respect to AD. As mentioned earlier in this review, the expression of most DNMTs are much higher in progenitor cells, but maintained at relatively low levels in most differentiated neurons (Goto, 1994), suggesting that DNMTs are unlikely to have a major role in AD. On the other hand, the TET enzymes have recently been linked to cognitive impairments in an AD mouse model. KD of Tet2 in the hippocampus of early-stage AD (5-6 months) 2xTg mice significantly augmented cognitive decline bringing them to a similar cognitive stat of late-stage AD mice (14 months) [262]. Importantly, Tet2 overexpression mitigated cognitive decline in 10-month AD mice. In support of this finding, it was demonstrated that by increasing Tet2 expression in the adult hippocampus, you could significantly improve age-related neurodegeneration and cognitive function [263]. Although this function of Tet2 in adult neurogenic rejuvenation has yet to be studied in an AD model, it would be an interesting avenue to pursue in terms of therapeutics.

Given that Tet proteins appear to be decreased in AD brains, research efforts have started to focus their attention on Tet's downstream product, 5hmC. Like 5mC, consensus of either a global increase or decrease of 5hmC in AD brains are inconsistent [254, 264-267], likely due to differences in brain regions and the degree of neurodegeneration of each sample. However, genome-wide sequencing studies have suggested that these aberrations in 5hmC distribution and function could be critical factors contributing to AD [267, 268]. One study functionally validated that several differentially hydroxymethylated loci (DhMLs) located near or in previously identified AD-associated SNPs could either exacerbate or rescue tau neurotoxicity in a *Drosophila* eye screen [269]. This suggests that these DhML could potentially be used to predict ones' AD disease risk.

Traditionally, aged, postmortem brains have been a primary model system to study AD; however, this model is only able to capture a snapshot of the disease state. In chapter 2, we further expand upon the role of 5hmC in AD by taking a unique approach. We utilized human forebrain organoids, which recapitulate embryonic development, to investigate developmental changes of 5hmC over time and see how perturbations in the 5hmC landscape could contribute to AD pathogenesis. This model system is the earliest human model available to study early neurodevelopment and provides a unique approach to studying age-related neurodegenerative diseases. Our research supports the notion that AD-specific 5hmC changes that occur early in development may cause subtle disruptions in the neuronal network that could contribute to the onset of AD later in life.

1.6.2. The Roles of Polycomb and Trithorax Proteins in AD

There are a handful of studies that observe some association of aberrant PcG and TrxG protein regulation in AD. For example, both lysine methyltransferases Kmt2a and Kmt2b (Mll1 and Mll2, respectively) are involved in memory formation [270], which is impaired in AD patients. In mouse hippocampal neurons, loss of Kmt2a partially recapitulates a down-regulated gene list similar to that observed in the mouse AD model. Another study identified that deficiency of PRC1 components responsible for the monoubiquitination of H2A, Bmi1/Ring1, are associated with late-onset AD [271]. This study observed that, in AD brains and induced pluripotent stem cell-differentiated neurons derived from late-onset individuals, Bmi1 is silenced. Notably, Bmi1 silencing is not seen in brains of familial AD patients or other dementia-like diseases. Finally, loss of the brain-specific, ATPase chromatin remodeler CHD5 in primary neurons augments genes with known roles in aging and AD [272, 273]. An interesting area for new research would be to identify more brain-specific, chromatin- remodeling proteins and elucidate any roles they could have in neurological diseases. Given that most remodelers are ubiquitously expressed, finding remodelers that are brain-specific could lead to the development of biomarkers.

To characterize and compare the human AD epigenome to the mouse AD epigenome, ChIP experiments on various histone marks, including H3K4me3 and H3K27me3, were computationally profiled [274]. Overall, human and mouse AD models show similar peak overlaps, especially at H3K27me3 peaks,

demonstrating conservation of the epigenome between mice and humans. Promoters with increased H3K4me3 correspond to immune genes, whereas decreased H3K4me3 promoters correspond to neuronal genes. This work supports the current hypothesis that AD development could be attributed to an immune response provoked from environmental factors (chronic diseases, obesity and type 2 diabetes) experienced during aging, and genetic factors (gene mutations and epigenetic dysregulations) contributing to cognitive impairments [274, 275].

1.7. Stress and Depression

Stress can be described as adverse experiences that contest the emotional and psychological well-being of an individual. In its most basic break down, stress is experienced either acutely or chronically. Acute stress, often referred to as "fight-or-flight" response, is a positive survival-based response that is only experienced for a limited duration. On the other hand, chronic stress reflects a prolonged period of enduring stress provoking situations that require constant efforts by the brain and body to adapt and survive [276]. Frequently, this adaptive coping turns into a cumulative physiological burden, whereby the risk of developing negative health-related problems and depression drastically increases. Individuals with depression or major depressive disorder (MDD) present clinically with not only a depressed mood, but can also suffer from anhedonia, dysregulated appetite and sleep, fatigue, poor concentration and suicidal ideations or acts [277]. In the United States, the incidence of depression in women is more than twice that of men [278]; however, reasons for this are inconsistent and often conflicting. Here we prioritize the impact of stress on the brain, given that it is the primary organ responsible for regulating how stress is perceived (threatening or not) and how one responds (susceptible or resilient) [276]. Specifically, we focus on the role of epigenetics and their corresponding machinery and whether or not they are involved in stress response.

1.7.1. Histone Modifications in Stress and Depression

To what extent epigenetic marks and the proteins that write, read and erase them serve in stress-induced depression is not well understood. Until recently, previous studies have directed their efforts at profiling global histone modifications in relation to stress. For example, in the hippocampus, chronic social defeat stress was observed to robustly increase the repressive histone methylation (H3K27me2) mark at the promoters of *Bdnf* transcripts 3 and 4 [279]. Chronic treatment with antidepressants reversed *Bdnf*

downregulation and increased H3 acetylation at these promoters and was observed to selectively downregulate the histone deacetylase *Hdac5*. Other studies have also suggested that dynamic regulation of histone acetylation marks such as H3K14ac and histone deacetylase levels could play a protective role against depression and confer a resilience to stress [280].

1.7.2. DNA Modifications in Stress and Depression

With regards to other epigenetic regulatory mechanisms, the impact of DNA modifications on stress has predominantly been studied in early-life. Since the early 2000s, it has been known that early-life exposure to chronic stress impacts epigenetic memory, where alterations to the epigenetic landscape have been shown to persist decades after the stressor. This suggests that affected individuals are likely to be more susceptible to neuropsychiatric diseases. Two of the earliest examples of this are maternal care or neglect and the Dutch famine cohort. Offspring who received more maternal care had increased expression of the glucocorticoid receptor (*GR*) gene due to decreased promoter methylation compared to neglected offspring [281]. Studies on prenatal exposure to the Dutch famine have shown prenatal malnutrition-associated differential methylated regions associated with genes that effect growth and lipid metabolism [282].

A major focus in depression therapeutics is to identify putative biomarkers that could be predictive of an individual's stress resilience or susceptibility. A top candidate gene that has been reported to act as a conceivable epigenetic biomarker is *BDNF* due to its two small CpG islands upstream of exons 1 and 4 [283]. Individuals with MDD have been reported to display increased methylation at the *BDNF* promoter resulting in reduced protein expression. Furthermore, it was found that the methylation status of exon 1 could be used to accurately distinguish between healthy controls and MDD patients who consistently showed a complete absence of methylation at certain CpG sites in exon 1 [284]. Methylation within *BDNF* or at specific exons has been associated with antidepressant drug efficacy; however, whether these effects are beneficial or not remains inconclusive [285, 286]. In addition to investigating the methylation of *BDNF*, recent work has explored how the downstream molecular targets of BDNF signaling could be involved in stress induced depression. One downstream target of BDNF signaling is the DNA demethylase Gadd45b, which removes methyl marks in the *Bdnf* gene during neurogenesis [287]. In the NAc of mice that have undergone chronic social defeat, Gadd45b

showed increased expression specifically in stress susceptible compared to stress resilient animals [288]. Moreover, knockdown of *Gadd45b* in susceptible animals rescued depressive-like behaviors. Another well-studied biological factor in MDD is the serotonin transporter gene *SLC6A4*. MDD individuals who had a family member with depression showed a higher percentage of *SLC6A4* methylation. In mother–child pairs that were concordant for depression, increased methylation of the *SLC6A4* promoter was seen in both mother and child [289]. These findings indicate that epigenetic regulation of this loci may be related to depression heritability.

With respect to stress and depression, the overwhelming majority of epigenetic studies have comprised of DNA methylation studies. The involvement of DNMTs, TET proteins and 5hmC in stress response is lacking, despite their overall abundance in the brain. In the context of chronic social defeat stress, *Dnmt3a* expression was significantly elevated in the NAc of stressed animals immediately following and 11 days post stress [290]. Interestingly, chronic inhibition of Dnmt3a methylation post social defeat attenuated the social avoidant behavior displayed in stressed animals to resemble that of animals chronically treated with the antidepressant fluoxetine.

Animal knockout (KO) studies have suggested that the loss of either Tet1 or Tet2 could influence stress susceptibility [291]. Prior to and following chronic stress, Tet1 KO animals displayed less anxiety/depressive-like behaviors compared to WT control littermates, suggesting that the loss of Tet1 could make the animals more resistant to stress. On the other hand, Tet2 KO animals behaved oppositely, suggesting the loss of Tet2 could increase stress susceptibility. Of note, the Tet1 and Tet2 KO animals are on different background strains (Tet1 on C57BL/6 and Tet2 on 129) making these finding strictly strain-dependent (i.e., increased stress susceptibility of Tet2 KO animals may not produce to the same effect if on the C57BL/6 background). It is possible that the behaviors observed could be influenced by differences in strain baseline predisposition to stress that can be attributed to differences in their genetic background [292]. Given that the Tet enzymes are responsible for generating 5hmC, it is conceivable that alterations in the 5hmC landscape could also play some role in stress. In fact, under chronic stress conditions, Tet1 interacts with the hypoxia-induced

factor HIF1α, shifting the 5hmC landscape in the prefrontal cortex [291]. Importantly, these differential 5hmC patterns occurred near the promoter regions of genes previously associated with MDD.

Cytosine modifications are arguably the most prevalent DNA modification in the brain; however, over the past 8 years a new modification known as N6-methyladenine (6mA) has surfaced. Originally thought to only be present in prokaryotes [293], 6mA has recently been discovered in mammalian genomes [294, 295]. During early mammalian embryonic development, 6mA is highly enriched but then quickly becomes depleted as development progress [294]. Further, it has been shown to regulate gene and transposon expression in mouse ESCs [296]. Similar to the cytosine modifications, it was presumed that 6mA would also have epigenetic machinery that function to "write" and "erase" this modification. In mouse, Mettl3-Mettl14 complex have been identified as putative enzymatic writers of 6mA while Alkbh1 is a putative eraser [296-298].

Given that 6mA is primarily enriched very early in development, initial studies examined how experiencing juvenile stress (P1-3) could impact stress response in male and female rat pups later in life (P33) [299]. In female rats, juvenile stress resulted in decreased expression of Alkbh1 in the amygdala, which corresponded to the observed increase of 6mA in the promoter region of the serotonin receptor Htr2a. This finding further explained the significant reduction in Htr2a expression in stressed females. On the other hand, stressed males expressed significantly higher levels of Alkbh1 compared to stressed females and male rats overall expressed considerably less Htr2a compared to females, regardless of stress. These findings suggest that exposure to juvenile stressors could have a sex-dependent response to serotonin signaling in the juvenile amygdala. In young adult mice, chronic stress increased 6mA levels in stress-responding brain regions (i.e. hippocampus, hypothalamus, amygdala and prefrontal cortex), where the most drastic affect was observed in the prefrontal cortex of stressed animals [300]. Of interest, regions with stress-induced changes in 6mA significantly overlapped with depression-associated genes, indicating strong association between 6mA and neuropsychiatric disorders. Another study found that neurons specifically activated by extinction learning displayed an increased in both N6amt1 and 6mA [301]. Notably, this accumulation predominately occurred at synapse genes and genes known to be involved in learning and memory.

1.7.3. Disruption of DNA Methylation from Environmental Stressors

There are two major neurological pathways involved in stress response: The hypothalamic–pituitary–adrenal (HPA) axis (**Figure 1.7:A**) and the Mesolimbic Dopamine Reward pathway (**Figure 1.7:B**) that initiate different physiological processes in the brain to modulate stress response. Beginning with the HPA-axis, acute stressors will trigger a burst of cortisol into the blood stream allowing for an immediate and nearly involuntary response to the stressor. Whereas during chronic stress, the prolonged release and elevated levels of cortisol result in HPA-axis and stress response dysregulating. The brain regions primarily involved in the HPA response are the prefrontal cortex and the hippocampus, both of which are cognitive brain regions and known to be affected by stress and depression [302, 303]. However, cognitive symptoms are not observed in most depressed patients, suggesting that these brain regions may be more broadly involved in regulating emotional behaviors [304]. This also suggests that there are other neural circuits in the brain that may be more closely linked to the emotional behaviors observed in depressed patients, like the mesolimbic dopamine reward pathway. There have been several studies showing that chronic stress activates the ventral tegmental area-nucleus accumbens (VTA-NAc) dopamine neurons, affecting how the NAc then releases its own neurotransmitters (reviewed elsewhere: [304]). Dysregulation of the nucleus accumbens is known to induces depressive-like phenotypes such as anhedonia, motivational loss and abnormalities in appetite, sleep, energy and circadian rhythms, most of which are exhibited in depressed patients [305].

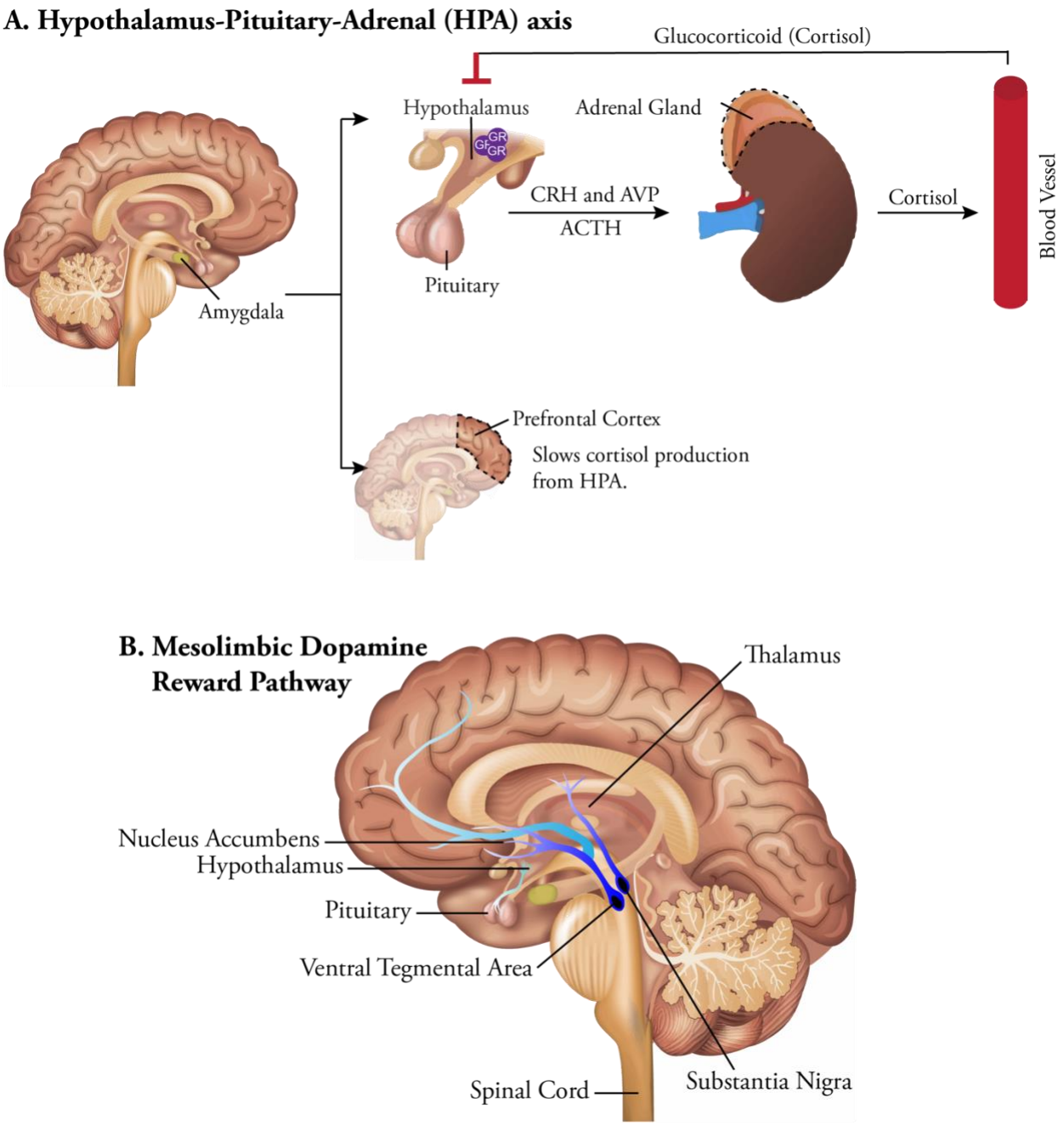

Figure 1.7: The Hypothalamic–Pituitary–Adrenal (HPA) Axis and Mesolimbic Dopamine Reward Pathways in Response to Stress

A. HPA-axis: The amygdala/hippocampus detects a stressor whether it is biological or emotional, provoking the HPA-axis to initiate the body's stress response signaling cascade. Neurons in the hypothalamus release corticotrophin-releasing hormone (CRH) and arginine vasopressin (AVP) stimulating the pituitary gland. The pituitary gland then releases adrenocorticotrophic hormone (ACTH) activating the adrenal gland on top of the kidneys. The adrenal gland releases the glucocorticoid hormone cortisol into the blood stream, activating additional downstream glucocorticoid receptors and their pathways. Elevated cortisol levels will induce a negative feedback loop to the hypothalamus where cortisol will bind to the glucocorticoid receptors and block further production of cortisol. Simultaneously, the amygdala signals to the prefrontal cortex to classify the stressor as life threatening or not. If classified as non-life threatening, the prefrontal cortex will signal the HPA-axis to attenuate its response. **B.** Mesolimbic Dopamine Reward Pathway: A collection of dopaminergic

neurons that project from the ventral tegmental area into various brain regions (shown in blue). The nucleus accumbens is one of the brain regions that receives the dopaminergic projects and is associated with the rewarding effects of food, sex and drugs of abuse [306, 307]. Images were modified from the following sources: https://www.thescienceofpsychotherapy.com/glossary/amygdala/; Bezdek et al. [308]; https://en.wikipedia.org/wiki/Dopaminergic_pathways.

Traumatic events experienced early in life are a major environmental risk factor for stress induced depression, and they have also been linked to global and loci-specific epigenetic aberrations that negatively impact the HPA-axis. Historically, some of the most renowned examples of stress-induced epigenetic changes are the Dutch famine study [282] and early maternal care/neglect [281]. Individuals that were exposed to prenatal malnutrition due to the Dutch famine have DMRs in growth and metabolic genes that have predisposed them to metabolic adversities such has increased cholesterol and BMI and poor glucose processing [282, 309]. Regarding early maternal care, offspring of low licking and grooming mothers had higher promoter methylation at the glucocorticoid receptor gene, affecting its expression levels and ability to shut down the HPA axis [281]. More recent studies have continued exploring the association between environmental stressors and epigenetic aberrations, providing a fuller picture of the role epigenetics plays in stress. Hypermethylation of the glucocorticoid receptor gene, NR3C1, has been observed in individuals with MDD [310] and known to have role in early life adversity [311]. In adolescent males, increased NR3C1 exon 1F methylation was associated with stressful experiences such as being bullied, lacking friends and internalizing symptoms, as assessed by a depression scale [312]. Polymorphisms in the glucocorticoid receptor co-chaperone protein, *FKBP5*, have also been associated with MDD. Interestingly, methylation of certain CpG sites in intron 7 significantly correlated with early life adversity in MDD patients (Farrell et al., 2018).

The corticotrophin-releasing hormone (CRH or CRF) is one of the primary HPA hormones released during stress response from hypothalamic neurons that is modulated by basal promoter methylation. Chronic social stress induced *Crf* promoter demethylation and a 3-fold increase in expression in stress susceptible animals, whereas stress resilient animals maintain basal levels of Crf expression and promoter methylation [313]. Moreover, increased blood corticosterone levels and anxiety-like behaviors due to hyper-active HPA signaling were also observed in animals with a conditional KO of Tet3 [314]. Additionally, Tet3 KO was also associated with a decrease in expression of the CRH receptor (Crhr2) and an enrichment in glucocorticoid signaling

pathway. Overall, evidence strongly supports that early life traumas can persist into adult hood predisposing the individual to depression and many negative health outcomes. Whether targeting HPA axis genes alone would be enough to improve stress induced depression, remains to be understood.

Chapter 2: 5-hydroxymethylcytosine is dynamically regulated during forebrain organoid development and aberrantly altered in Alzheimer's disease

This chapter is published as:
Kuehner, J.N., et al., *5-hydroxymethylcytosine is dynamically regulated during forebrain organoid development and aberrantly altered in Alzheimer's disease*. Cell Rep, 2021. 35(4): p.109042.

Author Contributions:
J.N.K., J.C., Z.W., J.Y. and B.Y. conceptualized and designed the experiments. **J.N.K.** and J.C. generated schematics and designed computational codes. **J.N.K.**, J.C., E.C.B., Y.L., Z.W., J.Y. and B.Y. wrote and revised the manuscript. **J.N.K.**, J.C., Y.L., L.C. and Z.L. performed computational analysis. Z.M. provided the control iPSC lines and C.M.H. provided the Alzheimer diseased iPSC lines that were used to generate the embryoid bodies and organoids. C.X. and Z.W. generated and provided the organoid cultures, and performed the organoid immunocytochemistry, Western Blot and ELISA assays. E.C.B. and F.W. performed the 5hmC-seq and RNA-seq studies. Z.W., J.Y. and B.Y. supervised all aspects of the project. All authors had the opportunity to discuss results and comment on the manuscript.

2.1. Summary

5-hydroxymethylcytosine (5hmC) undergoes dynamic changes during mammalian brain development, and its dysregulation is associated with Alzheimer's Disease (AD). The dynamics of 5hmC during early human brain development and how they contribute to AD pathologies, remain largely unexplored. We generate 5hmC and transcriptome profiles encompassing several developmental time points of healthy forebrain organoids and organoids derived from several familial AD patients. Stage-specific differentially hydroxymethylated regions demonstrate an acquisition or depletion of 5hmC modifications across development stages. Additionally, genes concomitantly increasing or decreasing in 5hmC and gene expression are enriched in neurobiological or early developmental processes, respectively. Importantly, our AD organoids corroborate cellular and molecular phenotypes previously observed in human AD brains. 5hmC is significantly altered in developmentally programmed 5hmC intragenic regions, in defined fetal histone marks and enhancers in AD organoids. These data suggest a highly coordinated molecular system that may be dysregulated in these early developing AD organoids.

2.2. Introduction

Epigenetics refers to heritable changes in gene expression without altering the DNA sequence through mechanisms such as DNA and histone modifications and non-coding RNAs. Mounting evidence implicates critical roles for DNA modifications, specifically 5-hydroxymethylcytosine (5hmC), in regulating brain development [315]. 5hmC emerged as a key DNA modification in the nervous system due to its significant enrichment in the brain [110] and its ability to regulate neuronal-specific gene expression during neural progenitor cell differentiation [316]. Due to the sample restraint, very few studies have investigated the 5hmC landscape during human early brain development spanning several developmental stages [317]. Previous studies that profiled 5hmC in human fetal brain tissues have lacked comprehensive genome wide coverage that expand beyond the coding regions of the genome [318]. Understanding the continuous dynamics of 5hmC throughout early brain development could reveal how crucial neurodevelopmental milestones are attained, and how failure to achieve these milestones could be detrimental to normal brain development and function, or even contribute to neurological diseases.

Genome-wide sequencing studies have suggested that abnormalities in 5hmC distribution and function could be critical factors contributing to Alzheimer's disease (AD) [268, 319]. AD is the most common neurodegenerative disease worldwide [320] and is characterized by extensive memory loss and cognitive impairments and the accumulation of β-amyloid plaques, phosphorylated Tau and neurofibrillary tangles [321]. Despite considerable efforts, the molecular mechanisms underlying AD pathogenesis remain elusive, especially before the onset of AD pathology and symptoms. Evidence suggests that long before the cognitive impairments of AD manifest, there are structural and functional brain defects [322, 323]; however, it is unknown whether alterations in DNA modifications have also manifested. Initial attempts to profile 5hmC in AD brains have revealed conflicting results due to differences between species (mouse vs. human), lack of comprehensive brain developmental time points and postmortem delay [254, 266]. Genome-wide and brain region-specific 5hmC profiling in late-stage mouse and postmortem AD samples have detected a global reduction in 5hmC as well as differentially hydroxymethylated regions (DhMRs) [268, 269]. These initial studies have laid the foreground for further investigation into how aberrations in the 5hmC landscape could contribute to AD pathology.

Transgenic mice and human postmortem brains have been leading models for studying the basic mechanisms and human specific features of late-stage AD, respectively. Another human specific model for AD is the 3-dimensional brain organoid derived from human iPSCs that recapitulates fetal brain development at the molecular level [324]. Brain organoids are an attractive model system for studying early development and neurological diseases as they I) can model disease progression spanning a comprehensive timeline, II) retain the complexity of a multicellular tissue/organ while being maintained in a cell culture-like environment [325] and III) can recapitulate human brain development in vitro [326]. Therefore, we generated 5hmC and transcriptome profiles encompassing several developmental time points of healthy forebrain organoids and organoids derived from several familial AD (fAD) patients. Our organoids are comparable to early human fetal brain development, spanning the 12-24 post-conception week period [324, 327]. Furthermore, they will allow us to obtain a comprehensive picture of 5hmC dynamics during early neural development and how aberrations in 5hmC might contribute to AD.

2.3. Results

2.3.1. Genome-wide profiling of 5hmC in forebrain organoids during early brain development

Forebrain organoids were cultured from a healthy iPSC line using miniature SpinΩ bioreactors [324] to study the dynamics of 5hmC during early brain development. We used embryoid body (EB) and forebrain organoids that had been cultured for 8 days (EBs), 56 days (D56), 84 days (D84) and 112 days (D112) (**Figure 2.1:A**) to model the early developing fetal brain. Using a 5hmC-selective chemical labeling method (hMe-Seal or 5hmC-seq) [131], we generated genome-wide 5hmC profiles from replicated samples at each of the organoid development time points. Our 5hmC and RNA-seq data showed high Pearson correlations (>0.9) and clustered together by principal component analysis (PCA), indicating sufficient reproducibility among multiple sample replicates (**Figure 2.2:A-F**). The different profiles of EBs compared to mature organoids occurs due to their distinct cellular composition [324].

Using the peak-calling tool MACS2, we observed that ~50% more 5hmC peaks were called in EBs compared to the later time points (**Figure 2.1:B**), which is in agreement with our global 5hmC dot blot and quantification analysis (**Figure 2.2:G** and **H**). In general, 5hmC is largely distributed in intronic and intergenic regions, specifically repetitive elements (**Figure 2.1:C** and **Figure 2.2:I**), and the proportion of 5hmC peaks in coding regions appeared to be relatively constant across all stages. Notably, the identified 5hmC regions do not appear to be the same regions retaining 5hmC peaks during development (**Figure 2.2:J**). Finally, enrichment analysis revealed that 5hmC peaks were enriched in intragenic regions and depleted in intergenic regions across the human genome (**Figure 2.1:D**), which is consistent with previous findings [125].

We next focused on the dynamic 5hmC patterns during organoid neurodevelopment. Average 5hmC read counts were plotted globally (**Figure 2.1:E, G, I** and **K**) and across gene bodies, promoters and intergenic regions (**Figure 2.2:A**). We observed that EBs have a distinct 5hmC pattern from the D56, D84 and D112 organoids, which were all comparable. For example, 5hmC is more enriched in the gene body and promoter region of ankyrin 1 (*ANK1*), a gene important for cellular proliferation, in EBs compared to the later developmental stages (**Figure 2.1:F**). Other neurodevelopmental specific genes such as *DRD2*, *NTRK1* and *TUBB2B* have stage-specific 5hmC enrichment in D56, D84 and D112 respectively (**Figure 2.1:H, J** and **L**).

Based on the data presented, we have shown that the 5hmC landscape is distinct from the multipotent EB stage to the neural-lineage committed developing organoid stages.

2.3.2. Dynamics of 5hmC regulation during forebrain organoid development

To investigate the detailed dynamics of 5hmC regulation during forebrain organoid development, we identified differentially hydroxymethylated regions (DhMRs) at each developmental stage. By comparing 5hmC peaks identified in D56 organoids with those from EB samples, we found this transition generated the most DhMRs (**Figure 2.3:A**). As the organoids became further differentiated, the number of established and disappearing DhMRs continued to decrease, but remained evenly distributed across all chromosomes (**Figure 2.4:A**). Given that a substantial amount of DhMR fluctuation occurs early in neurodevelopment, we identified stage-specific DhMRs (**Table 2.1:**and **Table 2.2:**). We observed a total of 101,907 stage-specific 5hmC enriched peaks (**Figure 2.3:B** and **Table 2.1:**). In the EB-specific 5hmC enriched peaks, functional analysis revealed that the annotated genes were largely within developmental genes such as *TNF* (**Figure 2.4:B**). Comparatively, stage-specific 5hmC peaks of the other 3 stages are enriched within genes critical for nervous system development and other neurobiological processes (e.g., *PAX6*, *AKT1* and *SNCA*) (**Figure 2.4:C-E**). Similar analyses were completed for stage-specific 5hmC depleted regions (**Figure 2.3:C** and **Table 2.2:**). Both the EB and D56-specific 5hmC depleted regions showed a reduction of 5hmC in key neurodevelopmental genes such as *NEUROG1* (**Figure 2.4:F**) and *GFAP* (**Figure 2.4:G**), suggesting that their expression may be specific to more mature neurodevelopmental stages. As expected, D84 and D112- specific 5hmC depleted regions were located in developmental genes such as *WNT10A* (**Figure 2.4:H**) and *FGFR1* (**Figure 2.4:I**), and involved in repressing multicellular organism development processes. Collectively, these findings support 5hmC as a critical epigenomic mark for brain development, especially during the differentiation of early nervous system structures to mature brain structures.

We next investigated DhMRs that showed continual 5hmC accumulation or depletion across the developmental stages, as these regions are more likely to be programmed and important for proper development (**Figure 2.3:D**). Among the total identified DhMRs, we found that 13,249 (13%) showed accumulation and 19,350 (19%) showed depletion in 5hmC levels (**Figure 2.4:J**), giving a total of 32,599

DhMRs of interest. Interestingly, DhMRs with continual 5hmC accumulation appeared to gradually gain 5hmC modifications during development (**Figure 2.3:E**), while DhMRs with continual 5hmC depletion show an instantaneous loss of 5hmC from the EB to other stages (**Figure 2.3:F**). This data suggests distinct dynamics for 5hmC acquisition versus 5hmC depletion throughout neuronal development.

Intragenic 5hmC is positively associated with gene expression [328], thus we further explored genes that harbored DhMRs with continual 5hmC accumulation or depletion and showed a continual increase or decrease in gene expression as determined by our RNA-seq data (**Figure 2.3:G**). We found 314 concomitantly increasing genes and 171 non-concomitantly increasing genes across the development stages (**Figure 2.4:K**). Using Gene Ontology (GO) analysis, we found that the 314 concomitantly increasing genes were enriched in neurodevelopmental processes, supporting the importance of 5hmC accumulation for proper brain development (**Figure 2.3:H**). These results were also confirmed using the Genomic Regions Enrichment of Annotations Tool (**Figure 2.4:N**). *SOX11*, a critical transcription factor in embryo and brain development [329], was identified among this group of genes (**Figure 2.3:J**). The 171 non-concomitantly increasing genes did not reveal any significant biological processes, potentially suggesting an indirect correlation with 5hmC and less relevance to neurodevelopment processes. Analysis of the continuously decreasing DhMRs revealed 601 concomitantly decreasing genes and 361 non-concomitantly decreasing genes across developmental stages (**Figure 2.4:L and M**). GO analyses showed that the 601 concomitantly decreasing genes were enriched in general developmental processes (**Figure 2.3:I** and **Figure 2.4:O**). The embryonic growth factor, *FGF8*, was identified among this group of genes and displayed enrichment that was restricted to the EB stage (**Figure 2.3:K**). Notably, the non-concomitantly decreasing genes were also enriched in neurobiological processes, but were more specifically involved in neuronal synapse processes (**Figure 2.4:M**). Overall, these data illustrate the synergism between 5hmC and gene expression during organoid development, where the continual regulation of 5hmC appears to strongly affect gene expression and foster proper neurodevelopment.

Recent studies have linked the presence of 5hmC at enhancer regions as a possible mechanism by which 5hmC promotes active gene expression [317]. We plotted all the 5hmC read counts from the developmental stages across all the fetal enhancer regions [330] to investigate their correlation. As the organoids

aged, higher 5hmC read counts were observed in fetal enhancer regions (**Figure 2.3:L**), further supporting a key role of 5hmC in gene regulation. Next, we wanted to consider the histone profile of enhancer regions that harbored either continuously increasing or decreasing 5hmC DhMRs to characterize the 5hmC-histone crosstalk at these enhancer regions. Interestingly, enhancer regions overlapped with DhMRs showing 5hmC accumulation (**Figure 2.3:M**, 4,222) were poised (enriched with H3K4me1), and may later become active as the accumulation of 5hmC is known to facilitate an accessible chromatin environment [331]. On the other hand, enhancers regions overlapped with DhMRs with continual 5hmC depletion (**Figure 2.4:N**, 751) were active (enriched with H3K27ac) and could become inactivated later during development as 5hmC levels continued decreasing. Collectively, these findings suggest that the level of 5hmC at enhancer regions could affect their ability to distally regulate their target genes.

2.3.3. Alzheimer's disease forebrain organoids recapitulate hallmark AD pathologies

We generated forebrain organoids from four fAD iPSC lines (AD-01: *PSEN1* Y155H; AD-02: *PSEN1* M139V; AD-03: *PSEN1* intron 4 deletion; AD-04: *APP* V717I) and three healthy controls (C-03, C-09, C-21). To confirm that our AD organoids recapitulated hallmark pathologies observed in the brain of AD patients, we performed immunofluorescence staining of phosphorylated Tau proteins and amyloid-beta (Aβ) aggregates on organoids cultured for 84 days (**Figure 2.5:A** and **B**). Consistent with previous findings [332], we found that both phosphorylated Tau proteins and Aβ aggregates were significantly increased in all AD organoid lines compared to controls. Immunoblotting and quantification revealed a 3-fold increase of phosphorylated Tau in AD organoids (**Figure 2.5:C**). Accumulation of Aβ-40 and Aβ-42 peptides are associated with AD pathogenesis, and our AD organoids showed significant enrichment of both peptides individually as measured by an ELISA assay (**Figure 2.5:D**).

To further investigate the genome-wide 5hmC alterations in AD human organoids, three organoid lines carrying fAD risk mutations (AD-01: *PSEN1* Y155H; AD-03: *PSEN1* intron 4 deletion; AD-04: *APP* V717I) and three control (C-03, C-09, C-21) lines were harvested at 84 days for 5hmC-seq profiling (**Figure 2.1:A**). The 5hmC-seq and RNA-seq data were of high quality, showing high Pearson correlations (>0.8) among replicates (**Figure 2.6:A** and **B**). Significantly, both our computational and experimental data revealed a global

reduction of 5hmC in AD organoids compared to their controls (**Figure 2.5:E-G**), which is consistent with previous studies using AD models [332]. Interestingly, despite the observed global 5hmC reduction, the overall distribution of the proportion of 5hmC enriched peaks at intra- and intergenic regions remained comparable, except at enhancer regions where the proportion of 5hmC enriched peaks increased from 20.5% in controls to 22.4% in AD organoids (**Figure 2.5:H**). Collectively, our AD organoids recapitulate human AD pathologies and known epigenomic signatures, validating them as an appropriate model system to study AD.

2.3.4. 5hmC is globally altered in Alzheimer's disease organoids

Using the same peak calling and DhMR identification approach described in **Figure 2.3:A**, overlapping 5hmC regions in 3 independent AD and control lines were first identified. We found a total of 67,466 common peaks across control organoids and 59,632 common peaks in the AD organoids. These overlapping 5hmC regions were then used to identify AD-specific DhMRs, where 9,428 AD-specific enriched DhMRs and 16,362 AD-specific depleted DhMRs were found (**Figure 2.7:A** and **B** and **Figure 2.8:A** and **B**). Given that 5hmC has been linked to gene expression [328], we analyzed the differential gene expression patterns between control and AD organoids using our RNA-seq data (**Figure 2.7:C**). Numerous neurodevelopmental genes and AD risk genes were identified amongst these differentially expressed genes (**Figure 2.8:B**). To ensure these findings were not due to changes in cell composition, we performed cellular deconvolution analysis using MuSiC [333]. No substantial changes in the estimated cellular proportions were observed (**Figure 2.8:C**). These findings suggest that in organoids derived from fAD patients, a reduction in 5hmC levels could consequently initiate subtle alterations in the early neuronal gene expression profile.

To further investigate how a reduction of 5hmC in AD organoids could reshape the gene expression profile, we annotated all of the AD-specific enriched or depleted DhMRs (**Figure 2.7:A** and **B**) to their respective genes. Of the AD-enriched DhMRs, we identified 676 genes that showed an increase in gene expression and enrichments exclusively in neurodevelopmental pathways (**Figure 2.7:D** and **Figure 2.8:D**). *GRIN3A*, which encodes a NMDA receptor subunit of a glutamate-gated ion channel (**Figure 2.7:F**) was found among this group of genes. On the other hand, 463 genes showing decreased expression were enriched in basic developmental process, although most of the terms were not found to be significant (**Figure 2.8:D**

and **E**). Investigation of the AD-depleted DhMRs revealed 1,172 genes with simultaneous decreasing gene expression (**Figure 2.7:E**) and 1,379 genes showing an increase in expression (**Figure 2.8:G** and **F**). The genes in both these groups were largely enriched in basic developmental process, like the centromere gene *CENPO* (**Figure 2.7:G**). Our data suggests that genes displaying increases of 5hmC and expression in AD organoids are enriched in neurodevelopmental process. On the other hand, irrespective of the impact on gene expression, the regions were 5hmC was lost are predominately occurring in genes that regulate basic developmental process. Interestingly, we found 17 AD risk genes previously identified from GWAS studies that contained at least one DhMR in our AD organoids (**Figure 2.8:H**). Taken together, these findings are reflective of the sophisticated nature of neurodevelopment and support that AD-specific 5hmC changes that are occurring early in development may cause subtle disruptions in the neuronal network that could contribute to the onset of AD later in life.

To determine how the loss of 5hmC in AD organoids could impact organoid development, we overlapped our AD-specific DhMRs with our continuously increasing (**Figure 2.7:H**) and decreasing regions (**Figure 2.7:J**) previously identified in Figure 2D. The combined AD-specific DhMRs that overlapped with continuously increasing DhMRs (n = 1,083) were also enriched in neurobiological processes (**Figure 2.7:I**). Similarly, the combined AD-specific DhMRs that overlapped with continuously decreasing DhMRs (n = 588) were enriched in early development process (**Figure 2.7:K**). Collectively, these data indicate that the dysregulation of 5hmC modifications found in fAD organoids could affect structural brain development as early as fetal development.

Given that cross talk between different epigenomic mechanisms can impact gene expression, we sought to understand how various histone marks may be affected by aberrant 5hmC levels in AD organoids. The Jaccard index [334] was used to quantify the overlap between our AD-specific DhMRs with published fetal brain histone marks [335, 336] (**Figure 2.7:L**). Interestingly, the Jaccard index between AD-depleted DhMRs and the active histone mark H3K4me3 showed the highest enrichment, suggesting that 5hmC depletion is more likely to orchestrate the presence of H3K4me3 to co-regulate gene expression. AD-enriched DhMRs appear to moderately overlap with the active enhancer marks H3K27ac and H3K4me1, which may indicate 5hmC

alterations in AD organoids could also affect the identity and activity of these enhancer regions. We next performed a similar analysis on the AD-specific DhMRs that was described for **Figure 2.3:M** and **N**. The common regions between fetal brain enhancers and AD-specific DhMRs appear to be more enriched with the active histone marks H3K27ac and H3K4me3, again suggesting that change of 5hmC in AD organoids could influence active enhancer activities (**Figure 2.7:M**). These observations indicate that altered 5hmC in our AD organoids could have multifaceted epigenomic roles such as directly modulating transcription, influencing histone marks and determining enhancer activities and identities.

Several recent studies have revealed strong 5hmC alteration in human postmortem brains of late-onset AD (**Table 2.3:**). However, whether these alterations have already occurred in early brain development remain unexplored. To that end, we compared the DhMRs identified from our AD organoid model with those from five published postmortem AD brains [261, 337-340] and found very little DhMR overlap between our early developing AD organoids and those from postmortem AD brain samples. On the other hand, a recent paper profiled DNA cytosine modifications in early and late onset AD using cultured, patient derived iPSCs differentiated into 2D cortical neurons [341]. We found 37-760 times more overlapping DhMRs between our AD-specific DhMRs and the 2D neurons derived from another fAD patient line (*PSEN1* mutation L286V) (**Table 2.3:)**. Many genes associated with these common DhMRs were also associated with key neurodevelopmental process. Overall, these findings provide conserved 5hmC alterations in two early AD models that could be further explored for mechanistic relevance in AD pathology.

2.4. Discussion

2.4.1. 5hmC Acquisition and Depletion in Coding and Non-coding Regions During Neurodevelopment

Our analyses support different dynamics for 5hmC acquisition versus 5hmC depletion throughout neuronal development. 5hmC modifications that showed a continuous enrichment throughout development did so in a more gradual manner. The steady accumulation of 5hmC could be important to promote neuronal maturation and thus brain development. On the contrary, 5hmC that showed a continuous depletion trend throughout development declined more rapidly from the pluripotent embryoid body stage to the neuronally-differentiated D56 stage, which may be required to commence the transitions between developmental stages.

In fact, when we examined the subset of concomitantly increasing genes (**Figure 2.3:H**), they were strongly represented in genes associated with general neurodevelopment processes, whereas concomitantly decreasing genes (**Figure 2.3:I**) were largely enriched in general development and proliferative processes. Interestingly, non-concomitantly decreasing genes were strongly represented in highly specified neuronal processes, like synapse development and function (**Figure 2.4:O**). From this, one could infer that 5hmC acquisition may have a role in overall neuronal architecture and morphology, while 5hmC depletion may be more involved in "fine-tuning" neuronal functions and transitioning away from undifferentiated stages and more towards neuronally committed lineages.

In the context of the central nervous system, our understanding of the relationship between 5hmC and enhancer regions is still premature. Crosstalk of 5hmC with other epigenetic modifications, like histone marks, can modulate the chromatin architecture and ultimately regulate gene expression [331]. We found that 5hmC was more strongly associated with enhancer regions in the developing organoids than it was in the undifferentiated embryoid bodies. When we specifically looked at DhMRs that continued to increase or decrease in 5hmC, these regions associated with poised or active enhancer regions, respectively, implying a role for 5hmC in promoting cell differentiation through its relationship with enhancers to upregulate cell-type specific differentiating genes [342]. Collectively, both pieces of data support the underappreciated importance of 5hmC regulation in non-coding and enhancer regions to induce neuronal-specific gene regulation during early fetal brain development.

2.4.2. Forebrain Organoid Model of Alzheimer's Disease and the Impact of 5hmC Global Alterations

In forebrain organoids derived from fAD patients carrying various *PSEN1* mutations or an APP mutation, we demonstrated at the cellular level that our AD organoids recapitulate hallmarks of human AD pathology, despite being reminiscent of fetal brain stages between 12-24 post-conception weeks [324]. Pluripotent stem cell derived models better recapitulate the structure and function of fetal tissues compared to their adult tissues [325], making them the earliest human model to study early neurodevelopment. These findings validate the use of AD forebrain organoids as a promising AD model.

In our study, we found a significant global reduction of 5hmC in the AD organoids compared to control. Although, we identified nearly 2-times fewer AD-enriched DhMRs compared to AD-depleted DhMRs, ectopic enrichment of 5hmC associated with increased gene expression specifically affected neurodevelopmental process. In support of this, we identified numerous critical neurodevelopmental genes and AD risk genes that were primarily upregulated in AD organoids. Regions that became ectopically depleted for 5hmC were involved in regulating basic developmental process irrespective of how their expression patterns changed. Noticeably, our RNA-seq data revealed that 56.7% of the dysregulated genes were inappropriately upregulated, despite the significant global 5hmC reduction we observed in the AD organoids. One possibility could be the increased proportion of 5hmC being distributed to enhancer regions that was observed only in AD organoids. Interestingly, we also found that enhancer regions overlapped with our AD-specific DhMRs were enriched for both active and poised enhancer histone marks. This speaks to a mechanism whereby these subtle 5hmC alterations during early brain development might not result in structural damage, but could affect the delicate neuronal networks making the AD-predisposed brain more vulnerable to AD pathogenesis. These findings collectively support that aberrant 5hmC dynamics disrupt the timing of neurodevelopment in the fetal brain carrying fAD risk mutations.

2.5. Figures and Figure Legends

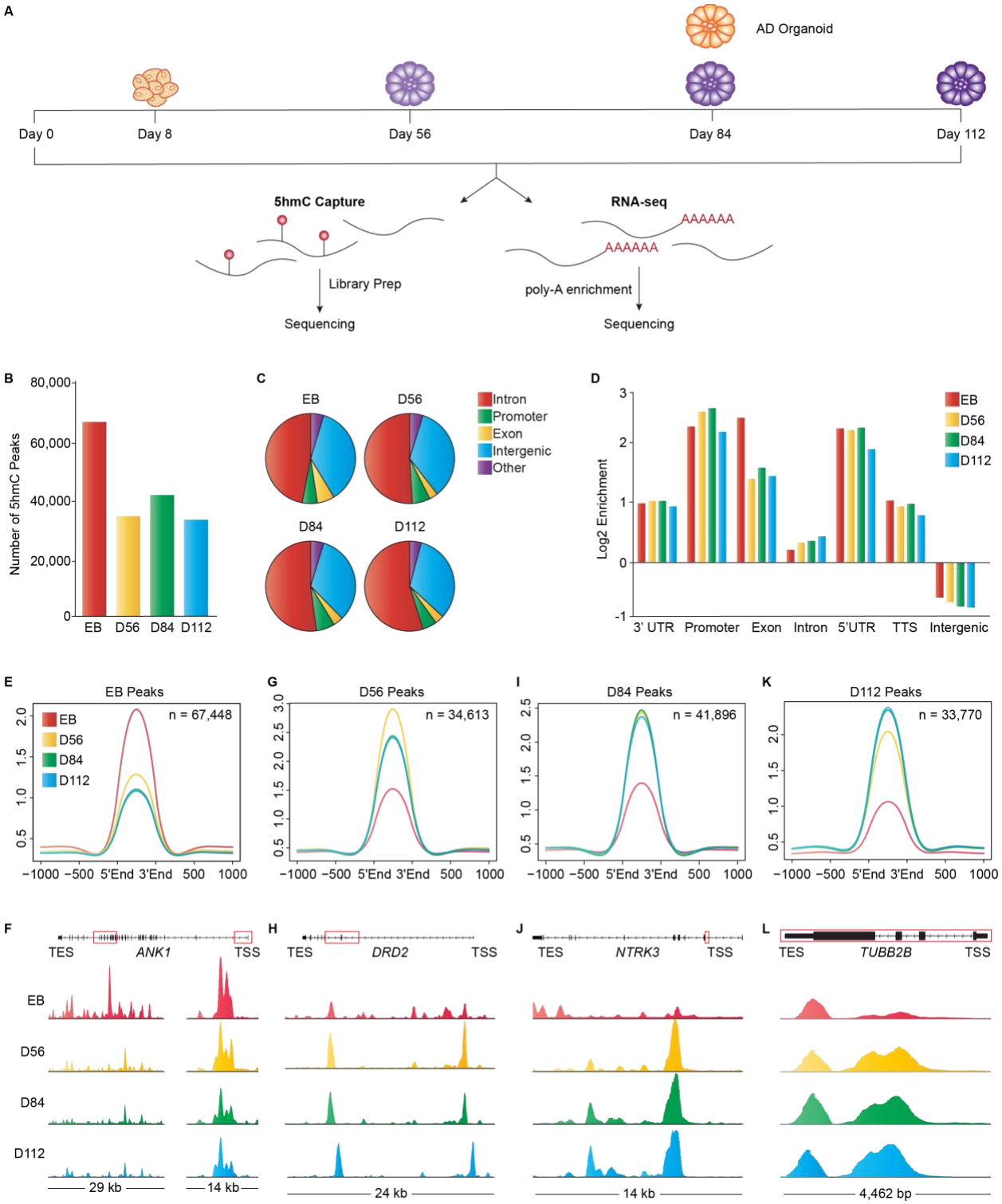

Figure 2.1: Genome-wide profiling of 5hmC in forebrain organoids during development

A. Schematic of the collection time points of forebrain organoids derived from controls and patients with Alzheimer's disease (AD) for genome-wide 5hmC and RNA sequencing: day 8 embryoid bodies (EBs), day 56 (D56), day 84 (D84) day 112 (D112) and AD organoid at day 84. **B.** Number of 5hmC peaks identified across

developmental stages. **C.** Distribution of 5hmC peaks across genomic features in the human genome. **D.** Enrichment of 5hmC peaks at 3' and 5' untranslated region (3'UTR and 5'UTR), promoters, exons, introns, transcription termination site (TTS) and intergenic regions. **E, G, I** and **K**. Average normalized 5hmC read counts across 5hmC peaks for EBs (**E**), D56 (**G**), D84 (**I**), and D112 (**K**). **F, H, J** and **L**. Normalized 5hmC counts at peak regions identified in ANK1 (**F**), DRD2 (**H**), NTRK3 (**J**) and TUBB2B (**L**) in forebrain organoids across developmental stages. Red box indicates where on the gene the displayed peak region(s) originated.

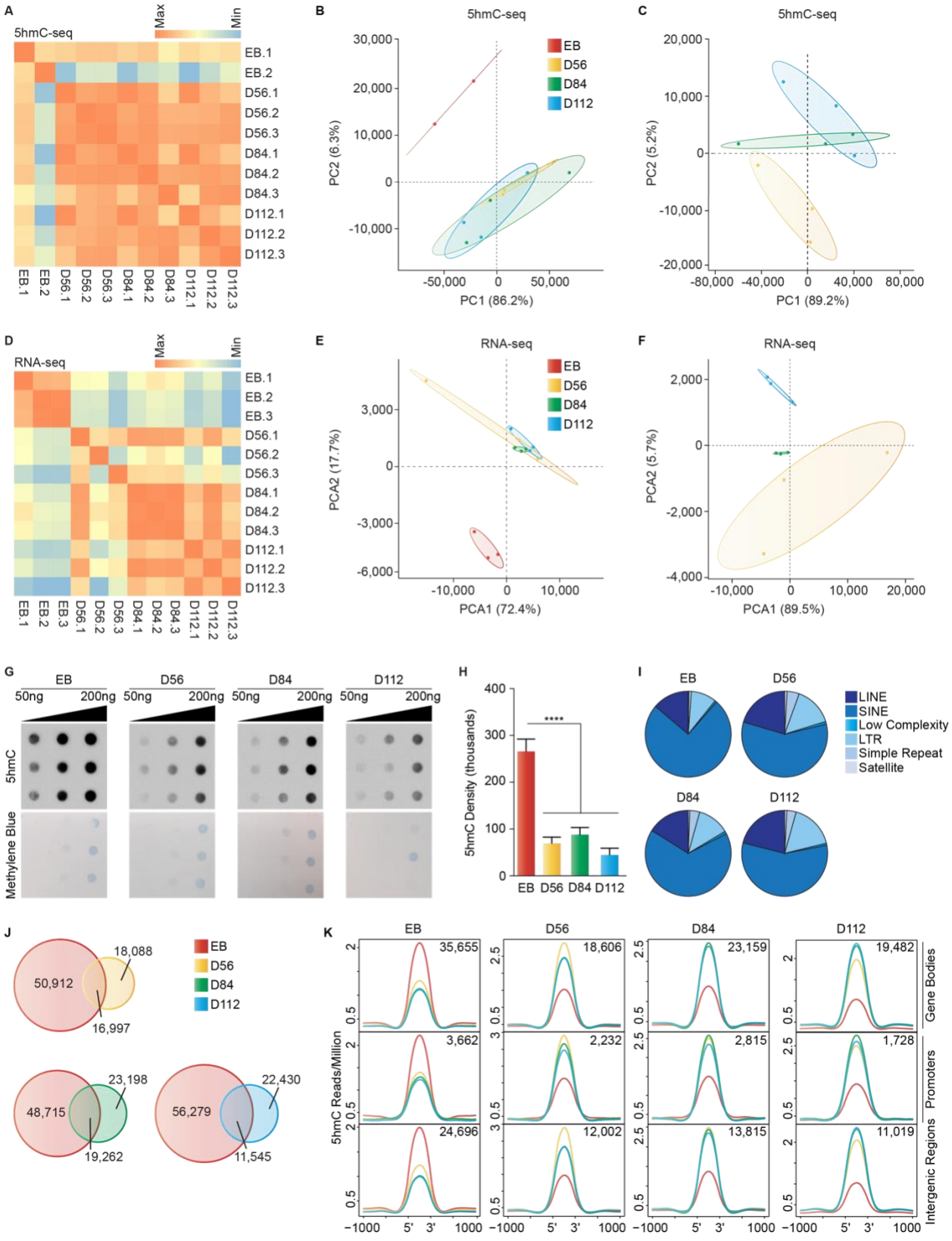

Figure 2.2: Validation of 5hmC in forebrain organoids during development

A and **D**. Correlation heat map of normalized read counts of all organoid samples with 5hmC-seq (**A**) and RNA- seq (**D**) data of forebrain organoids. **B** and **C.** Clustering of organoid samples by principal component analysis (PCA) using 5hmC-seq data with (**B**) and without (**C**) embryoid bodies. **E** and **F.** Clustering of organoid samples by PCA using RNA- seq data with (**E**) and without (**F**) embryoid bodies. **G.** Dot blot using a 5hmC-specific antibody showing whole organoid 5hmC enrichment (top). Methylene blue staining confirms equal concentrations of DNA were loaded per sample (bottom). **H.** Quantification of 5hmC dot blot, where EB organoids have significantly more 5hmC compared to other stages (One-way ANOVA; p-value < 0.0001). **I.** Distribution of 5hmC peaks across intergenic features: long interspersed nuclear element (LINE), short interspersed nuclear element (SINE), long terminal repeats (LTR), low complexity, simple repeat, and satellite. **J.** Number of stage-specific and shared 5hmC peaks between embryoid bodies and organoids: D56 (top left), D84 (bottom left) and D112 (bottom right). **K.** Average 5hmC read counts at 5hmC peaks identified per stage, with respect to gene bodies, promoters and intergenic regions

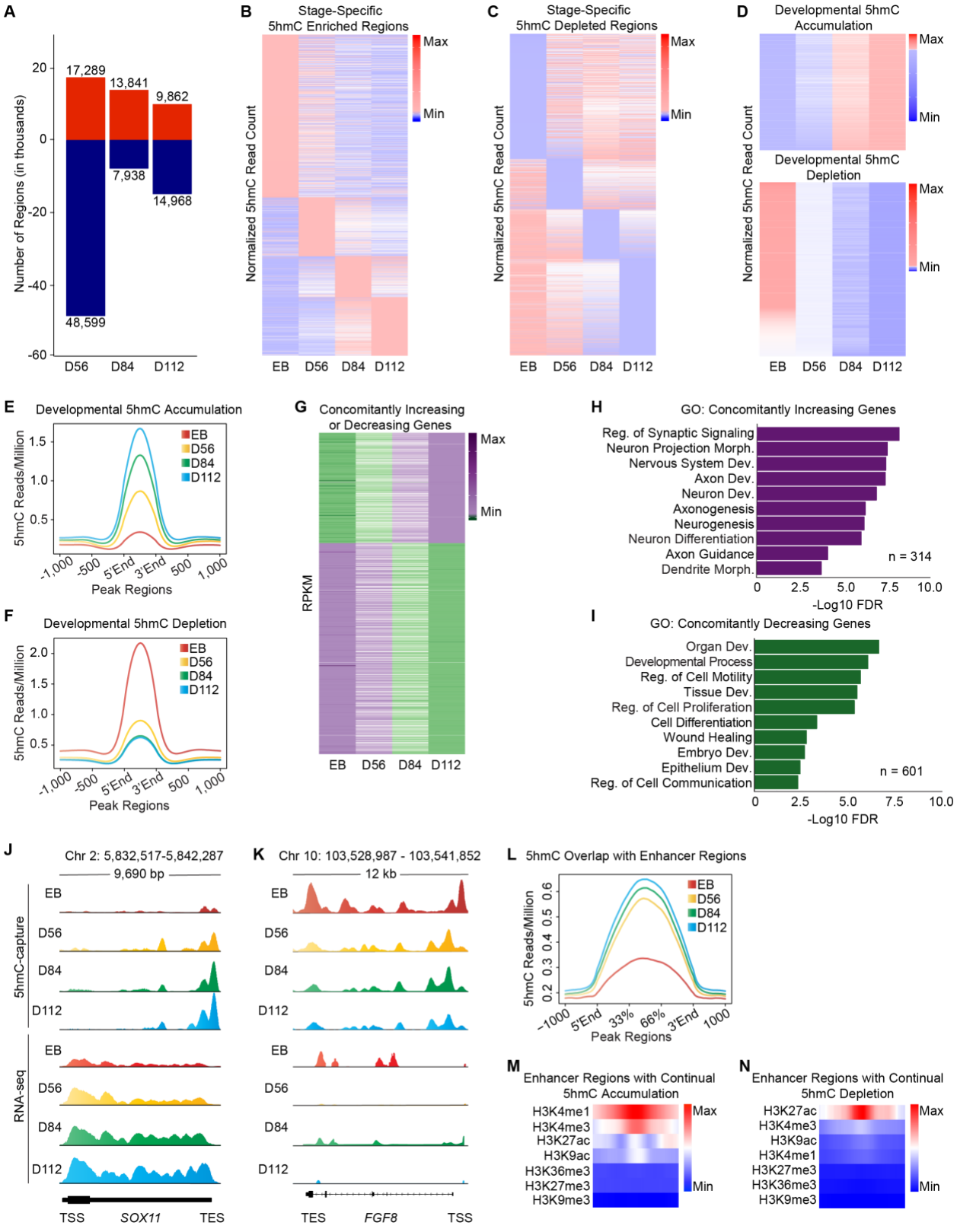

Figure 2.3: Dynamics of 5hmC regulation during forebrain organoid development

A. Number of established and disappeared 5hmC peaks at D56, D84, and D112. **B, C** and **D**. Heat maps of developmental stage specific DhMRs, where the color scale represents normalized 5hmC read counts. (**B**)

DhMRs that were enriched in developmental stages and (**C**) DhMRs that were depleted in developmental stages. (**D**) DhMRs with continual 5hmC accumulation (top) and continual 5hmC depletion (bottom) during organoid development. **E** and **F**. Average normalized 5hmC read counts per stage with continual 5hmC accumulation (**E**) and continual 5hmC depletion (**F**). G. Heat map of RPKM (reads per kilobase-per-million) for genes that concomitantly increase in 5hmC and gene expression (top) or concomitantly decrease in 5hmC and gene expression (bottom). **H** and **I.** Gene ontology (GO) analysis of the genes that concomitantly increase in 5hmC and gene expression (**H**) and concomitantly decrease in 5hmC and gene expression (**I**). Reg.: Regulation; Dev.: Development; Morph.: Morphogenesis. **J** and **K.** Normalized 5hmC read count and transcriptome across the concomitantly increasing SOX11 gene (**J**) or the concomitantly decreasing FGF8 gene (**K**). L. Average normalized 5hmC read counts per stage across enhancer regions. **M** and **N.** Enrichment of histone modifications at enhancer regions from fetal brains overlapped with DhMRs that continually accumulated (**M**) or lost (**N**) 5hmC.

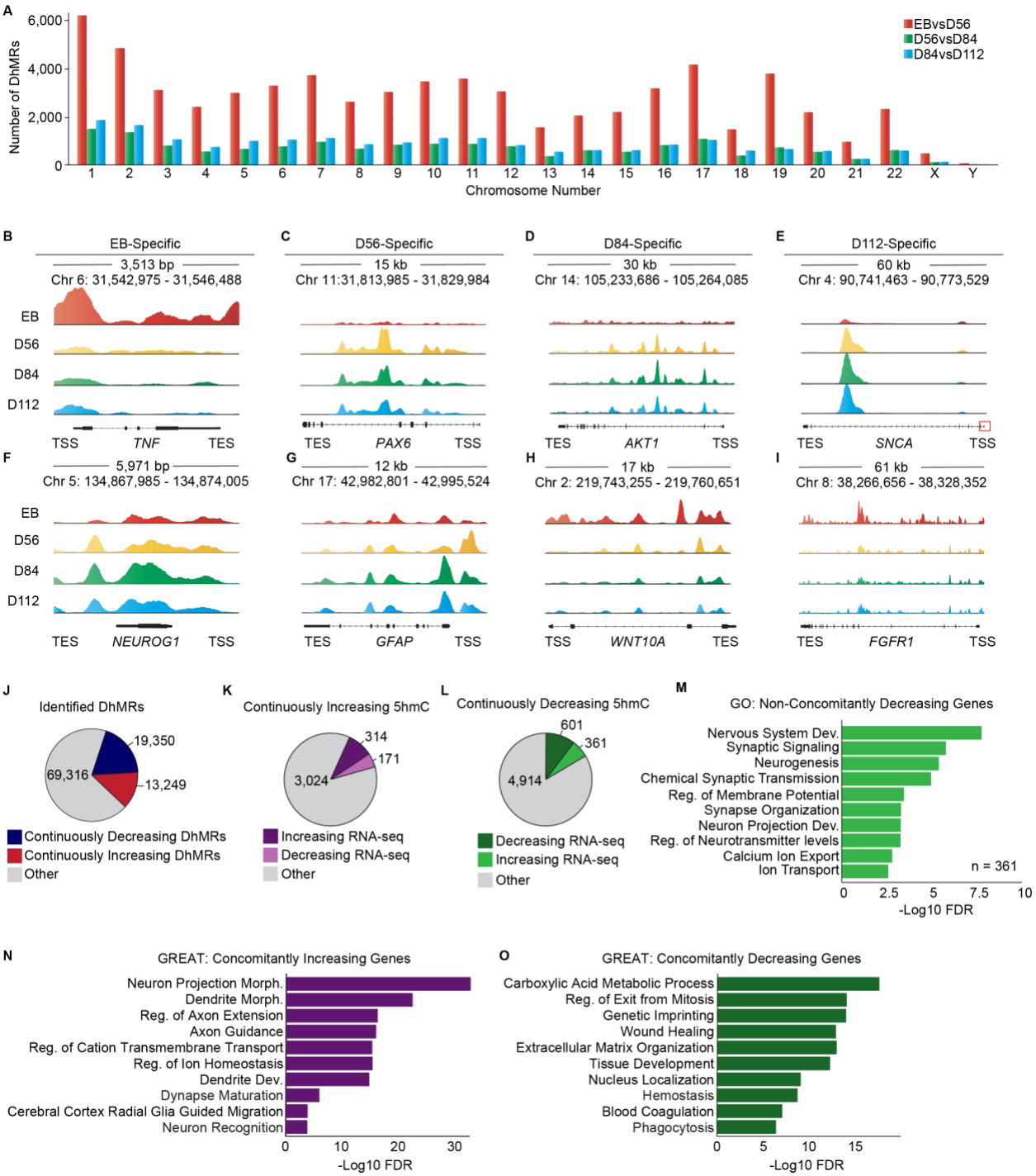

Figure 2.4: DhMR distribution observed in forebrain organoids across development

A. Number of stage-specific DhMRs at each chromosome. **B-I** Normalized 5hmC read counts per stage at stage-specific enriched (**B-E**) and depleted (**F-I**) 5hmC regions in forebrain organoids. Red box indicates where on the gene the displayed peak region originated from. **J.** Number of DhMRs identified that continuously increased or decreased in 5hmC levels. **K.** Number of concomitantly increasing (dark purple) and non-concomitantly decreasing (light purple) DhMRs. **L.** Number of concomitantly decreasing (dark green) and non-concomitantly increasing (light green) DhMRs. **M.** GO analysis results for genes with non-concomitantly decreasing DhMRs. Dev.: Development; Reg.: Regulation. **N** and **O.** Genomic Regions Enrichment of

Annotations Tool (GREAT) analysis of the concomitantly increasing (**N**) or concomitantly decreasing (**O**) DhMRs. Dev.: Development; Reg.: Regulation; Morph.: Morphogenesis.

Table 2.1: Number of stage-specific enriched DhMRs and annotated genes
Several of the most significant biological processes for each DhMR group is also provided.

	Num of Enriched DhMRs	Num of Genes	Biological Processes (-log 10 FDR)
EB	39,671	7,454	Anatomical Structure Development (24.7
			Multicellular Organism Development (23.2)
			System Development (20.5)
			Cell Differentiation (15.5)
D56	16,068	5,195	Nervous System Development (42.9)
			Cell Projection Organization (41.2)
			Neurogenesis (35.6)
			Neuron Differentiation (25.4)
D84	15,711	5,224	Nervous System Development (32.2)
			Developmental Process (30.8)
			Neurogenesis (29.3)
			Regulation of Signaling (28.7)
D112	30,457	8,224	Nervous System Development (31.3)
			Neurogenesis (27.9)
			Generation of Neurons (27.9)
			Regulation of Signaling (23.2)

Table 2.2: Number of stage-specific depleted DhMRs and annotated genes
Several of the most significant biological processes for each DhMR group is also provided.

	Num of Depleted DhMRs	Num of Genes	Biological Processes (-log 10 FDR)
EB	51,647	11,098	Nervous System Development (32.9)
			Detection of Stimulus (32.4)
			Neurogenesis (27.8)
			Generation of Neurons (26.3)
D56	18,690	4,517	Neurogenesis (27.6)
			Generation of Neurons (26.5)
			Nervous System Development (26.3)
			Detection of Stimulus (26.2)
D84	12,912	4,147	Multicellular Organism Development (26.5)
			Nervous System Development (20.5)
			Cell Development (18.8)
			Neurogenesis (17.3)
D112	18,666	4,505	Developmental Process (26.5)
			Multicellular Organism Development (25.3)
			Cell Differentiation (17.7)
			Nervous System Development (16.7)

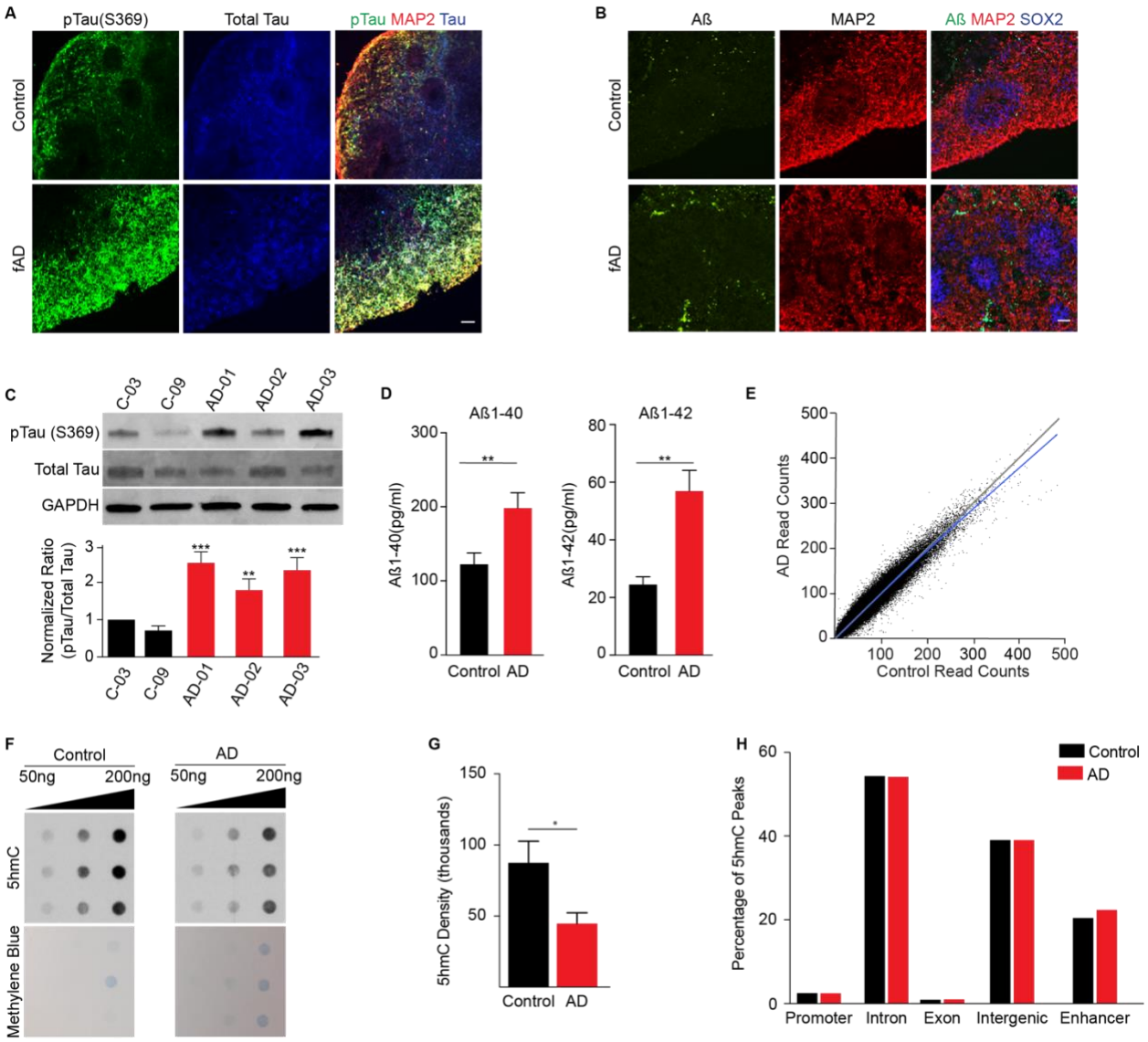

Figure 2.5: Alzheimer's organoids recapitulate hallmark pathologies of human Alzheimer's disease brains

A. Representative phosphorylated Tau immunostaining of fAD organoids at day 84 and controls. **B.** Representative amyloid beta (Aβ) immunostaining of fAD organoids at day 84 and controls. **C.** Immunoblot of phosphorylated and total Tau protein derived from independent control organoid lines (n=2 biological replicates done in triplicate) and independent fAD patient organoid lines (n=3 biological replicates done in triplicate) (*p-value < 0.05, ** p-value < 0.01, *** p-value < 0.001, unpaired t-test, data are represented as mean ± SEM). **D.** ELISA assay quantification of Aβ1-40 and Aβ1-42 peptide levels control and fAD organoids (**p-value < 0.01, unpaired t-test, n=3, biological replicates, data are represented as mean ± SEM). **E.** Average normalized 5hmC read counts across the whole genome show that 5hmC is significantly depleted (p-value = 2.513 x10-7 by unpaired t-test) in AD versus control organoids. **F.** 5hmC dot blot showing whole organoid 5hmC enrichment in controls versus AD organoids at day 84 (top). Methylene blue staining confirms equal amounts of DNA were loaded per sample (bottom). **G**. Quantification of 5hmC dot blot in controls and AD organoids (p-value < 0.05, unpaired t-test, n=3 biological replicates, data are represented as mean ± SEM). **H.** Proportions of 5hmC peaks across genomic features in control and AD organoids.

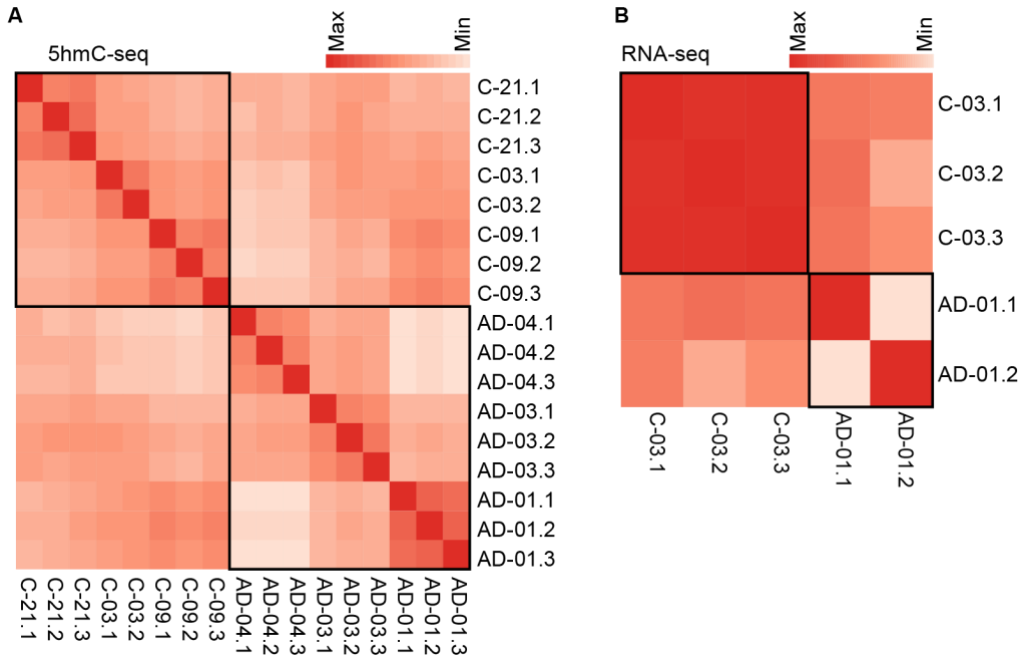

Figure 2.6: Distinctive genome-wide 5hmC profiling between healthy control- and AD patient-derived organoids

A and **B.** Correlation heat map of normalized read counts of 5hmC-seq (**A**) and RNA-seq (**B**) of control and AD forebrain organoids.

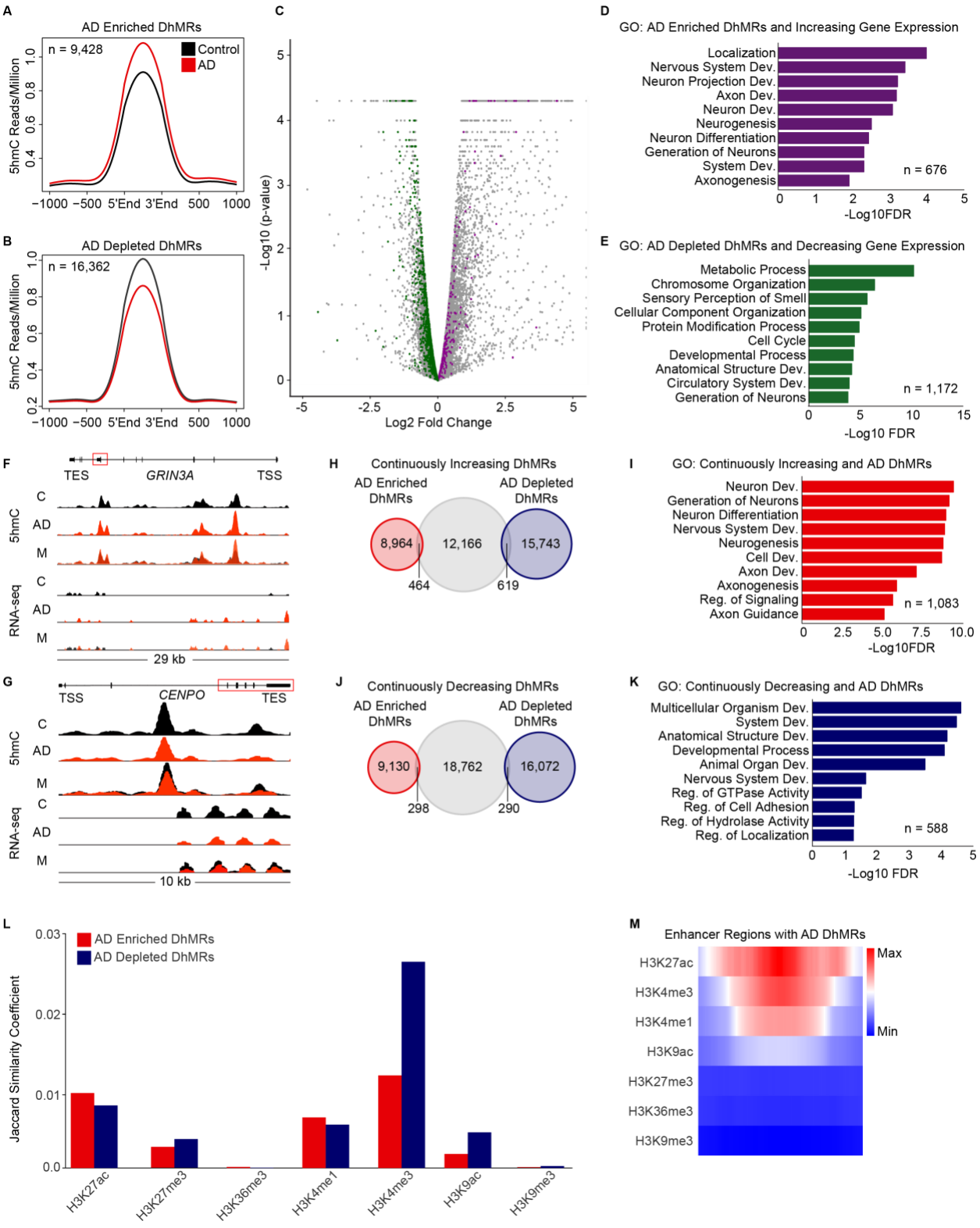

Figure 2.7: Aberrant alteration of 5hmC in Alzheimer's Organoids

A and **B.** Average normalized 5hmC read counts at AD enriched and AD depleted DhMRs. **C.** Differentially expressed genes (n = 7,976 down regulated genes and n = 10,458 up regulated genes in AD organoids). Green dots: AD depleted DhMRs with decreasing gene expression, Purple dots: AD enriched DhMRs with increasing

gene expression. **D** and **E.** Gene ontology analysis of genes annotated to AD enriched DhMRs with increasing gene expression (**D**) and AD depleted DhMRs with decreasing gene expression (**E**) in AD organoids. Dev.: Development. **F** and **G.** Normalized 5hmC read counts and transcriptome of GRIN3A, which depicts AD enriched DhMRs with increasing gene expression (**F**) or CENPO, which depicts AD depleted DhMRs with decreasing gene expression (**G**). Red box indicates where on the gene the displayed peak region(s) originated from. C: control, M; merge. **H-K**. Venn diagrams and corresponding gene ontology analysis results with respect to overlapped AD enriched and depleted DhMRs and continual 5hmC accumulation (**H** and **I**) or continual 5hmC depletion (**J** and **K**) during development. Dev.: Development; Reg.: Regulation. **L.** AD-depleted DhMRs are most similar with H3K4me3 regions, whereas AD-enriched DhMRs are most similar to H3K27ac and H3K4me1. **M.** Enrichment of fetal brain histone modifications in the overlapped regions between fetal brain enhancer regions and AD-specific DhMRs (n = 3,688 enhancers).

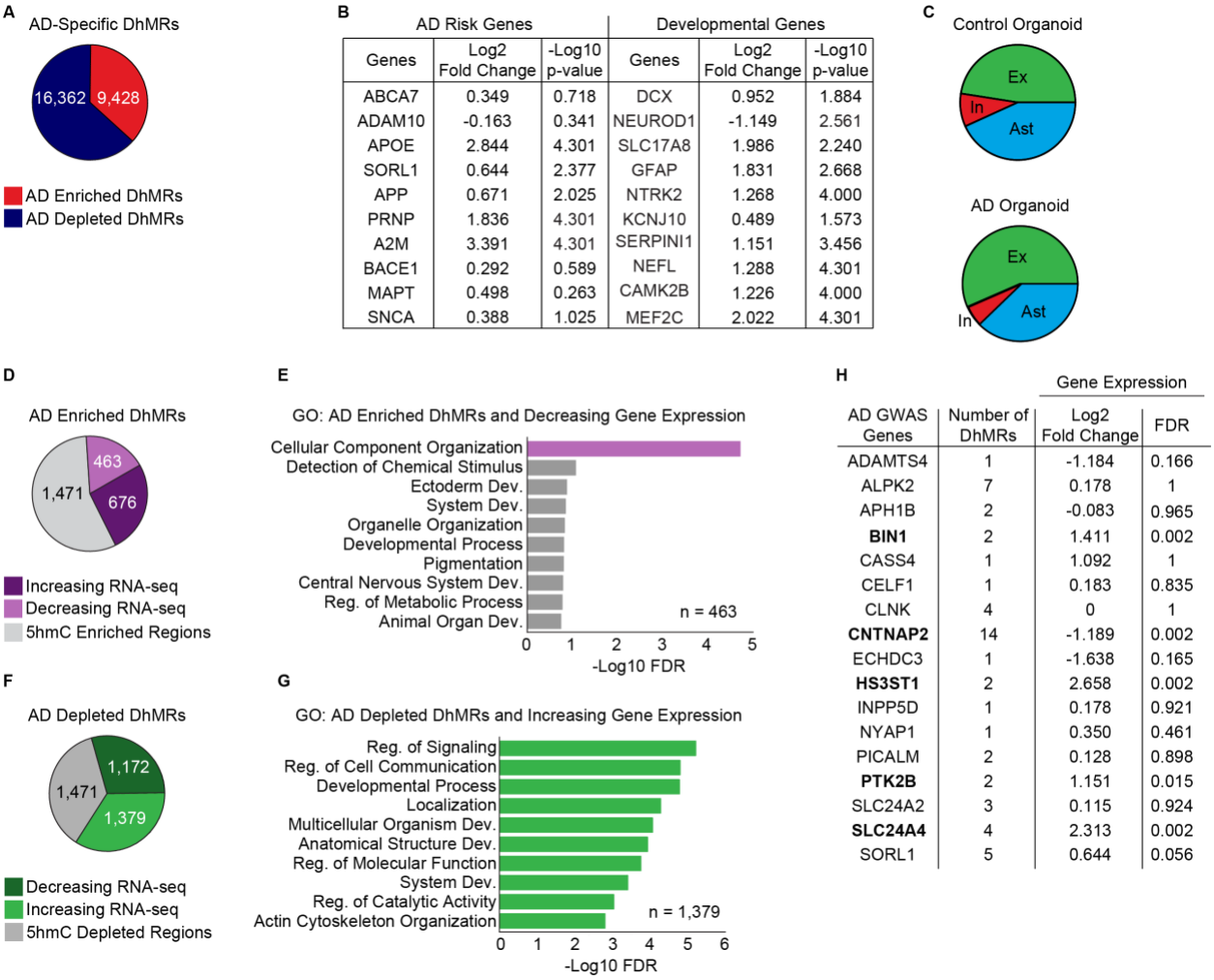

AD Risk Genes			Developmental Genes		
Genes	Log2 Fold Change	-Log10 p-value	Genes	Log2 Fold Change	-Log10 p-value
ABCA7	0.349	0.718	DCX	0.952	1.884
ADAM10	-0.163	0.341	NEUROD1	-1.149	2.561
APOE	2.844	4.301	SLC17A8	1.986	2.240
SORL1	0.644	2.377	GFAP	1.831	2.668
APP	0.671	2.025	NTRK2	1.268	4.000
PRNP	1.836	4.301	KCNJ10	0.489	1.573
A2M	3.391	4.301	SERPINI1	1.151	3.456
BACE1	0.292	0.589	NEFL	1.288	4.301
MAPT	0.498	0.263	CAMK2B	1.226	4.000
SNCA	0.388	1.025	MEF2C	2.022	4.301

		Gene Expression	
AD GWAS Genes	Number of DhMRs	Log2 Fold Change	FDR
ADAMTS4	1	-1.184	0.166
ALPK2	7	0.178	1
APH1B	2	-0.083	0.965
BIN1	2	1.411	0.002
CASS4	1	1.092	1
CELF1	1	0.183	0.835
CLNK	4	0	1
CNTNAP2	14	-1.189	0.002
ECHDC3	1	-1.638	0.165
HS3ST1	2	2.658	0.002
INPP5D	1	0.178	0.921
NYAP1	1	0.350	0.461
PICALM	2	0.128	0.898
PTK2B	2	1.151	0.015
SLC24A2	3	0.115	0.924
SLC24A4	4	2.313	0.002
SORL1	5	0.644	0.056

Figure 2.8: Alterations in the 5hmC landscape in Alzheimer's Organoids

A. Number of identified AD-specific DhMRs. **B.** List of various known AD risk genes and developmental genes with differential gene expression identified in Figure 4C. **C.** Proportion of specific cell types determined from the cellular deconvolution of D84 control and AD organoids RNA-seq data. Cell types: Ex: excitatory neurons; Ast: astrocytes; In: Inhibitory neurons. **D.** Number of AD enriched DhMRs that either increased (dark purple) or decreased (light purple) in gene expression. **E.** Gene ontology analysis results of genes annotated to AD enriched DhMRs with decreasing gene expression. Grey bars indicate non-significant GO terms. Reg.: Regulation; Dev.: Development. **F.** Number of AD depleted DhMRs that either decreased (dark green) or increase (light green) in gene expression. **G.** Gene ontology analysis results of genes annotated to AD

depleted DhMRs with increasing gene expression. Reg.: Regulation, Dev.: Development, Diff.: Differentiation. **H.** Number of DhMRs identified in known AD risk genes previously found in AD GWAS studies, where genes with a significant log2 fold change (FDR < 0.05) in gene expression are bolded.

Table 2.3: Overlapped DhMRs obtained from models of AD organoids, AD postmortem brains, and PSEN1 neurons

DhMRs were identified from AD organoids (this study), AD postmortem brains and a PSEN1 mutated 2D cortical neuron line. We identified significantly more common DhMRs between our AD organoids and those DhMRs from patient derived 2D cortical neurons compared to human AD postmortem brains.

Publication	AD Model	Number of Overlapping DhMRs
[341]	PSEN1 2D cortical neurons	2,279
[339]	AD postmortem brain	28
[340]	AD postmortem brain	3
[337]	AD postmortem brain	9
[261]	AD postmortem brain	4
[338]	AD postmortem brain	61

2.6. Materials and Methods

Experimental Model and Subject Details: The control iPSC lines were generously provided by Dr. Garry Basel's laboratory from Emory University. The fAD fibroblasts were generously provided by Dr. Selina Wray, from UCL Queen Square Institute of Neurology and then generated into fAD iPSCs by Dr. Chadwick Hales, from Emory University.

Human Forebrain-Specific Organoid Cultures: All fAD patient-derived iPSC lines (AD-01: *PSEN1* Y155H; AD-02: *PSEN1* M139V; AD-03: *PSEN1* intron4 deletion; AD-04: *APP* V717I) and the three sex- and age-matched healthy control (C-03, C-09, C-21) iPSC lines (provided by Dr. Chadwick Hales' laboratory at Emory University) were cultured on irradiated MEFs in human iPSC medium consisting of D-MEM/F12 (Invitrogen), 20% Knockout Serum Replacement (KSR, Invitrogen), 1X Glutamax (Invitrogen), 1X MEM Non-essential Amino Acids (NEAA, Invitrogen), 100 μM β- Mercaptoenthanol (Invitrogen), and 10 ng/ml human basic FGF (bFGF, PeproTech) as described [343]. Forebrain-specific organoids were generated as previously described [324]. Briefly, human iPSC colonies were detached from the feeder layer with 1 mg/ml collagenase treatment for 1 hour and suspended in embryonic body (EB) medium, consisting of FGF-2-free iPSC medium supplemented with 2 μM Dorsomorphin and 2 μM A-83 in non-treated polystyrene plates for 4 days with a daily medium change. On days 5-6, half of the medium was replaced with induction medium consisting of DMEM/F12, 1X N2 Supplement (Invitrogen), 10 μg/ml Heparin (Sigma), 1X Penicillin/Streptomycin, 1X Non-essential Amino Acids, 1X Glutamax, 4 ng/ml WNT-3A (R&D Systems), 1 μM CHIR99021 (Tocris), and 1 μM SB-431542 (Tocris). On day 7, organoids were embedded in Matrigel (BD Biosciences) and continued to grow in induction medium for 6 more days. On day 14, embedded organoids were mechanically dissociated from Matrigel by pipetting up and down onto the plate with a 5ml pipette tip. Typically, 10 - 20 organoids were transferred to each well of a 12-well spinning bioreactor (SpinΩ) containing differentiation medium, consisting of DMEM/F12, 1X N2 and B27 Supplements (Invitrogen), 1X Penicillin/Streptomycin, 100 μM β- Mercaptoenthanol (Invitrogen), 1X MEM NEAA, 2.5 μg/ml Insulin (Sigma). At day 71, differentiation medium was exchanged with maturation medium, consisting of Neurobasal (Gibco), 1X B27 Supplement, 1X Penicillin/Streptomycin, 1X β-Mercaptoenthanol, 0.2 mM Ascorbic Acid, 20

ng/ml BDNF (Peprotech), 20 ng/ml GDNF (Peprotech), 1 ng/ml TFGβ (Peprotech), and 0.5 mM cAMP (Sigma). All media were changed every other day.

Organoid Immunocytochemistry: Forebrain organoids were processed for immunocytochemistry as previously described [324]. Briefly, whole organoids were fixed in 4% Paraformaldehyde in Phosphate Buffered Saline (BPS) for 30-60 min at room temperature. Organoids were washed 3 times with PBS and then incubated in 30% sucrose solution overnight. Organoids were embedded in tissue freezing medium (General Data) and sectioned with a cryostat (Leica). For immunostaining, freezing medium was washed with PBS before permeabilization with 0.2% Triton-X in PBS for 1 hr. Tissues were then blocked with blocking medium consisting of 10% donkey serum in PBS with 0.1% Tween-20 (PBST) for 30 min. Primary antibodies diluted in blocking solution were applied to the sections overnight at 4ºC. After washing with PBST, secondary antibodies diluted in blocking solution were applied to the sections for 1hr at room temperature. Finally, sections were washed with PBST and stained with DAPI. All images were captured by Nikon Eclipse Ti-E microscope. Quantitative analyses were conducted on randomly picked cortical structures in a blind fashion using ImageJ software [344].

DNA and RNA Isolation: Embryoid bodies and organoids were collected after 56, 84 and 112 days of culture and were immediately frozen on dry ice and stored at -80°C. Tissue was first homogenized in a lysis buffer (10mM Tris pH 8.0, 5mM EDTA, 200mM NaCl, 0.2% SDS) with 25µl proteinase K (20mg/ml) using a hand-held pestle homogenizer then was incubated at 55°C overnight. After the overnight digestion, the lysates were brought to room temperature and incubated with 5µl of RNase A solution (20mg/ml) for at least 2 hours at room temperature. DNA was extracted by adding equal volume of buffered phenol:chloroform:isoamyl alcohol (25:24:1 ratio) and centrifuged in Phase-Lock tubes at 15,000 RPM at room temperature. Supernatant was transferred to clean tubes. An equal volume of isopropanol was then added to the supernatant and mixed well at room temperature to precipitate the DNA. The DNA was then centrifuged at 10,000g for 10 minutes at room temperature, and then washed in 70% ethanol. After all ethanol was removed, the DNA pellet was eluted in nuclease-free water and incubated at 55°C for 1 hour before storing at -20°C. The DNA was quantified by Nanodrop and Qubit, and quality confirmed by a gel.

A separate aliquot of tissue was used for RNA isolation. Tissue was homogenized in TRIzol using a hand-held pestle homogenizer and incubated in TRIzol for at least 5 minutes. Chloroform (1:5 ratio) was added, the tubes shaken, and incubated at room temperature for 15 minutes. Samples were then centrifuged at 12,000g for 15 minutes at 4°C. The top aqueous layer was transferred to a clean tube, and the RNA was precipitated in 3M NaAc pH 5.2 (10:1 ratio), 4μl of glycogen (5mg/ml), 100% isopropanol (1:1 ratio) overnight at -80°C. The next day, the samples were centrifuged at 15,000 RPM for 20 minutes at 4°C. The resulting RNA pellet was washed once in 75% ethanol, centrifuged at 7,500g for 10 minutes at 4°C. The washed RNA pellet was dissolved in nuclease-free water. RNA was quantified by Nanodrop and quality confirmed by a gel.

RNA-seq Cellular Deconvolution: Cellular deconvolution was conducted on the organoid RNA-seq data with MuSiC [333], a method that utilizes cell-type-specific single-cell RNA sequencing (scRNA-seq) data as a reference panel to quantify cell type compositions of samples with bulk RNA-seq data. We obtained the scRNA-seq data of postmortem human brain from the ROSMAP single cell study [345] as reference in the deconvolution. Following the software recommendations, we provided the raw read counts of both bulk RNA sequencing and the single cell RNA sequencing data as inputs. We applied MuSiC with all default settings and obtained cell type proportions in one step without clustering them into higher level groups. The output proportions "Est.prop.weighted" were used as the final proportion estimations.

Dot Blot: Genomic DNA was blotted onto a Hybond nylon membrane (Amersham, GE Healthcare) using a Bio-Rad Dot Blot apparatus (#1706545, Bio-Rad) and washed three times with 6X saline-sodium citrate buffer with 15 minutes of vacuum. The DNA was hybridized to the membrane at 85°C for 30 minutes. Immunoblotting was performed by first blocking the membrane in 5% milk/0.2% tris-buffered saline with Tween-20 for 30 minutes then incubating overnight in primary antibody in 5% milk (5hmC antibody 1:2000, Active Motif #39769) at 4°C with rotation. Secondary antibody incubation was anti-rabbit HRP-linked IgG (Cell Signaling #7074S) 1:5000 in 5% milk for 1 hour. Signal was detected with ECL substrate (Denville Scientific HyGLO #E2400) and imaged with autoradiography film and a Konica Minolta film processor (SRX-101A). Films were scanned into digital form, then pixel densitometry quantification was performed using ImageJ software [344].

Western blot analysis: Human iPSC-derived forebrain organoids were lysed in RIPA buffer (150 mM NaCl, 1% Triton X-100, 0.5% sodium deoxycholate, 0.1% SDS; 50 mM Tris, pH 8.0) containing Complete Protease Inhibitor Cocktail (Roche). Samples were left on ice for 30 min and sonicated briefly. The insoluble fraction was removed by centrifugation at 15,000 rpm for 15 min at 4°C. Protein concentration was determined by BCA protein assay kit (Bio-Rad). 2X SDS sample buffer (Bio-Rad) containing 5% β-mercaptoethanol (Sigma) was added to equal amounts of protein. Proteins were then separated by 4-15% SDS PAGE (Bio-Rad) and transferred to PVDF (0.2 μm) or nitrocellulose membrane (0.45 μm). 5% dried milk in TBST (Tris buffered saline with 0.1% Tween 20) was incubated for blocking, and membranes were applied with specific antibodies. After washing with TBST and incubation with horseradish peroxidase-conjugated anti-rabbit or anti-mouse IgG (Santa Cruz Biotechnology), the antigen-antibody was detected by chemiluminescence (ECL; Pierce) and X-ray film (GE Healthcare).

ELISA analysis: Aβ concentration was measured from forebrain organoid supernatants using commercial ELISA kit for Aβ (1–40) and Aβ (1–42) (Thermo Fisher Scientific #KHB3481 and #KHB3544 respectively) following the manufacturer's instruction. Briefly, media samples were incubated (4 hours) in primary antibodies against the COOH-terminus of the 1–40 or 1–42 Aβ sequence in pre-coated 96 well plates (pre-coated with monoclonal antibody specific to human Aβ 1–40 or 1–42) followed by aspiration and four washes (in washing buffer). And then the samples were subsequently incubated with HRP-conjugated secondary antibodies followed by aspiration, four washes, and addition of HRP substrate (3,3',5,5'-tetramethylbenzidine). The reaction was stopped using 1 N sulfuric acid and absorption was measured at 450 nm in a Synergy HT microplate reader (BioTek). Absolute values were calculated from a standard curve and plotted as either picogram/ml (pg/ml) or Aβ42/40 ratio per sample

5hmC Capture: Five μg of genomic DNA was sonicated to 300-400 base pair (bp) using a Covaris focused ultrasonicator. 5hmC capture was performed according to the method described in [131].First, a glucosyltransfer reaction was performed using 2.5μl of T4 phage ß-glucosyltransferase enzyme (10,000U/ml; New England BioLabs) and 100μM UDP-6-N3-glucose (Jena Biosciences) and incubated at 37°C for 2 hours. After purification with AMPure XP beads (Beckman Coulter), the glucosylated 5hmC-containing DNA

fragments were biotinylated with 150μM disulfide biotin linker (Click Chemistry Tools) at 37°C for 2 hours. After purification with AMPure XP beads, the biotinylated 5hmc-containing DNA fragments were pulled down using Dynabeads MyOne Streptavidin C1 beads (ThermoFisher Scientific) and were washed three times with Binding/Washing buffer (20mM Tris pH 7.5, 1mM EDTA, 2M NaCl, 0.01% Tween-20). The 5hmC-containing DNA fragments were then removed from the beads with fresh 100mM dithiothreitol for 2 hours with rotation at room temperature. After final purification with AMPureXP beads, the 5hmC-enriched DNA fragments were eluted in nuclease-free water and quantified by Qubit.

Library Preparation and High-Throughput Sequencing: Enriched DNA from 5hmC capture were subjected to library construction using the NEBNext Ultra II DNA Library Prep kit for Illumina (New England BioLabs) according to manufacturer's protocol. Briefly, 1-7ng of 5hmC-enriched DNA or un-enriched genomic DNA was utilized for each library construction. An Agilent 2100 Bioanalyzer was used to confirm purity and fragmentation size of the final libraries. RNA-seq libraries were generated using TruSeq RNA Sample Prep V2 kit (New England BioLabs) with 1μg of RNA to first obtain poly-A-enriched RNA and synthesize cDNA, and then the same library construction protocol was followed using 5ng of cDNA. Libraries were sequenced pair-end (150bp) on an Illumina HiSeq platform by Admera Health, LLC.

5hmC-seq and RNA-seq Data Processing: Raw 150 bp paired-end ChIP–seq reads were mapped to the hg19 reference genome using bowtie2 (v2.2.6) [346] with the parameters "--no-discordant --no-mixed" to prevent discordant alignments and alignments for the individual mates. Flags "-F 4" and "-q 10" were used in samtools (v 1.9) [347] to exclude unmapped reads and reads with low Mapping Quality (MAPQ) values less than 10 for each replicate in all stages. Technical replicates with multiple sequencings were combined using the "merge" function in samtools. The genome was segmented into 1-kb consecutive bins and the reads were normalized with respect to the sample with the smallest total numbers of read counts. Bins with less than 10 counts summed over all samples were removed and the correlation of the normalized reads intensity was calculated between biological replicates on remaining bins across all stages. Principal component analysis (PCA) was performed to visualize replicate clusters using the binned normalized read counts. All biological replicates with Pearson correlation > 0.8 per time point were included in our analysis. The MACS2 algorithm (v 2.1.0.)

[348] was used to call 5hmC enriched peaks for each organoid sample by comparing to the merged input organoid sample. By default, MACS2 normalizes all enriched peaks. Biological replicate peak files were combined using the "intersect" function in bedtools (v 2.27.0) [349] and only 5hmC peaks that were identified in all replicates were considered for our analyses. Based on a previous publication [350], the default parameters for the bedtools intersect function report a 1bp minimum overlap between regions. HOMER (Hypergeometric Optimization of Motif EnRichment) (v4.9) [351] was used to annotate identified peak regions to their corresponding nearby genes, with an additional flag "-annStats" to also annotate genomic features to these peak regions. 5hmC enrichment was estimated by calculating the ratio of observed verse expected probability for 5hmC peaks annotated to the specific genomic feature. The observed probability was the length of the 5hmc peaks that covers the related genomic regions versus the length of the total 5hmC peaks, and the expected probability was the length of the total regions of the specific genomic feature divided by the whole genome length. Further, EB peaks were overlapped with peak regions in other stages by using the "intersect" function in bedtools (v2.27.0).

Raw RNA-seq reads were aligned to the human genome build hg19 using TopHat2 (v1.3.3) **[352]**. Cufflinks (v2.2.1) [352] was used to generate fragments per kilobase million (FPKM) of all RefSeq genes and averaged per condition for downstream analyses. RNA-seq read count correlations were determined among all organoid samples and PCA was used to cluster organoid samples with FPKM data. All replicates per stage showed high correlation (Pearson's correlation > 0.85). Using these aligned RNA-seq data, differential gene expression analysis was conducted using Cuffdiff (v2.2.1) [352] with respect to control and AD organoids.

Identification of Differentially Hydroxymethylated Regions (DhMRs):

Developmental stage specific DhMRs were determined by established or disappeared 5hmC peaks in the current stage compared to the previous stage as previously described [350]. These peaks were identified by using the "windowbed" function in bedtools (v2.29.2) by extended 300bp on either side of the 5hmC peak regions. Peak regions with no surrounding peaks within 300bp in the previous stage were defined as established DhMRs and peak regions in the previous stage with no surrounding peaks within 300bp in current stage were defined as disappeared DhMRs in the current stage. To identify AD organoid-specific DhMRs, 5hmC peaks

from three replicate peak files for each AD organoid line were first overlapped using the "intersect" function in bedtools (v 2.27.0) to obtain common 5hmC peak regions per line. Then, using the same "windowbed" function described above, DhMRs per AD line were identified by comparing to the same age matched healthy control (C-03). Three sets of DhMRs from each line were finally overlapped, again using the "windowbed" function, to obtain shared AD-specific DhMRs to avoid person to person variations.

Bioinformatics Analysis: To identify stage-specific regions, 5hmC read counts were enumerated in all DhMRs per replicate and normalized to the sample with smallest total reads in the whole genome. The averages of the read counts of all replicates per stage were taken and compared across stages. DhMRs with inconsistent established or disappeared patterns were removed, for example, D56 established DhMRs with more averaged reads in EB stage than in D56 stage were excluded. Stage specific up-regulated DhMRs were defined as DhMRs with the highest read counts in the current stage and down-regulated DhMRs were defined as DhMRs with the lowest read counts in the current stage. Heatmaps and metaplots were generated by Ngsplot tool [353] to validate the enrichment patterns of 5hmc within these DhMRs. To enhance the visibility of the heatmaps, the read counts were normalized by subtracting the median count per region and divided by the median absolute deviation per region. The corresponding genes of these stage specific DhMRs were annotated by HOMER (v4.9) using default settings, and later used for Gene ontology (GO) analysis [354, 355] or Genomic Regions Enrichment of Annotations Tool (GREAT) analysis [356]. To identify DhMRs that showed a continual increase or decrease in 5hmC read counts across developmental stages, averaged normalized 5hmC read counts were counted and grouped based on the stage with either the highest or lowest number or read counts. These DhMRs were then annotated to their corresponding genes by HOMER (v4.9), and those located in intergenic regions were removed from further analysis. Only genes also showing a continual increase or decrease in expression were used for gene ontology. GO analysis were performed to identify functional patterns enriched with these genes. To investigate possible links between 5hmC and enhancer regions, published enhancer regions from human fetal brains and astrocytes available on the online database EnhancerAtlas [330] were overlapped with DhMRs that showed either a continual increase or decrease in 5hmC. EnhancerAtlas was also used to predict and annotate genes that may be regulated by these enhancers. Furthermore, raw sequence data from human

fetal brain histone modifications from the Epigenome Roadmap Project [335] were also obtained, mapped and overlapped with the above enhancer regions, where the average normalized read counts of these histone marks per stage were plotted. These histone marks were also used to assess the Jaccard similarity coefficient [334, 357] between 5hmC peaks and histone peaks at enhancer regions that overlapped with AD-specific DhMRs. To compare AD organoid DhMRs to published human postmortem AD brains or patient derived iPSCs differentiated into 2D cortical neurons, DhMRs were identified using the same analysis for identifying the organoid DhMRs described above. Overlapping DhMRs were annotated to their corresponding genes and used for gene ontology.

Gene Ontology (GO) Analysis: Functional annotation analysis was conducted in the GO Consortium classification system (http://geneontology.org) [354, 355]. We then clustered GO terms to a representative functional term and plotted the most significant (-log10(FDR)) to show their statistical significance. These results were confirmed using GREAT [356] which assigns biological processes directly from our identified DhMRs.

Chapter 3: Social Defeat Stress Induces Genome-Wide 5mC and 5hmC Alterations in the Mouse Brain

This chapter is submitted as:

Kuehner, J.N., et al., Social Defeat Stress Induces Genome-Wide 5mC and 5hmC Alterations in the Mouse Brain. Human Molecular Genetics, 2023 (*Submitted*).

Author Contributions:

J.N.K. and B.Y. conceptualized and designed the experiments. **J.N.K.**, N.R.W. and R.S. performed all animal experiments and behavior analysis. **J.N.K.**, N.R.W. and R.S. performed the 5mC-seq, 5hmC-seq and RNA-seq studies. J.N.K. and Y.L. generated schematics and designed computational codes. **J.N.K.**, N.R.W., R.S. and B.Y. wrote and revised the manuscript. **J.N.K.** and Y.L. performed computational analysis. B.Y. supervised all aspects of the project. All authors had the opportunity to discuss results and comment on the manuscript.

3.1. Summary

Stress is adverse experiences that require constant adaptation to reduce the emotional and physiological burden, or "allostatic load", of an individual. Despite their everyday occurrence, a subpopulation of individuals is more susceptible to stressors, while others remain resilient. In this study, we investigated the contribution of the DNA modifications, 5-methylcytosine (5mC) and 5-hydroxymethylcytosine (5hmC), underlying the individual differences in stress susceptibility and resilience. Genome-wide 5mC and 5hmC profiles from 3- and 6-month adult male mice that underwent various durations of social defeat were generated. In 3-month animals, 5mC and 5hmC work in parallel and do not distinguish between stress susceptible and resilient phenotypes, while in 6-month animals, 5mC and 5hmC show distinct enrichment patterns. Acute stress responses may epigenetically "prime" the animals to either increase or decrease their predisposition to depression susceptibility. In support of this, re-exposure studies reveal that the enduring effects of social defeat affect differential biological process between susceptible and resilient animals. Finally, the stress-induced 5mC and 5hmC fluctuations across the acute-chronic-longitudinal time course demonstrate that the negative outcomes of chronic stress do not discriminate between susceptible and resilient animals. However, resilience is more associated with neuroprotective processes while susceptibility is linked to neurodegenerative process. Furthermore, 5mC appears to be responsible for acute stress response, whereas 5hmC may function as a persistent and stable modification in response to stress. Our study broadens the scope of previous research offering a comprehensive analysis of the role of DNA modifications in stress-induced depression.

3.2. Introduction

Stress can be described as adverse experiences that contest the emotional and psychological well-being of an individual. Despite stressful events being a part of everyday life, some individuals are more susceptible to these stressors, while others remain resilient. The molecular mechanisms underlying stress susceptibility and resilience remain elusive. In addition, the duration to which the stressor is experienced can also impact susceptibility. Stress can be categorized into different classes according to duration: instantaneous, acute (short-term), chronic (persistent), and longitudinal (re-exposure). The more prolonged the exposure to the stressor, the more likely an individual is to become vulnerable to anxiety and depressive behaviors predisposing them to Major Depressive Disorder (MDD) [358].

Stress-induced depression is robustly affiliated with the hyper-activation of the hypothalamus-pituitary-adrenal (HPA) axis, causing an increase in blood corticosterone levels and neurological phenotypes [359, 360]. However, stress-induced alterations to the epigenetic landscape, particularly chemical modifications on the DNA paired with gene expression, are less well characterized. Several pioneering studies investigated how prenatal or early life traumas could epigenetically "prime" an individual to inherently be more predisposed to neuropsychiatric disorders later in life [281, 282, 361]. Nevertheless, how stress-induced epigenetic alterations in the brain could regulate differences in stress response remains an open question.

Epigenetics broadly refers to heritable changes in gene expression that occur without altering the DNA sequence, through mechanisms such as DNA covalent modifications [2]. Importantly, these epigenetic variations can arise as a consequence of environmental factors and have a lasting physiological and pathological impact [361]. Previous studies have primarily focused on loci-specific and global histone modification profiles concerning stress. For example, exposure to chronic stress was shown to induce repressive histone methylation at the promoter of specific brain-derived neurotrophic factor (*Bdnf*) splice variants resulting in decreased expression [279]. We and others have previously demonstrated the importance of the DNA modifications 5-methylcytosine (5mC) and 5-hydroxymethylcytosine (5hmC) in neurodevelopment and neurodegenerative disorders [362-364]. In terms of DNA modifications in stress response, there is a large body of work concentrating on loci-specific alterations associated with chronic stress. For instance, loss of promoter methylation at the *Crf* gene [365], increased expression of the active DNA demethylase inducer *Gadd45b* [288] and the persistent upregulation of *Dnmt3a* [290] have all been observed to coincide with stress susceptibility. Ubiquitous knockout of either *Tet1* or *Tet2* DNA demethylase in mice resulted in increased baseline resilience or susceptibility to chronic restraint stress, respectively [291]. This provides a clear link between epigenetic regulation and differences in stress response. In addition, there is a multitude of evidence supporting the role of epigenetics in neuropsychiatric diseases [315]; however, a systematic assessment of global 5mC and 5hmC in relation to various stress durations is needed.

In this study, we generated genome-wide 5mC, 5hmC and transcriptome profiles from animals that underwent various durations of social defeat. Stress-induced alteration of both DNA modifications were

observed with respect to age and duration of stress. We further defined 5mC and 5hmC fluctuations across the acute-chronic-longitudinal time course. Our study broadens the scope of previous research from a locus-specific perspective to a global perspective, offering a comprehensive analysis of the role of DNA modifications in stress-induced depression.

3.3. Results

3.3.1. Chronic social defeat stress induces social avoidance in young and mature adult mice

Chronic social defeat stress (CSDS) is an ethologically relevant paradigm that has been shown to induce depressive and anxiety-like behaviors in rodents [366]. Over the span of 10 days, naïve 3-month (young) and 6-month (mature) mice were repeatedly subjected to bouts of physical defeat by an aggressor (**Figure 3.1:A** and **B**). Defeats were followed by a 24-hour sensory stress in the aggressor's home cage through a clear, perforated divider. Nest building and food consumption were measured daily as indicators of distress in the animals (**Figure 3.2:A-D**). Interestingly, during the first 2 days of defeat, more low-quality nests and a reduction in food consumption were observed in both age groups. After the second defeat, nest quality improved and significantly more food was consumed for the remainder of the experiment. These behaviors uncovered an initial acute response followed by stress adaptation, recapitulating stress habituation behaviors, or allostasis, observed in humans [367]. Social avoidant-like behavior was measured using the social interaction (SI) test (**Figure 3.1:C**). Three and six-month stressed animals exhibited social avoidant behavior compared to controls (**Figure 3.1:D**), as indicated by the significant decrease in time spent interacting with the target and the strong preference towards the avoidant zones (**Figure 3.2:E** and **F**). Out of all the stressed animals, just over 20%, regardless of age, displayed social behavior indistinguishable from control animals and were designated as resilient (**Figure 3.1:E**). Sucrose preference testing suggested that age may play a role in the development of anhedonic-like behavior. While sucrose consumption did not significantly change in the 3-month animals, we did observe increased anhedonic-like behavior in the 6-month animals (**Figure 3.1:F**). Finally, blood corticosterone levels were measured approximately 36 hours after the final defeat and a significant increase in corticosterone was observed in defeated animals (**Figure 3.1:G**). Cumulatively, our data confirm that the CSDS paradigm induces physiological and biological symptoms of depression as well as distinguishes between stress-susceptible and resilient animals, which can be used to elucidate how epigenetics contributes to stress response.

3.3.2. Global characterization of susceptible and resilient DMRs and DhMRs in young and mature adult mice

Given that stress-susceptible and resilient animals were obtained, we investigated how DNA modifications, including 5mC and 5hmC, could contribute to differences in stress response and be responsible for the increased stress sensitivity observed with age. Using established 5mC and 5hmC enrichment methods (5mC-seq and 5hmC-seq, respectively) [364], we generated genome-wide 5mC and 5hmC profiles of the cortex, an important stress-responding brain region [368]. Concerning 5mC, we found that 6-month animals overall had more 5mC peaks compared to 3-month animals (**Figure 3.3:A**). Notably, stress-resilient animals regardless of age, have approximately 1.5 times less 5mC and the highest level of 5hmC compared to control and susceptible animals. This suggests a trend towards global hypo-methylation and hyper-hydroxymethylation that is strongly associated with resilient animals. Enrichment analysis revealed expected genomic patterning for both 5mC and 5hmC peaks [125, 369] (**Figure 3.4:A-D**). 5mC is primarily enriched in exons while 5hmC is distributed across gene bodies with strong depletion in intergenic regions. Overall, stress did not induce any global changes to the enrichment patterns of either 5mC or 5hmC compared to expected values, suggesting that after the initial defeats, the epigenetic landscapes could have stabilized as a stress adaptation, similar to the feeding and nesting behaviors.

We next identified differentially methylated and hydroxymethylated regions, DMRs and DhMRs respectively, in 3- and 6-month stress susceptible and resilient animals by comparing each stress condition to its corresponding control using our established computational approach [364]. Regardless of age, stress susceptible animals consistently gained more and lost fewer DMRs compared to resilient animals (**Figure 3.3:B**). Furthermore, the opposite was observed for DhMRs, where the resilient animals gained more DhMRs (**Figure 3.3:C**). To determine if the cyclic conversion of 5mC to 5hmC to unmodified C could be important for promoting the resilient phenotype, we compared gained and lost DMRs to lost and gained DhMRs, respectively (**Figure 3.4:E** and **F**), but observed very little overlap. In the brain, it has previously been demonstrated that fluctuations of 5hmC occur independent of 5mC level changes [126]. This data supports 5hmC as a *de novo* and independent epigenetic mark in the mammalian brain, so we separately analyzed 5mC

and 5hmC in the following sections. Collectively, our data support that chronic stress induces alterations to the 5mC and 5hmC landscape of the cortex and that these changes correspond to differences in stress response.

Although, 5mC is generally associated with gene repression, particularly at promoter regions, in the mammalian genome, 5mC within the gene body of actively transcribed genes has been reported [7, 370]. Thus, we focused on the positive association between both DNA modifications and gene expression throughout our entire study. To characterize susceptible- and resilient-related DNA modifications that correspond to age, we grouped the regions into either susceptible or resilient 5mC gain or 5mC loss groups (**Figure 3.3:D** and **K**) and correlated these changes in DNA modifications to concomitant changes in gene expression. Using Gene Ontology (GO) analysis, we found that 3-month concomitantly increasing DMRs and DhMRs from susceptible and resilient animals show a strong bias towards nervous system process (**Figure 3.3:E** and **Table 3.3:** and **Table 3.4:**). For both susceptible and resilient gained DMRs and resilient gain DhMRs, the nervous system bias appears to focus specifically on synaptic function. Meanwhile, the susceptible gain DhMRs also function in signaling pathways. Three-month concomitantly decreasing DMRs and DhMRs reside in genes involved in cellular signaling, communication and vasculature morphogenesis, regardless of the stress response (**Figure 3.3:F** and **Table 3.3:** and **Table 3.4:**). Moreover, inspection of 3-month resilient associated DMRs and DhMRs, we discovered several genes with critical roles in neurotransmitter activity such as the dopamine receptor gene *Drd2* (**Figure 3.3:G**), the serotonin synthesizing enzyme *Tph2* (**Figure 3.3:H**) and the glutamate receptor gene *Gria2* (**Figure 3.3:I**). Additionally, susceptible specific regions that gained 5hmC were found in the klotho gene *KI* (Figure 3.3:J), which has been linked to chronic stress-induced depression through its modulation of the glutamate receptor subunit GluN2B [371]. Overall, these findings suggest that in 3-month animals, 5mC and 5hmC are working in parallel, functioning in similar biological processes in response to chronic stress, and do not appear to distinguish between stress susceptible and resilient phenotypes.

Compared to 3-month animals, 6-month animals displayed more distinctive 5mC and 5hmC enrichment patterns in response to chronic stress. We found that concomitantly increasing DMRs in 6-month susceptible animals are involved in immune response processes such as leukocyte activation, inflammatory response and the regulation of cytokine production, whereas DMRs from mature resilient animals are associated

with cell-cell signaling, cilium and cell motility (**Figure 3.3:L** and **Table** 3.3:). With regards to DhMRs, 6-month susceptible animals expressed gene enrichment in signaling pathways or cascades, one of which was the regulation of insulin in response to glucose stimulation (**Table 3.4:**). Resilient DhMRs are involved in basic cellular processes with an emphasis on metabolic and protein-modifying processes (**Table 3.4:**). Based on the data presented, the concomitant increase of DNA modifications and gene expression show distinct enrichment patterns between 6-month susceptible and resilient animals. Gain of either 5mC or 5hmC in mature susceptible animals is associated with canonical stress responding processes (i.e., immune, wounding, insulin and glucose, homeostasis), whereas the gain of 5mC or 5hmC in mature resilient animals is associated with basic cellular signaling (cell-cell signaling and metabolism). For the concomitantly decreasing 6-month DMRs, both susceptible and resilient animals showed a bias for general nervous system processes, but resilient animal DMRs are also involved in signaling, vasculature development, hormone regulation and the immune system (**Figure 3.3:M** and **Table 3.1:**). Regarding susceptible and resilient DhMRs, both annotated to genes primarily functioning in basic cellular and enzymatic activities (**Table 3.2:**). Corroborating chronic stress affecting signaling pathways, DMRs were found in the circadian rhythm gene *Per2* (**Figure 3.3:N**). We also observed an increase in promoter methylation of the *Pvalb* gene (**Figure 3.3:O**), which has previously been observed in patients with MDD [372]. DMRs were also observed in the transcription factor *Foxo1* (**Figure 3.3:P**) which is known to directly regulate the expression of the sestrin gene *Sesn3* (**Figure 3.3:Q**) [373]. Moreover, *Foxo1* and *Sesn3* function in insulin and glucose energy metabolism [374, 375], the main energy sources of the brain. Given that the demand for energy metabolites increases during extended periods of stress to maintain a balanced allostatic state, perhaps resilience in mature animals is associated with improved regulation of energy homeostasis.

3.3.3. Comparison Between Shared DMRs and DhMRs in Young and Mature Adult Mice

We next sought to directly compare our 3- and 6-month chronically stressed animals and identify shared susceptible or resilient DMRs and DhMRs. Using the gain and loss susceptible and resilient DMRs and DhMRs identified in 3-month animals (**Figure 3.3:B** and **C**), we determined which of those regions were also gained or lost in susceptible and resilient 6-month animals (**Figure 3.5:A** and **B**), respectively. Given that the

6-month animals displayed increased stress susceptibility, we wanted to determine if 6-month differential regions had a more drastic gain or loss of either DNA modification. Close to 90% overlap between 3- and 6-month DMRs and DhMRs was observed (**Figure 3.6:A** and **B**), suggesting that when 5mC or 5hmC was gained or lost in response to stress in 3-month animals, it was also gained or lost to the same magnitude in 6-month animals. This indicates that with age, there is not a more sever gain or loss of either DNA modification, suggesting that the shared regions are likely not the principal drivers for increased stress susceptibility in mature animals, and are instead contributing to the overall stress response. To investigate the biological functions of the common DMRs and DhMRs, we correlated the corresponding genes to our gene expression data and only considered those genes that had a concomitant increase or decrease in both 3- and 6-month animals and used STRING to cluster the genes into functional groups (**Figure 3.5:C** and **D** and **Table 3.3:** and **Table 3.4:**). In addition, we overlapped our genes with a large-scale published MDD gene list [376]. Finally, we validate that our susceptible and resilient DNA profiles are independent of each other by overlapping the concomitantly increasing or decreasing susceptible and resilient gene lists and found marginal overlap (**Figure 3.5:E** and **F**).

We identified 341 3- and 6-month common susceptible genes that concomitantly decreased in 5mC and gene expression that were found to have functions in the heart/circulatory system, ion transport, nervous system development and catalytic activity (**Table 3.3:**). We observed a large number of genes involved in the management of calcium release associated with synaptic neurotransmission and other genes linked to synaptic function. Genes that regulate calcium-induced neuro-vasculature blood flow, blood brain barrier (BBB) composition and vascular growth signals were also observed. Encouragingly, we uncovered several genes linked to nutrient-sensing and glucose transport, further supporting our findings that disruption of glucose and energy homeostasis in chronically stressed animals could promote stress susceptibility. With respect to stress and anxiety, we identified *Glp1r,* which directly interacts with the HPA axis to trigger the secretion of glucocorticoids [377] and *Gpr3* which modulates anxiety- and depressive-related behaviors by regulating monoaminergic neurotransmitters and their metabolites [378]. Of the 54 genes found to overlap with the published MDD genes, 32 function in the above biological process, supporting the idea that compromised brain health and energy homeostasis could be key contributors to stress susceptibility. In the 5mC concomitantly increasing

susceptible group, 61 genes were found to function in the endocrine system (**Table 3.3:**). Genes pertaining to lipid biosynthesis, metabolism, homeostasis, peripheral immune system activation and male reproduction, were identified. Importantly, all of these processes are highly interconnected with HPA-axis activation during an adaptive stress response [379].

5mC concomitantly decreasing genes in our common resilient category were found to be involved in pathways regulating heart/circulatory development, immune response and various signaling pathways such as PI3k-Akt, MAPK, ERK1/2, etc. (**Table 3.3:**). Although most of the genes in the heart/circulatory development pathway function primarily in muscle and heart tissue, there are several interesting genes that could function in the vasculature system of the brain. For example, *Agtr1a* is the receptor for angiotensin ll, a vasoconstrictor that regulates blood pressure. Recently, it was determined that angiotensin II induced hypertension increased BBB permeability and that Agtr1a receptors present in brain endothelial cells of the BBB increase its permeability [380]. In the immune response category, we predominately observed genes that regulate inflammation and cytokine production. Traditionally, chronic stress-induced neuroinflammation compromises the integrity of the BBB which in turn has adverse effects on the neuro-vasculature architecture that supplies the brain with blood and other nutrients. Our data insinuates that the shared resilient regions between 3- and 6-month animals could repress these pathways through the loss of 5mC, proposing a neuroprotective role. In the overlapped MDD genes, we found several genes with various nervous system roles such as the adenosine deaminase, *Adarb2*, which can edit the serotonin receptor 2C mRNA and drastically affect its affinity for serotonin binding [381] and the NADPH-dependent enzyme *Hsd11b1*, which converts cortisone to the stress hormone cortisol [382]. On the other hand, in resilient animals when 5mC and gene expressed concomitantly increased, genes involved in anion and ATP binding were identified (**Table 3.3:**). We found several genes involved in neuroprotection, GABAergic signaling and anxiety regulation. Overall, these findings lay out a mechanism whereby stress-induced alterations to 5mC in resilient animals exert a neuroprotective effect through the inhibition of neuroinflammatory and blood vessel constriction and the promotion of genes thought to protect against anxiety.

Concerning 5hmC in susceptible animals, 269 3- and 6-month common concomitantly decreasing genes were found to function in processes ranging from signaling cascades to the nervous system. More specifically, process such as oligoprogenitor cell (OPC) differentiation, BBB permeability, neuroinflammatory response and the trafficking of glutamate receptors were observed (**Table** 3.4:). One gene of interest includes *Dag1*, which is speculated to function in BBB integrity due to its expression in astrocytic feet that surround blood vessels and in endothelial cells that make up the BBB [383]. Importantly, many genes within all the clusters were involved in depression and anxiety-related behaviors in mice. For example, *Adarb1* targets the pre-mRNA of the $GABA_A$ receptor [384] and serotonin receptor [385] for A-to-I editing. Moreover, 12 genes, 9 of which overlap with the published MDD genes, are implicated in Alzheimer's disease (AD). Also in the MDD overlap list, is *Sik1,* a critical regulator of the corticotrophin releasing hormone, a major hormone in the HPA-axis [386]. 144 concomitantly increasing 5hmC genes in susceptible animals localized to the nucleus and membrane-bound organelles (**Table** 3.4:). Among them, many genes function as epigenetic regulators of the chromatin and histone landscape, in microglia activation and neuroinflammation, as transporters across the BBB or are linked to depression-related behaviors in mice. We again observed numerous genes associated with AD pathology, specifically the Aβ-plaques, neurofibrillary tangles and neurodegeneration. Nineteen of our genes overlapped with the published MDD data set, and were found to function processes such as dopaminergic health, microglia activation, BBB permeability and energy/metabolic homeostasis. Collectively, alterations to the 5hmC landscape in stress susceptible animals appears to be linked to the dysregulation of neuroprotective processes, that under normal conditions, reinforce BBB permeability, regulate glutamate receptor availability and neuroinflammatory process. Interestingly, many of the genes were found to also be associated with AD, supporting the proposed theory that chronic stress is a risk factor for AD [387].

The 228 shared concomitantly decreasing 5hmC genes identified in resilient animals function in cytoskeleton organization and the nervous system (**Table 3.4:**). Gene analysis from both clusters demonstrated that processes such as synaptic vesicle trafficking and transmission, microglia activation, BBB regulation, sphingolipid metabolism and Notch/Wnt signaling regulation could be disrupted. In the MDD cluster, we identified: *Brd4* which is associated with neuroinflammation, anxiety-like behavior and impaired memory [388],

the postsynaptic scaffolding protein, *Dlgap4*, which forms a protein complex to regulate glutamatergic synapses [389] and *Slc36a1,* which has been proposed to be a putative biomarker for patients who experience their first depressive episode after the age of 50 (known as late-onset MDD) [390]. Regarding the 204 genes displaying a concomitant increase in 5hmC and gene expression, their gene products were found to localize to cellular or nuclear membranes and synapses (**Table 3.4:**). Of interest, the gene encoding β-catenin, *Ctnnb1*, was found and has previously been shown in the regulate stress resilience in the nucleus accumbens [391]. Other synaptic localizing genes include those that encode ion channels and synaptic vesicle endocytosis machinery. Notably, there appeared to be a significant bias towards GABAergic and glutamatergic synapse function and composition compared to other synapses. A serendipitous finding was the number of genes implicated in the regulation of adult neurogenesis and adult OPCs. Perturbations to both processes have been observed to influence anxiety and mood disorders [392, 393]. Our findings imply that the loss of intragenic 5hmC in resilient animals appears to encourage the resilient phenotype by repressing neurodegenerative processes to some extent; suggesting that resilient animals are not impervious to the negative consequences of chronic stress. On the other hand, the gain of 5hmC could promote adult neuro- and gliogenesis.

3.3.4. Acute social defeat induced epigenetic alterations that prime chronic stress response

Given the acute stress response observed during the first 2 days of CSDS, we modified the paradigm to recapitulate a short-term, acute social defeat stress (ASDS). ASDS animals underwent 2 days of social defeat followed by social interaction testing (**Figure 3.8:A**). Nest building and food consumption were measured daily, and as expected, on days 3 and 4 when the social defeat occurred, a reduction in nest quality and food consumption was observed (**Figure 3.8:B** and **C**). There was a significant decrease in social interaction (**Figure 3.8:D**) and sucrose consumption (**Figure 3.8:E**), indicating that 2 days of stress is sufficient to induce depressive-like behavior. Importantly, a significant increase in corticosterone levels was only observed immediately preceding the final defeat (**Figure 3.8:F**) and not 36 hours after when tissues were collected (**Figure 3.8:G**). This corresponds to the negative feedback mechanism of the HPA-axis, allowing for the maintenance of relatively low concentrations of corticosterone in the bloodstream. With this in mind, the

resulting DNA modification profiles are more likely to represent a "recovery" period indicative of the lingering effects and not the immediate consequence of corticosterone.

Initial analysis of the 5mC and 5hmC peaks revealed a specific increase in 5mC peaks, and not 5hmC, in response to acute stress (**Figure 3.7:A**). In support of this, nearly 3.5-times more gained DMRs compared to lost were reported and the DhMRs were equivalently affected (**Figure 3.7:B**). Enrichment analysis uncovered inversely correlated 5mC profiles in every intragenic region except exons, whereas 5hmC enrichment was unaltered from the expected distribution in acute versus control samples (**Figure 3.8:H** and **I**). These data suggest that the early accumulation of 5mC in response to acute stress could be a driving factor in the re-establishment of adaptive homeostasis whereas 5hmC could be more stable and less impacted by stress. ASDS-specific DMRs were identified in the neuronal calcium binding protein, *Necab2*, the high-affinity adenosine receptor, *Adora2*, and the dopamine receptor subunit, *Drd2* (**Figure 3.8:J - L**). Notably, in the 3-month CSDS analysis, we also observed a resilient specific loss of 5mC in *Drd2*, suggesting reduced methylation of *Drd2* could be an early indicator of stress resilience.

After the differential regions were correlated with RNA-seq data, GO analysis was used to determine the biological processes affected by ASDS (**Table 3.5:**). Concomitantly increasing 5mC genes are involved in modulating a cell's response to stress. This suggests that a drastic or sudden change in activity, such as alterations in phosphorylation-mediated signaling, cell death or the transport of ions, could contribute to the re-establishment of a homeostatic state. There is also the potential activation of a humoral immune response, which could be indicative of the immune system "preparing" to respond to insults such as the wounding that occurs during the social defeat. Although no significant biological processes were found in the concomitantly decreasing 5mC gene list (**Table 3.5:**), more genes involved in signaling response to stress, like through cell surface receptors, were observed. This is in contrast to "fight-or-flight" related responses (reproduction, heart rate, muscle contraction and blood pressure regulation) stimulated through the release of corticosterone where less genes were observed. Genes containing regions that concomitantly gained 5hmC function in metabolic and signaling processes such as glycerolipid metabolism (**Table 3.5:**). In the brain, lipids facilitate synaptic membrane composition, energy homeostasis and intracellular signaling process which could be regulating the

protein localization or modification processes found in our data. Surprisingly, we also observed processes like molting and hair follicle and epidermis development. This could be a result of stress-induced shedding or hair and skin regrowth after injury. In the 5hmC concomitantly decreasing genes (**Table 3.5:**), processes that regulate RNA transcription and biosynthetic processes, as well as histone modifying mechanisms were observed. This suggests some degree of dysregulation in gene expression. Downregulation of catecholamine secretion, which regulates "fight-or-flight" responses was also observed. Given that catecholamines can stimulate an immune response [394], a decrease in their secretion could also explain the observed decrease in immune response and NF-kB signaling in our data. Overall, the analysis suggests that after acute stress and when corticosterone levels return to baseline, the reminiscent changes in 5mC appear to regulate cellular signals at the global scale, where 5hmC seems to be "fine-tuning" or perhaps orchestrating these global signals into more precise stress responding pathways.

We next wanted to identify common concomitant genes between ASDS and CSDS to identify differential regions that could be indicative of a "priming" for stress susceptibility or resilience. To accomplish this, ASDS DMRs and DhMRs were overlapped with 3-month susceptible-specific or resilient-specific DMRs and DhMRs, respectively (**Figure 3.7:C**). Those common 2,472 regions annotated to 420 concomitant genes between ASDS gained DMRs and CSDS susceptible-specific gained DMRs. Furthermore, they are involved in processes that regulate neurovascular response to stress and cell-cell signaling likely mediated through cell junction, adhesion and extracellular matrix mechanisms (**Table 3.6:**). On the other hand, those susceptible genes that share a common loss of 5mC function in various synaptic processes. For example, both *Farp1* and *Ptpro* promote synapse formation [395, 396] while *Mertk* helps mediate astrocyte-driven phagocytosis of synapses [397]. In resilient animals, 136 genes were annotated from the 751 regions shared between ASDS and CSDS resilient-specific gain DMRs (**Table** 3.6:). These genes function in adult neurogenesis, microglia-induced innate immune responses, BBB permeability, cell adhesion and glutamate and glucose transport. Of interest, the *Dagla* gene encodes an enzyme that produces one of the main endocannabinoids in the adult brain and when *Dagla* expression is lost, animals develop anxiety and depressive-like behavior in mice [398]. Those

common resilient 5mC loss genes function in ion transport as well as neuron-specific processes like differentiation, generation and projection (**Figure 3.7:D**).

Common concomitant genes between ASDS gain DhMRs and CSDS susceptible-specific gain DhMRs (**Table 3.6:**) function in signaling cascades mediated through enzyme-linked receptor proteins and/or the transport of ions across membranes in response to a stimulus to re-establish a homeostatic state. The regulation of fat cell differentiation could be indicative of an adaptive response to compensate for the increased energy demand due to stress. Other processes include the upregulated response to transforming growth factor-β (TGF-β) signaling, which in turn is known to activate blood vessel development. Importantly, acute and chronic insult are both known to significantly upregulate TGF-β signaling [399], corroborating our finding. Interestingly, susceptible genes that share a common loss of 5hmC and gene expression encode subunits of the SWI-SNF ATP-dependent chromatin remodeling complex or polycomb repressive complex 1 (**Table 3.6:**). The ASDS gain DhMRs that overlapped with the CSDS resilient-specific gain DhMRs annotated to genes that are primarily involved in signaling through phosphorylation and the organization of dendritic synapses (**Figure 3.7:E**). There was also a significant enrichment for gliogenesis, supporting our findings from the CSDS resilient DhMRs that stress could be disrupting the maturation or differentiation of adult oligoprogenitor cells. Those genes found to be in common with CSDS resilient-specific DhMR loss, appear to function in energy homeostasis and have neuroprotective roles (**Table 3.6:**). Other genes of interest include *Pkce* and *Tet3*, both of which have been affiliated with depression or anxiety-like behaviors [314, 400]. These results are surprising considering the loss of neuroprotective properties are contradictory to the expected stress resilient phenotype. It is possible that these findings are specific to acute stress response and that animals primed to be resilient have the potential to rectify these processes.

In summary, our comparison of 5mC and 5hmC between ASDS and CSDS to identify putative epigenetic priming patterns for stress susceptibility or resilience was informative. In general, the DNA profiles across susceptible and resilient animals demonstrate that both groups are affected by the dysregulation of stress-responding pathways. Susceptible animals specifically repressed subunits of chromatin remodeling complexes, while resilient animals appear to promote neuro- and oligo-genesis.

3.3.5. Longitudinal social defeat suggests that epigenetic memory may protect against chronic stress

Previous work has demonstrated that CSDS has an enduring influence on social behavior [401]; however, how this effect differs between susceptible and resilient stress responders is poorly understood. To model this behavior, we employed a longitudinal social defeat stress (LSDS) paradigm that incorporates an "incubation" period into the CSDS paradigm followed by a second re-exposure social interaction (**Figure 3.10:A**). Animals were divided into 2 groups based on their behavior in the social interaction test: Animals who maintained susceptibility (SS) and those who remained stress resilient (RR) (**Figure 3.10:B**). Initial peak analysis showed that overall, re-exposure induced an increase in both 5mC and 5hmC peak number compared to controls (**Figure 3.10:C**). The number of gained and lost DMRs was approximately equal across all stress groups (**Figure 3.9:A**) whereas, for 5hmC, the SS animals have more than twice as many gained DhMRs compared to the RR animals (**Figure 3.9:B**). Our data suggests that re-exposure simulates acute stress, given that both ASDS and LSDS display a spike in 5mC peak number and gained DMRs compared to CSDS and in terms of the stress duration. Regarding 5hmC, although SS animals have over twice as many gained DhMRs compared to RR, when considered across all stress conditions (**Figure 3.3:C**, **Figure 3.5:B** and **Figure 3.9:B**), 5hmC dynamics appear to be decreasing or displaying minimal alterations. This suggests once 5hmC is added or removed from a region, it functions as a stable epigenetic mark. To investigate how DNA modifications can modulate stress response after a re-exposure event, we applied the same overlapping method described for **Figure 3.5:C** to compare CSDS susceptible and resilient specific differential regions to LSDS SS (L_{SS}) and RR (L_{RR}) gained and lost differential regions (**Figure 3.9:C**). We identified 711 overlapping concomitant genes that gained 5mC between L_{SS} and CSDS susceptible DMRs (**Table 3.7:**). Interestingly, these genes were enriched in numerous peripheral body systems such as ear, circulatory, renal, kidney, skeletal and respiratory development. These findings could be indicative of the central nervous system signaling specifically through the autonomic-sympathetic regulatory pathways of the peripheral nervous system. The regions that overlapped between L_{SS} and CSDS susceptible lost DMRs only annotated to the two genes *Prdm16* and *Zswim4*, whose functions in the adult brain are unclear (**Table 3.7:**). On the other hand, the overlap of L_{RR} and CSDS resilient gained DMRs revealed 234 genes, where the only significant biological processes are neuromuscular process

and intracellular signal transduction (**Table 3.7:**). Despite their lack of statistical significance, the synaptic vesicle cycling and ionotropic glutamate receptor signaling processes could suggest an important function for glutamate receptor recycling homeostasis in developing stress resilience. Furthermore, the HPA-axis and circadian regulation are deeply interconnected in their efforts to regulate stress response. Very few genes overlapped between L_{RR} and CSDS resilient loss DMRs (**Table 3.7:**). Among the genes identified, we observed the BBB transporter (*Abcc4*) [402], the neural tissue-specific chromatin remodeler (*Chd5*) and the myelinating protein (*Mopb*) [403].

We identified 173 overlapping concomitant genes that gained 5hmC between L_{SS} and CSDS susceptible DhMRs (**Figure 3.9:D** and **Table 3.7:**). There is a strong enrichment for signaling cascades such as Wnt, MAPK, TGF-β and BMP signaling, which all utilize cell surface receptors and serine/threonine kinase signaling to facilitate their signal transduction. Importantly, these signaling cascades function in the brain and have broad impacts on how the brain responds to stress. Regarding the overlapping L_{SS} and CSDS susceptible lost DhMRs, 113 genes were identified and preferentially function in the nervous/neurovascular systems and signaling pathways (**Table 3.7:)**. Deficiency in the zinc finger *Zfp462* has recently been found to cause anxiety-like behavior [404] and could be a critical stress susceptibility gene. Similar to the gained DhMRs shared between L_{SS} and CSDS susceptible animals, the shared gained DhMRs between the L_{RR} and CSDS resilient animals also annotated to genes involved in cellular signaling utilizing cell surface receptors and serine/threonine kinase (**Figure 3.9:E** and **Table 3.7:**). In addition, processes that regulate gene expression, potential through transcription and RNA metabolic processes were also observed. Positive and negative regulation of cellular signaling are likely ubiquitous consequences of stress and are not necessarily distinguishing characteristics of stress susceptibility or resilience. However, our data hints at a possible mechanism whereby the processing of mRNA transcripts could be contributing to the diverging stress response phenotypes. Only 67 genes overlapped between L_{RR} and CSDS resilient loss DhMRs (**Table 3.7:**). From these genes, we identified chromatin remodelers and transcription factors that function in various components of adult neurogenesis such as inducing adult neural stem cell proliferation (*Ankrd11*) [405], differentiation (*Chd7*) [406] or quiescence (*Foxo3*) [407].

In summary, after stressor re-exposure, 5mC was found to regulate the brain's communication network with peripheral organ systems in susceptible animals. For resilient animals, upregulation of 5mC is linked to the putative recycling of glutamate receptors and promotes HPA—circadian synergism. With respect to 5hmC, both susceptible and resilient animals express an upregulation of intracellular signaling cascades in response to stress. For susceptible animals, these signals could be contributing to the downregulation of nervous/neurovascular processes, whereas in resilient animals, the mRNA transcripts downstream of these signals could be undergoing various metabolic processes affecting gene expression.

3.3.6. 5mC and 5hmC dynamics across the ASDS-CSDS-LSDS time course

To investigate stress-induced patterns that expand across the acute, chronic and longitudinal (ASDS-CSDS-LSDS) time course, we examined DMRs and DhMRs that either continually increased or decreased (**Figure 3.9:H** and **Figure 3.10:F**, Groups 1 and 2 respectively) or returned to baseline (**Figure 3.9:H** and **Figure 3.10:F**, Groups 3 and 4 respectively). Given that the handling conditions and time between defeats, SI and tissue collection were constant across each social defeat variation, the three conditions are suitable for a linear comparison to estimate a stress-dependent epigenetic timeline. Only those genes whose expression pattern matched the 5mC/5hmC pattern (i.e., both 5mC and gene expression increased between ASDS and CSDS and decreased between CSDS and LSDS) were considered (**Figure 3.10:G**). Furthermore, we prioritized those genes that showed the most drastic pattern fluctuations for further discussion.

Genes that continuously increase or decrease in either DNA modification across the ASDS-CSDS-LSDS time course are likely to function as major contributors to stress response. For example, genes found along the depression-susceptible course (A_S-C_S-L_{SS}) would be of great interest, because they are most likely to impact stress-induced depression. In the susceptible 5mC continuously increasing group, we identified 334 genes (**Figure 3.9:F**, Group 1; top). This list contained several ion channels such as *Kcnj16* (**Figure 3.9:G**) as well as pyrimidine metabolizing and anxiety-related genes. On the other hand, 107 genes were observed to continuously decrease in 5mC (**Figure 3.9:F**, Group 2; top). Of those genes, *Ctr9* and *St6galnac2* expressed the most significant decreases. *Ctr9* (**Figure 3.9:H**) functions in a protein complex that traffics dopamine transporters to the plasma membrane [408]. The sialyltransferase enzyme, *St6galnac2*, transfers sialic acid onto

the sugar N-acetylgalactosamine on the cell surface [409]. The brain contains the highest levels of sialic acids which regulate a variety of functions such as neuronal plasticity, the myelination of axons, myelin stability and neuronal network remodeling [410]. These observations are consistent with the idea that chronic stress-induced neurodegeneration is tightly linked with depression susceptibility. Those genes whose 5mC and gene expression returned to base line in susceptible animals represent genes that may be working to reduce the allostatic load induced by chronic stress (**Figure 3.9:F**, Group 3 and 4; top). We identified clusters that either displayed a gain-loss (29 genes) or loss-gained (2,698 genes) pattern. From the gain-loss cluster, one of the most dramatic changes was observed in *Sgk3*. *Sgk3* has been shown to mediate corticosterone-induced autophagic cell death in neural stem cells after chronic stress [411]. In the loss-gain cluster, we observed a series of genes involved in hormone transport (*Ttr*), vitamin A metabolism (*Rbp2*, *Rbp7* and *Stra6*), metal ion homeostasis (*Steap1*) and brain transporter proteins (*Kcne2*, *Slc4a5* and *Aqp1*). Based on the data presented, epigenetic recovery is predominantly occurring in genes that function in very primal and highly conserved processes, but there is also evidence to suggest some degree of HPA-axis recovery in susceptible animals.

Peculiarly, for both the 5mC continually increasing and decreasing resilient clusters (A_S-C_R-L_{RR}) (**Figure 3.9:F,** Group 1 and 2; bottom), there were minimal pattern fluctuations compared to the depression susceptibility model. In the continuously increasing cluster, we identified genes that participate in synapse morphology (*Cadm1* and *Ap3b1*), non-homologous end joining of DNA double-strand breaks (*Xrcc5*), inflammation-induced cell death (*Irf2*) and brain cholesterol metabolism (*Ephx2*). In the continuously decreasing cluster, genes related to intracellular iron homeostasis (*Bdh2*) and neurotransmitter release (*P2rx2*) were observed. Given the minimal increase or decrease of 5mC in depression resilient animals, this provides additional support to our prior observations: Firstly, that 5mC is functioning as an acute stress response modulator and secondly, that the LSDS re-exposure stressor is more analogous to an acute stressor. Resilient genes that returned to baseline also appear to work in basal neurological processes essential for proper cellular and brain function, similar to the susceptible animals. Only 29 genes make up the 5mC gain-loss cluster (**Figure 3.9:F**, Group 3), but the most significantly altered genes function in important processes like DNA damage regulation during replication (*Rfc5*), synapse morphology (*Musk* and *Zdhhc2*) and cholesterol-mediated steroid

production (*Atad3a*). The loss-gain cluster contains 2,385 genes (**Figure 3.9:F**, Group 4; bottom). Several genes localize to the microvessels of the brain (*Slc47a1* and *Enpep*) or function in different aspects of nervous system inflammation and immunity (*Pf4*, *Mamdc2* and *Slc9b2*). Overall, these data suggest that despite their resilient phenotype, depression resilient animals are not impervious to the negative physiological consequences of chronic stress. An unexpected finding was the recovery and prevention of DNA damage processes. Accordingly, the promotion of adult neurogenesis and DNA damage prevention may be the processes most responsible for easing the long-standing effects of chronic stress, to a certain degree in resilient individuals.

Regarding 5hmC, 31 genes were found to continuously increase in both 5hmC and gene expression in our depression susceptibility model (**Figure 3.10:F**, Group 1; top). The *Qrfpr* receptor showed the most significant increase (nearly 11-fold) of all the genes and has recently been implicated in rodent feeding behavior and dietary fat intake [412]. In the 5hmC continuously decreasing group (**Figure 3.10:F**, Group 2; top), many of the genes (*Ifgbp7*, *Tspan18*, *Flt4*, and *Acvrl1*) are expressed in the endothelial cells that make up the brain's vasculature or the BBB (*Pecam1*). We also identified the circadian clock gene, *Per1*, as being one of the most repressed genes in our list. Of particular interest, the DNA modifying proteins Dnmt3a, Tet2 and Tet3 were found, suggesting that the loss or reduced expression of epigenetic machinery could be a key contributor to stress-induced depression. Our data demonstrate that the continual worsening of 5hmC dynamics in susceptible animals is associated with the development of a compromised neurovasculature system and BBB. These phenotypes are reminiscent of early AD pathology and further support chronic stress as a major risk factor for AD. Subsequently, many of the genes from both groups, such as *G3bp2, Grhl1, Flt4 and Pecam1*, have all been previously associated with AD [413-416]. The genes that returned to baseline expression in the depression susceptible (**Figure 3.10:F**, Groups 3 and 4; top) pathway work in diverse biological functions such as ion transport (*Scn1a*), lipid metabolism (*Cyb5r3*), neurovasculature (*Slc4a5* and *Mgp*), neuroinflammation regulation (*Adora2b*) and excitatory synapse formation (*Syndig1*). Interestingly, we again identified the Klotho gene (*Kl*), which we previously found in 3-month CSDS susceptible animals. In the central nervous system, *Kl* is secreted into the CSF and acts as a circulating hormone allowing it to exert its biological functions (mediating the effects

of nitric oxide, oxidative stress, inflammation and calcium metabolism) over the brain [417]. More importantly, dysregulation of *Kl* has also been to neuropsychiatric disorders including MDD [371].

In depression resilient animals, 117 genes were found to continuously and concomitantly increase in 5hmC (**Figure 3.10:F,** Group 1; bottom) and several of the most drastic increases were observed in Ada, *Hpse2*, *Smoc2* and *Disc1*. Adenosine deaminases (*Ada*) have multiple functions, one of which is to protect the nervous system from high levels of adenosine that can occur when nervous system activity is enhanced like under conditions of chronic stress [418]. Both *Hpse2* and *Smoc2* function in the positive regulation of heparin sulfate. Heparan sulfates account for 50-90% of the residues in glycosaminoglycan side chains on glycocalyx, which coats the endothelial cells of the BBB, and reinforce impermeability to peripheral circulating molecules [419]. Generally, SNPs and mutations in *Disc1* are a well-established contributor to neuropsychiatric diseases. In the context of promoting resilience to depression, the increase in *Disc1* transcription in response to chronic stress could reflect an effort to manage the demands of its expansive interactome. Of the 269 genes that continued to decrease in 5hmC in resilient animals (**Figure 3.10:F**, Group 2; bottom), we identified two transporter proteins (*Slc2a8* and *Slc38a4*) that facilitate the transport of glucose and large amino acids across the BBB, respectively. Furthermore, 425 gain-loss and 729 loss-gain genes for the 5hmC return to baseline clusters (**Figure 3.10:F**, Groups 3 and 4; bottom) were observed. In these groups, we observed the metalloproteinase (*Mmp21*) and neuroinflammatory modulators *Tlr6* and *Alox5*. Importantly, prolonged activation of MMPs in the brain could weaken the BBB, over activate neuroinflammatory pathways and cause demyelination of neurons [420]. In addition, we found thymine DNA glyucosylase (*Tdg*) which functions in the base excision repair mechanism to regenerate an unmodified C in the DNA cytosine modification biochemical pathway [421]. In the depression susceptible model, we found a continual decrease in the DNA modifying proteins (Dnmt3a, Tet2 and Tet3) while resilient animals display TDG returning to baseline. These observations would imply a role for DNA modifying machinery in influencing stress-induced depression.

In conclusion, our analysis of 5mC and 5hmC alterations spanning across the acute, chronic and longitudinal time course provide a systematic and linear comparison of how DNA covalent modifications are regulated in response to various forms of stress. This analysis has shed light onto the molecular mechanisms of

how critical stress response genes are epigenetically regulated. Our final gene list represents the most likely ones to influence stress response and offer potential therapeutic targets for MDD.

3.4. Discussion

In this study, we investigated how the DNA modifications 5mC and 5hmC could contribute to the individual differences in stress susceptibility and resilience by comparing their genome-wide profiles between animals that underwent various durations of social defeat: acute (short-term), chronic (persistent), and longitudinal (re-exposure). We characterized CSDS in 3-month-old and 6-month-old naive adult male mice. In 3-month animals, 5mC and 5hmC work in parallel and were not found to distinguish between stress susceptible and resilient phenotypes, while 6-month animals displayed distinct 5mC and 5hmC enrichment patterns. Analyses of acute stress responses revealed a potential "priming" mechanism for 5mC that could foreshadow chronic stress response. The overlap of ASDS and CSDS differential regions revealed a potential 5hmC suppression of chromatin remodeling subunits in susceptible animals. On the other hand, resilient animals supported an epigenetic environment that promoted adult neuro- and glio-genesis. These findings insinuate that stress susceptibility may be predisposed if the epigenetic architecture is unable to rearrange during times of stress and that promotion of adult neurogenesis may serve as a critical factor for priming stress resilience. Comparison between CSDS and LSDS differential regions suggest that the enduring effects of social defeat affect differential biological process between susceptible and resilient animals. Susceptible animals display an upregulation of peripheral organ systems, likely induced from the acute re-exposure stress, and repression of nervous and neurovascular process whereas resilient animals express an upregulation of metabolic processes of mRNA transcripts. Finally, the stress-induced 5mC and 5hmC fluctuations across the ASDS-CSDS-LSDS time course demonstrate that resilient animals are not impervious to the negative consequences of chronic stress and susceptible animals do display some degree of neuroinflammatory and synaptic processes recovery. These findings are summarized in **Figure 3.11:**.

Because constant conditions were maintained across all social defeat paradigms, we systematically compare fluctuations in 5mC and 5hmC dynamics across different durations of stress. We observed an accumulation of 5mC in response to acute stress that we hypothesized could be a driving factor in the re-

establishment of adaptive homeostasis. Encouragingly, in our CSDS 5mC analysis, both susceptible and resilient animals show a significant decrease in their number of 5mC peaks and gained DMRs, compared to ASDS. However, susceptible animals gained nearly 1.5 times more DMRs compared to resilient. In addition, susceptible and resilient animals showed another significant increase in 5mC and gained DMRs in our re-exposure LSDS analysis. Accordingly, this suggests that the "re-exposure" stressor simulates acute stress, resulting in a sizeable 5mC increase that was also observed in ASDS. This is further supported by the minimal continual increase or decrease of 5mC in depression resilient animals observed over the ASDS-CSDS-LSDS time course. Taken together, our data suggests that large fluctuations in 5mC could be driving acute stress response, whereas 5mC loss could be necessary to reduce the "allostatic load" and achieve adaptive homeostasis. Furthermore, the degree of 5mC loss could be critical as stress persists in that resilient animals achieve 5mC levels closer to baseline. Regarding 5hmC, there were minimal alterations in its dynamics between acute, chronic and longitudinal stress. This possibly indicates that once 5hmC is added or removed from a region, it functions as a permanent epigenetic/transcriptomic architectural rearrangement in response to stress.

An emerging component of stress habituation is the role epigenetic memory is playing, as it can impact gene expression acutely or chronically. Epigenetic memory, more specifically transcriptional memory, requires changes in the chromatin architecture that then allow the cells to amount a more robust response upon re-exposure [422]. From our 5hmC ASDS analysis, we found that animals "primed" for stress susceptibility had reduced expression of chromatin remodeling complex subunits (*Arid1b, Arid2, Smarca2, Rest* and *Ring1*). Animals confirmed to be susceptible after CSDS also exhibited a concomitant 5hmC reduction and repression of chromatin (*Smarca2*) and histone (*Smyd1, Rcor2* and *Pwwp2a*) modifying genes. Furthermore, in our depression susceptible model where 5hmC continuously decreased along the ASDS-CSDS-LSDS continuum, the DNA modifying proteins Dnmt3a, Tet2 and Tet3 were found. Cumulatively, these data propose a mechanism whereby depression susceptibility could be connected to insufficient expression of the epigenetic machinery necessary to promote chromatin rearrangement, and acquire the epigenetic memory that would allow for a resilient stress response. To the contrary, resilient animals appear to be "primed" through the activation or protection of adult neuro/oligogenesis as independently observed in all three stress paradigms. Although

chronic stress is known to impair adult neurogenesis [393], studies have shown that if this process can be protected, it can actually defends against stress susceptibility [423, 424]. Our findings that stress resilient animals exhibit an upregulation of genes that facilitate adult neurogenesis and oligodendrocyte precursor cells support these findings and suggest that these mechanisms could serve as a critical contributor towards stress resilience.

The monoaminergic neurotransmitter hypothesis for MDD has dominated the field of study and still continues to be the primary source for available treatment options [425]. This is likely attributed to the fact that serotonin, norepinephrine and dopamine levels and their relationship with mood (focus/calmness, alternes/energy, anhedonia/pleasure, respectively) make them effective targets for treatment [426]. Interestingly, our data showed a strong bias towards GABAergic and glutamatergic synapse function, composition and release compared to other synapses, particularly in resilient animals. In particular, in the L_{RR} and CSDS resilient gained DMRs overlap, we observed an enrichment in synaptic vesicle cycling and ionotropic glutamate receptor signaling processes. During chronic stress, glutamate uptake and synaptic clearance are impaired by several factors: the loss of glutamate receptors on postsynapses and glial cells and/or impaired receptor cycling [427]. This results in a spillover effect whereby extrasynaptic glutamate receptors become activated and induce downstream cell death signaling [428]. Out data suggest that 5mC and 5hmC could be encouraging resilience by managing glutamatergic synapses and protecting against these neurotoxic effects. Importantly, both glutamate and GABA have been observed to contribute to MDD behaviors in prior experiments and are receiving more immediate attention as treatment options for MDD [425, 429].

In addition to GABA and glutamate, our results also uncovered a role for adenosine in modulating stress response. In the CNS, adenosine functions in a neuroprotective manner by preventing its own accumulation during ischemia, glutamate excitotoxicity or seizures [418]. Moreover, adenosine receptors are present in dopaminergic and glutamatergic neurons and co-localize with various neurotransmitter receptors. Intriguingly, we identified ASDS specific DMRs in the neuronal calcium binding protein, *Necab2*, the high-affinity adenosine receptor, *Adora2*, and the dopamine receptor subunit, *Drd2*. Both the dopaminergic and adenosinergic systems have been implicated in anxiety disorders [430]. Moreover, Necab2 interacts with and controls the cell surface expression and function of Adora2a [431], which directly interacts with Drd2 forming

heterodimers, dampening the binding affinity Drd2 has for dopamine [432]. This protein network insinuates a mechanism whereby Necab2—Adora2a interaction reduces Adora2a plasma membrane expression, creating an environment where more dopamine can bind to its receptor and potentially protect against anxiety-like behaviors. Further supporting the role of adenosine in stress-induced depression, we also identified three adenosine deaminases (*Ada*, *Adarb1* and *Adarb2*) in our CSDS and ASDS-CSDS-LSDS analyses. In addition to their neuroprotective properties, *Adarb1/2* target the pre-mRNA of the $GABA_A$ receptor [384] and serotonin receptor [381, 385] for A-to-I editing, drastically affect the affinity for neurotransmitter binding.

Our results indicate that stress susceptible animals show patterns of genetic dysregulation associated with compromised neurovasculature system, impaired BBB function, altered lipid metabolism, and microglia-mediated neuroinflammation. These phenotypes are reminiscent of early AD pathology and support the hypothesis that exposure to chronic stress is a major risk factor for AD [387]. In both concomitantly increasing and decreasing 5hmC susceptible genes identified from our CSDS analysis, we found many genes associated with later stage AD pathology. For example, *Prkag2*, *Dctn6*, *Bag3* and *Rer1* have been linked to Aβ-plaques [433-436], *Hs3st1* with neurodegeneration [437] and *Lgmn* and *Ppp2cb* with neurofibrillary tangles [438, 439]. Furthermore, the 5hmC dynamics across the ASDS-CSDS-LSDS time line revealed *G3bp2*, *Grhl1*, *Flt4* and *Pecam1*, all of which been previously associated with AD [100-103]. These findings point to an increase in the severity of AD-related gene expression changes across our epigenetic stress timeline. Overall, our results suggest that changes to the DNA modification landscape could potentially be part of the mechanism through which chronic stress creates the characteristic cellular pathology associated with AD in stress-susceptible individuals.

An interesting question not addressed in our analysis is how resilience is lost over time? In addition to the SS and RR animals identified in the LSDS analysis, we also observed a third group, resilient animals that became susceptible after stress re-exposure (data not shown). Initial investigations into differential regions and corresponding biological pathways and genes affected by stress induced alterations in 5mC and 5hmC were strikingly similar to RR and SS animals. This suggests that other mechanisms are likely at hand.

In conclusion, our study expands upon previous research and provides a much needed global and comprehensive perspective of the contributions from DNA modifications in stress-induced depression. Our

study is the first to simultaneously profile paired 5mC, 5hmC and transcriptome data on the genome-wide scale across three different durations of social defeat. This allowed us to investigate the dynamics of DNA modifications in relation to stress and offer potential therapeutic targets for MDD.

3.5. Figures and Legends

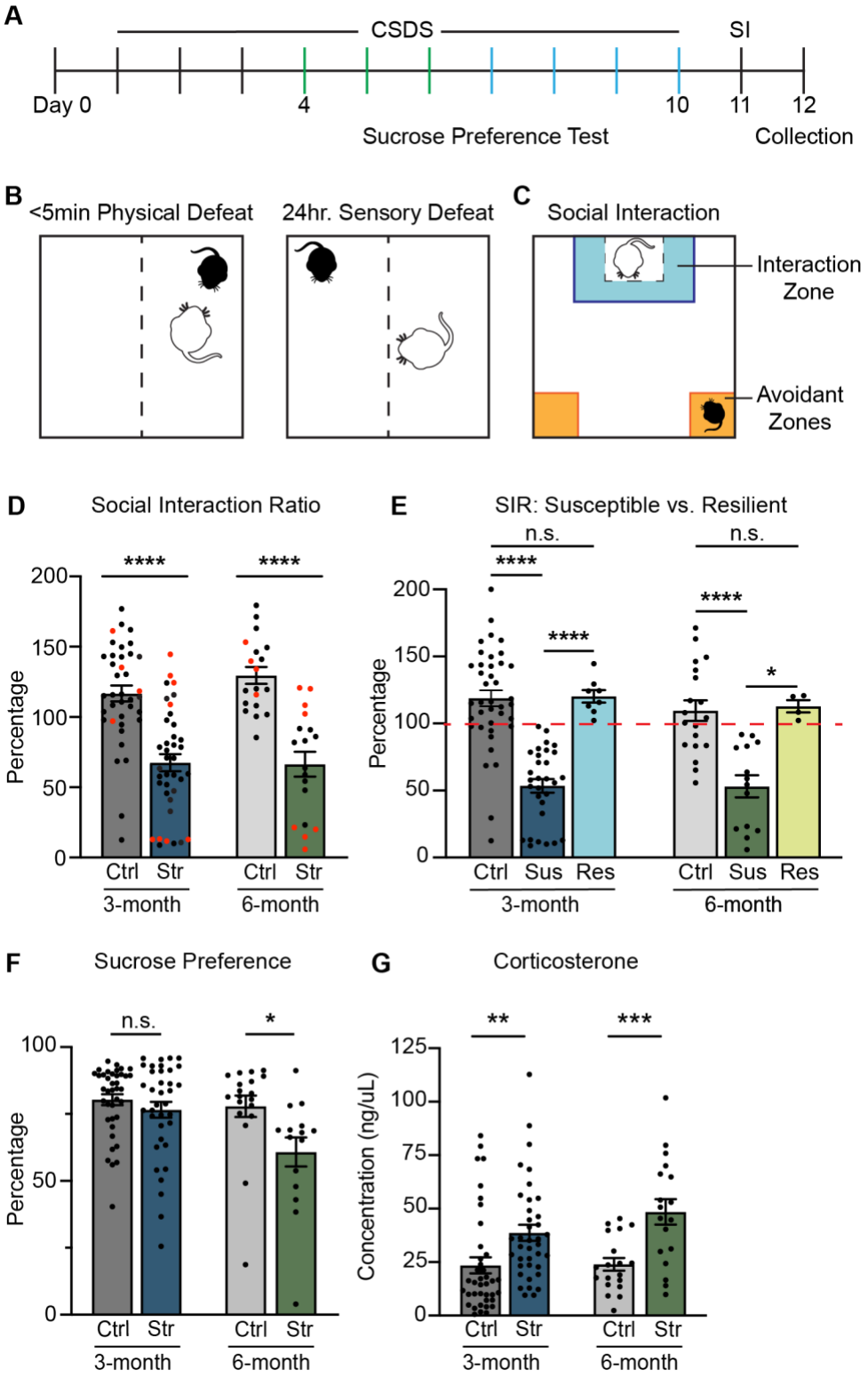

Figure 3.1: Chronic social defeat stress induces social avoidance in young and mature adult mice
A. Schematic of chronic social defeat stress (CSDS) paradigm. **B.** Schematic of social interaction (SI) behavior test. **C.** Experimental design of CSDS paradigm, behavior tests and tissue and blood collection. **D.** Defeated

3- and 6-month-old animals display a significant reduction in social behavior (*3-month: n = 39 Ctrl, n = 38 Str, independent cohorts = 4; 6-month: n = 19 Ctrl, n = 18 Str, independent cohorts = 2; Unpaired t-test, ****P < 0.0001 versus aged matched and littermate controls*). Red dots indicate randomly selected animals used for downstream 5mC and 5hmC enrichment and RNA-seq experiments. **E.** Social interaction ratios (SIR). Stress susceptible (SIR < 100) and stress resilient (SIR > 100) 3- and 6-month animals as indicated by the dashed red line *(*P < 0.05 and ****P < 0.0001 in Tukey's post hoc test after One-way ANOVA*). **F.** Sucrose preference testing for anhedonic-like behavior in 3- and 6-month animals (*Unpaired t-test, *P < 0.05*). **G.** Blood corticosterone was significantly elevated in both 3- and 6-month animals following CSDS (Unpaired t-test, **P < 0.01 and ***P < 0.001).

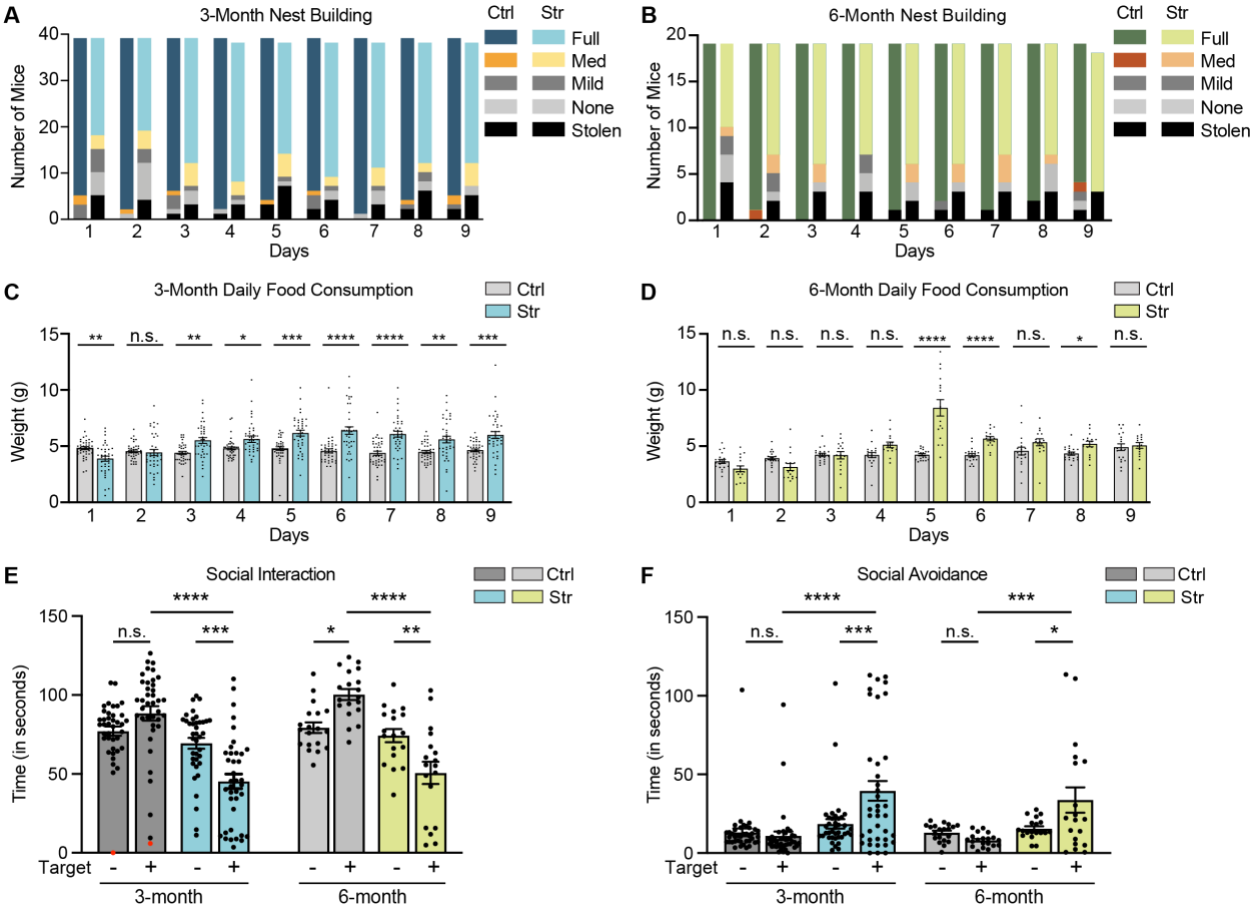

Figure 3.2: Chronic social defeat stress induces social avoidance in young and mature adult mice
A and **B.** 3- and 6-month animals daily nest building. **C and D.** 3- and 6-month animals daily food consumption *(*P < 0.05, **P < 0.01 and ***P < 0.001, ****P < 0.0001 in Holm-Sidak method for multiple comparisons after unpaired t-test).* **E** and **F.** Time spent in the interaction zone (**E**) and avoidant zone (**F**) when target was either absent (-) or present (+) *(*P < 0.05, **P < 0.01 and ***P < 0.001, ****P < 0.0001 in Tukey's post hoc test after One-way ANOVA*).

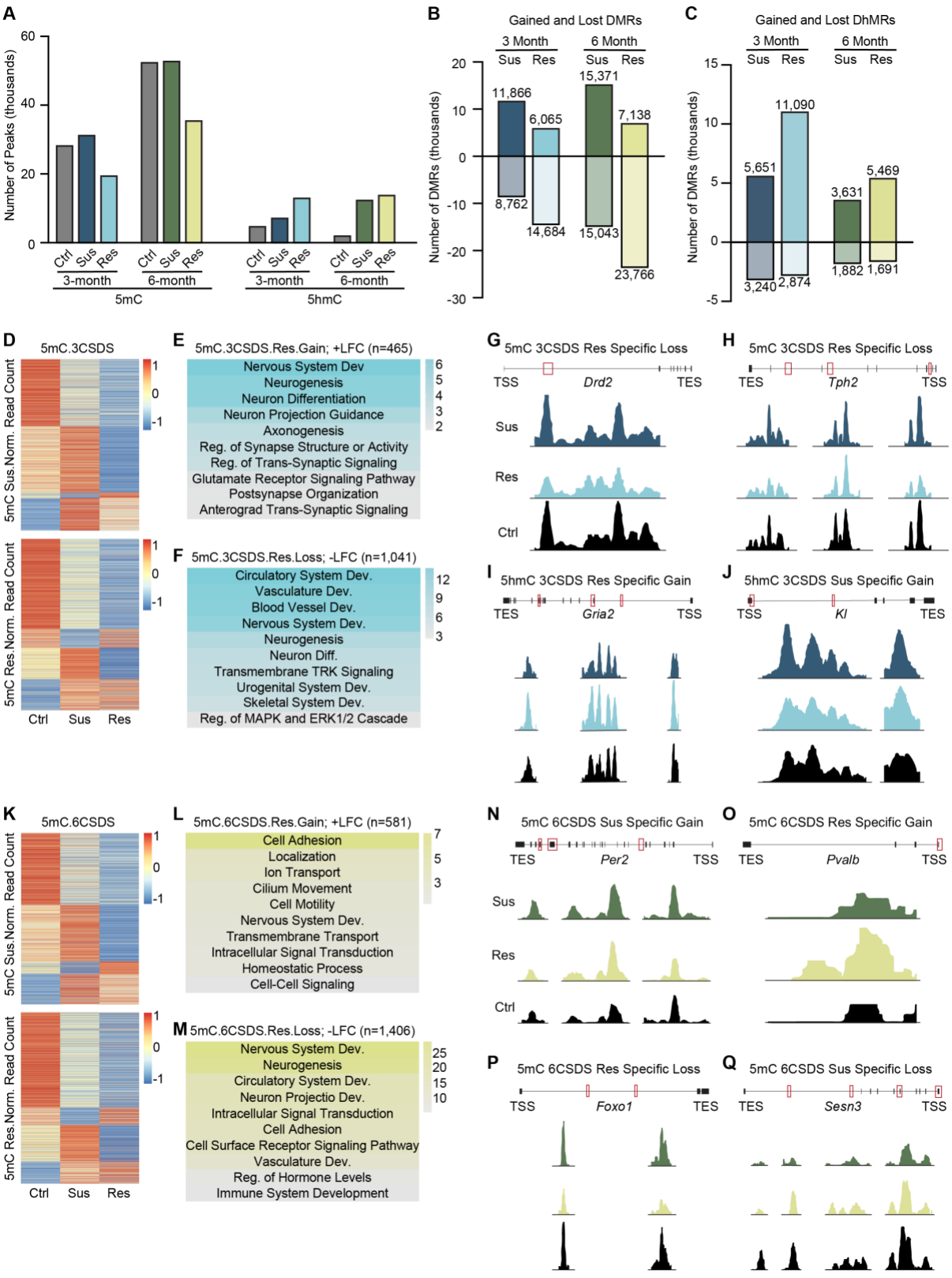

Figure 3.3: Characterization of susceptible and resilient chronic stress-induced DMRs and DhMRs
A. Number of 5mC and 5hmC peaks identified in control (Ctrl), susceptible (Sus) and resilient (Res) 3- and 6-month animals. **B** and **C.** Number of gain and lost 5mC (**B**) and 5hmC (**C**) peaks in stress susceptible and

resilient 3- and 6-month animals. **D** and **K.** Heatmap of susceptible and resilient DMRs from 3-month (**D**) and 6-month (**K**) chronically stressed animals, where the color scale represents normalized 5mC read counts. **E** and **F.** Representative gene ontology (GO) analysis of the genes from 3-month (**E** and **F.**) and 6-month (**L** and **M.**) stress resilient animals that either concomitantly increased in 5mC and gene expression (**E** and **L.** Gain; +LFC) or concomitantly decreased in 5mC and gene expression (**F** and **M.** Loss; -LFC). Color scale represents $-\log_{10}$ FDR. GO analysis for remaining 5mC and 5hmC analysis are in Tables 1 and 2. **G-J** and **N-Q.** Normalized 5mC or 5hmC counts at specific peak regions identified in 3-month (**G-J**) CSDS animals: *Drd*2 (**G**), *Tph2* (**H**), *Gria2* (**I**) and *Kl* (**J**) and 6-month (**N-Q.**) CSDS animals: *Per2* (**N**), *Pvalb* (**O**), *Foxo1* (**P**) and *Sesn3* (**Q**).

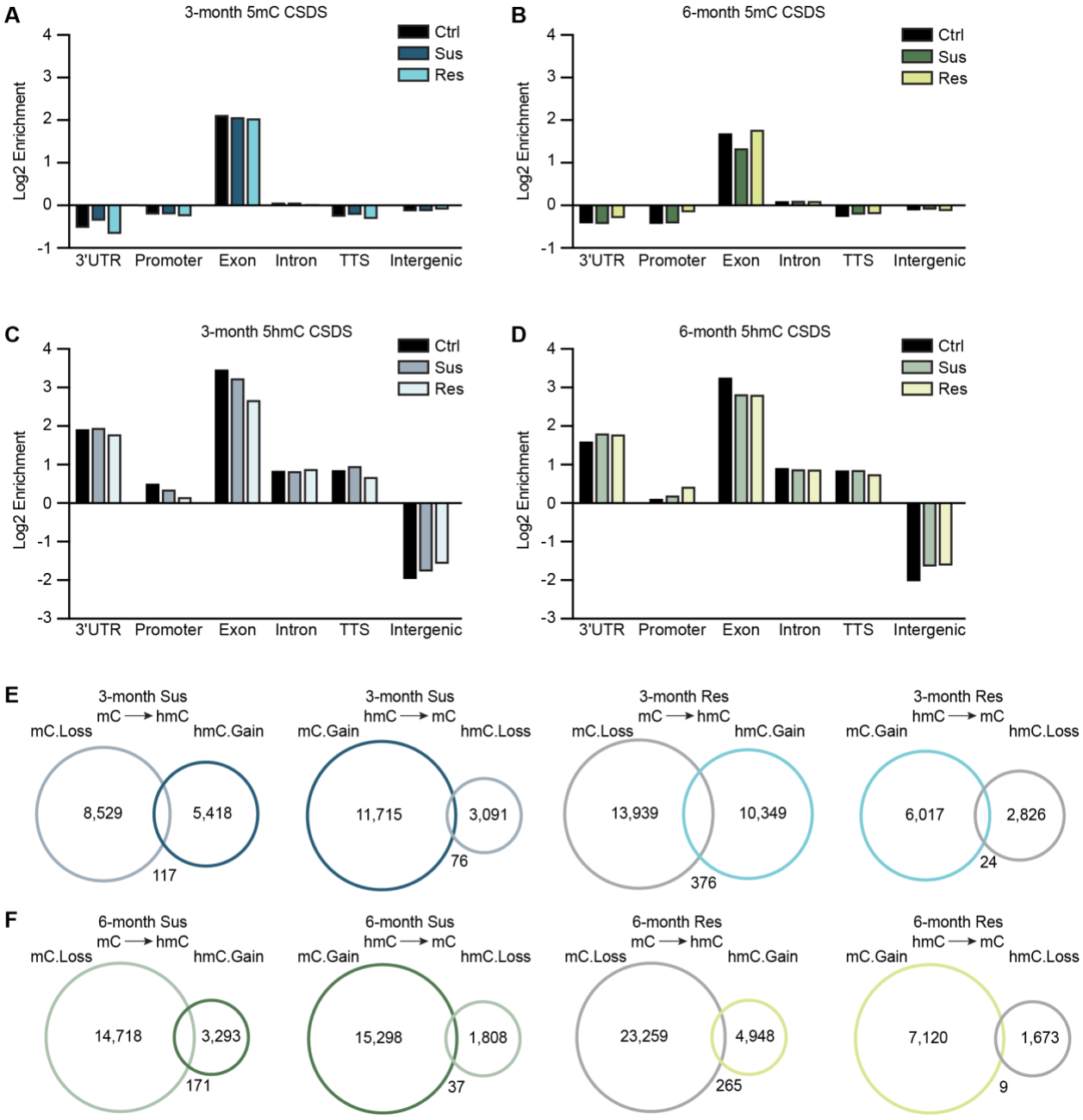

Figure 3.4: Characterization of susceptible and resilient chronic stress-induced DMRs and DhMRs
A-D. Enrichment of 5mC (**A** and **B**) and 5hmC (**C** and **D**) peaks at 3' and 5' untranslated regions (3' and 5'UTR), promoters, exons, introns, transcription termination sites (TTS) and intergenic regions. **E** and **F.** Overlap of 5mC and 5hmC differential regions demonstrating there is minor conversion of 5mC to 5hmC or vice versa.

Table 3.1: Biological processes corresponding to the gained/lost DMRs from 3- and 6-month susceptible and resilient animals.
GO analysis on the 5mC regions that either concomitantly increase (Gain; +LFC) or decrease (Loss; -LFC) in 5mC and gene expression (n = number of concomitantly increase/decrease genes). Table is a continuation from Figure 2.

Animal (Numb genes gain/loss)	5mC Gain; +LFC (-log 10 FDR)	5mC Loss; -LFC (-log 10 FDR)
3-month susceptible (n=947/281)	Nervous System Dev. (10.2) Neurogenesis (9.8) Generation of Neurons (7.8) Neuron Diff. (6.5) Cell Adhesion (6.1) Neuron Projection Dev. (3.2) Reg. of Trans-Synaptic Signaling (2.9) Synapse Org. (2.2) Cell Surface Receptor Signaling Pathway (2.1) Reg. of Neurotransmitter Levels (2.0)	Cell Adhesion (9.4) Cell Diff. (6.0) Cell Junction Org. (4.2) Nervous System Dev. (3.9) Neurogenesis (3.0) Circulatory System Dev. (2.9) Blood Vessel Morph. (2.8) Vasculature Dev. (2.8) Neuron Projection Morph. (1.7) Cell Surface Receptor Signaling Pathway (1.4)
3-month resilient (n=465/1,041)	Nervous System Dev. (6.4) Neurogenesis (5.7) Neuron Diff. (5.6) Neuron Projection Guidance (4.1) Axonogenesis (3.6) Reg. of Synapse Structure or Activity (3.3) Reg. of Trans-Synaptic Signaling (3.1) Glutamate Receptor Signaling Pathway (2.1) Post-synapse Org. (1.9) Anterograde Trans-Synaptic Signaling (1.8)	Circulatory System Dev. (14.1) Vasculature Dev. (12.9) Blood Vessel Dev. (12.8) Nervous System Dev. (11.9) Neurogenesis (8.6) Neuron Diff. (6.9) Transmembrane TRK Signaling (6.9) Urogenital System Dev. (6.7) Skeletal System Dev. (5.7) Reg. of MAPK and ERK1/2 Cascade (2.4)
6-month susceptible (n=1,014/697)	Transmembrane Transport (6.5) Small Molecule Metabolic Process (3.7) Response to Wounding (2.9) Homeostatic Process (2.8) Ion Transmembrane Transport (2.5) Leukocyte Activation (2.2) Reg. of Response to Stress (1.8) Activation Involved in Immune Response (1.8) Inflammatory Response (1.7) Reg. of Cytokine Production (1.5)	Nervous System Dev. (21.0) Neurogenesis (19.9) Neuron Diff. (17.4) Generation of Neurons (16.9) Neuron Projection Morph. (14.4) Circulatory System Dev. (13.4) Axon Guidance (12.4) Reg. of Cell Communication (12.1) Axonogenesis (11.9) Muscle Structure Dev. (9.3)
6-month resilient (n=581/1,406)	Cell Adhesion (7.2) Localization (3.5) Ion Transport (3.2) Cilium Motility (2.6) Cell Motility (2.6) Nervous System Dev. (2.4) Transmembrane Transport (2.2) Intracellular Signal Transduction (2.0) Homeostatic Process (1.9) Cell-Cell Signaling (1.3)	Nervous System Dev. (29.3) Neurogenesis (26.5) Circulatory System Dev. (18.2) Neuron Projection Dev. (17.7) Intracellular Signal Transduction (16.5) Cell Adhesion (15.5) Cell Surface Receptor Signaling Pathway (14.9) Vasculature Dev. (12.0) Reg. Hormone Levels (6.2) Immune System Dev. (5.3)

Table 3.2: Biological processes corresponding to the gained/lost DhMRs from 3- and 6-month susceptible and resilient animals.
GO analysis on the 5hmC regions that either concomitantly increase (Gain; +LFC) or decrease (Loss; -LFC) in 5hmC and gene expression (n = number of concomitantly increase/decrease genes). Table is a continuation from Figure 2.

Animal (Numb genes gain/loss)	5hmC Gain; +LFC (-log 10 FDR)	5hmC Loss; -LFC (-log 10 FDR)
3-month susceptible (n=712/343)	Nervous System Dev. (11.3) Reg. of Signal Transduction (9.5) Neuron Diff. (8.8) Neuron Projection Dev. (7.5) Cytoskeleton Org. (5.7) Macromolecule Mod. (4.3) Wnt Signaling Pathway (3.7) Homeostatic Process (3.5) Cell Surface Receptor Signaling (2.9) Neuromuscular Process (2.0)	Developmental Process (8.3) Cell Differentiation (5.6) Nervous System Dev. (5.5) Reg. of Signal Transduction (4.8) Cell Junction Org. (3.6) Cytoskeleton Org. (2.9) Phosphorylation (2.8) +Reg. of Cell Communication (2.4) Protein Modification Process (2.2) Macromolecule Localization (2.2)
3-month resilient (n=1,719/228)	Nervous System Dev. (23.6) Macromolecule Mod. (21.9) Neuron Projection Dev. (19.1) Neuron Diff. (16.7) Chemical Synaptic Transmission (13.4) Synapse Org. (12.3) Metabolic Process (10.8) Reg. of Dendrite Dev. (7.1) Synaptic Signaling (5.2) Vesicle Mediated Transport in Synapse (5.1)	Reg. of Cell Migration (6.5) Transmembrane Receptor TK Signaling (5.9) Cell Surface Receptor Signaling (5.4) Angiogenesis (5.0) Blood Vessel Morph. (4.1) Vasculature Dev. (3.8) Reg. of Cell Junction Assembly (3.8) Reg. of Cell Communication (3.7) Reg. of Catalytic Activity (3.0) Reg. of MAPK cascade (3.0)
6-month susceptible (n=313/213)	Reg. of Cell Communication (2.1) Reg. of Signaling (1.9) Reg. of Signal Transduction (1.7) Developmental Process (1.6) Reg. of Insulin Secretion Involved in Response to Glucose Stimulus (1.4) Wnt Signaling Pathway (1.4) Homeostatic Process (1.4) Reg. of Response to Stimulus (1.4) Cell-Cell Signaling by Wnt (1.3)	Intracellular Signal Transduction (6.8) Reg. of Cell Diff. (5.7) Nervous System Dev. (4.5) Protein Phosphorylation (4.4) Reg. of Macromolecule Mod. (4.2) Reg. of Catalytic Activity (4.1) +Reg. of Hydrolase Activity (3.9) Reg. of Cell Adhesion (3.5) Reg. of GTPase Activity (3.3) Reg. of Gene Expression (2.1)
6-month resilient (n=610/116)	Metabolic Process (7.8) Reg. of Cell Diff. (4.2) Protein Localization (4.2) Reg. of Cell Communication (3.8) Protein Modification Process (3.6) Catabolic Process (2.8) Nervous System Dev. (2.8) Cellular Homeostasis (2.3) Reg. of Cell Death (1.9) Energy Reserve Metabolic Process (1.6)	Reg. of Cellular Process (3.2) Reg. of Biological Process (3.1) Reg. of Metabolic Process (2.7) Reg. of Macromolecules (2.1) Reg. of Signaling (1.8) Reg. of Cell Communication (1.8) Dephosphorylation (1.5) Golgi Plasma Membrane Protein Transport (1.5) Vesicle Cytoskeletal Trafficking (1.5) Reg. of Dev. Process (1.3)

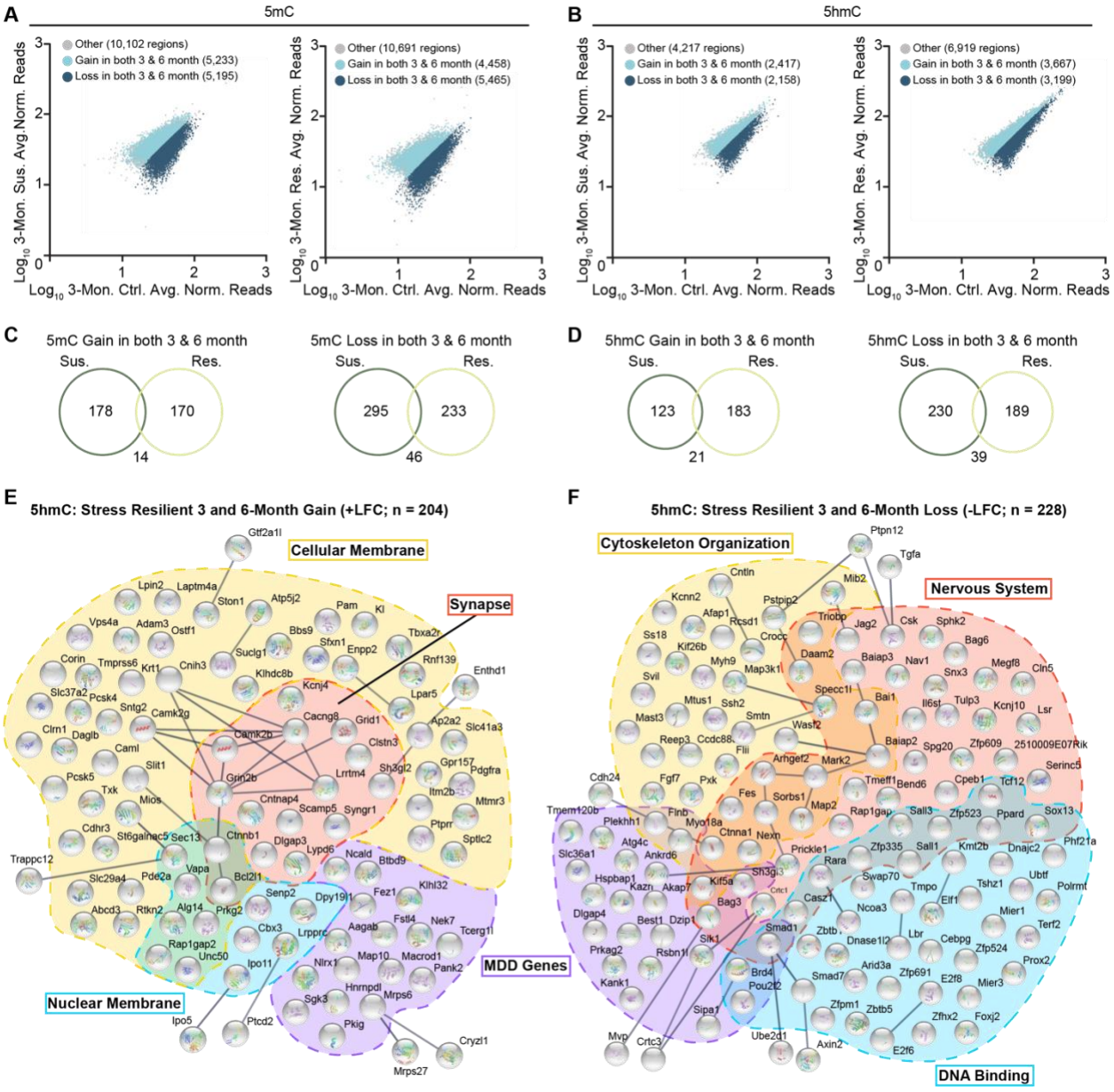

Figure 3.5: Comparison of shared DMRs and DhMRs in 3- and 6-month animals

A and **B.** 5mC (**A**) and 5hmC (**B**) regions that are gained or lost in 3-month susceptible or resilient animals. Colored dots indicate 6-month regions. **C** and **D.** Representative STRING analysis of the shared genes between 3- and 6-month stress resilient animals that either concomitantly increase (**C**) or decrease (**D**) in 5hmC and gene expression. Analysis of the remaining 5mC and 5hmC STRINGs are in Tables 3 and 4. **E** and **F.** The overlap of shared 3- and 6-month genes observed between susceptible and resilient animals.

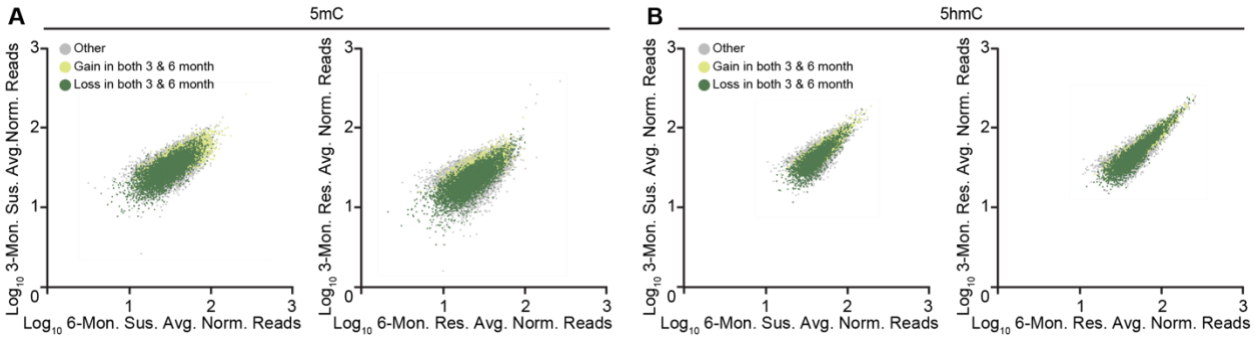

Figure 3.6: Comparison of shared DMRs and DhMRs in 3- and 6-month animals
A and **B.** 5mC (**A**) and 5hmC (**B**) regions that are gained or lost in both 3- and 6-month susceptible or resilient animals. 6-month CSDS animals gain and lose 5mC and 5hmC to the same magnitude as 3-month CSDS animals.

Table 3.3: Gene list of annotated DMRs shared between 3- and 6-month animals.
STRING analysis on the 5mC regions that are shared between 3- and 6-month susceptible or resilient animals that also showed either a concomitant increase (+LFC) or decrease (-LFC) in 5mC and gene expression. We then compared our gene list to a published list of MDD genes. Table is a continuation from Figure 3.

	No. of Genes in Data Set	Genes in Network	Biological Process
Stress Susceptible 3 and 6-month Loss -LFC	341	*Agtr1a, Akap13, Asxl2, Bicc1, Bmp7, Cacna1c, Cad, Cdkn1a, Col4a2, Dchs1, E2f8, Ece1, Eln, Epas1, Ephb3, Erbb2, Flt1, Gatad2a, Greb1, Heg1, Heyl, Hif3a, Loxl2, Megf8, Myh9, Myom1, Nebl, Nfatc1, Ngfr, Notch2, Nrp1, Pdlim5, Ppard, Prokr1, Ptch1, Rps6ka2, Sgcd, Smad1, Svep1, Syk, Tenm4, Zfpm1*	Heart/Circulatory System
		Abcc2, Ano1, Atp8a2, Cacna1c, Cacna1d, Cacna1h, Cnnm4, Glp1r, Grid2, Hephl1, Kcnb1, Kcnh7, Klhl3, Nfatc1, Panx2, Piezo1, Plch1, Rasa3, Rimbp2, Slc10a7, Slc16a7, Slc1a5, Slc4a11, Slc6a1, Slc6a11, Slc6a20a, Slc8a2, Slco2a1, Slco2b1, Spx, Steap3, Syk, Xker7, Trpc2	Ion Transport
		Abca2, Adam22, Adcy6, Atp8a2, Bcl2l11, Bmp7, Boc, Bsn, Btbd3, Celsr3, Clmn, Dchs1, Dclk1, Egflam, Eif2ak4, Ephb3, Erbb2, Farp1, Fat3, Fos, Foxo3, Foxo6, Gas7, Gatad2a, Gpr98, Grid2, Hap1, Heyl, Ikbkb, Ipmk, Itsn1, Kdr, Lpar3, Mdga1, Megf8, Mertk, Mturn, Myo7a, Nes, Ngfr, Nrp1, Obsl1, Pak4, Pdlim5, Plxnc1, Ppard, Prex1, Ptch1, Ptprs, Rab17, Rap1gap2, Ret, Sema3d, Slc6a11, Smad1, Sox13, Spen, Srrm4, St6gal1, Tenm4, Tmem108, Trim71, Tshr, Ttbk2, Vax1, Zeb1, Zswim4	Nervous System Development
		Abca2, Agtr1a, Akap13, Arfgap3, Bcl2l11, Bmp7, Ddx11, Dusp18, Elf2, Emp2, Ephb3, Erbb2, Farp1, Flt1, Git2, Gpr98, Gpsm2, Heg1, Hip1, Ikbkb, Itsn1, Kdr, Kiaa1324, Ksr1, Lats2, Lpar3, Nek10, Nes, Ngfr, Nrp1, Pak4, Parp8, Plxnc1, Prex1, R3hdml, Rabep2, Rap1gap2, Ret, Sash1, Sgsm1, St18, Stk10, Tbc1d1, Tbc1d2, Tbc1d4, Timp3, Tshr, Uaca	Catalytic Activity
		Akap13, Ankrd6, Cacna1d, Cdkn1a, Celsr3, Cep128, Clmn, Clstn2, Dclk1, Dhx8, Dip2a, Elfn2, Emp2, Flt1, Fos, Gpd2, Gpr3, Heg1, Heyl, Hip1, Itpkb, Itsn1, Jmjd1c, Kcnb1, Kcnh7, Kif13b, Klf12, Mturn, Nrp1, Olfm2, Osbpl3, Parp8, Pde1c, Phldb2, Plekhg3, Prima1, Ptch1, Ptprs, Rap1gap2, Rasa3, Rimbp2, Rnd3, Sgcd, Slc16a7, Smad1, Sorbs1, Spen, Srrm4, St18, St6gal1, Tmem151b, Tshr, Uaca, Wdr7	MDD
Stress Susceptible 3 and 6-month Gain +LFC	192	*Acot7, Adam32, Ak8, Aldh1l1, Ank3, Bckdhb, Ccdc91, Cd83, Cdc34, Celf2, Cpn1, Ctss, Dnah1, Dtnbp1, Echdc3, Efhd1, Fabp4, Fsip1, Fyb, Hao1, Hpn, Hydin, Kiz, Lck, Lsp1, Map2k5, Mlycd, Msra, N4bp3, Neu2, Ngf, Osbp2, Pdlim3, Pecr, Pex7, Plb1, Plod2, Prkag2, Rab3ip, Ranbp17, Rarres2, Rbm25, Rbm47, Rbp1, Rbpms, Rgs10, Rrp7a, Siglec1, Slc45a3, Smarca4, Soat2, Socs2, Spata19, Spatc1l, Taf1b, Tagln2, Tdrd9, Terf2, Thyn1, Wipi1, Zbtb20*	Endocrine Gland Expressing Genes
		Acot7, Bckdhb, Bend5, Ccdc91, Csrp1, Dnah1, Dnajc12, Efhd1, Foxp1, Hs3st4, Inpp5a, Kcnip3, Kiz, Map2k5, Mccc2, Ogfod3, Olfm1, Pdlim3, Pdpn, Prkag2, Rgs10, Scnn1a, Sftpc, Stk39, Taf1b, Vit, Zbtb20	MDD
Stress Resilient 3 and 6-month Loss -LFC	279	*Agtr1a, Alx4, Amotl1, Bbs2, Bmp6, Bmp7, Casq2, Ccm2l, Cdh5, Cntfr, Col4a1, Col4a2, Dab2, Dchs1, Dlx3, Dtnbp1, Eln, Epas1, Ets1, Fgf1, Fli1, Flt1, Frem2, Gpr116, Gpr124, Heg1, Hhip, Hmga2, Kat2b, Kdr, Lmod3, Ltbp1, Megf10, Myh11, Myom1, Ncor2, Nfatc1, Ngfr, Notch1, Pdlim5, Pgm5, Prdm1, Ptprb, Ryr3, Sall1, Stat1, Tead1, Tfap2a, Tmem67, Tnfrsf1a, Tpm2, Trp53bp2*	Heart/Circulatory Development
		Bach2, Bmp6, Cd276, Cdh17, Chst3, Crtc3, Csf1, Dab2, Epas1, Ets1, Fli1, Flt1, Fyn, Gpr116, Hck, Ikzf1, Ikzf3, Il31ra, Jarid2, Kdr, Mitf, Mpl, Nbeal2, Nfatc1, Nod1, Orai1, Pdcd1lg2, Plcg2, Prdm1, Rtp4, Stat1, Stat2, Syk, Tirap, Usp18	Immune Response
		Ankrd6, Cacna1d, Cacng4, Capn2, Ccdc88c, Cdh5, Chst3, Col4a1, Col4a2, Csf1, Csnk1g2, Drd2, Ezr, Fam83d, Fgf1, Flt1, Fyn, Fzd6, Gdnf, Gng12, Gpr124, Hck, Hmga2, Igfbp1, Insrr, Irs1, Itga6, Kank2, Kdr,	Signaling Pathways (PI3k-Akt, MAPK, ERK1/2,

		Lamb2, Lamc1, Map3k1, Ncf4, Ncor2, Nfatc1, Ngfr, Nod1, Notch1, Osmr, Pde8a, Pik3ap1, Plcg2, Ptpn7, Rps6ka1, Sh2d2a, Spry4, Stat1, Syk, Timp3, Tirap, Tnfrsf1a, Tnn, Trp63	Tyrosine kinase, Wnt, Steroid Hormone)
		Adarb2, Amotl1, Ankrd6, Bcas1, Cabin1, Cacna1d, Cacng4, Cald1, Cat, Ccdc91, Cdk5rap2, Chst3, Clip4, Ets1, Ezr, Fat1, Filip1l, Flt1, Hsd11b1, Igf2bp1, Iqsec3, Kndc1, Lamc1, Lrch1, Myh11, Pde1c, Plcg2, Prdm1, Prkcb, Ptr, Rcbtb1, Rnd3, Sbk1, Sdc4, Spry4, Tns3, Tph2, Tshr	MDD
Stress Resilient 3 and 6-month Gain +LFC	184	*Aadat, Amph, Cryz, Gap43, Hyal2, Mocs1, Mpo, Mtg1, Pon1, Popdc2, Prkar1b, Ptprf, Rxra, Scarb2, Syt17, Zfyve28*	Anion Binding
		Acss1, Actr3b, Ak5, Ak7, Atp9a, Camk2b, Cdkl4, Chd5, Clcn4-2, Fgr, Galk1, Gck, Gucy2c, Hunk, Iars2, Iqca, Mcm2, Myh6, Myo15, Nek7, Nlrc3, Nlrp1a, Nuhpl, Pfkm, Prkce, Prkg2, Sgk3, Slfn9, Trpm4, Ulk4	ATP Binding
		Amph, Bcap29, Fez2, Inpp5a, Mvb12b, Nek7, Nkx6-3, Sgk3, Tmem259, Tpd52	MDD

Table 3.4: Gene list of annotated DhMRs shared between 3- and 6-month animals.
STRING analysis on the 5hmC regions that are shared between 3- and 6-month susceptible or resilient animals that also showed either a concomitant increase (+LFC) or decrease (-LFC) in 5hmC and gene expression. We then compared our gene list to a published list of MDD genes. Table is a continuation from Figure 3.

	No. of Genes in Data Set	Genes in Network	Biological Process
Stress Susceptible 3 and 6-month Loss -LFC	269	*Bag3, Cbl, Csnk1d, Daam1, Dag1, Dagla, Dzip1, Fam53b, Fat4, Fgf7, Grin2d, Hnf1a, Ift172, Il17rd, Itga2, Jag2, Lrp6, Mark1, Nedd9, Nlk, Pkd1, Plxna1, Ptk2, Rap2a, Sel1l, Sema4d, Sort1, Sufu, Tgfbr2, Tle3, Tnks, Usp15*	Cell Surface Receptor Signaling Pathway
		Aak1, Adarb1, Adat3, Asxl1, Brap, Camk1d, Cand1, Ccnd3, Cdk19, Csnk1d, Cttnbp2nl, Dcst1, Dyrk1a, Egln1, Epc1, Galnt2, Hdac4, Hnf1a, Kansl1, Kdm4a, Kdm5b, Kdm6b, Klhl21, Klhl24, Klhl3, Klhl42, Map3k2, Mark1, Mast4, Morc3, Nlk, Pkd1, Ptpn1, Ptprb, Pxk, Setd7, Sik1, Srpk1, St3gal2, St6gal1, Stat5b, Stk4, Tmtc2, Tnks, Trrap, Ube2h, Ubr5, Usp10, Usp15, Usp19, Usp24, Yeats2	Macromolecule Modification
		Adra1b, Akap12, Dag1, Dstyk, Dusp4, Ece1, Fn1, Hmgcr, Iqgap1, Map3k14, Map3k2, Map3k5, Mfhas1, Mid1, Mink1, Nod1, Pik3r5, Ptpn1, Rap2a, Rara, Sema4c, Spred3, Timp3, Trib2, Wwc1	MAPK and ERK1/2 Signaling Cascade
		Ak4, Ankrd27, Arhgef10, Atrn, Avil, Bag3, Bhlhe40, Btbd3, Cic, Clmn, Dagla, Dock10, Dock7, Dpysl3, Fat4, Gnpat, Hspa5, Ift172, Jag2, Kif5a, Lrp6, Ncan, Omp, Sdk1, Serinc5, Slc38a2, Sox5, Sufu, Tmem108, Zfp365, Zfp609	Nervous System
		Aak1, Agfg1, Ank1, Ankrd6, Arl10, Asxl1, Bag3, Cadps, Camk1d, Ccnd2, Cdk19, Clmn, Dcp2, Dstyk, Dusp4, Dzip1, Entpd1, Fbxo28, Flnb, Galnt2, Heg1, Hmgcr, Hspa5, Iqgap1, Itga2, Itpkb, Kank1, Kif5a, Klhl24, Map3k, Mcf2l, Mink1, Ncan, Nedd9, Osbpl3, Pde4a, Pdzd2, Pfkfb3, Plxna1, Ptpn1, Sik1, Slc4a4, Sox5, St6gal1, Synpo2, Trib2	MDD
Stress Susceptible 3 and 6-month Gain +LFC	144	*Ascc1, Bag5, Cct8, Cd1d1, Celf2, Celf4, Corin, Cotl1, Ctnnbip1, Ddx24, Dnajc8, Eefsec, Enoph1, Fam192a, Hsf5, Insm2, Kcnk2, Keap1, Lpin1, Lrpprc, Map2k5, Mark2, Mef2c, Mgmt, Ndufab1, Nmnat3, Nosip, Nsmce2, Nudt3, Pard6g, Pdlim7, Ppargc1b, Ppp2cb, Prkag2, Pwwp2a, Qsox2, Rab3ip, Rbm25, Rcor2, Sap30bp, Smarca2, Smyd2, Spdef, Tacc2, Taf3, Taf9, Tcf7l1, Terf2, Tjp3, Tkt, Trappc12, Txk, Usp42, Vrk1, Wdr70, Xab2, Xrcc5, Ybx3, Yeats4, Zbtb8a, Zc3h10, Zfp30, Zfp536*	Nuclear Localization
		Adora1, Bloc1s5, Caml, Cspg5, Dctn6, Emid1, Fam110b, Fars2, Fpgs, H2-DMa, Hs3st1, Idh2, Lgmn, Lipc, Mthfd1l, Oca2, Pcsk5, Pde9a, Rab4a, Rap1gap, Rer1, Rffl, Scnn1a, Slc37a1, Slc38a9, Slc48a1, Stambpl1, Tbxas1, Trf, Wnt3, Wnt4, Zdhhc20	Membrane Bound Organelles
		Bckdhb, Celf2, Dtnb, Emid1, Fbxo9, Kiz, Map2k5, Mark2, Nudt3, Oca2, Ppargc1b, Prkag2, Scnn1a, Slc38a9, Smyd2, Tspan3, Vrk1, Yeats4, Zc3h10	MDD
Stress Resilient 3 and 6-month Loss -LFC	228	*Arhgef2, Bai1, Baiap2, Ccdc88c, Cntln, Crocc, Ctnna1, Daam2, Fes, Fgf7, Flii, Flnb, Kcnn2, Kif26b, Kif5a, Map2, Map3k1, Mark2, Mast3, Mib2, Mtus1, Myh9, Myo18a, Nexn, Pstpip2, Pxk, Rcsd1, Sorbs1, Specc1l, Ss18, Triobp, Wasf2*	Cytoskeleton Organization
		2510009E07Rik, Arhgef2, Bag3, Bag6, Bai1, Baiap2, Baiap3, Bend6, Casz1, Cln5, Cpeb1, Crtc1, Csk, Ctnna1, Daam2, Fes, Il6st, Jag2, Kcnj10, Kif5a, Lsr, Map2, Mark2, Megf8, Nav1, Nexn, Ppard, Prickle1, Rap1gap, Rara, Sall1, Sall3, Serinc5, Sh3gl3, Smad1, Snx3, Sorbs1, Sox13, Specc1l, Spg20, Sphk2, Tcf12, Tmeff1, Triobp, Tulp3, Zfp335, Zfp523, Zfp609	Nervous System
		Akap7, Ankrd6, Atg4c, Bag3, Best1, Brd4, Daam2, Dlgap4, Dzip1, Flnb, Hsphap1, Kank1, Kazn, Kif5a, Mark2, Myo18a, Nexn, Plekhh1, Pou2f2, Prkag2, Rsbn1l, Sh3gl3, Sik1, Slc36a1, Smad1, Sorbs1, Tmem120b	MDD

Stress Resilient 3 and 6-month Gain +LFC	204	*Abcd3, Adam3, Ap2a2, Atp5j2, Bbs9, Camk2g, Caml, Cdhr3, Clrn1, Cnih3, Corin, Daglb, Enpp2, Gpr157, Itm2b, Kl, Klhdc8b, Krt1, Laptm4a, Lpar5, Lpin2, Mios, Mtmr3, Ostf1, Pam, Pcsk4, Pcsk5, Pde2a, Pdgfra, Ptprr, Rnf139, Rtkn2, Sfxn1, Slc29a4, Slc37a2, Slc41a3, Slit1, Sntg2, Sptlc2, St6galnac5, Ston1, Suclg1, Tbxa2r, Tmprss6, Txk, Vps4a*	Cellular Membrane
		Alg14, Bcl2l1, Cbx3, Ctnnb1, Dpy19l1, Ipo11, Lrpprc, Prkg2, Rap1gap2, Sec13, Senp2, Unc50, Vapa	Nuclear Membrane
		Bcl2l1, Cacng8, Camk2b, Clstn3, Cntnap4, Ctnnb1, Dlgap3, Grid1, Grin2b, Kcnj4, Lrrtm4, Lypd6, Scamp5, Sh3gl2, Syngr1	Synapse
		Aagab, Btbd9, Dpy19l1, Fez1, Fstl4, Hnrnpdl, Itm2b, Klhl32, Macrod1, Map10, Mrps6, Mtmr3, Ncald, Nek7, Nlrx1, Pank2, Pdgfra, Pkig, Ptprr, Rap1gap2, Sgk3, Sh3gl2, Sptlc2, Syngr1, Tceg1l	MDD

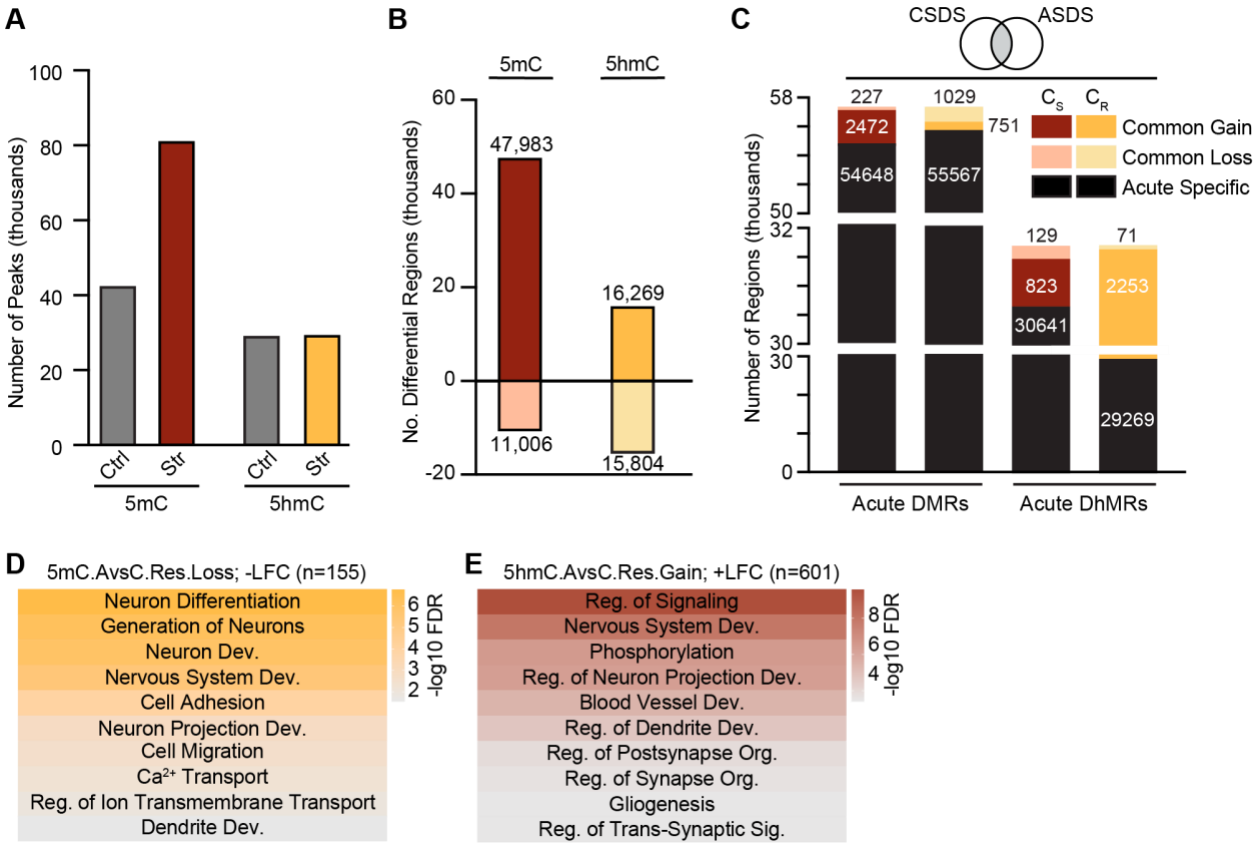

Figure 3.7: Characterization of DMRs and DhMRs from acute social defeat stress
A. Number of 5mC and 5hmC peaks identified in control and acutely stressed animals. **B.** Number of gained and lost 5mC and 5hmC peaks. GO analysis of the gain or loss of DMRs and DhMRs are in Table 5. **C.** Overlap between ASDS DMRs or DhMRs with CSDS susceptible or resilient specific DMRs or DhMRs. **D** and **E.** Representative GO analysis of the common genes identified between ASDS stressed and CSDS resilient mice that either concomitantly decreased in 5mC and gene expression (**D.** Loss; -LFC) or concomitantly increased in 5hmC and gene expression (**E.** Gain; +LFC). Color scale represents -$\log_{10}$ FDR. GO analysis for remaining 5mC and 5hmC analysis are in Table 6.

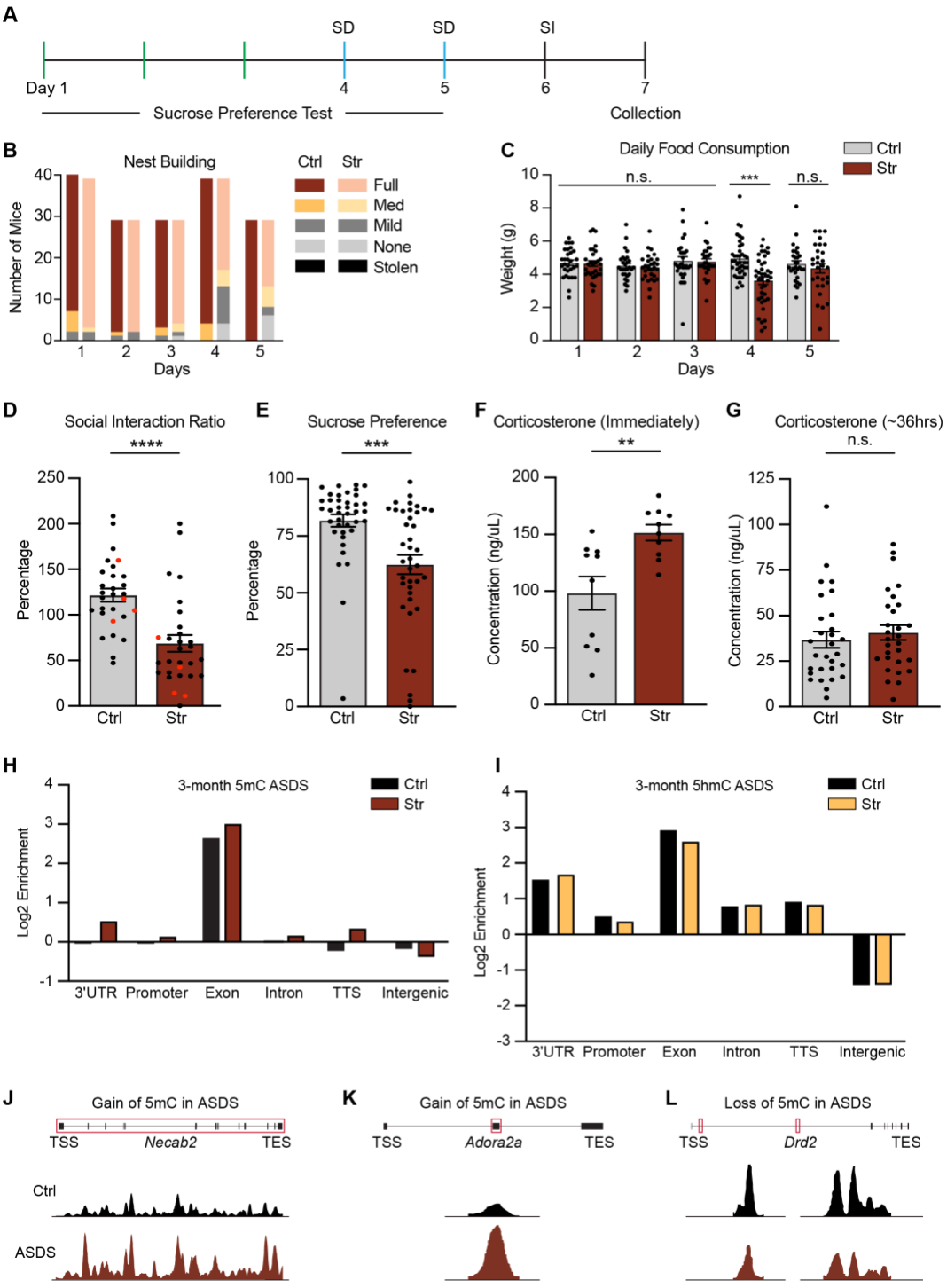

Figure 3.8: Acute social defeat stress is sufficient to induce social avoidant-like behavior
A. Experimental design of ASDS paradigm, behavior tests and tissue and blood collection. **B.** Daily nest building. **C.** Daily food consumption *(***P < 0.001 in Holm-Sidak method for multiple comparisons after unpaired t-test).* **D.** ASDS causes a social avoidant-like phenotype. (Unpaired t-test, *****P < 0.0001*). Red dots indicate randomly selected animals used for downstream 5mC and 5hmC enrichment and RNA-seq experiments. **E.** Sucrose preference (*Unpaired t-test, ***P < 0.001*). **F** and **G.** Blood corticosterone was significantly elevated in stressed animals immediately following ASDS (**F**), but not 36 hours post stress (**G**) (*Unpaired t-test, **P < 0.01*). **H-I.** Enrichment of 5mC (**H**) and 5hmC (**I**) peaks at 3' and 5' untranslated regions (3' and 5'UTR), promoters,

exons, introns, transcription termination sites (TTS) and intergenic regions. **J-L.** Normalized 5mC counts at peak regions identified in ASDS animals: *Necab2* (**J**), *Adora2a* (**K**), *Drd2* (**L**).

Table 3.5: Biological processes corresponding to the ASDS gained/lost DMRs and DhMRs.
GO analysis of the genes from acutely stressed animals that either concomitantly increased in 5mC/5hmC and gene expression (Gain; +LFC) or concomitantly decreased in 5mC/5hmC and gene expression (Loss; -LFC). n = number of concomitantly increase/decrease genes. Italicized terms indicate those processes found not to be significant. Table corresponds to Figure 4.

DNA Modification (Numb genes gain/loss)	Gain; +LFC (-log 10 FDR)	Loss; -LFC (-log 10 FDR or genes)
5mC (n=2,914/248)	Nervous System Dev. (9.5) Phosphorylation (8.3) Ion Transport (7.6) Homeostatic Process (7.5) Chemical Homeostasis (6.6) Reg. of Response to Stress (4.7) Reg. of Cell Death (4.3) Vesicle-Mediated Transport (4.2) Humoral Immune Response (4.1) Response to Wounding (4.1) Vasculature Dev. (3.9)	*Signal Transduction (55 genes)* *Response to Stress (27)* *Cell Surface Receptor Signaling (23)* *Nervous System Dev. (20)* *Immune Response (15)* *Reproductive Processes (15)* *Reg. of Heart Rate (2)* *Muscle Contraction (1)* *Blood Pressure Reg. (0)*
5hmC (n=963/900)	Metabolic Process (9.8) Reg. of Signaling (8.8) Protein Localization (5.2) Reg. of Response to Stimulus (4.8) Protein Modification Process (4.6) Glycerolipid Metabolic Process (3.8) Nervous System Process (3.7) Hair Follicle Dev. (3.0) Respiratory System Dev. (2.9) Molting Cycle Process (2.8) Skin Epidermis Dev. (2.8) Response to Hormone (2.1)	+Reg. of RNA Biosynthetic Process (2.8) +Reg. of DNA-Templated Transcription (2.8) Reg. of Signaling (2.0) Macromolecule Modification (2.0) Reg. of Transcription by RNA pol ll (1.6) Reg. of Catecholamine Secretion (1.4) *-Reg. of MAPK Cascade (1.2)* *Histone Modification (1.2)* *Vascular Process in Circulatory System (0.9)* *Immune Response (0.9)* *NIK/NF-kappaβ Signaling (0.8)*

Table 3.6: Identification of genes that could act as "primers" for stress response.
GO and gene analysis of the overlapped genes found between ASDS DMRs or DhMRs and CSDS susceptible or resilient specific DMRs or DhMRs. Table corresponds to Figure 4.

ASDS	CSDS Specific File	No. of Genes in Data Set	Biological Process (-log10 FDR) or Genes
Stress Gain 5mC	Sus. Gain 5mC	420	Circulatory System (4.0) Blood Vessel Morphogenesis (3.1) Vasculature Development (3.1) Response to Wounding (2.5) Cell Junction Organization (2.3) Enzyme-Linked Receptor Protein Signaling (2.2) Extracellular Matrix Organization (1.9) Nervous System Development (1.7) Cell Adhesion (1.7) +Regulation of Catalytic Activity (1.5) Synapse Organization (1.5)
Stress Loss 5mC	Sus. Loss 5mC	41	*0610043K17Rik, 1700010I14Rik, 4930539M17Rik, Adam2, Amotl1, Ankrd55, Cacna2d3, Cpped1, Crnde, Dnah8, Ebf1, Ephx2, Farp1, Gabrg3, Gm10635, Grm8, Itga2, Itgad, Mertk, Myo3a, Optc, Osbpl9, Pan2, Pard3, Pcdh15, Pde9a, Pou6f2, Ppp1r1c, Prkce, Prmt3, Ptpro, Rec114, Sec24d, Smoc1, Sorcs3, Spon1, Srgap1, Stk32b, Trdmt1, Ush2a, Zfp521*
Stress Gain 5mC	Res. Gain 5mC	136	*A730036I17Rik, Abca4, Adamts17, Ankrd44, Arhgef10l, Arhgef3, Asap1, Atp9a, Atrnl1, Bcar3, Brca2, Cadm3, Camta1, Capn9, Catsperg1, Cdc42bpg, Col5a1, Creb5, D830013O20Rik, Dagla, Dapk2, Dcaf4, Disc1, Dock2, Dock5, Dock8, Dysf, E330021D16Rik, Efcab6, Erc2, Esrrb, Fam221b, Fancd2, Fcgbp, Fli1, Fto, Gdpd5, Gm6249, Gna15, Gng2, Gpr68, Grhl2, Grik3, Haao, Hebp1, Hs3st3b1, Hunk, Hydin, Kalrn, Kank2, Kcnb2, Kcnk10, Kif26a, Kit, Ksr2, Lama4, Lmna, Lnx1, Lrig3, Lrrc28, Ltbp2, Megf11, Mgmt, Micu1, Morc1, Mras, Mvb12b, Myo16, Myrip, Naaa, Nlrp1a, Npc1, Nuak1, Nubpl, Nudt12, Nxph1, Osbpl3, Pde6c, Pex5, Phldb3, Piezo2, Plxnc1, Ppl, Prdm16, Prex1, Prkaa1, Ptprf, Rfx8, Rgs3, Rhbdd1, Rnf144b, Rora, Rrp9, Scfd1, Scgn, Sdk2, Shc3, Shq1, Slc13a3, Slc1a7, Slc22a1, Slc45a1, Slit1, Smad3, Smyd3, Snx18, Snx8, Sohlh2, Sorcs2, Spag16, Spats2l, St3gal4, Ston2, Stox2, Susd1, Swap70, Syne2, Tanc1, Tecta, Tgfbr2, Tmem117, Tmem178b, Tnfaip8, Tns1, Tpcn2, Trappc11, Trim47, Trp63, Ttc23, Usp43, Wdr63, Wdr70, Wnt7b, Wwc2, Zbtb7c, Zc3h18*
Stress Loss 5mC	Res. Loss 5mC	155	Neuron Differentiation (6.8) Generation of Neurons (6.2) Neuron Development (6.0) Nervous System Development (5.4) Cell Adhesion (4.0) Neuron Projection Development (2.8) Cell Migration (2.6) Ca^{2+} Transport (2.2) Regulation of Ion Transmembrane Transport (2.0) Dendrite Development (1.6)
Stress Gain 5hmC	Sus. Gain 5hmC	261	-Regulation of Response to Stimulus (2.9) Regulation of Fat Cell Differentiation (2.7) Enzyme-Linked Receptor Protein Signaling (2.6) Homeostatic Process (2.4)

			Regulation of K^+ Transmembrane Transport (2.0) Response to TGFβ (1.8) Neuron Projection Development (1.8) Blood Vessel Development (1.6) Ion Transport (1.5) Regulation of Smooth Muscle Cell Migration (1.4)
Stress Loss 5hmC	Sus. Loss 5hmC	53	*2410004B18Rik, Actn4, Acvr2b, Ahsa2, Alkbh2, Arhgap10, Arid1b, Arid2, Bcr, Chst11, Chst12, Cmip, Coro1c, Daam1, Ddah1, Dnm3, Eif3h, Eif4g3, Eml1, Ephb1, Farp1, Foxj2, Grap2, Katnal1, Lims2, Lrrc1, Lrrc42, Map4k4, Mapre2, Mtcl1, Mtus2, Myl12b, Prep, Prrc2c, Rest, Ring1, Rnf126, Rptor, Serac1, Sik3, Slc12a1, Slc16a7, Smarca2*, *Spata13, Spock1, Tenm3, Thrsp, Ubr5, Vangl1, Zdhhc14, Zdhhc18, Zfp462, Zfp865*
Stress Gain 5hmC	Res. Gain 5hmC	601	Regulation of Signaling (9.6) Nervous System Development (8.0) Phosphorylation (6.5) Regulation of Neuron Projection Development (6.3) Blood Vessel. Development (5.5) Regulation of Dendrite Development (4.7) Regulation of Post-Synapse Organization (3.9) Regulation of Synapse Organization (3.7) Gliogenesis (3.4) Regulation of Dendrite Morphogenesis (3.4)
Stress Loss 5hmC	Res. Loss 5hmC	26	*Atxn7l1, Bcdin3d, Camkmt, Chst11, Chsy1, Dst, Gna12, Lrrn1, Maml3, Map4k4, Matn4, Mfsd5, Msantd1, Park7, Picalm, Prkce, Ric8b, Rnf114, Rnpep, Scn8a, Sept8, Slc9a9, Soga1, Tet3, Zfp513, Zfp710*

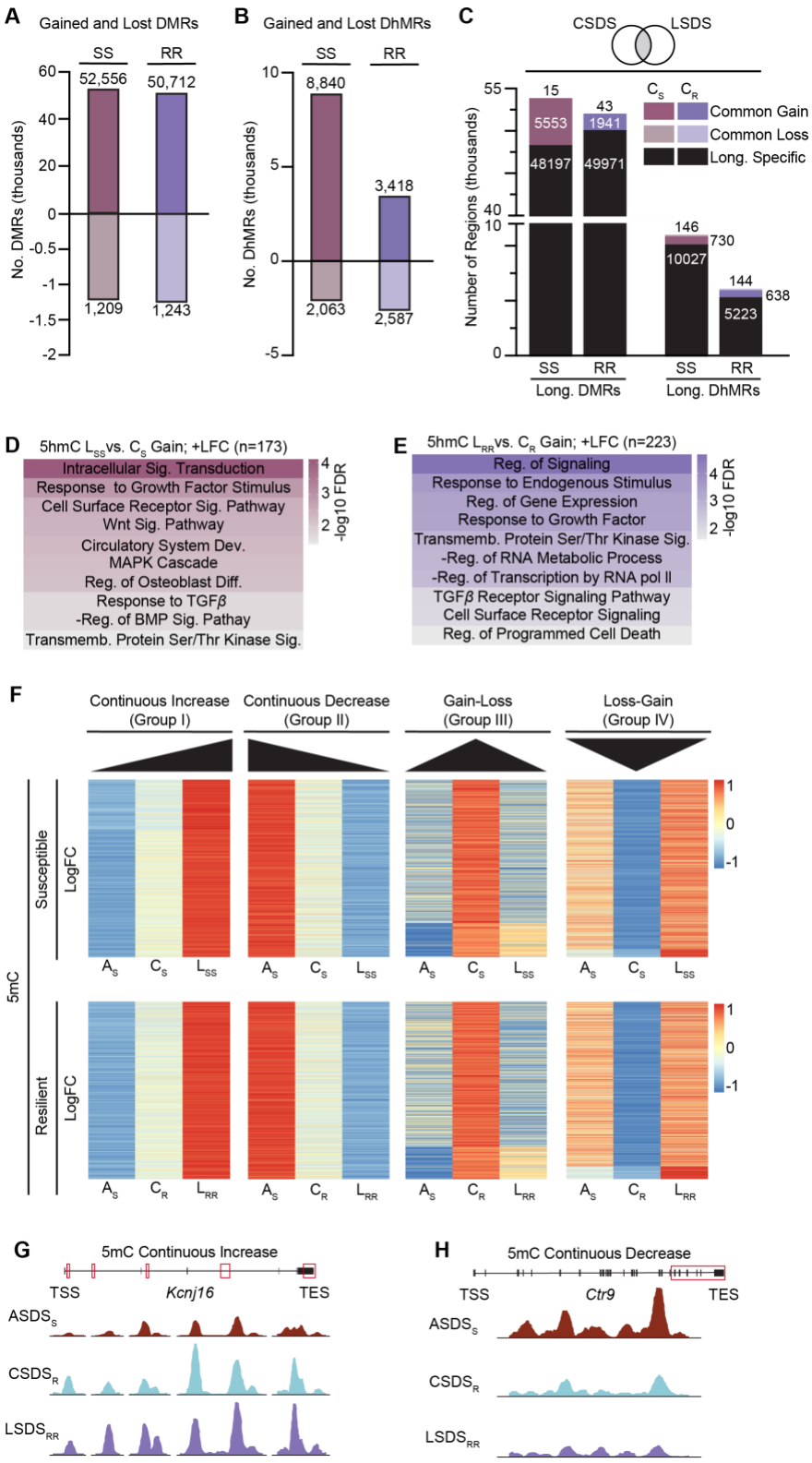

Figure 3.9: Characterization of DMRs and DhMRs from longitudinal social defeat stress
A and **B.** Number of gained and lost 5mC (**A**) and 5hmC (**B**) peaks in longitudinally stressed animals. **C.** LSDS SS and RR gained or lost DMRs or DhMRs overlapped with CSDS susceptible or resilient specific DMRs or

DhMRs. **D** and **E.** Representative GO analysis of the common genes identified between L_{SS} and CSDS susceptible (**D**) and L_{RR} and CSDS resilient (**E**) mice that concomitantly increased in 5hmC and gene expression (Gain; +LFC). GO analysis for remaining 5mC and 5hmC analysis are in Table 7. **F.** Average normalized 5mC read count across ASDS, CSDS and LSDS susceptible (top) or resilient (bottom) continuum with continual 5mC accumulation (Group I), depletion (Group II), or a return to base line (Groups III and IV). **G** and **H.** Normalized 5mC counts at peak regions identified across ASDS, CSDS and LSDS: *Kcnj16* (**G**), *Ctr9* (**H**).

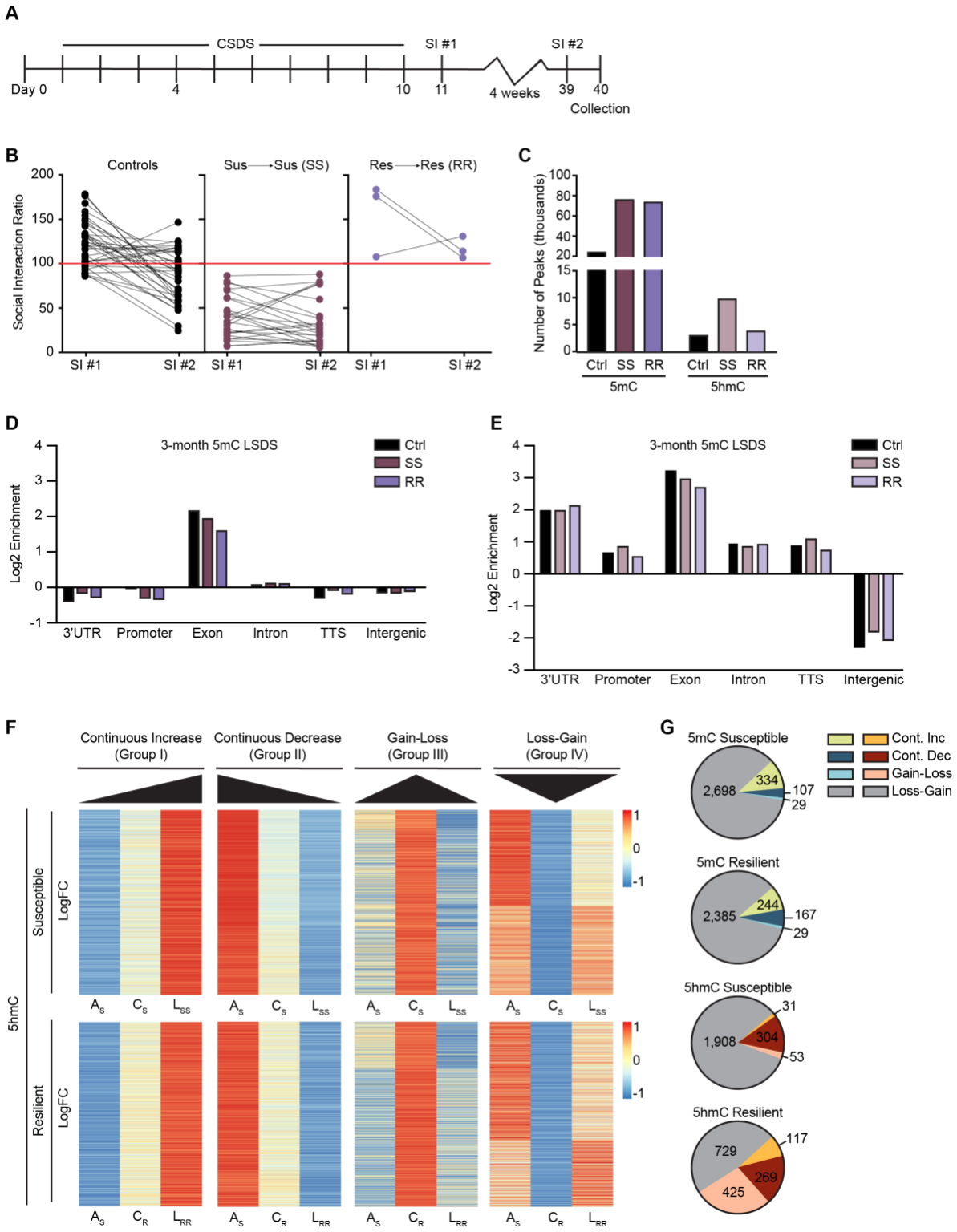

Figure 3.10: Social avoidant phenotype is maintained after incubation period

A. Experimental design of LSDS paradigm and tissue and blood collection. **B.** SI data subcategorizing animals into L_{SS} (Susceptible remained susceptible) or L_{RR} (Resilient remained resilient). **C.** Number of 5mC and 5hmC peaks identified in control and longitudinally stressed animals. **D** and **E.** Enrichment of 5mC and 5hmC peaks at 3' and 5' untranslated regions (3' and 5'UTR), promoters, exons, introns, transcription termination sites

(TTS) and intergenic regions. **F.** Average normalized 5hmC read count across ASDS, CSDS and LSDS susceptible (top) or resilient (bottom) continuum with continual 5hmC accumulation (Group I), depletion (Group II), or a return to base line (Groups III and IV). **G.** Number of genes annotated from Groups I-IV for both 5mC/5hmC susceptible/resilient regions.

Table 3.7: Biological processes and genes affected after stress re-exposure.
GO and gene analysis of LSDS DMRs and DhMRs overlapped with CSDS susceptible or resilient specific DMRs or DhMRs. Table corresponds to Figure 5.

DNA Modification	LSDS	CSDS Specific File	RNA-seq	No. of Genes in Data Set	Biological Process (-log10 FDR) or Genes
5mC	L_{SS} Gain	Sus. Gain	+LFC	711	System Development (12.2) Nervous System Development (6.4) Ear Development (5.9) Circulatory System Development (5.3) Tissue Development (5.3) Renal System Development (4.7) Kidney Development (4.6) Vasculature Development (3.8) Skeletal System Development (2.5) Respiratory System Development (2.5)
	L_{SS} Loss	Sus. Loss	-LFC	2	*Prdm16 and Zswim4*
	L_{RR} Gain	Res. Gain	+LFC	234	Neuromuscular Process (1.4) Intracellular Signal Transduction (1.4) *Synaptic Vesicle Cycle* *Circadian Regulation of Genes Expression* *Cilium Organization* *Ionotropic Glutamate Receptor Signaling Pathway*
	L_{RR} Loss	Res. Loss	-LFC	13	*Abcc4, Adprh, Chd5, Dennd3, Edar, Igf2bp2, Itpr3, Lamb2, Mobp, Ptprg, Rbm45, Rtn1, Sec14l5*
5hmC	L_{SS} Gain	Sus. Gain	+LFC	173	Intracellular Signal Transduction (4.1) Cellular Response to Growth Factor Stimulus (2.9) Cell Surface Receptor Signaling Pathway (2.5) Wnt Signaling Pathway (2.4) Circulatory System Development (2.3) MAPK Cascade (2.2) Response to TGF-β Stimulus (1.7) -Regulation of BMP Signaling Pathway (1.7) Transmemb. Receptor Protein Serine/Threonine Kinase Sig. (1.4)
	L_{SS} Loss	Sus. Loss	-LFC	113	*Afap1l1, Akt1, Aldh4a1, Arhgap23, Asap1, Asap2, Atp9a, Bmp2k, Ccdc6, Chst12, Clic4, Clip2, Cmip, Ctdspl, Ddx54, Dnah8, Eml1, Foxo3, Foxp1, Frmd4b, Fyn, Gatc, Gpr146, Grip1, Lmf1, Lnx2, Lrrc8d, Map4k4, Mast4, Mbd3, Mob3b, Mtcl1, Ncor2, Nfia, Nfkb1, Ntm, Pik3r1, Pkp4, Prrc2c, Ptpru, Rap1gds1, Sema6a, Sik1, Smc5, Sox5, Spata13, Spock1, Spred2, Stox2, Tmcc2, Tmem63b, Trio, Trub1, Upp2, Zbtb43, Zfp462, Zfp532, Zfp768, Zswim6*
	L_{RR} Gain	Res. Gain	+LFC	223	Regulation of Signaling (4.7) Response to Endogenous Stimulus (3.6) Regulation of Gene Expression (3.4) Response to Growth Factor (3.3) Transmemb. Receptor Protein Serine/Threonine Kinase Sig. (2.9)

				-Regulation of RNA Metabolic Process (2.9) -Regulation of Transcription by RNA pol ll (2.7) TGFβ Receptor Signaling Pathway (2.0) Cell Surface Receptor Signaling Pathway (2.0) Regulation of Programed Cell Death (1.6)
L_{RR} Loss	Res. Loss	-LFC	67	*2810013P06Rik, Abhd2, Acot8, Acvr1, Ankrd11, Apc2, Arhgef10, Arhgef2, Arid3a, Atp13a2, ,Atp9a, Atxn1, Bcdin3d, Best1, Camsap1, Cebpg, Chd7, Cmip, Col27a1, Csrnp1, Ctdspl, Dnajb3, Dock9, Eif4g3, Elfn2, Eml1, Fam110b, Farp1, Foxo3, Gna12, Gramd1a, Iffo2, Il4i1, Itpk1, Kank2, Klf3, Ksr1, Lrfn3, Map3k1, Map3k4, Mcu, Mical1, Micu1, Mmp15, Nphp4, Pced1b, Pkp4, Ppm1b, Prkce, Rapgef3, Rara, Rbpms, Rusc2, Ski, Slc25a51, Slc38a10, Srgap1, St3gal3, Tceanc2, Tet3, Tmem184b, Vgll4, Wnk2, Zbtb5, Zfhx2, Zfp513, Zswim6*

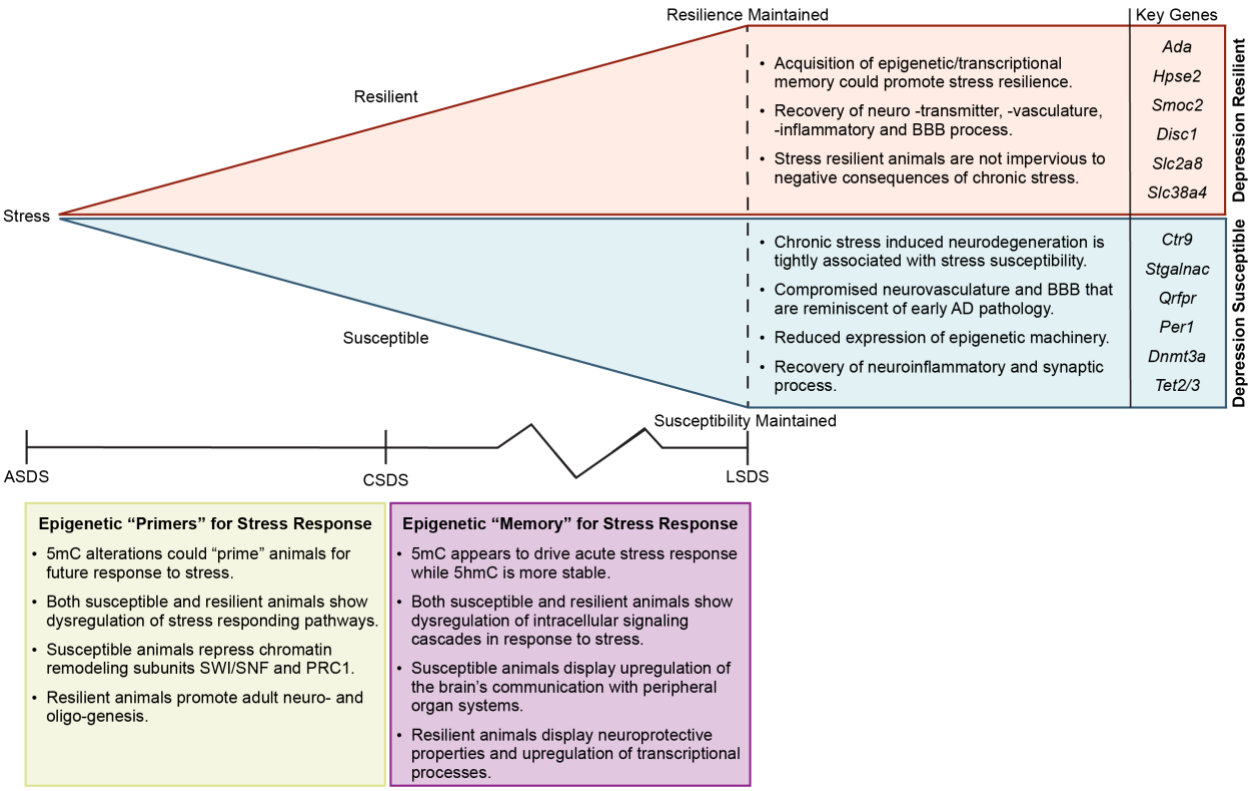

Figure 3.11: Summary of the 5mC and 5hmC dynamics across the ASDS-CSDS-LSDS time course
Diagram summarizing the key findings and putative key genes of the 5mC and 5hmC dynamics between ASDS and CSDS (green box), CSDS and LSDS (purple box) and across the ASDS-CSDS-LSDS time course (red and blue triangles).

3.6. Materials and Methods

Animals: C57BL/6J male (Jackson Labs, stock #:000664) mice were used as experimental animals. CD1 male retired breeders (Charles River Laboratories, stock #022) that were greater than 4 months in age were used as aggressor animals and singly housed. Experimental animals were grouped housed with littermates in cages of 2-5, unless otherwise indicated. All animals were maintained on a 12-hour light/dark cycle (lights on from 7:00am – 7:00pm) and provided ad libitum food and water. Social defeats and behavior tests occurred during the beginning of their dark cycle and animals were randomly distributed into control and stress groups. All procedures were approved by Emory University's IACUC committee guidelines and followed NIH Guide for the Ethical Treatment of Animals.

Social Defeat Stresses: Naïve C57BL/6J male experimental animals approximately 3 or 6 months in age were subjected to different durations of social defeat stress (chronic social defeat (CSDS) and longitudinal social defeat (LSDS) 10 consecutive days and acute social defeat (ASDS) 3 consecutive days) in white light as previously described [366]. Every day, each experimental mouse was placed into the home cage of a novel aggressor for ≤5 minutes and was readily defeated by the aggressor. Animals were immediately removed from the aggressor's cage at the first sign of blood or other injury. Aggressor mice were retired CD1 breeders that had previously been selected for aggressive behavior (an attack latency less than 60s upon 2+ consecutive screening tests). After 5 minutes of physical interaction, experimental and aggressor mice are separated by a clear perforated cage divider so that sensory contact was maintained for 24 hours. Each day, experimental mice were exposed to a new aggressor's home cage. Control animals were housed by pair, one on each side of a clear perforated cage divider, rotated daily and never allowed to physically encounter their cage mate. Each variation of the social defeat paradigm (i.e., CSDS, ASDS and LSDS) was conducted with 4-5 independent cohorts (n = 8-10 controls and n = 8-10 stressed animals per cohort).

Social Interaction (SI): Video recordings were used to score interaction and avoidance behaviors towards an unfamiliar CD1 target animal. The arena was a white open field (40x40xcm height; Maze Engineers) maintained in complete darkness supplemented with red lamp lights. 24 hours after the final defeat, defeated and control mice were introduced into the open field for two consecutive sessions of 2.5 minutes each. During the first

session ("no target"), the open arena contained an empty wire enclosure (enclosure: 10x6.5x30cm high; wire mesh: 10x6.5x8cm high; Maze Engineers) placed at one end of the arena in the center of the interaction zone. During the second session ("target"), an unfamiliar CD1 target animal was placed in a new wire enclosure. The time spent in the interaction zone and avoidance zone was scored for "no target" and "target" conditions. The Social Interaction Ratio (SIR) was calculated as the time spent in the interaction zone with target divided by the time spent in the interaction zone without target. Susceptible animals were defined as having a SIR < 1 and resilient animals had an SIR ≥1. Animals in the LSDS cohorts underwent 2 rounds of SI, one 24 hours after the final defeat and a second round 4 weeks later after an "incubation" period. During the incubation period, LSDS animals were singly housed and injuries were treated daily. All videos were scored manually using a stop watch; however, because repeated defeats can leave visible injuries, it was not always possible for the experimenter to be blinded during scoring thus two independent scores were used and averaged. To avoid artificially inflating the average, animals whose "no target" score time was < 1 second or SIR > 300 were removed from the data set. This resulted in the removal of 1 animal from the analysis.

Sucrose Preference Testing: Mice were provided two bottles daily, one with water and the other with 1% (wt/vol) fresh sucrose solution that were counterbalanced for position. Animals were habituated for 3 days with 24-hour access to water and sucrose in the experimental cages. Preference testing occurred for 4 days and the animals were given access to water and sucrose after the social defeat session for 12 hours. Bottles were weighed the following morning and the sucrose solution was replaced with a water bottle. Sucrose preference was calculated as the percentage of sucrose solution consumed out of the total fluid consumption: 100 x sucrose / (sucrose + water).

Nest Building: Nest quality was assessed daily 24 hours following social defeat. Quality was based on a scale ranging from 0-3. A score of 0 indicate the nestlet had not been touched, 1 indicated minimal shredding; nestlet shape could still be discerned, 2 indicated medium shredding; nestlet shape nearly undiscernible and 3 indicated full shredding; no nestlet shape could be seen.

Food Consumption: Before the social defeat, food was weighed daily to determine how much was consumed over a 24-hour period. As necessary, food was replenished to ensure animals had ad libitum access to food.

Corticosterone Measurement: Blood was collected approximately 36 hours after the final defeat except for the ASDS animals whose blood was collected immediately following defeat. All animals were anesthetized with isoflurane and blood was collected from the axillary (armpit) vessel and put into EDTA-coated tubes (VWR 101094-004) and chilled on ice. Blood was centrifuged for 20 min at 3,000 rpm at 4°C, plasma was collected and stored at -80°C. CORT was measured using the Enzo Life Sciences kit (VWR, ADI-900-097) following the manufacturer's small volume protocol for blood plasma, including diluting samples 1:40 with a steroid displacement reagent solution. Absorption was read at 405 nm in a Synergy H4 hybrid reader (BioTek). Absolute concentrations (pg/mL) were calculated from a standard curve and converted to ng/mL and adjusted for 1:40 dilution.

RNA Isolation: Brain tissue was placed in TRIzol and homogenized using a hand-held pestle homogenizer and allowed to incubate for at least 5 minutes. Chloroform was added to the homogenate in a 1:5 ratio, the tubes shaken, and allowed to incubated at room temperature for 15 minutes. Samples were centrifuged at 12,000g for 15 minutes at 4°C. The top aqueous layer was transferred to a clean tube, and the RNA was precipitated in 3M NaAc pH 5.2 (10:1 ratio), 4µl of glycogen (5mg/ml), 100% isopropanol (1:1 ratio) overnight at -37°C. The next day, samples were centrifuged at 15,000 RPM for 20 minutes at 4°C. The resulting RNA pellet was washed twice in 75% ethanol and centrifuged at 7,500g for 10 minutes at 4°C. The washed RNA pellet was dissolved in nuclease-free water. RNA was quantified by Nanodrop and quality confirmed by a gel.

RNA-sequencing: RNA was isolated from brain tissue as described above. Bulk RNA was sent to Admera Health, LLC for library construction and sequencing on an Illumina HiSeq platform.

DNA Isolation: Brain tissue was harvested either immediately (ASDS), 36 hours (CSDS) or 4 weeks (LSDS) following the final social defeat and after were immediately frozen on dry ice and stored at -80°C. Tissue was digested in a lysis buffer (10mM Tris pH 8.0, 5mM EDTA, 200mM NaCl, 0.2% SDS) with 30µl proteinase K (20mg/ml) and incubated at 55°C overnight. After the overnight digestion, the lysates were brought to room temperature and incubated with 5µL of RNase A solution (20mg/ml) for at least 2 hours at room temperature. DNA was extracted by adding equal volume of buffered phenol:chloroform:isoamyl alcohol (25:24:1 ratio) and

centrifuged at 14,000 RPM at room temperature. Supernatant was transferred to clean tubes and 5µl of 5M NaCl, 2µl Glycogen and equal volume of 100% ethanol were added. After overnight incubation at -20°C, DNA was centrifuged at 10,000g for 10 minutes at room temperature, and then washed in 70% ethanol. After all ethanol was removed, the DNA pellet was eluted in nuclease-free water and incubated overnight at 4°C before storing at -20°C before being quantified by Nanodrop.

5hmC Capture: 5hmC capture was performed according to the method described in [364]. In brief, 5µg of genomic DNA was sonicated to 300-400 base pairs and 5hmC containing fragments were glucosylated (T4 phage ß-glucosyltransferase enzyme and UDP-6-N3-glucose). The glucosylated fragments were purified and then biotinylated (disulfide biotin linker) and pulled down with Dynabeads MyOne Streptavidin C1 beads. The 5hmC fragments were released from the beads using dithiothreitol and purified for a final time. DNA fragments were eluted in nuclease-free water and quantified by Qubit.

Methylated DNA Immunoprecipitation (MeDIP) and Library Construction: 5mC capture was performed according to the method described in [440] with slight modifications. 3µg of genomic DNA was sonicated to 300-400 base pairs using a Covaris focused ultrasonicator. The DNA fragments were then subjected to end repair, A-tailing, adaptor ligation and USER digestion using the NEBNext Ultra II DNA Library Prep kit for Illumina (New England BioLabs, E7645S) according to the manufacturer's protocol. Following USER digestion and purification, DNA was denatured for 10 minutes at 95°C and immunoprecipitated overnight at 4°C with 4µL of either 5mC antibody (Active Motif, 39649) or IgG antibody (Sigma 12-371) in IP buffer (500mM Tris-HCl, pH 7.4, 750mM NaCl and 0.25% TritonX). The mixture was then incubated with Protein G coated Dynabeads for at least 2 hours at 4°C, washed with ice cold IP buffer and finally washed in ice cold high salt (300mM NaCl) IP buffer. After the final washing, the beads were treated with 200µL digest buffer (1X TE Buffer, pH 7.4, 0.25% SDS, 0.25% Proteinase K (2.5mg/mL)) and shaken at 1000rpm for 2 hours at 55°C. The methylated DNA was recovered by phenol:chloform:isoamyl alcohol (25:24:1) extraction followed by precipitation in 3X volume of 100% ethanol supplemented with 3µL glycogen(5mg/mL) and 15µL NaAC pH 5.2 overnight at -20°C. The next day, the DNA was pelleted and

washed with 75% ethanol and dissolved in nuclease-free water. Illumina indexes were added, PCR enriched and purified using the NEBNext Ultra II DNA Library Prep kit for Illumina following the manufacturer's protocol.

Library Preparation and High-throughput Sequencing: Library preparation and sequencing were performed according to the method described in [364]. The NEBNext Ultra II DNA Library Prep kit for Illumina (New England BioLabs, E7645S) was used per the manufacturer's protocol for enriched and unenriched genomic DNA. An Agilent 2100 Bioanalyzer was used to confirm purity and fragmentation size of the final libraries. Libraries were sequenced pair-end (150bp) on an Illumina HiSeq platform by Admera Health, LLC. The accession number for the 5mC-seq, 5hmC-seq and RNA-seq data generated in this paper is GSE223301.

5mC/5hmC-seq and RNA-seq data processing: Data mapping and processing was performed as previously described [364]. Briefly, bowtie2 (v2.3.5.1) [346] was used to map pair-end reads to the mm9 reference genome followed by MACS2 peak calling (v 2.1.2) [348]. Technical replicates were combined using the bedtools (v2.28.0) "window" function with a 300bp extension applied up and downstream of the peak. Only the common peaks in all the replicates were considered for further analysis. Peaks were then annotated to their corresponding genes using HOMER (Hypergeometric Optimization of Motif EnRichment) (v4.11.1) [351] and the flag "-annStat" was added to annotate these peaks to genomic features. Raw RNA-seq reads were aligned to the mouse mm9 genome using TopHat2 (v2.1.0) [352] and differential gene expression analysis was conducted using Cuffdiff (v2.2.1).

Identification of differentially methylated and hydroxymethylated regions (DMRs and DhMRs): Using the bedtools "window" function with the same parameters as described above, gained and lost differential regions were identified by comparing control samples to their appropriate stress condition. Peak regions only found in stress samples compared to control were defined as gained, whereas peak regions found to be absent in stress compared to control were defined as lost.

Bioinformatics analysis: Using susceptible gained and lost DMRs/DhMRs, we compared susceptible and resilient DNA modification profiles. 5mC or 5hmC reads were counted for all the replicates, normalized by

their corresponding mapped read counts, averaged and the $\log_2$ fold change observed between stress and control samples was determined. Susceptible gained and lost DMRs/DhMRs were grouped by the resilient $\log_2$ fold change and heatmaps were generated to validate the enrichment patterns. This process was repeated using resilient gained and lost DMRs/DhMRs. Susceptible and resilient gained and lost DMRs/DhMRs were annotated to their nearest gene by HOMER and those regions located in intergenic regions were removed from further analysis. Only those genes showing a positive correlation with gene expression data were used for either Gene Ontology (GO) analysis [354, 355]. Genes that gained 5mC or 5hmC and have a positive $\log_2$ fold change in gene expression will be referred to as concomitantly increasing genes. Whereas genes that lost 5mC or 5hmC and have a negative $\log_2$ fold change in gene expression will be referred to as concomitantly decreasing genes. To visualize example DMRs/DhMRs, the Integrative Genomics Viewer (IGV) (v2.14.0) was used [441].

Comparisons between 3- and 6-month susceptible and resilient animals were made using the corresponding gained and lost DMRs/DhMRS. After taking the averaged normalized read count, the $\log_2$ fold change observed between stress and control samples was used to categorize the regions into either a group that gained or lost 5mC/5hmC in both 3- and 6-month animals. After annotating the regions to genes, duplicate genes between susceptible gain and loss or resilient gain and loss were removed. Only those genes that showed a positive correlation in 3- and 6-month gene expression (as described above) were used for String Analysis (https://string-db.org/) [442]. The final gene list was then overlapped with published MDD gene expression data set [376]. To identify top potential susceptible and resilient candidate genes, only those genes whose $\log_2$ fold change in gene expression was greater than 0.25 in both 3- and 6-month animals were considered.

Between stress comparisons (i.e. CSDS vs. ASDS or CSDS vs. LSDS) were done using the bedtools "window" function with the same parameters as described above. Gain and lost ASDS or LSDS DMRs/DhMRs were overlapped with either CSDS gain/loss-specific DMRs/DhMRs respectively. To identify regions that showed either a continual increase, decrease, or return to baseline of 5mC/5hmC across the ASDS-CSDS-LSDS time course, averaged normalized reads were counted and grouped based on the $\log_2$ fold change observed between corresponding stress and control samples. HOMER gene annotation, RNA-seq correlation, GO analysis and IGV were performed as previously described.

Gene ontology (GO) analysis: Functional annotation analysis was conducted in the GO Consortium classification system (http://geneontology.org) [354, 355]. We then clustered GO terms to a representative term and plotted by $-\log_{10}$FDR to show their statistical significance.

Chapter 4: Epigenetic Machinery: Tet2 KO and Stereotaxic Experiments

This chapter is unpublished data pertaining to Chapter 3

Contributions:

J.N.K. and B.Y. conceptualized and designed the experiments. **J.N.K.**, N.R.W. and R.S. performed all animal experiments and behavior analysis. **J.N.K.**, N.R.W. and R.S. performed the 5mC-seq, 5hmC-seq and RNA-seq studies. **J.N.K.** and Jennifer Wong performed the ICV injections. **J.N.K.** and Thomas Shiu performed perfusions, immunofluorescence staining and imaging. **J.N.K.** and F.W. performed Western Blot analysis. B.Y. supervised all aspects of the project.

4.1. Introduction

Prior research has insinuated that the DNA eraser enzymes Tet1/2/3 could influence stress response. For example, ubiquitous knockout of either *Tet1* or *Tet2* in mice resulted in increased baseline resilience or susceptibility to chronic restraint stress, respectively [291]. In addition, conditional knock-out of Tet3 in the mouse hippocampus increased both anxiety-like behaviors and blood corticosterone levels [443]. Moreover, we also found that depression susceptible animals had a continual decrease in DNA modifying proteins (Dnmt3a, Tet2 and Tet3) while resilient animals displayed TDG returning to baseline. All of this evidence implies a role for DNA modifying machinery in influencing stress-induced depression [316].

4.2. Preliminary Results and Discussion

To investigate if the loss of Tet2 machinery would increase stress susceptibility in mice, WT and $Tet2^{KO}$ siblings underwent the same CSDS paradigm used in **Chapter 3:**. Nest building and food consumption were again measured daily as indicators of distress in the animals (**Figure 4.1:A** and **B**). Like we observed prior, the first several days of defeat had more low-quality nests and reduced food consumption, followed by stress habituation behaviors. Social avoidant-like behavior was again measured using the social interaction (SI) test. Significant social avoidant behavior was observed for both WT and $Tet2^{KO}$ defeated animals, compared to paired controls (**Figure 4.1:C** and **D**); however, there was no significant difference between stressed WT and $Tet2^{KO}$. Sucrose preference testing did not reveal significantly changes between paired controls and stressed animals (**Figure 4.1:E**), nor did blood corticosterone levels (**Figure 4.1:F**). It remains unclear as to why corticosterone levels were not significantly higher in stressed animals. Cumulatively, our behavior data did not support the loss of Tet2 as a mechanism that increases stress susceptibility as analyzed through behavioral experiments. Computational follow up comparing these animals to the susceptible and resilient CSDS animals in our above study could shed some light onto the possible HPA-axis disruption and epigenetic differences.

A likely reason as to why we were unable to replicate the increased stress susceptibility phenotype observed in prior studies could be due to the type of stress paradigms performed. Cheng et al. measured baseline stress response without any prior exposure to stressors. Whereas in our study, we performed a robust stressor and then measured stress response. Although we observed 2 resilient WT and 3 resilient $Tet2^{KO}$ animals, this amounts to only an 11% and 13% resilient rate, respectively, compared to the 20% rate we observed in our

canonical WT CSDS experiment. Another important consideration to take into account when comparing our study with the Cheng et al. study is that their Tet1^{KO} and Tet2^{KO} animals were on different strain backgrounds. This makes direct comparisons of stress susceptibility between the animals less reliable. To further demonstrate the importance of strain background, we observed that the stressed WT siblings from the Tet2^{KO} line appeared more sensitive during CSDS compared to the WT animals from the pure C57BL/6J background (data not provided). The WT and Tet2^{KO} sibling pairs and the WT animals used in our CSDS experiments are considered to be on the same C57BL/6J background. However, the Tet2^{KO} line express 5 markers from their parent strain (C57BL/6N) that segregate from the C57BL/6J background (Jackson Lab).

One way that we could resolve background strain differences would be to knock-down experiments in WT C57BL/6J mice. We performed shRNA targeted Tet2 knock-down experiments that specifically target Tet2 in the brain. Because the transgenic animals express a ubiquitous loss of Tet2, we also wanted to confirm that any behavioral or computational differences observed, would not be attributed to the loss of Tet2 during embryonic or early brain development. Accordingly, we first validated our AAV-lentivirus construct and several siRNAs targeting Tet2 in HEK293 cells to confirm a sufficient decrease in protein levels (**Figure 4.1:G**). Intracerebroventricular (ICV) injections of either control or Tet2 targeted lentivirus were administered to WT animals at 6-weeks of age followed by 6-weeks of incubation to allow for optimal expression. Immunofluorescence staining and microscopy revealed minimal plasmid expression and dispersion (**Figure 4.1:H**), suggesting the need for additional experiment optimization.

4.3. Figures and Figure Legends

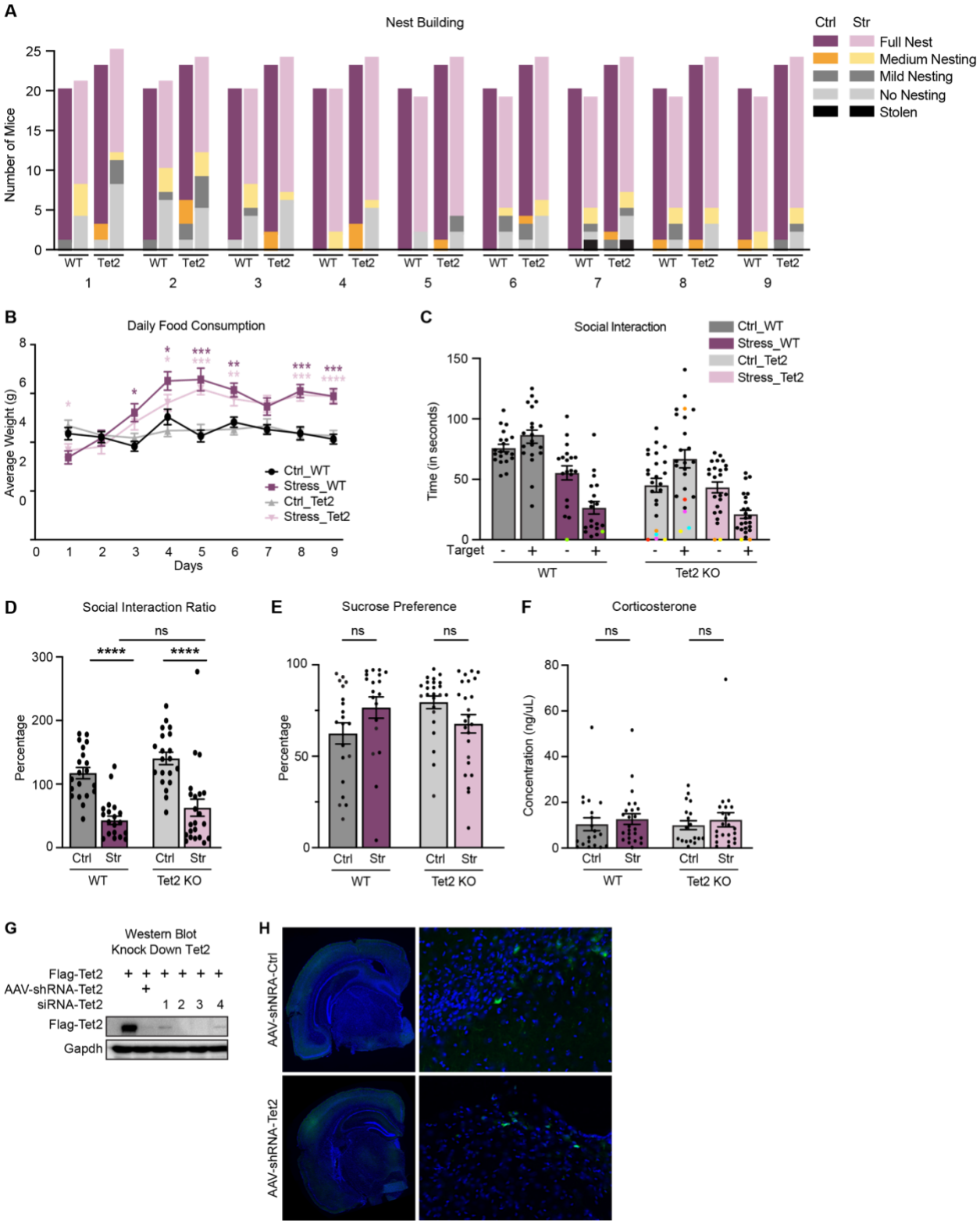

Figure 4.1: Chronic Social Defeat Stress Induces Social Avoidance in Tet2KO Animals

A. Daily nest building for WT and Tet2KO controls and stressed animals. **B.** Daily food consumption for WT and Tet2KO controls and stressed animals (*P < 0.05, **P < 0.01 and ***P < 0.001, ****P < 0.0001 in Holm-Sidak method for multiple comparisons after unpaired t-test). **C.** Time spent in the interaction zone when target was either absent (-) or present (+). **D.** Defeated WT and Tet2KO animals display a significant reduction in social behavior (WT: n = 20 Ctrl, n = 18 Str, independent cohorts = 5; Tet2KO: n = 20 Ctrl, n = 22 Str, independent cohorts = 5; Unpaired t-test, ****P < 0.0001 versus aged matched and littermate controls). **E.** Sucrose preference testing for anhedonic-like behavior in WT and Tet2KO animals (Unpaired t-test, *P < 0.05). **F.** Blood corticosterone was not significantly elevated in both WT and Tet2KO animals following CSDS (Unpaired t-test, **P < 0.01 and ***P < 0.001). **G.** Immunoblot of Tet2 knock-down efficiency by either shRNA or siRNA targeting in HEK293 cells. H. Representative immunostaining of intracerebroventricular (ICV) injections of either control or Tet2 lentivirus.

4.4. Material and Methods

Animals: Tet2 knockout (*Tet2*$^{-/-}$) male mice were used as experimental animals. Tet2 heterozygous males were purchased from Jackson Labs (stock#023359) and backcrossed for one generation to C57BL/6J. Resulting heterozygous mice from this cross were then mated to generate wild type and homozygous knockout Tet2 animals used in experiments. CD1 male retired breeders (Charles River Laboratories, stock #022) that were greater than 4 months in age were used as aggressor animals and singly housed. Experimental animals were grouped housed with littermates in cages of 2-5, unless otherwise indicated. All animals were maintained on a 12-hour light/dark cycle (lights on from 7:00am – 7:00pm) and provided ad libitum food and water. Social defeats and behavior tests occurred during the beginning of their dark cycle and animals were randomly distributed into control and stress groups. All procedures were approved by Emory University's IACUC committee guidelines and followed NIH Guide for the Ethical Treatment of Animals.

Social Defeat Stress, Social Interaction (SI), Sucrose Preference Testing, Nest Building, Food Consumption, Corticosterone Measurements, 5mC and 5hmC enrichment and library prep: Please refer to Chapter 3 Materials and Methods

Western Blot Analysis: Mouse cortex was lysed in RIPA buffer (150 mM NaCl, 1% Triton X-100, 0.5% sodium deoxycholate, 0.1% SDS; 50 mM Tris, pH 8.0) containing Complete Protease Inhibitor Cocktail (Roche). Samples were left on ice for 30 min and sonicated briefly. The insoluble fraction was removed by centrifugation at 15,000 rpm for 15 min at 4°C. Protein concentration was determined by BCA protein assay kit (Bio-Rad). 2X SDS sample buffer (Bio-Rad) containing 5% β-mercaptoethanol (Sigma) was added to equal amounts of protein. Proteins were then separated by 4%–15% SDS-PAGE (Bio-Rad) and transferred to PVDF (0.2 mm) or nitrocellulose membrane (0.45 mm). 5% dried milk in TBST (Tris buffered saline with 0.1% Tween 20) was incubated for blocking, and membranes were applied with specific antibodies. After washing with TBST and incubation with GAPDH or FLAG antibody, the antigen-antibody was detected by chemiluminescence (ECL; Pierce) and X-ray film (GE Healthcare).

Intracerebroventricular (ICV) injections: Six-week-old C57BL/6J male animals were administered 5mg/kg meloxicam (Med-Vet International, RXLOXICOM) prior to the surgical procedure to aid in analgesia.

Anesthesia was maintained with 1.5% isoflurane (Med-Vet International, RXISO-100) throughout the surgical procedure. The right lateral ventricle (RLV) was targeted using the following coordinates relative to bregma: anterior-posterior (AP): -0.3mm, medial-lateral (ML): 1.0mm, and dorsal-ventral (DV): -3.0mm. 4uL of either AAV-shRNA-control or AAV-shRNA-Tet2 [444] were injected into the RLV at 1uL/min. All mice were given 6-weeks to recover from surgery and to allow for optimal expression of each AAV. AAV-shRNA-Control and AAV-shRNA-Tet2 was a gift from Hongjun Song (Addgene plasmid #85743; http://n2t.net/addgene:85743 ; RRID:Addgene_85743).

Immunofluorescent Staining: Brains were harvested 6-weeks after ICV injections using perfusion and fixed in 4% paraformaldehyde (wt/vol) for 24 hours at 4°C. After, brains were rinsed in phosphate-buffered saline (PBS) then immersed in 30% sucrose solution for 1-2 days and stored at 4°C. Brains were embedded in optimal cutting temperature (O.C.T) embedding medium (Fisher Health Care) and sectioned with a cryostat (Lecia) to 40μm sections. For immunostaining, sections were washed in PBS before permeabilization and blocked in 0.2-0.5% TritonX and 5% normal goat serum in PBS for 1 hour. GFP primary antibody (Invitrogen G1036) was diluted (1:100) in blocking solution and sections were incubated overnight at 4°C. After washing in PBS, Alexa fluor 568 secondary antibody (Invitrogen A10042) was diluted (1:100) in blocking solution and sections were incubated at room temperature for 1 hour. Finally, sections were washed with PBS and stained with DAPI. All images were captured on Keyence microscope.

Chapter 5: The Third DNA Modification: 6mA and its Writer Alkbh1

This chapter is unpublished data pertaining to Chapter 3

Contributions:

J.N.K. and B.Y. conceptualized and designed the experiments. **J.N.K.**, N.R.W. and R.S. performed all animal experiments and behavior analysis. **J.N.K.**, N.R.W. and R.S. performed the 6mA and RNA-seq studies. **J.N.K.** and Jennifer Wong performed the ICV injections. **J.N.K.** and Thomas Shiu performed perfusions, immunofluorescence staining and imaging. **J.N.K.**, Y.H. and F.W. performed Western Blot and RTqPCR experiments and analysis. B.Y. supervised all aspects of the project.

5.1. Introduction

Originally recognized as the most abundant modification on RNA [445], N6-methyladenine (6mA) has surfaced as a new DNA modification. 6mA was previously thought to only exist in the prokaryotic genome where it functions as a defense mechanism by labeling host DNA to distinguish it from foreign pathogenic DNA [446]. More recently, 6mA has been identified in higher order eukaryotic genomes like flies and mammals [294, 447, 448]; however, its function has remained unclear. Studies have revealed that 6mA is highly enriched during mammalian embryonic development, but quickly becomes depleted as development progresses [294]. In addition, 6mA has been shown to regulate gene and transposon expression in mouse ESCs [296]. As one would expect, 6mA also has a set of epigenetic machineries that 'writes' and 'erases' it onto and from the DNA. In mouse, N6amt1, Mettl4 and Mettl3-Mettl14 complex have been identified as putative enzymatic writers of 6mA while Alkbh1 is a putative eraser [296-298, 449, 450].

Regarding the role of 6mA in stress response, it has previously been shown that chronic restraint stress increased 6mA levels in stress-responding brain regions, especially in the mouse prefrontal cortex [300]. Genome-wide analysis revealed that intergenic regions and repressive chromatin transcription factor binding cites are enriched for 6mA, while enhancers and Pol II binding sites were depleted. Furthermore, genes upregulated in response to chronic restrain that lost 6mA were suggested to be involved in neuronal development and learning. More importantly, a significant overlap between depression-associated genes and genes with dynamic 6mA were observed, indicating a strong association between 6mA and neuropsychiatric disorders. Moreover, studies focusing on Alkbh1 in stress suggest that exposure to stressors at a young age could have a sex-dependent response that affect serotonin signaling [299]. Given the evidence at hand, we sought to investigate how chronic stress could alter the 6mA landscape in the cortex and if loss of the eraser protein Alkbh1 had any effect on stress response.

5.2. Preliminary Results and Discussion

In addition to 5mC and 5hmC, we also enriched for 6mA from the same 3-month animals analyzed in our CSDS experiments. Although this data has yet to be fully analyzed, we did observe differential 6mA regions in the cortex of susceptible and resilient animals (**Figure 5.1:A**). Notably, chronically stressed animals display a similar number of gained and lost 6mA regions with lost regions being most prevalent. In addition, we also

started preliminary knock-down studies on Alkbh1 similar to the Tet2 knock-down experiments described in **Chapter 5:**. shRNAs targeting Alkbh1 were experimentally validated *in vitro* for sufficient mRNA and protein loss (**Figure 5.1:B** and **C**). Given that shRNA_1 displayed the best knock-down efficiency, we proceeded with ICV injections of both control and Alkbh1 targeted lentiviruses. RTqPCR analysis revealed a decrease of *Alkbh1* in the cortex and hippocampus of two independent animals (**Figure 5.1:D**). Immunofluorescence staining and microscopy showed that the shRNA-Alkbh1 plasmid was predominately expressed in the hippocampus (cell bodies of the dentate gyrus and nerites of granule cells) and not in the cortex (**Figure 5.1:E**). In conclusion, a full computational analysis of global 6mA alterations in response to chronic stress still needs to be completed.

5.3. Figures and Figure Legends

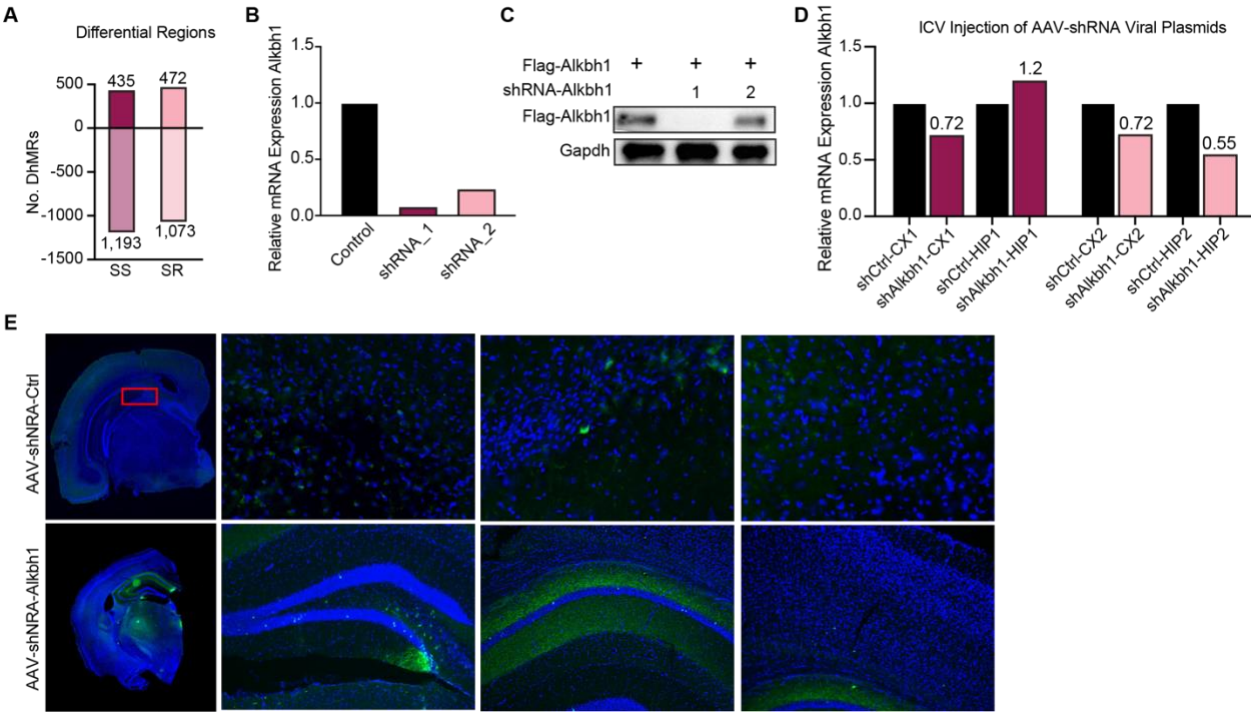

Figure 5.1: Preliminary 6mA analysis
A. Number of gain and lost 5hmC peaks in stress susceptible and resilient 3-month animals. **B.** Relative expression of Alkbh1 mRNA after shRNA targeted knock-down in HEK293 cells. **C.** Immunoblot of Alkbh1 knock-down efficiency by either shRNA targeting in HEK293 cells. **D.** Relative Alkbh1 expression in the cortex and hippocampus of 2 independent animals after ICV injection of either control or Alkbh1 lentivirus. **E.** Representative immunostaining of intracerebroventricular (ICV) injections of either control or Alkbh1 lentivirus.

5.4. Materials and Methods:

RNA Isolation and RTqPCR: RNA was isolated as described in Chapter 3. RTqPCR was performed using Thermo Fisher's Super Script III First-Strand Synthesis (18080051) kit and manufactures protocol was followed.

Western Blot Analysis: Please see Chapter 5 Materials and Methods

6mA DNA Immunoprecipitation: 6mA capture was performed according to the method described in [451, 452]. 10μg of genomic DNA was sonicated to 300-400 base pairs using a Covaris focused ultrasonicator. The fragmented DNA was incubated with rotation overnight at 4°C with 8μL of 6mA antibody (Synaptic Systems) in IP buffer (50mM Tris-HCl, pH 7.5, 150mM NaCl, 0.1% NP-40). The mixture was then incubated with Protein G coated Dynabeads for at least 2 hours at 4°C, washed with ice cold IP and finally washed in ice cold high salt buffer (50mM Tris-HCl, pH 7.5, 1M NaCl, 1mM EDTA, 0.1% NP-40, 0.1% SDS). After the final wash, the beads were treated with DNA extraction buffer (10mM Tris, pH 7.5, 100mM NaCl, 10mM EDTA, 0.2% SDS) warmed to 37°C and Proteinase K and shaken at 1200rpm for 2 hours at 56°C. The 6mA enriched DNA was recovered by adding 200μL DNA extraction buffer and 300μL phenol:chloform:isoamyl alcohol with Tris/EDTA to the DNA followed by precipitation in 2X volume of 100% isopropanol supplemented with 10μL glycogen(5mg/mL) and 10μL 5M NaCl overnight at -32°C. The next day, samples were brought to room temperature, centrifuged at max speed for 20 minutes at 4°C and DNA pellets were washed in 70% ethanol before being eluted in nuclease-free water overnight at 4°C. Concentration was quantified by Qubit and all precipitated samples were stored at -20°C.

Library prep: Please refer to Chapter 3 Materials and Methods.

Chapter 6: Conclusions and Future Directions

Overall, the work presented in this thesis explored how the epigenetic landscape, specifically DNA modifications, change during normal brain development and are influenced by neurological disorders. We advanced the field of Alzheimer's research by profiling the 5hmC landscape in the earliest model system available to date, the forebrain organoid. Traditionally, AD studies prioritize aged and/or late disease stages for research; however, our analysis suggests that dysregulation of 5hmC in individuals predisposed to familial AD could appear within neuronal networks as early as fetal development. This finding opens the door to a new way to approach AD treatment options that could be preventative rather than consisting of symptom management. The possibility that early preventative measures could one day exist as a prenatal supplement or vitamin is an exciting new concept and avenue for the field.

In addition to AD, this work is also the first to provide a systematic global profiling of the 5mC and 5hmC landscapes spanning various durations of stress. What affects individual differences in stress response is a vastly heterogeneous combination of life experiences, personality and adaptive practices. Thus, it is likely that the genetic/epigenetic contribution to stress response is also heterogeneous. Our work symbolizes the beginning of an opportunity to incorporate global multi-omic profiles of stress responding brain regions into the field of depression. The key to understanding heterogeneous conditions, like stress response, is to consider the big picture in its entirety and focus less on the individual pieces of the puzzle. The development of data sets that are expansive and inclusive of proteomic, transcriptomic, epigenomic data, etc. is supported by our analysis whereby the downregulation of various epigenetic machinery that regulate chromatin, histone and DNA modification dynamics/interactions could predispose depression susceptibility. Moreover, such a comprehensive and interactive data set could help reduce the amount of ambiguity that goes into prescribing drug treatments and so earlier relief can be provided to patients.

6.1. General Conclusions on Alzheimer's Disease

Both genetic and epigenetic regulation are critical for brain development, function and prevention of neurological diseases. Currently, clear molecular mechanisms underlying neurological diseases and effective treatment options are lacking. The field of epigenetics provides alternative avenues for therapeutic exploration

given that many diseases are not monogenic and likely have a significant environmental contribution. The epigenome can be greatly influenced by environmental factors such as nutrition, chemical pollutants, traumatic early life experiences, temperature changes and exercise [453, 454], but how these aversions affect brain development is poorly understood. Importantly, the effect of the environment on epigenetics is not limited to development after birth, but can also affect development in utero. Early life stressors have been hypothesized to induce long-lasting epigenetic changes that may be caused by cellular epigenetic "priming." For example, when an environmental exposure is experienced, altering the epigenetic state of a gene, that gene remains in a state of "primed responsiveness," promoting a more rapid response if re-exposure occurs [455]. This concept of epigenetic memory in response to environmental stimuli could serve as a mechanism to identify individuals predisposed to developing neurological diseases.

6.1.1. Alzheimer's Disease Background

The canonical pathologies of Alzheimer's Disease (AD), Aβ plaques and neurofibrillary tangles, were first clinically described in 1906 by Alois Alzheimer and are still recognized today as the official hallmarks for disease diagnosis [456]. As technologies progressed, heritable mutations in the genes *APP*, *PSEN1* and *PSEN2* and their symbiotic roles in the production of Aβ plaques [457] eventually led to the proposition of the amyloid hypothesis in 1992 by Hardy and Higgins [321]. For decades, the AD field has vigorously pursued therapeutic treatments through the direct targeting of amyloid plaques and tau-proteins, but this approach has only had minimal success [458]. Subsequently, the field was forced to reassess their definition of "canonical" AD pathology and revisit prior observations implicating the immune [459-461] and vascular [462, 463] systems as more significant contributors to disease onset and progression than previously accredited. Finally, despite decades of new research, the AD field has yet to make further advancements towards an effective treatment option, largely due to the lack of clinical translatability in animal models for AD.

6.1.2. A Discussion on Alzheimer's Disease Model Systems

A major challenge in studying any disease is overcoming the inherit limitations of the model systems available for study. For neurodegenerative diseases, like AD, mouse models, postmortem human brain tissues and nonhuman primates are heavily relied upon to provide insight into neurological disease pathology and etiology. A major criticism of AD mouse models is that no transgenic line fully recapitulates all the

neurodegenerative phenotypes observed in humans. Although mouse and human brains are similar at genetic, structural and general circuitry levels, key differences limit mice as models of human diseases that are characterized by complex dysfunction of behavior and thought. Another important consideration is that AD mouse models were originally generated by overexpressing human genes at levels significantly higher than what is observed at physiological levels perturbing the clearing and metabolic abilities of affected cells. Furthermore, plaques can appear much earlier in mice compared to humans creating an asynchronous environment between plaque formation, which normally occur in an aged brain, and the immune system of a young versus aged animal [464]. This second point illustrates the importance of temporal expression of disease pathology and could contribute to the lack of success in clinical trials. An underappreciated characteristic of mouse models in general, is that they lack genetic diversity due to extensive inbreeding with most of the models being generated on the same genetic background. To address this, a recent study breed established AD mouse lines with three different wild mouse lines and found clear differences in amyloid deposition, neuronal cell loss and neuroinflammation that were sex and strain dependent [465]. This suggests that the incorporation of genetic diversity into AD models would more accurately represent the genetic diversity found in the human population, and allow for better correlations between phenotype variations and disease outcome.

Postmortem human brain tissue has been critical for characterizing the morphological brain alterations that occur by the most sever stages of disease. However, herein lies their short coming, they are severely biased towards the later stages of disease and are unable to provide a progressive timeline. Furthermore, there are concerns as to whether postmortem tissues can accurately recapitulate the epigenomic landscape of a living brain. Alternatively, nonhuman primates pose as an attractive model that would allow for all AD stages to be studied, especially because their nervous system is so comparable to humans. Despite this seemingly fortuitous advancement, it appeared that nonhuman primates would suffer from some of the same pitfalls as their mouse counterparts because neurodegenerative diseases were thought to be unique to humans. Excitingly, several research groups have observed that tau tangles can naturally occur in the brains of sufficiently aged chimpanzees [466], macaques [467], and potentially vervets [468] nonhuman primate species. As a result, several longitudinal studies utilizing nonhuman primates are underway, utilizing various behaviors and modifiable risks (i.e., diet,

exercise, environmental stimulation, and stress and depression) as measurements, with the hope of gaining some clairvoyance into the initial stages of AD. The primary concerns for using nonhuman primates are the ethics, feasibility of maintaining large enough colonies to have a powered study, the time it takes the animals to age and the cost of such programs. Given that the greatest risk factor for AD is age, the wait for such data may just be worth it.

A new and promising model system that can compensate for the limitations of mice, postmortem brains and nonhuman primates, and one we took advantage of in our own AD study, is organoids. Organoids are three-dimensional cultures that model whole developing organs [326]. This system evolved from embryoid cultures, which are 3D aggregates of stem cells that are grown in a suspension that will induce their differentiation. When organoids are used to generate neuronal lineages, they can recapitulate human brain development *in vitro*. Morphological studies have further confirmed that forebrain organoids have similar developmental patterns as the developing human cortex [324, 469]. For example, developing organoids can undergo neural differentiation, form multi-layer progenitor zones, form discrete brain regions and portray typical neuron morphologies such as spine-like structures [324, 470]. Epigenomic studies have also confirmed that brain organoids recapitulate the fetal brain epigenome [471]. Whole-genome methylome profiling revealed that mCH accumulation in both fetal brain and cerebral organoid occurred at super-enhancers that are specifically active during fetal development, and later became repressed. Additionally, organoid mCG signatures at DNA methylated valleys, large domains depleted of mCG, were comparable to fetal cortex and localized to genes with roles in brain development.

In terms of disease modeling, patient-derived mature epithelial cells can be collected non-invasively, reverted to induced pluripotent stem cells and cultured into brain organoids. This provides researchers with a model that is genetically identical to the patient, avoiding background signals attributed to artificially overexpressing an exogenous construct to induce disease phenotypes. In addition to not facing the same restrictions as animal models in terms of space, cost and ethical considerations, organoids can be cultured on a large enough scale for high-throughput drug screenings to be developed. In the future, the use of organoids could allow for the development of unique therapeutic options specific to each patient.

As with any model, organoids are not without their own set of limitations. Until recently, organoids did not naturally develop anterior–posterior and dorsal–ventral axes [327]. Cederquist et al. developed a human pluripotent cell line that expresses an inducible sonic hedgehog (SHH) signaling factor [472]. When these cells are embedded into a pole of a developing organoid, they will express SHH, generating topographically-patterned organoids. Research is underway to generate more sophisticated organoid models that better recapitulate organogenesis. These improvements include developing methods to further drive anterior–posterior and dorsal–ventral axes, as well as vascular systems to improve oxygen and nutrient distribution for better growth [325].

6.1.3. The Incorporation of Inclusive Practices in AD Studies

Understanding and carefully considering the limitations of one's model system is critical to the design of any experiment. However, two overarching concerns remain in the AD field that are only just beginning to be addressed. The first is that, regardless of the model system used, researchers have hyper-focused on the high genetic risk genes *APP*, *PSEN1* and *PSEN2* found in early onset familial AD patients, which only constitute approximately 5% of the entire AD population [468]. The apolipoprotein E (*APOE*) gene is a known major risk factor for sporadic late onset AD and contains 3 alleles: $\varepsilon 2$, $\varepsilon 3$ and $\varepsilon 4$, where $\varepsilon 3$ and $\varepsilon 4$ are thought to strongly impact the rate of cognitive decline in a race specific manner [473-475]. This highlights the second major concern, that minority populations are grossly underrepresented in AD studies. Given that non-Hispanic blacks (NHB) are at a significantly higher risk of developing AD compared to their non-Hispanic white (NHW) counterparts [476, 477], it is critical that conventional inclusion criteria, which tend to positively bias towards White, well-educated and privileged individuals, be reevaluated [478]. To demonstrate this point, one study noted that NHB were disproportionately excluded from a trial specifically due to low test scores in the Mini-Mental State Exam (MMSE) [479], which is known to bias against individuals with lower educational levels [480].

The lack of inclusive practices in AD studies has consequently resulted in the misrepresentation of the population. Two possible strategies to address this could be considered. First, implementing more tailored inclusion criteria for racial and ethnic minorities that consider socioeconomic status, disease comorbidities,

negative cultural experiences and adjustments for unique cultural norms [478, 481, 482]. A main limitation of this approach would be the high variability generated across studies due to inconsistent inclusion criteria, making cross comparison difficult. To address this, the second strategy that could be established is group-specific inclusion baselines from cognitively healthy individuals representing various racial and ethnic backgrounds.

To illustrate the impact of racial and ethnic background on AD progression is the interaction between *APOE* and *TOMM40'523* (*'523*) genes. Interestingly, *APOE* is in strong linkage disequilibrium with poly-T variants (short (S), long (L) and very long (VL)) in intron 6 of the TOMM40'523 gene ('523) [483]. In fact, how APOE alleles combine with the different haplotypes of '523 is known to impact AD risk. For example, in older NHWs who were APOE ε3/3 homozygous with S/S '523 haplotype had significantly faster cognitive decline compared to individuals with S/VL or VL/VL [474]. Furthermore, 94.2% of NHWs who carry an APOE ε4 allele also carry the '523-L allele, suggesting almost perfect linkage. Additionally, each ε4 and '523-L allele doubled the risk for AD in NHWs. However, in the NHB population, while ε4 allele is more prevalent and appears to have a protective effect, the linkage between the **ε**4 and '523-L haplotype was lost (47.8%). The authors suggest that admixture between people of African ancestry and Caucasian ancestry could be a possible explanation [475]. In support of this, it was observed that the percentage of African ancestry affected amyloid levels in NHBs [479]. For example, cognitively normal NHB with a high percentage of African ancestry exhibited lower amyloid levels compared to NHW, whereas lower percentages had more amyloid detected. Clearly, consideration of epigenetic, ancestry and environmental interactions affect disease risk and susceptibility and the ability to obtain an accurate diagnosis.

6.1.4. Future Experiments for Alzheimer's Disease Organoids

As discussed in the introduction, the interplay between 5mC, 5hmC and Tet enzymes are critical for proper brain development and function and have also been strongly implicated in age-related diseases like AD. Despite some controversy over the exact global landscape of 5mC and 5hmC in AD brains, it is clear that dysregulation of these DNA modifications contributes in some manner to AD development and progression. Until recently, nearly every AD study has focused on and modeled later stages of the disease, leaving the earlier

stages before the detection of disease pathology largely unexplored, especially at the epigenetic level. To begin addressing this gap, our lab took advantage of fAD forebrain organoids modeling 12–24-week fetal brains, which is one of the youngest AD models to date [364]. From our work, we observed that despite a significant global 5hmC reduction in AD organoids, over 50% of identified dysregulated genes were upregulated in AD organoids. We further postulated that this inappropriate upregulation in gene expression could be connected to the observed increase of 5hmC across enhancer regions that was only seen in the AD organoids. Our findings support that during early brain development of an AD-predisposed brain, subtle 5hmC alterations could affect the immature neuronal networks, increasing the vulnerability of developing AD later in life. Of note, our study did not find any difference in gene expression for any of the *TET* proteins or *DNMTs* between AD and control organoids (data not shown). Given that the expression levels of *DNMTs* in most differentiated cells are maintained at low levels, it is unlikely that they play a role in AD. However, mice studies have demonstrated that either knockdown or overexpression of *Tet2* can either increase or decrease cognitive decline in AD mice models respectively, as discussed in the introduction. This could suggest that at some point during AD progression, a regulatory "switch" may be flipped, altering *Tet2* expression. A longitudinal study that encapsulates time points starting embryonically through old age could be used to test if such a "switch" exists. Another possibility could be that TET2 dysregulation could distinguish or be predictive of those individuals who transition from cognitive dementia to AD-dementia.

An important future study for our AD organoids would be to incorporate global 5mC profiling so cross-comparisons between 5mC and 5hmC and their relationship in early AD could be explored. This analysis would again be a first of its kind, as all prior profiling of 5mC in AD have been conducted at later stages. Characterizing global epigenetic profiles is critical for developing and understanding big picture epigenetic cross-talk; however, to more precisely define molecular mechanisms, single base resolution is needed. A major caveat to global sequencing is that signal resolution is limited to 300-500bp. To identify which cytosine base(s) and/or how many are modified in a single read, single base technology is required. Bisulfite based methodologies (bisulfite sequencing (BS), oxidative BS and Tet-assisted BS) have been considered the gold standards for identifying modified cytosines, 5mC or 5hmC, respectively. The use of bisulfite treatment is

extremely damaging to the DNA and the global conversion of cytosines to thymines destabilizes the genome. Consequently, these methods require a large amount of starting DNA input and yield poor sequence quality and require lengthy computational processing [484]. To combat these issues, the newer technologies (Tet-assisted pyridine borane sequencing (TAPS), TAPSβ and chemical-APS) exploit a bisulfite-free approach [484, 485]. The replacement of bisulfite with pyridine borane treatment creates very mild reaction conditions preventing DNA damage, thus allowing for low starting DNA inputs. Moreover, by preventing DNA damage, sequencing costs and data processing times can be greatly reduced while significantly improving sequencing quality. Because of these improvements, single-base resolution experiments are now far more feasible to attempt in organoids and can therefore be incorporated into future experiments.

Other challenging, but crucial future experiments would be to generate cell-type specific transcriptomic and epigenomic profiles using AD and control organoids. As our study used bulk genomic and transcriptomic data, we were unable to investigate the precise cellular changes that could contribute to AD. To begin answering this question, there have been several single cell profiles generated using human AD brains. For example, *APOE* expression has been observed in a cell-type specific pattern in the entorhinal cortex of AD brains [486]. In oligodendrocyte progenitors and astrocyte subpopulations, *APOE* was found to be significantly repressed, but in microglial subpopulations its transcription was upregulated. Another analysis using the prefrontal cortexes of early-stage AD brains revealed that AD-associated transcriptomic changes are highly cell-type specific [345]. On the other hand, genes found to be upregulated in late-stage brains were observed across all examined cell types. It would be interesting to cross compare these early- and late-stage AD single cell profiles with those studying the progressive transition from normal cognition to mild cognitive impairment to various severities of AD-dementia [487] to possibly better refine transition probability models.

With respect to applying single cell technology to organoids, only neural ectodermal derived cell types, (i.e., neuronal and glial populations) could be profiled in organoid models. Importantly, a single human cortical spheroid on average contains 500,000 – 1,000,000 cells and after FACS sorting for specific cell types, there is sufficient starting material to perform single-cell RNAseq [488]. Despite the impressive number of cells that can be isolated from organoids, single-cell epigenomic profiling has yet to be developed. This is predominately

due to the large amount of input DNA required by current DNA modification capture protocols. Alternatively, cell-type specific epigenomic data could be captured by immunopanning, a purification method that uses cell-type specific antibodies to deplete cell types of interest from a heterogeneous population of cells [489]. Although large quantities of organoids would be required to isolate sufficient genomic DNA from neurons, astrocytes and oligodendrocytes, epigenomic profiles could conceivably be generated. Immunopanning can also be applied to complex tissues like the brain; however, tissues cannot be frozen and thawed due to cell lysing. Because much of AD brain tissues available are obtained from brain banks such as RUSH, other methods for isolating specific cell types, such as FACTS sorting, would need to be considered.

6.1.5. Alzheimer's Disease Conclusions

In summary, a body of work has been presented outlining the current state and future directions of the AD field. We described the importance of utilizing forebrain organoids to investigate the epigenetic landscape during early brain development and during the early-stages of AD. Collectively, our neurodevelopment findings support the importance of 5hmC for brain development, especially during the differentiation of early nervous system structures to mature brain structures. Furthermore, we showed that during early brain development of an AD-predisposed brain, subtle 5hmC alterations could affect the immature neuronal networks, increasing the vulnerability of developing AD later in life. The observations reported here support the need for new models or the adaptation of current models to more precisely define AD-associated cognitive decline and preclinical AD stages.

6.2. General Conclusions for Chronic Stress

Stressful life events are an inevitable part of life; thus, our brains have developed sophisticated mechanisms for managing how we perceive and respond to adverse events. In today's environment, individuals routinely experience acute (short-term), chronic (persistent) and/or longitudinal (re-exposure) stressor that will challenge their psychopathology. Generally, most people will maintain normal psychological function and adapt to the stressor; however, a subset of individuals will respond negatively and be at higher risk for developing anxiety or major depressive disorder (MDD). Individuals that display characteristics of cognitive flexibility, strong emotional regulation and positive affectivity and optimism are often more likely to fall into the stress resilient category [490, 491]. An important consideration to reflect on when studying stress resilience, is that,

despite an individual phenotypically presenting as depression resilient; molecularly, the negative consequences of chronic stress will still take a toll on the brain and total body health. Both stress susceptible and resilient individuals will display elevated levels of corticosterone, disruptions to sleep and feeding behaviors, and eventually neuro-inflammatory and degenerative pathologies. This suggests that differences in affirmative behaviors are not just regulated by neuro-circuitry, but are also impacted by genetic and epigenetic modifiers. Whether DNA modifications and their machinery are involved in stress-induced depression is not well understood. We therefore sought to address this gap and generated some of the first global 5mC and 5hmC profiles from the cortex of mice that underwent various durations of social defeat.

6.2.1. Validations and Functional Experiments

An important continuation of the work described in Chapter 3 would be to experimentally validate the computational predictions. One way to approach this would be from the RNA perspective rather than the DNA. By starting with our significantly differentially expressed genes (DEGs) and overlapping our differentially methylated regions (DMRs) and differentially hydroxymethylated regions (DhMRs) with them, we could more confidently suggest that the dysregulation of DNA modifications is the primary driver for the significant change in gene expression observed. Early efforts focusing on this approach revealed interesting preliminary findings after we conducted within group (**Figure 6.1:A**) and between group analyses (**Figure 6.1:B**). For the within group, it was immediately apparent that when we compared control animals to their corresponding stress resilient counterparts, there were considerably less differentially expressed genes compared to the control and susceptible animal comparisons. The exception to this observation is the chronically stressed resilient animals. This suggests that resilient and control animals share a similar transcriptomic profile and those significant DEGs regulated by 5mC and 5hmC could indicate critical genes necessary to maintain a resilient phenotype. Notably, the 6-month chronically stressed animals contained the most significant DEGs, supporting the idea that age increases sensitivity to stress. When we preformed between group comparisons, very few significant DEGs were conserved; however, those that were appeared to have critical roles in the nervous system. The neuropilin receptor, *Nrp2*, was identified from the acute social defeat stress (ASDS) stress vs. chronic social defeat stress (CSDS) resilient comparison and shows increased promoter methylation coinciding with reduced

gene expression in CSDS resilient animals (**Figure 6.1:C**). This gene canonically functions with its semaphorin ligand, Sema3f, to facilitate embryonic development of the sympathetic nervous system [492]. In the adult brain, *Nrp2* has been linked to increased recruitment of oligo-progenitor cells [493]. From the ASDS stress vs. CSDS susceptible significant DEGs, we identified the synaptic protein *Rims3* which is essential for neurotransmitter release (**Figure 6.1:D**) [494]. Finally, we observed the *Ptprb* gene (**Figure 6.1:E**) that functions in angiogenesis and can facilitate the restoration of the blood brain barrier by activating downstream signaling molecules [495]. *Ptprb* showed reduced expression in L_{RR} compared to resilient animals. Given its function as an activator of vessel development, it is likely chronically stressed animals benefit more to higher expression than those who have a re-exposure. Overall, our brief analysis revealed new avenues worth exploring in functional studies.

A

Within Group Analysis	5mC	5hmC
ASDS Ctr. vs. Stress	17	13
CSDS Ctr. vs. Susceptible	13	1
CSDS Ctr. vs. Resilient	16	12
6 CSDS Ctr. vs. Susceptible	370	264
6 CSDS Ctr. vs. Resilient	6	3
LSDS Ctr. vs. L_{SS}	32	8
LSDS Ctr. vs. L_{RR}	5	0

B

Between Group Analysis	5mC	5hmC
ASDS Stress. vs. CSDS Sus.	6	4
ASDS Stress. vs. CSDS Res.	3	2
CSDS Sus. vs . L_{SS}	4	0
CSDS Res. vs. L_{RR}	4	2

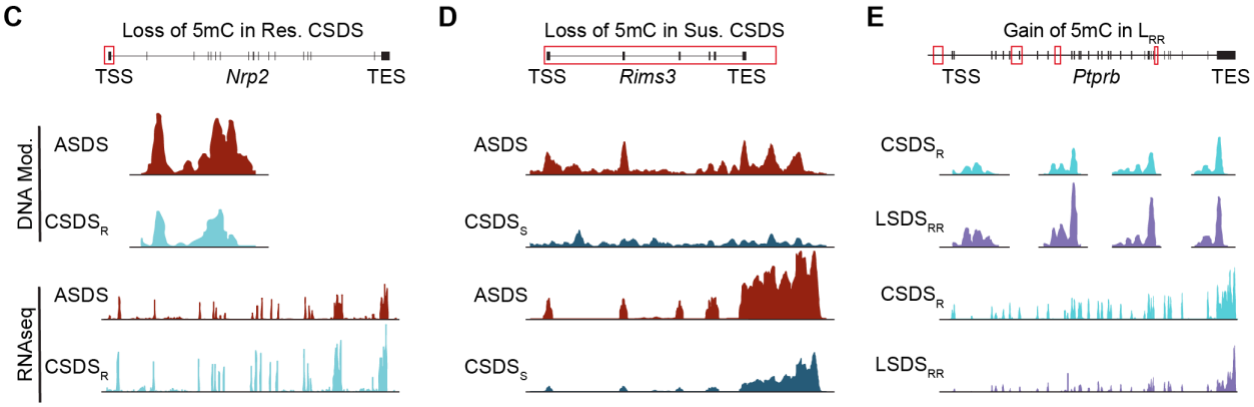

Figure 6.1: RNA-seq based targeting of stress responding genes for functional validation
A. Number of significantly differentially expressed genes identified from within group analysis overlapped with DMRs or DhMRs. **B.** Number of significantly differentially expressed genes identified from between group analysis overlapped with DMRs or DhMRs. **C-E.** Normalized 5mC counts at specific peak regions identified in 3-month CSDS or LSDS animals: *Nrp2* (**C**), *Rims3* (**D**) and *Ptbrb* (**E**).

6.2.2. Additional Stress Responding Brain Regions

In addition to the cortex, several additional stress-responding brain regions were collected including the hippocampi, hypothalamus and cerebellum for epigenetic profiling. The hippocampus is the region of the brain that consolidates information into short-term, long-term and spatial memory and further regulates memory recall. Furthermore, the hippocampus serves as a critical inhibitor of HPA-axis activation, which is largely attributed to the high expression of glucocorticoid receptors [496]. Chronic stress studies have demonstrated that persistently elevated levels of glucocorticoid exposure affect memory recall [497] and induce structural and functional damage. For example, there are reports of increased neuronal cell death, cytoskeletal defects (dendrite morphology), glutamate excitotoxicity, reduced neurogenesis and suppression of long-term-potentiation and synaptic plasticity [498]. The hypothalamus is responsible for regulating certain metabolic processes and autonomic processes like breathing, digestion, organ function, body temperature, hunger and circadian rhythms. Importantly, secretion of the corticotrophin-releasing hormone (CRH) from paraventricular

nuclei in the hypothalamus, initiates stress induced activation of the HPA-axis. Outside of its role in HPA-axis activation, the hypothalamus also is a major contributor to the abnormalities in appetite, sleep, circadian rhythms and sexual behaviors frequently observed in depressed patients. Finally, the cerebellum has been underappreciated for its contribution to stress response, potentially because its roles are traditionally devoted to motor function, despite it having all the machinery required to respond to stress. Over the years, more and more studies have demonstrated disruptions in cerebellar networks [499] and emotion regulation [500] as contributors to MDD. Furthermore, both acute and chronic stress studies have shown alterations in cerebellar neurotransmitter regulation and glucocorticoid receptor gene expression [501]. The incorporation of the epigenetic profiles from these additional brains will provide a complete DNA modification database encompassing the major stress responding brain regions.

6.2.3. Cell Type Specific Epigenetic Profiling Using Immunopanning

The second aim of this project was to profile stress-induced DNA modification changes in a cell-type specific manner. To achieve this, we collaborated with Dr. Steven Sloan's lab and implemented his immunopanning method to isolate purified neurons, microglia and astrocytes (**Figure 6.2:A**) [469]. Immunopanning is a depletion-based method that utilizes antibodies against cell-type specific surface receptors to enrich for a specific cell type. There were a number of experimental and technical challenges that needed to be overcome to accomplish these experiments. First, immunopanning requires the use of fresh, never frozen tissue. Accordingly, all social interaction videos had to be scored same day so the phenotype of each stressed mouse was known. Second, the 5mC and 5hmC capture protocols used require 3-5μg of genomic DNA for efficient capture. After immunopanning, only 0.5μg or less of DNA was isolated, therefore we were only able to perform 5hmC-seq on microglia and neurons from control, susceptible and resilient animals. This leads into the third challenge in that for every round of CSDS performed, an average of 1-3 resilient animals were obtained, which leads into the fourth and final challenge. Because a sufficient number of resilient animals is not guaranteed from each round of CSDS, purified microglia and neurons from resilient mice were not analyzed in duplicate like they were for control and susceptible animals. Preliminary analysis of the 5hmC read count suggests that microglia from resilient animals have a very unique epigenetic profile unlike either control or

susceptible animals (**Figure 6.2:B**). Unfortunately, the neurons from resilient animals did not pass the sequencing for quality control and could not be used for downstream analysis. Data from our manuscript suggested that properties or functions of adult oligo-precursor cells and adult oligodendrocytes could be important for supporting a resilient phenotype. Accordingly, it may be worthwhile to isolate these cell types in future immunopanning experiments to validate these findings. Finally, to combat the need for high input DNA concentrations, a new method was developed, termed nano-hmC-Seal, that has been effectively utilized to profile the 5hmC landscape in ~1,000 cells [502].

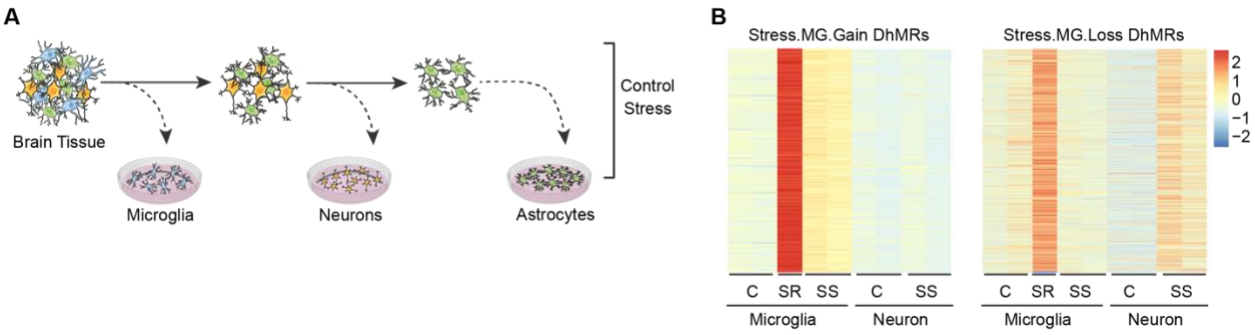

Figure 6.2: Preliminary Immunopanning Analysis
A. Schematic of immunopanning procedure. **B.** Preliminary heatmap of susceptible and resilient DhMRs from isolated microglia and neurons where the color scale represents normalized 5hmC read counts.

6.2.4. Investigating Stress Response in Females and Alternative Stress Approaches

An important research area not covered in our investigation of stress response, is the sex-dependent differences observed between men and women. Given that females are twice as likely to experience depression as compared to men [503], it is critical that future studies incorporate female animals into their studies so that the mechanism underlying stress induced sex-specific biases can be elucidated. Many possible explanations have been suggested regarding why there are drastic sex-dependent difference in depression prevalence, such as differing HPA axis activity during the menstrual cycle or differing social pressures experienced by females [504, 505]. However, inconsistent results indicate that the cause of the increased susceptibility of depression in females remains largely unknown. This lack of understanding in sex-dependent differences in stress-response, depression and anxiety primarily stem from the fact that many animal behavior models do not use female subjects. Female animals have been excluded from behavioral studies due to the misconception that their

estrous cycle causes hormonal changes, which then introduce significantly increased variability in behavioral data. In addition, many chronic stress paradigms in rodents, including CSDS, have proven difficult to implement in female mice since under most conditions, neither male nor female resident mice attack intruder females [506]. To address this challenge, the standard CSDS paradigm was modified to take advantage of odorants and pheromones in urine to stimulate aggressive behavior in male mice towards females [506]. This protocol involved collecting urine from a novel CD1 male, unknown to the resident aggressor CD1, and applying it to the base of the female tail and vaginal orifice just before the social defeat. Aggressive behavior was observed in approximately half of the resident-intruder pairings and was not affected by the estrous cycle. Importantly, canonical social avoidant and depressive behaviors were observed in stress susceptible females, further supporting the use of this adapted method in future studies where mechanistic studies could be considered.

Another variation of CSDS, known as vicarious social defeat stress (VSDS), could also be used to incorporate females into stress studies. During VSDS, male-male resident intruder defeats are still used over the course of 10 days, but a witness component is added (i.e., a third mouse witnesses the social defeat of another mouse) [507]. This paradigm proposes a scenario that would avoid the absence of aggressive behavior exhibited toward female animals. However, the few studies that have attempted to use female animals have reported conflicting success [507, 508]. In male witness mice, VSDS induces depressive and anxiety-like phenotypes; however, the initial social-avoidant behavior robustly observed in the defeated animals is less pronounced [507, 509]. Interestingly, one-month after the final defeat, witness animals develop a very robust avoidant phenotype, suggesting behavioral delay or the possible "loss" of resilience. Another exciting avenue that VSDS offers is the opportunity to differentiate between stress-induced depression caused by either physical or emotional stress. This becomes evident in PTSD studies given that the development of PTSD is not limited to those exposed to physical abuse, but can also develop in individuals who witness or perceive a traumatic event [510, 511]. Furthermore, VSDS can be a great tool to uncouple the immune response caused by physical injury verse emotional stress when studying stress-induced neuroinflammation. Overall, the inclusion of

females in stress studies will allow for a more defined understanding of sex-based biases that could ultimately lead to better preventative care and improved treatments for neuropsychiatric illnesses.

6.2.5. Stress Conclusions

In summary, a body of work has been presented outlining the current state and future directions for the field of depression. We described the importance of utilizing various durations of social defeat to identify key target genes that are most likely to contribute to differences in stress response. Collectively, our ASDS study suggests that the priming of adult neuro- and glio-genesis could promote a resilience phenotype, while the downregulation of chromatin remodelers could prevent the chromatin rearrangement leading to stress susceptibility. Furthermore, chronic stress induced alterations to 5mC and 5hmC do not appear to account for the increase in stress susceptibility related to age. In addition, younger animals did not display 5mC or 5hmC dependent differences in the biological pathways affected whereas this distinction was observed in mature animals. Stress re-exposure appears to activate an acute stress response. The maintenance of resilience appears to be facilitated by improved regulation of metabolic and energy based homeostatic process. Finally, the stress-induced 5mC and 5hmC fluctuations across the ASDS-CSDS-LSDS time course demonstrate that resilient animals are not impervious to the negative consequences of chronic stress and susceptible animals do display some degree of neuroinflammatory and synaptic processes recovery. The observations reported here support the need for experimental validation of top candidate genes and global profiling of additional stress responding brain regions to more precisely define individual differences in stress response.

6.3. Overall Conclusions

In conclusion, this thesis encompasses a body of work that profiled DNA modifications across brain development and in response to AD and stress-induced depression. An important future direction for this work would be to integrate the AD and stress studies, given that chronic stress has been hypothesized to be a risk factor for AD [387]. As the acceptance that amyloid plaques and tau-proteins are no longer the predominant pathologies significantly contributing to AD progression has taken hold, this has allowed for a shift in focus, accrediting the immune and vasculature systems of the brain as critical contributors to AD. Importantly, results from our study suggest that stress susceptible animals display patterns of genetic dysregulation associated with early pathologies of AD including compromised neurovasculature system, impaired BBB function, altered lipid

metabolism, and microglia-mediated neuroinflammation. In addition to these early phenotypes, we also observed many genes associated with later stage AD pathology such as Aβ-plaques, neurodegeneration and neurofibrillary tangles. Overall, our stress data support the hypothesis that exposure to chronic stress is a major risk factor for AD and warrant further investigation in the future.

References

1. Waddington, C.H., *An introduction to modern genetics*. 1939, New York,: The Macmillan company. 2 p.l., 7 -441 p.
2. Goldberg, A.D., C.D. Allis, and E. Bernstein, *Epigenetics: a landscape takes shape.* Cell, 2007. **128**(4): p. 635-8.
3. Allis, C.D. and T. Jenuwein, *The molecular hallmarks of epigenetic control.* Nat Rev Genet, 2016. **17**(8): p. 487-500.
4. Gayon, J., *From Mendel to epigenetics: History of genetics.* C R Biol, 2016. **339**(7-8): p. 225-30.
5. Atladottir, H.O., et al., *The increasing prevalence of reported diagnoses of childhood psychiatric disorders: a descriptive multinational comparison.* Eur Child Adolesc Psychiatry, 2015. **24**(2): p. 173-83.
6. Reik, W., *Stability and flexibility of epigenetic gene regulation in mammalian development.* Nature, 2007. **447**(7143): p. 425-32.
7. Suzuki, M.M. and A. Bird, *DNA methylation landscapes: provocative insights from epigenomics.* Nat Rev Genet, 2008. **9**(6): p. 465-76.
8. Bird, A.P., *CpG-rich islands and the function of DNA methylation.* Nature, 1986. **321**(6067): p. 209-13.
9. Jones, P.A., *Functions of DNA methylation: islands, start sites, gene bodies and beyond.* Nat Rev Genet, 2012. **13**(7): p. 484-92.
10. Neri, F., et al., *Intragenic DNA methylation prevents spurious transcription initiation.* Nature, 2017. **543**(7643): p. 72-77.
11. Maunakea, A.K., et al., *Intragenic DNA methylation modulates alternative splicing by recruiting MeCP2 to promote exon recognition.* Cell Res, 2013. **23**(11): p. 1256-69.
12. Illingworth, R.S. and A.P. Bird, *CpG islands--'a rough guide'.* FEBS Lett, 2009. **583**(11): p. 1713-20.
13. Norton, N. and M.J. Owen, *HTR2A: association and expression studies in neuropsychiatric genetics.* Ann Med, 2005. **37**(2): p. 121-9.
14. Ladd-Acosta, C., et al., *DNA methylation signatures within the human brain.* Am J Hum Genet, 2007. **81**(6): p. 1304-15.

15. Borsani, G., et al., *Characterization of a murine gene expressed from the inactive X chromosome.* Nature, 1991. **351**(6324): p. 325-9.

16. Brown, C.J., et al., *The human XIST gene: analysis of a 17 kb inactive X-specific RNA that contains conserved repeats and is highly localized within the nucleus.* Cell, 1992. **71**(3): p. 527-42.

17. Beard, C., E. Li, and R. Jaenisch, *Loss of methylation activates Xist in somatic but not in embryonic cells.* Genes Dev, 1995. **9**(19): p. 2325-34.

18. Sati, S., et al., *Genome-wide analysis reveals distinct patterns of epigenetic features in long non-coding RNA loci.* Nucleic acids research, 2012. **40**(20): p. 10018-10031.

19. Liu, W.M., et al., *Alu transcripts: cytoplasmic localisation and regulation by DNA methylation.* Nucleic Acids Res, 1994. **22**(6): p. 1087-95.

20. Woodcock, D.M., et al., *Asymmetric methylation in the hypermethylated CpG promoter region of the human L1 retrotransposon.* J Biol Chem, 1997. **272**(12): p. 7810-6.

21. Walsh, C.P., J.R. Chaillet, and T.H. Bestor, *Transcription of IAP endogenous retroviruses is constrained by cytosine methylation.* Nat Genet, 1998. **20**(2): p. 116-7.

22. Ma, D.K., et al., *Epigenetic choreographers of neurogenesis in the adult mammalian brain.* Nat Neurosci, 2010. **13**(11): p. 1338-44.

23. Muotri, A.R., et al., *Somatic mosaicism in neuronal precursor cells mediated by L1 retrotransposition.* Nature, 2005. **435**(7044): p. 903-10.

24. Muotri, A.R. and F.H. Gage, *Generation of neuronal variability and complexity.* Nature, 2006. **441**(7097): p. 1087-93.

25. Coufal, N.G., et al., *L1 retrotransposition in human neural progenitor cells.* Nature, 2009. **460**(7259): p. 1127-31.

26. Li, E., C. Beard, and R. Jaenisch, *Role for DNA methylation in genomic imprinting.* Nature, 1993. **366**(6453): p. 362-365.

27. Barlow, D.P., *Genomic imprinting: a mammalian epigenetic discovery model.* Annu Rev Genet, 2011. **45**: p. 379-403.

28. Bourc'his, D., et al., *Dnmt3L and the establishment of maternal genomic imprints.* Science, 2001. **294**(5551): p. 2536-9.

29. Kaneda, M., et al., *Role of de novo DNA methyltransferases in initiation of genomic imprinting and X-chromosome inactivation.* Cold Spring Harb Symp Quant Biol, 2004. **69**: p. 125-9.

30. Wilkinson, L.S., W. Davies, and A.R. Isles, *Genomic imprinting effects on brain development and function.* Nat Rev Neurosci, 2007. **8**(11): p. 832-43.

31. Aizawa, T., et al., *Expression of necdin, an embryonal carcinoma-derived nuclear protein, in developing mouse brain.* Brain Res Dev Brain Res, 1992. **68**(2): p. 265-74.

32. Mohn, F., et al., *Lineage-specific polycomb targets and de novo DNA methylation define restriction and potential of neuronal progenitors.* Mol Cell, 2008. **30**(6): p. 755-66.

33. Teter, B., et al., *Methylation of the rat glial fibrillary acidic protein gene shows tissue-specific domains.* J Neurosci Res, 1994. **39**(6): p. 680-93.

34. Takizawa, T., et al., *DNA methylation is a critical cell-intrinsic determinant of astrocyte differentiation in the fetal brain.* Dev Cell, 2001. **1**(6): p. 749-58.

35. Pensold, D., et al., *The DNA Methyltransferase 1 (DNMT1) Controls the Shape and Dynamics of Migrating POA-Derived Interneurons Fated for the Murine Cerebral Cortex.* Cereb Cortex, 2017. **27**(12): p. 5696-5714.

36. Symmank, J., et al., *DNMT1 modulates interneuron morphology by regulating Pak6 expression through crosstalk with histone modifications.* Epigenetics, 2018. **13**(5): p. 536-556.

37. Kumar, R., et al., *Structure, biochemistry, and biology of PAK kinases.* Gene, 2017. **605**: p. 20-31.

38. Civiero, L., et al., *Leucine-rich repeat kinase 2 interacts with p21-activated kinase 6 to control neurite complexity in mammalian brain.* J Neurochem, 2015. **135**(6): p. 1242-56.

39. Toyoda, S., et al., *Developmental epigenetic modification regulates stochastic expression of clustered protocadherin genes, generating single neuron diversity.* Neuron, 2014. **82**(1): p. 94-108.

40. Sano, K., et al., *Protocadherins: a large family of cadherin ‐ related molecules in central nervous system.* The EMBO journal, 1993. **12**(6): p. 2249-2256.

41. Lefebvre, J.L., et al., *Protocadherins mediate dendritic self-avoidance in the mammalian nervous system.* Nature, 2012. **488**(7412): p. 517-21.

42. Wang, X., et al., *Gamma protocadherins are required for survival of spinal interneurons.* Neuron, 2002. **36**(5): p. 843-54.

43. Garrett, A.M., et al., *gamma-protocadherins control cortical dendrite arborization by regulating the activity of a FAK/PKC/MARCKS signaling pathway.* Neuron, 2012. **74**(2): p. 269-76.

44. Kohmura, N., et al., *Diversity revealed by a novel family of cadherins expressed in neurons at a synaptic complex.* Neuron, 1998. **20**(6): p. 1137-1151.

45. Wu, Q. and T. Maniatis, *A striking organization of a large family of human neural cadherin-like cell adhesion genes.* Cell, 1999. **97**(6): p. 779-790.

46. Hirayama, T. and T. Yagi. *Regulation of clustered protocadherin genes in individual neurons*. in *Seminars in cell & developmental biology*. 2017. Elsevier.

47. Morris, R.G., et al., *Place navigation impaired in rats with hippocampal lesions.* Nature, 1982. **297**(5868): p. 681-3.

48. Squire, L.R., *Mechanisms of memory.* Science, 1986. **232**(4758): p. 1612-9.

49. Miller, C.A., et al., *Cortical DNA methylation maintains remote memory.* Nature neuroscience, 2010. **13**(6): p. 664-666.

50. Levenson, J.M., et al., *Evidence that DNA (cytosine-5) methyltransferase regulates synaptic plasticity in the hippocampus.* Journal of Biological Chemistry, 2006. **281**(23): p. 15763-15773.

51. Miller, C.A. and J.D. Sweatt, *Covalent modification of DNA regulates memory formation.* Neuron, 2007. **53**(6): p. 857-869.

52. Guo, J.U., et al., *Neuronal activity modifies the DNA methylation landscape in the adult brain.* Nat Neurosci, 2011. **14**(10): p. 1345-51.

53. Weaver, I.C., et al., *Epigenetic programming by maternal behavior.* Nat Neurosci, 2004. **7**(8): p. 847-54.

54. McGowan, P.O., et al., *Epigenetic regulation of the glucocorticoid receptor in human brain associates with childhood abuse.* Nat Neurosci, 2009. **12**(3): p. 342-8.

55. Yu, N.K., S.H. Baek, and B.K. Kaang, *DNA methylation-mediated control of learning and memory.* Mol Brain, 2011. **4**: p. 5.

56. Bestor, T.H. and G.L. Verdine, *DNA methyltransferases.* Curr Opin Cell Biol, 1994. **6**(3): p. 380-9.

57. Frauer, C., et al., *Different binding properties and function of CXXC zinc finger domains in Dnmt1 and Tet1.* PLoS One, 2011. **6**(2): p. e16627.

58. Dhayalan, A., et al., *The Dnmt3a PWWP domain reads histone 3 lysine 36 trimethylation and guides DNA methylation.* J Biol Chem, 2010. **285**(34): p. 26114-20.

59. Hata, K., et al., *Dnmt3L cooperates with the Dnmt3 family of de novo DNA methyltransferases to establish maternal imprints in mice.* Development, 2002. **129**(8): p. 1983-93.

60. Bestor, T.H. and V.M. Ingram, *Two DNA methyltransferases from murine erythroleukemia cells: purification, sequence specificity, and mode of interaction with DNA.* Proc Natl Acad Sci U S A, 1983. **80**(18): p. 5559-63.

61. Chuang, L.S., et al., *Human DNA-(cytosine-5) methyltransferase-PCNA complex as a target for p21WAF1.* Science, 1997. **277**(5334): p. 1996-2000.

62. Delgado, S., et al., *Initiation of DNA replication at CpG islands in mammalian chromosomes.* EMBO J, 1998. **17**(8): p. 2426-35.

63. Li, E., T.H. Bestor, and R. Jaenisch, *Targeted mutation of the DNA methyltransferase gene results in embryonic lethality.* Cell, 1992. **69**(6): p. 915-26.

64. Okano, M., S. Xie, and E. Li, *Cloning and characterization of a family of novel mammalian DNA (cytosine-5) methyltransferases.* Nat Genet, 1998. **19**(3): p. 219-20.

65. Okano, M., et al., *DNA methyltransferases Dnmt3a and Dnmt3b are essential for de novo methylation and mammalian development.* Cell, 1999. **99**(3): p. 247-57.

66. Okano, M., S. Xie, and E. Li, *Dnmt2 is not required for de novo and maintenance methylation of viral DNA in embryonic stem cells.* Nucleic Acids Res, 1998. **26**(11): p. 2536-40.

67. Goll, M.G., et al., *Methylation of tRNAAsp by the DNA methyltransferase homolog Dnmt2.* Science, 2006. **311**(5759): p. 395-8.

68. Schaefer, M., et al., *RNA methylation by Dnmt2 protects transfer RNAs against stress-induced cleavage.* Genes & development, 2010. **24**(15): p. 1590-1595.

69. Bourc'his, D. and T.H. Bestor, *Meiotic catastrophe and retrotransposon reactivation in male germ cells lacking Dnmt3L.* Nature, 2004. **431**(7004): p. 96-9.

70. Goto, K., et al., *Expression of DNA methyltransferase gene in mature and immature neurons as well as proliferating cells in mice.* Differentiation, 1994. **56**(1-2): p. 39-44.

71. Feng, J., et al., *Dynamic expression of de novo DNA methyltransferases Dnmt3a and Dnmt3b in the central nervous system.* J Neurosci Res, 2005. **79**(6): p. 734-46.

72. Fan, G., et al., *DNA hypomethylation perturbs the function and survival of CNS neurons in postnatal animals.* J Neurosci, 2001. **21**(3): p. 788-97.

73. Feng, J., et al., *Dnmt1 and Dnmt3a maintain DNA methylation and regulate synaptic function in adult forebrain neurons.* Nat Neurosci, 2010. **13**(4): p. 423-30.

74. Guo, J.U., et al., *Distribution, recognition and regulation of non-CpG methylation in the adult mammalian brain.* Nat Neurosci, 2014. **17**(2): p. 215-22.

75. Shirane, K., et al., *Mouse oocyte methylomes at base resolution reveal genome-wide accumulation of non-CpG methylation and role of DNA methyltransferases.* PLoS Genet, 2013. **9**(4): p. e1003439.

76. Xie, W., et al., *Base-resolution analyses of sequence and parent-of-origin dependent DNA methylation in the mouse genome.* Cell, 2012. **148**(4): p. 816-31.

77. Varley, K.E., et al., *Dynamic DNA methylation across diverse human cell lines and tissues.* Genome Res, 2013. **23**(3): p. 555-67.

78. Lister, R., et al., *Human DNA methylomes at base resolution show widespread epigenomic differences.* Nature, 2009. **462**(7271): p. 315-22.

79. Laurent, L., et al., *Dynamic changes in the human methylome during differentiation.* Genome Res, 2010. **20**(3): p. 320-31.

80. Lister, R., et al., *Global epigenomic reconfiguration during mammalian brain development.* Science, 2013. **341**(6146): p. 1237905.

81. Mo, A., et al., *Epigenomic Signatures of Neuronal Diversity in the Mammalian Brain.* Neuron, 2015. **86**(6): p. 1369-84.

82. Ballestar, E. and A.P. Wolffe, *Methyl-CpG-binding proteins. Targeting specific gene repression.* Eur J Biochem, 2001. **268**(1): p. 1-6.

83. Hendrich, B. and A. Bird, *Identification and characterization of a family of mammalian methyl-CpG binding proteins.* Mol Cell Biol, 1998. **18**(11): p. 6538-47.

84. Jones, P.L., et al., *Methylated DNA and MeCP2 recruit histone deacetylase to repress transcription.* Nat Genet, 1998. **19**(2): p. 187-91.

85. Fuks, F., et al., *The methyl-CpG-binding protein MeCP2 links DNA methylation to histone methylation.* J Biol Chem, 2003. **278**(6): p. 4035-40.

86. Nan, X., et al., *Transcriptional repression by the methyl-CpG-binding protein MeCP2 involves a histone deacetylase complex.* Nature, 1998. **393**(6683): p. 386-389.

87. Gabel, H.W., et al., *Disruption of DNA-methylation-dependent long gene repression in Rett syndrome.* Nature, 2015. **522**(7554): p. 89-93.

88. Mellén, M., et al., *MeCP2 binds to 5hmC enriched within active genes and accessible chromatin in the nervous system.* Cell, 2012. **151**(7): p. 1417-1430.

89. Shahbazian, M.D., et al., *Insight into Rett syndrome: MeCP2 levels display tissue- and cell-specific differences and correlate with neuronal maturation.* Hum Mol Genet, 2002. **11**(2): p. 115-24.

90. Cassel, S., et al., *Expression of the methyl-CpG-binding protein MeCP2 in rat brain. An ontogenetic study.* Neurobiol Dis, 2004. **15**(2): p. 206-11.

91. Mullaney, B.C., M.V. Johnston, and M.E. Blue, *Developmental expression of methyl-CpG binding protein 2 is dynamically regulated in the rodent brain.* Neuroscience, 2004. **123**(4): p. 939-49.

92. Chen, W.G., et al., *Derepression of BDNF transcription involves calcium-dependent phosphorylation of MeCP2.* Science, 2003. **302**(5646): p. 885-9.

93. Martinowich, K., et al., *DNA methylation-related chromatin remodeling in activity-dependent BDNF gene regulation.* Science, 2003. **302**(5646): p. 890-3.

94. Horike, S., et al., *Loss of silent-chromatin looping and impaired imprinting of DLX5 in Rett syndrome.* Nat Genet, 2005. **37**(1): p. 31-40.

95. Amir, R.E., et al., *Rett syndrome is caused by mutations in X-linked MECP2, encoding methyl-CpG-binding protein 2.* Nat Genet, 1999. **23**(2): p. 185-8.

96. Fujita, N., et al., *Methyl-CpG binding domain 1 (MBD1) interacts with the Suv39h1-HP1 heterochromatic complex for DNA methylation-based transcriptional repression.* J Biol Chem, 2003. **278**(26): p. 24132-8.

97. Fujita, N., et al., *MCAF mediates MBD1-dependent transcriptional repression.* Mol Cell Biol, 2003. **23**(8): p. 2834-43.

98. Sarraf, S.A. and I. Stancheva, *Methyl-CpG binding protein MBD1 couples histone H3 methylation at lysine 9 by SETDB1 to DNA replication and chromatin assembly.* Mol Cell, 2004. **15**(4): p. 595-605.

99. Zhang, Y., et al., *Analysis of the NuRD subunits reveals a histone deacetylase core complex and a connection with DNA methylation.* Genes Dev, 1999. **13**(15): p. 1924-35.

100. Zhao, X., et al., *Mice lacking methyl-CpG binding protein 1 have deficits in adult neurogenesis and hippocampal function.* Proc Natl Acad Sci U S A, 2003. **100**(11): p. 6777-82.

101. Jung, B.P., et al., *Differential expression of methyl CpG-binding domain containing factor MBD3 in the developing and adult rat brain.* J Neurobiol, 2003. **55**(2): p. 220-32.

102. Monk, M., M. Boubelik, and S. Lehnert, *Temporal and regional changes in DNA methylation in the embryonic, extraembryonic and germ cell lineages during mouse embryo development.* Development, 1987. **99**(3): p. 371-82.

103. Kafri, T., et al., *Developmental pattern of gene-specific DNA methylation in the mouse embryo and germ line.* Genes Dev, 1992. **6**(5): p. 705-14.

104. Tada, T., et al., *Epigenotype switching of imprintable loci in embryonic germ cells.* Dev Genes Evol, 1998. **207**(8): p. 551-61.

105. Howlett, S.K. and W. Reik, *Methylation levels of maternal and paternal genomes during preimplantation development.* Development, 1991. **113**(1): p. 119-27.

106. Mertineit, C., et al., *Sex-specific exons control DNA methyltransferase in mammalian germ cells.* Development, 1998. **125**(5): p. 889-97.

107. Rougier, N., et al., *Chromosome methylation patterns during mammalian preimplantation development.* Genes Dev, 1998. **12**(14): p. 2108-13.

108. Howell, C.Y., et al., *Genomic imprinting disrupted by a maternal effect mutation in the Dnmt1 gene.* Cell, 2001. **104**(6): p. 829-838.

109. Valinluck, V. and L.C. Sowers, *Endogenous cytosine damage products alter the site selectivity of human DNA maintenance methyltransferase DNMT1.* Cancer Res, 2007. **67**(3): p. 946-50.

110. Kriaucionis, S. and N. Heintz, *The nuclear DNA base 5-hydroxymethylcytosine is present in Purkinje neurons and the brain.* Science, 2009. **324**(5929): p. 929-30.

111. Tahiliani, M., et al., *Conversion of 5-methylcytosine to 5-hydroxymethylcytosine in mammalian DNA by MLL partner TET1.* Science, 2009. **324**(5929): p. 930-935.

112. Ito, S., et al., *Role of Tet proteins in 5mC to 5hmC conversion, ES-cell self-renewal and inner cell mass specification.* Nature, 2010. **466**(7310): p. 1129-33.

113. Ito, S., et al., *Tet proteins can convert 5-methylcytosine to 5-formylcytosine and 5-carboxylcytosine.* Science, 2011. **333**(6047): p. 1300-3.

114. He, Y.F., et al., *Tet-mediated formation of 5-carboxylcytosine and its excision by TDG in mammalian DNA.* Science, 2011. **333**(6047): p. 1303-7.

115. Bhutani, N., D.M. Burns, and H.M. Blau, *DNA demethylation dynamics.* Cell, 2011. **146**(6): p. 866-72.

116. Amouroux, R., et al., *De novo DNA methylation drives 5hmC accumulation in mouse zygotes.* Nat Cell Biol, 2016. **18**(2): p. 225-233.

117. Iyer, L.M., et al., *Prediction of novel families of enzymes involved in oxidative and other complex modifications of bases in nucleic acids.* Cell Cycle, 2009. **8**(11): p. 1698-710.

118. Yildirim, O., et al., *Mbd3/NURD complex regulates expression of 5-hydroxymethylcytosine marked genes in embryonic stem cells.* Cell, 2011. **147**(7): p. 1498-1510.

119. Deplus, R., et al., *TET2 and TET3 regulate GlcNAcylation and H3K4 methylation through OGT and SET1/COMPASS*. The EMBO journal, 2013. **32**(5): p. 645-655.

120. Costa, Y., et al., *NANOG-dependent function of TET1 and TET2 in establishment of pluripotency*. Nature, 2013. **495**(7441): p. 370-4.

121. Vella, P., et al., *Tet proteins connect the O-linked N-acetylglucosamine transferase Ogt to chromatin in embryonic stem cells*. Molecular cell, 2013. **49**(4): p. 645-656.

122. Gu, T.P., et al., *The role of Tet3 DNA dioxygenase in epigenetic reprogramming by oocytes*. Nature, 2011. **477**(7366): p. 606-10.

123. Iqbal, K., et al., *Reprogramming of the paternal genome upon fertilization involves genome-wide oxidation of 5-methylcytosine*. Proceedings of the National Academy of Sciences, 2011. **108**(9): p. 3642-3647.

124. Wossidlo, M., et al., *5-Hydroxymethylcytosine in the mammalian zygote is linked with epigenetic reprogramming*. Nature communications, 2011. **2**(1): p. 1-8.

125. Szulwach, K.E., et al., *5-hmC-mediated epigenetic dynamics during postnatal neurodevelopment and aging*. Nat Neurosci, 2011. **14**(12): p. 1607-16.

126. Hahn, M.A., et al., *Dynamics of 5-hydroxymethylcytosine and chromatin marks in Mammalian neurogenesis*. Cell reports, 2013. **3**(2): p. 291-300.

127. Rudenko, A., et al., *Tet1 is critical for neuronal activity-regulated gene expression and memory extinction*. Neuron, 2013. **79**(6): p. 1109-1122.

128. Li, X., et al., *Neocortical Tet3-mediated accumulation of 5-hydroxymethylcytosine promotes rapid behavioral adaptation*. Proceedings of the National Academy of Sciences, 2014. **111**(19): p. 7120-7125.

129. Orsini, C.A. and S. Maren, *Neural and cellular mechanisms of fear and extinction memory formation*. Neuroscience & Biobehavioral Reviews, 2012. **36**(7): p. 1773-1802.

130. Globisch, D., et al., *Tissue distribution of 5-hydroxymethylcytosine and search for active demethylation intermediates*. PLoS One, 2010. **5**(12): p. e15367.

131. Song, C.X., et al., *Selective chemical labeling reveals the genome-wide distribution of 5-hydroxymethylcytosine*. Nat Biotechnol, 2011. **29**(1): p. 68-72.

132. Wang, T., et al., *Genome-wide DNA hydroxymethylation changes are associated with neurodevelopmental genes in the developing human cerebellum*. Human molecular genetics, 2012. **21**(26): p. 5500-5510.

133. West, A.E., et al., *Calcium regulation of neuronal gene expression.* Proc Natl Acad Sci U S A, 2001. **98**(20): p. 11024-31.

134. Shieh, P.B., et al., *Identification of a signaling pathway involved in calcium regulation of BDNF expression.* Neuron, 1998. **20**(4): p. 727-40.

135. Tao, X., et al., *Ca2+ influx regulates BDNF transcription by a CREB family transcription factor-dependent mechanism.* Neuron, 1998. **20**(4): p. 709-26.

136. Guo, J.U., et al., *Hydroxylation of 5-methylcytosine by TET1 promotes active DNA demethylation in the adult brain.* Cell, 2011. **145**(3): p. 423-34.

137. Song, C.-X., et al., *Genome-wide profiling of 5-formylcytosine reveals its roles in epigenetic priming.* Cell, 2013. **153**(3): p. 678-691.

138. Bachman, M., et al., *5-Formylcytosine can be a stable DNA modification in mammals.* Nat Chem Biol, 2015. **11**(8): p. 555-7.

139. Kellinger, M.W., et al., *5-formylcytosine and 5-carboxylcytosine reduce the rate and substrate specificity of RNA polymerase II transcription.* Nature structural & molecular biology, 2012. **19**(8): p. 831-833.

140. Cortazar, D., et al., *Embryonic lethal phenotype reveals a function of TDG in maintaining epigenetic stability.* Nature, 2011. **470**(7334): p. 419-23.

141. Cortellino, S., et al., *Thymine DNA glycosylase is essential for active DNA demethylation by linked deamination-base excision repair.* Cell, 2011. **146**(1): p. 67-79.

142. Spruijt, C.G., et al., *Dynamic readers for 5-(hydroxy) methylcytosine and its oxidized derivatives.* Cell, 2013. **152**(5): p. 1146-1159.

143. Kornberg, R.D. and J.O. Thomas, *Chromatin structure; oligomers of the histones.* Science, 1974. **184**(4139): p. 865-8.

144. Hyun, K., et al., *Writing, erasing and reading histone lysine methylations.* Exp Mol Med, 2017. **49**(4): p. e324.

145. Cedar, H. and Y. Bergman, *Linking DNA methylation and histone modification: patterns and paradigms.* Nat Rev Genet, 2009. **10**(5): p. 295-304.

146. Jobe, E.M., A.L. McQuate, and X. Zhao, *Crosstalk among epigenetic pathways regulates neurogenesis.* Frontiers in neuroscience, 2012. **6**: p. 59.

147. Schwartz, Y.B. and V. Pirrotta, *Polycomb complexes and epigenetic states.* Current opinion in cell biology, 2008. **20**(3): p. 266-273.

148. Franke, A., et al., *Polycomb and polyhomeotic are constituents of a multimeric protein complex in chromatin of Drosophila melanogaster.* EMBO J, 1992. **11**(8): p. 2941-50.

149. Locke, J., M.A. Kotarski, and K.D. Tartof, *Dosage-dependent modifiers of position effect variegation in Drosophila and a mass action model that explains their effect.* Genetics, 1988. **120**(1): p. 181-198.

150. Shao, Z., et al., *Stabilization of chromatin structure by PRC1, a Polycomb complex.* Cell, 1999. **98**(1): p. 37-46.

151. Ng, J., et al., *A Drosophila ESC-E (Z) protein complex is distinct from other polycomb group complexes and contains covalently modified ESC.* Molecular and cellular biology, 2000. **20**(9): p. 3069-3078.

152. Kuzmichev, A., et al., *Histone methyltransferase activity associated with a human multiprotein complex containing the Enhancer of Zeste protein.* Genes & development, 2002. **16**(22): p. 2893-2905.

153. Tie, F., et al., *The Drosophila Polycomb Group proteins ESC and E (Z) are present in a complex containing the histone-binding protein p55 and the histone deacetylase RPD3.* Development, 2001. **128**(2): p. 275-286.

154. Cao, R., et al., *Role of histone H3 lysine 27 methylation in Polycomb-group silencing.* Science, 2002. **298**(5595): p. 1039-43.

155. Fischle, W., et al., *Molecular basis for the discrimination of repressive methyl-lysine marks in histone H3 by Polycomb and HP1 chromodomains.* Genes Dev, 2003. **17**(15): p. 1870-81.

156. Min, J., Y. Zhang, and R.-M. Xu, *Structural basis for specific binding of Polycomb chromodomain to histone H3 methylated at Lys 27.* Genes & development, 2003. **17**(15): p. 1823-1828.

157. de Napoles, M., et al., *Polycomb group proteins Ring1A/B link ubiquitylation of histone H2A to heritable gene silencing and X inactivation.* Developmental cell, 2004. **7**(5): p. 663-676.

158. Schuettengruber, B., et al., *Trithorax group proteins: switching genes on and keeping them active.* Nature reviews Molecular cell biology, 2011. **12**(12): p. 799-814.

159. Roguev, A., et al., *The Saccharomyces cerevisiae Set1 complex includes an Ash2 homologue and methylates histone 3 lysine 4*. The EMBO journal, 2001. **20**(24): p. 7137-7148.

160. Miller, T., et al., *COMPASS: a complex of proteins associated with a trithorax-related SET domain protein*. Proceedings of the National Academy of Sciences, 2001. **98**(23): p. 12902-12907.

161. Wu, M., et al., *Molecular regulation of H3K4 trimethylation by Wdr82, a component of human Set1/COMPASS*. Molecular and cellular biology, 2008. **28**(24): p. 7337-7344.

162. Bernstein, B.E., et al., *A bivalent chromatin structure marks key developmental genes in embryonic stem cells*. Cell, 2006. **125**(2): p. 315-26.

163. Mikkelsen, T.S., et al., *Genome-wide maps of chromatin state in pluripotent and lineage-committed cells*. Nature, 2007. **448**(7153): p. 553-560.

164. Burgold, T., et al., *The histone H3 lysine 27-specific demethylase Jmjd3 is required for neural commitment*. PLoS One, 2008. **3**(8): p. e3034.

165. Jiang, H., et al., *Role for Dpy-30 in ES cell-fate specification by regulation of H3K4 methylation within bivalent domains*. Cell, 2011. **144**(4): p. 513-525.

166. Pereira, J.D., et al., *Ezh2, the histone methyltransferase of PRC2, regulates the balance between self-renewal and differentiation in the cerebral cortex*. Proceedings of the National Academy of Sciences, 2010. **107**(36): p. 15957-15962.

167. Hirabayashi, Y., et al., *Polycomb limits the neurogenic competence of neural precursor cells to promote astrogenic fate transition*. Neuron, 2009. **63**(5): p. 600-613.

168. Sher, F., Rossler, R., Brouwer, N., Balasubramaniyan, V., Boddeke, E., and Copray, S., *Differentiation of neural stem cells into oligodendrocytes: involvement of the polycomb group protein Ezh2*. Stem Cells, 2008. **26**: p. 2875-2883.

169. Di Meglio, T., et al., *Ezh2 orchestrates topographic migration and connectivity of mouse precerebellar neurons*. Science, 2013. **339**(6116): p. 204-207.

170. Wu, H., et al., *Dnmt3a-dependent nonpromoter DNA methylation facilitates transcription of neurogenic genes*. science, 2010. **329**(5990): p. 444-448.

171. Inoue, A. and D. Fujimoto, *Histone deacetylase from calf thymus.* Biochimica et Biophysica Acta (BBA)-Enzymology, 1970. **220**(2): p. 307-316.

172. Racey, L.A. and P. Byvoet, *Histone acetyltransferase in chromatin: Evidence for in vitro enzymatic transfer of acetate from acetyl-coenzyme A to histones.* Experimental Cell Research, 1971. **64**(2): p. 366-370.

173. Yang, H.L., et al., *Affinity Purification of Hepatitis B Virus Surface Antigen Containing PreS1 Region.* Sheng Wu Hua Xue Yu Sheng Wu Wu Li Xue Bao (Shanghai), 1996. **28**(4): p. 412-417.

174. Sterner, D.E. and S.L. Berger, *Acetylation of histones and transcription-related factors.* Microbiology and molecular biology reviews, 2000. **64**(2): p. 435-459.

175. Kouzarides, T., *Chromatin modifications and their function.* Cell, 2007. **128**(4): p. 693-705.

176. Saha, R. and K. Pahan, *HATs and HDACs in neurodegeneration: a tale of disconcerted acetylation homeostasis.* Cell Death & Differentiation, 2006. **13**(4): p. 539-550.

177. Gray, S.G. and T.J. Ekstrom, *The human histone deacetylase family.* Exp Cell Res, 2001. **262**(2): p. 75-83.

178. Abel, T. and R.S. Zukin, *Epigenetic targets of HDAC inhibition in neurodegenerative and psychiatric disorders.* Curr Opin Pharmacol, 2008. **8**(1): p. 57-64.

179. Cao, X. and T.C. Sudhof, *A transcriptionally [correction of transcriptively] active complex of APP with Fe65 and histone acetyltransferase Tip60.* Science, 2001. **293**(5527): p. 115-20.

180. Fischer, A., et al., *Recovery of learning and memory is associated with chromatin remodelling.* Nature, 2007. **447**(7141): p. 178-82.

181. Nitarska, J., et al., *A Functional Switch of NuRD Chromatin Remodeling Complex Subunits Regulates Mouse Cortical Development.* Cell Rep, 2016. **17**(6): p. 1683-1698.

182. Son, E.Y. and G.R. Crabtree. *The role of BAF (mSWI/SNF) complexes in mammalian neural development*. in *American Journal of Medical Genetics Part C: Seminars in Medical Genetics*. 2014. Wiley Online Library.

183. Kaeser, M.D., et al., *BRD7, a novel PBAF-specific SWI/SNF subunit, is required for target gene activation and repression in embryonic stem cells.* Journal of Biological Chemistry, 2008. **283**(47): p. 32254-32263.

184. Lessard, J., et al., *An essential switch in subunit composition of a chromatin remodeling complex during neural development.* Neuron, 2007. **55**(2): p. 201-215.

185. Wang, W., et al., *Purification and biochemical heterogeneity of the mammalian SWI - SNF complex.* The EMBO journal, 1996. **15**(19): p. 5370-5382.

186. Wang, W., et al., *Diversity and specialization of mammalian SWI/SNF complexes.* Genes & development, 1996. **10**(17): p. 2117-2130.

187. Bultman, S., et al., *A Brg1 null mutation in the mouse reveals functional differences among mammalian SWI/SNF complexes.* Mol Cell, 2000. **6**(6): p. 1287-95.

188. Ho, L., et al., *An embryonic stem cell chromatin remodeling complex, esBAF, is essential for embryonic stem cell self-renewal and pluripotency.* Proceedings of the National Academy of Sciences, 2009. **106**(13): p. 5181-5186.

189. Ho, L., et al., *esBAF facilitates pluripotency by conditioning the genome for LIF/STAT3 signalling and by regulating polycomb function.* Nature cell biology, 2011. **13**(8): p. 903-913.

190. Tuoc, T.C., et al., *Chromatin regulation by BAF170 controls cerebral cortical size and thickness.* Developmental cell, 2013. **25**(3): p. 256-269.

191. Gotz, M., A. Stoykova, and P. Gruss, *Pax6 controls radial glia differentiation in the cerebral cortex.* Neuron, 1998. **21**(5): p. 1031-44.

192. Chong, J.A., et al., *REST: a mammalian silencer protein that restricts sodium channel gene expression to neurons.* Cell, 1995. **80**(6): p. 949-57.

193. Schoenherr, C.J. and D.J. Anderson, *Silencing is golden: negative regulation in the control of neuronal gene transcription.* Curr Opin Neurobiol, 1995. **5**(5): p. 566-71.

194. Chen, Z.F., A.J. Paquette, and D.J. Anderson, *NRSF/REST is required in vivo for repression of multiple neuronal target genes during embryogenesis.* Nat Genet, 1998. **20**(2): p. 136-42.

195. Andres, M.E., et al., *CoREST: a functional corepressor required for regulation of neural-specific gene expression.* Proc Natl Acad Sci U S A, 1999. **96**(17): p. 9873-8.

196. Grimes, J.A., et al., *The co-repressor mSin3A is a functional component of the REST-CoREST repressor complex.* J Biol Chem, 2000. **275**(13): p. 9461-7.

197. Battaglioli, E., et al., *REST repression of neuronal genes requires components of the hSWI.SNF complex.* J Biol Chem, 2002. **277**(43): p. 41038-45.

198. Olave, I., et al., *Identification of a polymorphic, neuron-specific chromatin remodeling complex.* Genes & development, 2002. **16**(19): p. 2509-2517.

199. Naik, S.H., et al., *Development of plasmacytoid and conventional dendritic cell subtypes from single precursor cells derived in vitro and in vivo.* Nature immunology, 2007. **8**(11): p. 1217-1226.

200. Wu, J.I., et al., *Regulation of dendritic development by neuron-specific chromatin remodeling complexes.* Neuron, 2007. **56**(1): p. 94-108.

201. Aizawa, H., et al., *Dendrite development regulated by CREST, a calcium-regulated transcriptional activator.* Science, 2004. **303**(5655): p. 197-202.

202. Cech, T.R. and J.A. Steitz, *The noncoding RNA revolution-trashing old rules to forge new ones.* Cell, 2014. **157**(1): p. 77-94.

203. Bartel, D.P., *MicroRNAs: genomics, biogenesis, mechanism, and function.* Cell, 2004. **116**(2): p. 281-97.

204. Lewis, B.P., C.B. Burge, and D.P. Bartel, *Conserved seed pairing, often flanked by adenosines, indicates that thousands of human genes are microRNA targets.* cell, 2005. **120**(1): p. 15-20.

205. Lim, L.P., et al., *Microarray analysis shows that some microRNAs downregulate large numbers of target mRNAs.* Nature, 2005. **433**(7027): p. 769-773.

206. Kim, J., et al., *Identification of many microRNAs that copurify with polyribosomes in mammalian neurons.* Proceedings of the National Academy of Sciences, 2004. **101**(1): p. 360-365.

207. Krichevsky, A.M., et al., *Specific microRNAs modulate embryonic stem cell–derived neurogenesis.* Stem cells, 2006. **24**(4): p. 857-864.

208. Miska, E.A., et al., *Microarray analysis of microRNA expression in the developing mammalian brain.* Genome biology, 2004. **5**(9): p. 1-13.

209. Sempere, L.F., et al., *Expression profiling of mammalian microRNAs uncovers a subset of brain-expressed microRNAs with possible roles in murine and human neuronal differentiation.* Genome biology, 2004. **5**(3): p. 1-11.

210. Lagos-Quintana, M., et al., *Identification of tissue-specific microRNAs from mouse.* Current biology, 2002. **12**(9): p. 735-739.

211. Makeyev, E.V., et al., *The MicroRNA miR-124 promotes neuronal differentiation by triggering brain-specific alternative pre-mRNA splicing.* Molecular cell, 2007. **27**(3): p. 435-448.

212. Sharma, S., A.M. Falick, and D.L. Black, *Polypyrimidine tract binding protein blocks the 5′ splice site-dependent assembly of U2AF and the prespliceosomal E complex.* Molecular cell, 2005. **19**(4): p. 485-496.

213. Wagner, E.J. and M.A. Garcia-Blanco, *Polypyrimidine tract binding protein antagonizes exon definition.* Molecular and cellular biology, 2001. **21**(10): p. 3281-3288.

214. Silber, J., et al., *miR-124 and miR-137 inhibit proliferation of glioblastoma multiforme cells and induce differentiation of brain tumor stem cells.* BMC medicine, 2008. **6**(1): p. 1-17.

215. Kapranov, P., et al., *RNA maps reveal new RNA classes and a possible function for pervasive transcription.* Science, 2007. **316**(5830): p. 1484-1488.

216. Pang, K.C., M.C. Frith, and J.S. Mattick, *Rapid evolution of noncoding RNAs: lack of conservation does not mean lack of function.* Trends in genetics, 2006. **22**(1): p. 1-5.

217. Ravasi, T., et al., *Experimental validation of the regulated expression of large numbers of non-coding RNAs from the mouse genome.* Genome research, 2006. **16**(1): p. 11-19.

218. Brannan, C.I., et al., *The product of the H19 gene may function as an RNA.* Mol Cell Biol, 1990. **10**(1): p. 28-36.

219. Brockdorff, N., et al., *Conservation of position and exclusive expression of mouse Xist from the inactive X chromosome.* Nature, 1991. **351**(6324): p. 329-31.

220. Plath, K., et al., *Role of histone H3 lysine 27 methylation in X inactivation.* Science, 2003. **300**(5616): p. 131-135.

221. Silva, J., et al., *Establishment of histone h3 methylation on the inactive X chromosome requires transient recruitment of Eed-Enx1 polycomb group complexes.* Developmental cell, 2003. **4**(4): p. 481-495.

222. Rinn, J.L., et al., *Functional demarcation of active and silent chromatin domains in human HOX loci by noncoding RNAs.* cell, 2007. **129**(7): p. 1311-1323.

223. Mercer, T.R., et al., *Long noncoding RNAs in neuronal-glial fate specification and oligodendrocyte lineage maturation.* BMC Neurosci, 2010. **11**: p. 14.

224. Ponting, C.P., P.L. Oliver, and W. Reik, *Evolution and functions of long noncoding RNAs.* Cell, 2009. **136**(4): p. 629-641.

225. Ng, S.-Y., et al., *Long noncoding RNAs in development and disease of the central nervous system.* Trends in Genetics, 2013. **29**(8): p. 461-468.

226. Iyer, M.K., et al., *The landscape of long noncoding RNAs in the human transcriptome.* Nature genetics, 2015. **47**(3): p. 199-208.

227. Mercer, T.R., et al., *Noncoding RNAs in Long-Term Memory Formation.* Neuroscientist, 2008. **14**(5): p. 434-45.

228. Bernard, D., et al., *A long nuclear-retained non-coding RNA regulates synaptogenesis by modulating gene expression.* EMBO J, 2010. **29**(18): p. 3082-93.

229. Lipovich, L., et al., *Activity-dependent human brain coding/noncoding gene regulatory networks.* Genetics, 2012. **192**(3): p. 1133-1148.

230. Clemson, C.M., et al., *An architectural role for a nuclear noncoding RNA: NEAT1 RNA is essential for the structure of paraspeckles.* Mol Cell, 2009. **33**(6): p. 717-26.

231. Lamond, A.I. and D.L. Spector, *Nuclear speckles: a model for nuclear organelles.* Nature reviews Molecular cell biology, 2003. **4**(8): p. 605-612.

232. Hutchinson, J.N., et al., *A screen for nuclear transcripts identifies two linked noncoding RNAs associated with SC35 splicing domains.* BMC genomics, 2007. **8**(1): p. 1-16.

233. Lv, J., et al., *Identification and characterization of long non-coding RNAs related to mouse embryonic brain development from available transcriptomic data.* PloS one, 2013. **8**(8): p. e71152.

234. Lin, M., et al., *RNA-Seq of human neurons derived from iPS cells reveals candidate long non-coding RNAs involved in neurogenesis and neuropsychiatric disorders.* PloS one, 2011. **6**(9): p. e23356.

235. Kleaveland, B., et al., *A network of noncoding regulatory RNAs acts in the mammalian brain.* Cell, 2018. **174**(2): p. 350-362. e17.

236. Memczak, S., et al., *Circular RNAs are a large class of animal RNAs with regulatory potency.* Nature, 2013. **495**(7441): p. 333-338.

237. Piwecka, M., et al., *Loss of a mammalian circular RNA locus causes miRNA deregulation and affects brain function.* Science, 2017. **357**(6357): p. eaam8526.

238. Grimson, A., et al., *MicroRNA targeting specificity in mammals: determinants beyond seed pairing.* Mol Cell, 2007. **27**(1): p. 91-105.

239. Saetrom, P., et al., *Distance constraints between microRNA target sites dictate efficacy and cooperativity.* Nucleic Acids Res, 2007. **35**(7): p. 2333-42.

240. Anand, R., K.D. Gill, and A.A. Mahdi, *Therapeutics of Alzheimer's disease: Past, present and future.* Neuropharmacology, 2014. **76 Pt A**: p. 27-50.

241. Ramirez-Bermudez, J., *Alzheimer's disease: critical notes on the history of a medical concept.* Arch Med Res, 2012. **43**(8): p. 595-9.

242. Bertram, L. and R.E. Tanzi, *The genetics of Alzheimer's disease.* Prog Mol Biol Transl Sci, 2012. **107**: p. 79-100.

243. Blennow, K., M.J. de Leon, and H. Zetterberg, *Alzheimer's disease.* Lancet, 2006. **368**(9533): p. 387-403.

244. Horvath, S., *DNA methylation age of human tissues and cell types.* Genome biology, 2013. **14**(10): p. 1-20.

245. Christensen, B.C., et al., *Aging and environmental exposures alter tissue-specific DNA methylation dependent upon CpG island context.* PLoS genetics, 2009. **5**(8): p. e1000602.

246. Hernandez, D.G., et al., *Distinct DNA methylation changes highly correlated with chronological age in the human brain.* Human molecular genetics, 2011. **20**(6): p. 1164-1172.

247. Siegmund, K.D., et al., *DNA methylation in the human cerebral cortex is dynamically regulated throughout the life span and involves differentiated neurons.* PloS one, 2007. **2**(9): p. e895.

248. Hannum, G., et al., *Genome-wide methylation profiles reveal quantitative views of human aging rates.* Molecular cell, 2013. **49**(2): p. 359-367.

249. Breitling, L.P., et al., *Frailty is associated with the epigenetic clock but not with telomere length in a German cohort.* Clinical epigenetics, 2016. **8**(1): p. 1-8.

250. Levine, M.E., et al., *DNA methylation age of blood predicts future onset of lung cancer in the women's health initiative.* Aging (Albany NY), 2015. **7**(9): p. 690.

251. De Jager, P.L., et al., *Alzheimer's disease: early alterations in brain DNA methylation at ANK1, BIN1, RHBDF2 and other loci.* Nat Neurosci, 2014. **17**(9): p. 1156-63.

252. Chouliaras, L., et al., *Consistent decrease in global DNA methylation and hydroxymethylation in the hippocampus of Alzheimer's disease patients.* Neurobiol Aging, 2013. **34**(9): p. 2091-9.

253. Mastroeni, D., et al., *Epigenetic changes in Alzheimer's disease: decrements in DNA methylation.* Neurobiol Aging, 2010. **31**(12): p. 2025-37.

254. Condliffe, D., et al., *Cross-region reduction in 5-hydroxymethylcytosine in Alzheimer's disease brain.* Neurobiol Aging, 2014. **35**(8): p. 1850-4.

255. Lashley, T., et al., *Alterations in global DNA methylation and hydroxymethylation are not detected in A lzheimer's disease.* Neuropathology and applied neurobiology, 2015. **41**(4): p. 497-506.

256. Lunnon, K., et al., *Methylomic profiling implicates cortical deregulation of ANK1 in Alzheimer's disease.* Nat Neurosci, 2014. **17**(9): p. 1164-70.

257. Smith, R.G., et al., *Elevated DNA methylation across a 48‐kb region spanning the HOXA gene cluster is associated with Alzheimer's disease neuropathology.* Alzheimer's & Dementia, 2018. **14**(12): p. 1580-1588.

258. Zhang, L., et al., *Epigenome-wide meta-analysis of DNA methylation differences in prefrontal cortex implicates the immune processes in Alzheimer's disease.* Nature communications, 2020. **11**(1): p. 1-13.

259. Smith, R.G., et al., *A meta-analysis of epigenome-wide association studies in Alzheimer's disease highlights novel differentially methylated loci across cortex.* Nature communications, 2021. **12**(1): p. 1-13.

260. Soreq, L., et al., *Major shifts in glial regional identity are a transcriptional hallmark of human brain aging.* Cell reports, 2017. **18**(2): p. 557-570.

261. Gasparoni, G., et al., *DNA methylation analysis on purified neurons and glia dissects age and Alzheimer's disease-specific changes in the human cortex.* Epigenetics Chromatin, 2018. **11**(1): p. 41.

262. Li, L., et al., *Role of Ten eleven translocation‐2 (Tet2) in modulating neuronal morphology and cognition in a mouse model of Alzheimer's disease.* Journal of Neurochemistry, 2021. **157**(4): p. 993-1012.

263. Gontier, G., et al., *Tet2 rescues age-related regenerative decline and enhances cognitive function in the adult mouse brain.* 2018. **22**(8): p. 1974-1981.

264. Coppieters, N., et al., *Global changes in DNA methylation and hydroxymethylation in Alzheimer's disease human brain.* Neurobiol Aging, 2014. **35**(6): p. 1334-44.

265. Cadena-del-Castillo, C., et al., *Age-dependent increment of hydroxymethylation in the brain cortex in the triple-transgenic mouse model of Alzheimer's disease.* J Alzheimers Dis, 2014. **41**(3): p. 845-54.

266. Bradley-Whitman, M.A. and M.A. Lovell, *Epigenetic changes in the progression of Alzheimer's disease.* Mech Ageing Dev, 2013. **134**(10): p. 486-95.

267. Shu, L., et al., *Genome-wide alteration of 5-hydroxymenthylcytosine in a mouse model of Alzheimer's disease.* BMC genomics, 2016. **17**(1): p. 1-11.

268. Zhang, Y., et al., *Selective loss of 5hmC promotes neurodegeneration in the mouse model of Alzheimer's disease.* FASEB J, 2020. **34**(12): p. 16364-16382.

269. Bernstein, A.I., et al., *5-Hydroxymethylation-associated epigenetic modifiers of Alzheimer's disease modulate Tau-induced neurotoxicity.* Hum Mol Genet, 2016. **25**(12): p. 2437-2450.

270. Kerimoglu, C., et al., *KMT2A and KMT2B Mediate Memory Function by Affecting Distinct Genomic Regions.* Cell Rep, 2017. **20**(3): p. 538-548.

271. Flamier, A., et al., *Modeling Late-Onset Sporadic Alzheimer's Disease through BMI1 Deficiency.* Cell Rep, 2018. **23**(9): p. 2653-2666.

272. Potts, R.C., et al., *CHD5, a brain-specific paralog of Mi2 chromatin remodeling enzymes, regulates expression of neuronal genes.* PLoS One, 2011. **6**(9): p. e24515.

273. Thompson, P.M., et al., *CHD5, a new member of the chromodomain gene family, is preferentially expressed in the nervous system.* Oncogene, 2003. **22**(7): p. 1002-11.

274. Gjoneska, E., et al., *Conserved epigenomic signals in mice and humans reveal immune basis of Alzheimer's disease.* Nature, 2015. **518**(7539): p. 365-9.

275. Forno, L.S., *Neuropathology of Parkinson's disease.* J Neuropathol Exp Neurol, 1996. **55**(3): p. 259-72.

276. McEwen, B.S., *Physiology and neurobiology of stress and adaptation: central role of the brain.* Physiological reviews, 2007. **87**(3): p. 873-904.

277. Belmaker, R.H. and G. Agam, *Major depressive disorder.* N Engl J Med, 2008. **358**(1): p. 55-68.

278. Brody, D.J., L.A. Pratt, and J.P. Hughes, *Prevalence of depression among adults aged 20 and over: United States, 2013-2016*. 2018.

279. Tsankova, N.M., et al., *Sustained hippocampal chromatin regulation in a mouse model of depression and antidepressant action.* Nat Neurosci, 2006. **9**(4): p. 519-25.

280. Sun, H., P.J. Kennedy, and E.J. Nestler, *Epigenetics of the depressed brain: role of histone acetylation and methylation.* Neuropsychopharmacology, 2013. **38**(1): p. 124-137.

281. Meaney, M.J. and M. Szyf, *Maternal care as a model for experience-dependent chromatin plasticity?* Trends in neurosciences, 2005. **28**(9): p. 456-463.

282. Tobi, E.W., et al., *DNA methylation signatures link prenatal famine exposure to growth and metabolism.* Nature communications, 2014. **5**(1): p. 1-14.

283. Angelucci, F., S. Brene, and A.A. Mathe, *BDNF in schizophrenia, depression and corresponding animal models.* Mol Psychiatry, 2005. **10**(4): p. 345-52.

284. Fuchikami, M., et al., *DNA methylation profiles of the brain-derived neurotrophic factor (BDNF) gene as a potent diagnostic biomarker in major depression.* PLoS One, 2011. **6**(8): p. e23881.

285. Hutchinson, A.N., et al., *Phosphorylation of MeCP2 at Ser421 contributes to chronic antidepressant action.* Journal of Neuroscience, 2012. **32**(41): p. 14355-14363.

286. Tadić, A., et al., *Methylation of the promoter of brain-derived neurotrophic factor exon IV and antidepressant response in major depression.* Molecular psychiatry, 2014. **19**(3): p. 281-283.

287. Ma, D.K., et al., *Neuronal activity-induced Gadd45b promotes epigenetic DNA demethylation and adult neurogenesis.* Science, 2009. **323**(5917): p. 1074-7.

288. Labonte, B., et al., *Gadd45b mediates depressive-like role through DNA demethylation.* Sci Rep, 2019. **9**(1): p. 4615.

289. Mendonca, M.S., et al., *Epigenetic variation at the SLC6A4 gene promoter in mother-child pairs with major depressive disorder.* J Affect Disord, 2019. **245**: p. 716-723.

290. LaPlant, Q., et al., *Dnmt3a regulates emotional behavior and spine plasticity in the nucleus accumbens.* Nature neuroscience, 2010. **13**(9): p. 1137-1143.

291. Cheng, Y., et al., *Ten-Eleven Translocation Proteins Modulate the Response to Environmental Stress in Mice.* Cell Rep, 2018. **25**(11): p. 3194-3203 e4.

292. Vogt, M.A., et al., *May the use of different background strains 'strain'the stress-related phenotype of GR+/− mice?* Behavioural brain research, 2017. **335**: p. 71-79.

293. Wion, D. and J. Casadesús, *N6-methyl-adenine: an epigenetic signal for DNA–protein interactions.* Nature Reviews Microbiology, 2006. **4**(3): p. 183-192.

294. Liu, J., et al., *Abundant DNA 6mA methylation during early embryogenesis of zebrafish and pig.* Nature communications, 2016. **7**(1): p. 1-7.

295. Koziol, M.J., et al., *Identification of methylated deoxyadenosines in vertebrates reveals diversity in DNA modifications.* Nature structural & molecular biology, 2016. **23**(1): p. 24-30.

296. Wu, T.P., et al., *DNA methylation on N6-adenine in mammalian embryonic stem cells.* Nature, 2016. **532**(7599): p. 329-333.

297. Woodcock, C.B., et al., *Human MettL3–MettL14 complex is a sequence-specific DNA adenine methyltransferase active on single-strand and unpaired DNA in vitro.* Cell discovery, 2019. **5**(1): p. 63.

298. Yu, D., et al., *Human MettL3-MettL14 RNA adenine methyltransferase complex is active on double-stranded DNA containing lesions.* Nucleic acids research, 2021. **49**(20): p. 11629-11642.

299. Kigar, S.L., et al., *N(6)-methyladenine is an epigenetic marker of mammalian early life stress.* Sci Rep, 2017. **7**(1): p. 18078.

300. Yao, B., et al., *DNA N6-methyladenine is dynamically regulated in the mouse brain following environmental stress.* Nat Commun, 2017. **8**(1): p. 1122.

301. Li, X., et al., *The DNA modification N6-methyl-2'-deoxyadenosine (m6dA) drives activity-induced gene expression and is required for fear extinction.* Nature neuroscience, 2019. **22**(4): p. 534-544.

302. Duman, R.S. and L.M. Monteggia, *A neurotrophic model for stress-related mood disorders.* Biological psychiatry, 2006. **59**(12): p. 1116-1127.

303. Müller, M.B. and F. Holsboer, *Mice with mutations in the HPA-system as models for symptoms of depression.* Biological psychiatry, 2006. **59**(12): p. 1104-1115.

304. Nestler, E.J. and W.A. Carlezon Jr, *The mesolimbic dopamine reward circuit in depression.* Biological psychiatry, 2006. **59**(12): p. 1151-1159.

305. American Psychiatric Association, D. and A.P. Association, *Diagnostic and statistical manual of mental disorders: DSM-5*. Vol. 5. 2013: American psychiatric association Washington, DC.

306. Wise, R.A., *Drug-activation of brain reward pathways.* Drug and alcohol dependence, 1998. **51**(1-2): p. 13-22.

307. Koob, G.F. and M. Le Moal, *Drug addiction, dysregulation of reward, and allostasis.* Neuropsychopharmacology, 2001. **24**(2): p. 97-129.

308. Bezdek, K.G. and E.H. Telzer, *Have no fear, the brain is here! How your brain responds to stress.* Age, 2017. **8**(15): p. 1-5.

309. Tobi, E.W., et al., *DNA methylation differences after exposure to prenatal famine are common and timing-and sex-specific.* Human molecular genetics, 2009. **18**(21): p. 4046-4053.

310. Farrell, C., et al., *DNA methylation differences at the glucocorticoid receptor gene in depression are related to functional alterations in hypothalamic-pituitary-adrenal axis activity and to early life emotional abuse.* Psychiatry Res, 2018. **265**: p. 341-348.

311. Daskalakis, N.P. and R. Yehuda, *Site-specific methylation changes in the glucocorticoid receptor exon 1F promoter in relation to life adversity: systematic review of contributing factors.* Front Neurosci, 2014. **8**: p. 369.

312. Efstathopoulos, P., et al., *NR3C1 hypermethylation in depressed and bullied adolescents.* Transl Psychiatry, 2018. **8**(1): p. 121.

313. Elliott, E., et al., *Resilience to social stress coincides with functional DNA methylation of the Crf gene in adult mice.* Nature neuroscience, 2010. **13**(11): p. 1351-1353.

314. Antunes, C., et al., *Tet3 ablation in adult brain neurons increases anxiety-like behavior and regulates cognitive function in mice.* Molecular psychiatry, 2021. **26**(5): p. 1445-1457.

315. Kuehner, J.N., et al., *Epigenetic Regulations in Neuropsychiatric Disorders.* Frontiers in genetics, 2019. **10**.

316. Li, X., et al., *Ten-eleven translocation 2 interacts with forkhead box O3 and regulates adult neurogenesis.* Nat Commun, 2017. **8**: p. 15903.

317. Wen, L., et al., *Whole-genome analysis of 5-hydroxymethylcytosine and 5-methylcytosine at base resolution in the human brain.* Genome Biol, 2014. **15**(3): p. R49.

318. Spiers, H., et al., *5-hydroxymethylcytosine is highly dynamic across human fetal brain development.* BMC Genomics, 2017. **18**(1): p. 738.

319. Shu, L., et al., *Genome-wide alteration of 5-hydroxymenthylcytosine in a mouse model of Alzheimer's disease.* BMC Genomics, 2016. **17**: p. 381.

320. James, B.D., et al., *Contribution of Alzheimer disease to mortality in the United States.* Neurology, 2014. **82**(12): p. 1045-50.

321. Hardy, J.A. and G.A. Higgins, *Alzheimer's disease: the amyloid cascade hypothesis.* Science, 1992. **256**(5054): p. 184-5.

322. Busche, M.A. and A. Konnerth, *Impairments of neural circuit function in Alzheimer's disease.* Philos Trans R Soc Lond B Biol Sci, 2016. **371**(1700).

323. Sun, B., et al., *Imbalance between GABAergic and Glutamatergic Transmission Impairs Adult Neurogenesis in an Animal Model of Alzheimer's Disease.* Cell Stem Cell, 2009. **5**(6): p. 624-33.

324. Qian, X., et al., *Brain-Region-Specific Organoids Using Mini-bioreactors for Modeling ZIKV Exposure.* Cell, 2016. **165**(5): p. 1238-1254.

325. Takebe, T. and J.M. Wells, *Organoids by design.* Science, 2019. **364**(6444): p. 956-959.

326. Itskovitz-Eldor, J., et al., *Differentiation of human embryonic stem cells into embryoid bodies compromising the three embryonic germ layers.* Molecular medicine, 2000. **6**(2): p. 88.

327. Kelava, I. and M.A. Lancaster, *Stem Cell Models of Human Brain Development.* Cell Stem Cell, 2016. **18**(6): p. 736-48.

328. Pastor, W.A., et al., *Genome-wide mapping of 5-hydroxymethylcytosine in embryonic stem cells.* Nature, 2011. **473**(7347): p. 394-7.

329. Bergsland, M., et al., *The establishment of neuronal properties is controlled by Sox4 and Sox11.* Genes Dev, 2006. **20**(24): p. 3475-86.

330. Gao, T. and J. Qian, *EnhancerAtlas 2.0: an updated resource with enhancer annotation in 586 tissue/cell types across nine species.* Nucleic Acids Res, 2020. **48**(D1): p. D58-D64.

331. Mahe, E.A., et al., *Cytosine modifications modulate the chromatin architecture of transcriptional enhancers.* Genome Res, 2017. **27**(6): p. 947-958.

332. Raja, W.K., et al., *Self-Organizing 3D Human Neural Tissue Derived from Induced Pluripotent Stem Cells Recapitulate Alzheimer's Disease Phenotypes.* PLoS One, 2016. **11**(9): p. e0161969.

333. Wang, X., et al., *Bulk tissue cell type deconvolution with multi-subject single-cell expression reference.* Nat Commun, 2019. **10**(1): p. 380.

334. Jaccard, P., *The distribution of the flora in the alpine zone. 1.* New phytologist, 1912. **11**(2): p. 37-50.

335. Roadmap Epigenomics, C., et al., *Integrative analysis of 111 reference human epigenomes.* Nature, 2015. **518**(7539): p. 317-30.

336. Yan, L., et al., *Epigenomic Landscape of Human Fetal Brain, Heart, and Liver.* J Biol Chem, 2016. **291**(9): p. 4386-98.

337. Lardenoije, R., et al., *Alzheimer's disease-associated (hydroxy)methylomic changes in the brain and blood.* Clin Epigenetics, 2019. **11**(1): p. 164.

338. Li, P., et al., *Epigenetic dysregulation of enhancers in neurons is associated with Alzheimer's disease pathology and cognitive symptoms.* Nat Commun, 2019. **10**(1): p. 2246.

339. Qin, L., et al., *Ethnicity-specific and overlapping alterations of brain hydroxymethylome in Alzheimer's disease.* Hum Mol Genet, 2020. **29**(1): p. 149-158.

340. Zhao, J., et al., *A genome-wide profiling of brain DNA hydroxymethylation in Alzheimer's disease.* Alzheimers Dement, 2017. **13**(6): p. 674-688.

341. Fetahu, I.S., et al., *Epigenetic signatures of methylated DNA cytosine in Alzheimer's disease.* Sci Adv, 2019. **5**(8): p. eaaw2880.

342. Serandour, A.A., et al., *Dynamic hydroxymethylation of deoxyribonucleic acid marks differentiation-associated enhancers.* Nucleic Acids Res, 2012. **40**(17): p. 8255-65.

343. Wen, Z., et al., *Synaptic dysregulation in a human iPS cell model of mental disorders.* Nature, 2014. **515**(7527): p. 414-8.

344. Schneider, C.A., W.S. Rasband, and K.W. Eliceiri, *NIH Image to ImageJ: 25 years of image analysis.* Nat Methods, 2012. **9**(7): p. 671-5.

345. Mathys, H., et al., *Single-cell transcriptomic analysis of Alzheimer's disease.* Nature, 2019. **570**(7761): p. 332-337.

346. Langmead, B., et al., *Ultrafast and memory-efficient alignment of short DNA sequences to the human genome.* Genome Biol, 2009. **10**(3): p. R25.

347. Li, H., et al., *The Sequence Alignment/Map format and SAMtools.* Bioinformatics, 2009. **25**(16): p. 2078-9.

348. Zhang, Y., et al., *Model-based analysis of ChIP-Seq (MACS).* Genome Biol, 2008. **9**(9): p. R137.

349. Quinlan, A.R. and I.M. Hall, *BEDTools: a flexible suite of utilities for comparing genomic features.* Bioinformatics, 2010. **26**(6): p. 841-2.

350. Wang, C., et al., *Reprogramming of H3K9me3-dependent heterochromatin during mammalian embryo development.* Nat Cell Biol, 2018. **20**(5): p. 620-631.

351. Heinz, S., et al., *Simple combinations of lineage-determining transcription factors prime cis-regulatory elements required for macrophage and B cell identities.* Mol Cell, 2010. **38**(4): p. 576-89.

352. Trapnell, C., et al., *Differential gene and transcript expression analysis of RNA-seq experiments with TopHat and Cufflinks.* Nat Protoc, 2012. **7**(3): p. 562-78.

353. Shen, L., et al., *ngs.plot: Quick mining and visualization of next-generation sequencing data by integrating genomic databases.* BMC Genomics, 2014. **15**: p. 284.

354. Ashburner, M., et al., *Gene ontology: tool for the unification of biology. The Gene Ontology Consortium.* Nat Genet, 2000. **25**(1): p. 25-9.

355. The Gene Ontology, C., *The Gene Ontology Resource: 20 years and still GOing strong.* Nucleic Acids Res, 2019. **47**(D1): p. D330-D338.

356. McLean, C.Y., et al., *GREAT improves functional interpretation of cis-regulatory regions.* Nat Biotechnol, 2010. **28**(5): p. 495-501.

357. Tanimoto, T.T., *Elementary mathematical theory of classification and prediction*. 1958.

358. Tafet, G.E. and R. Bernardini, *Psychoneuroendocrinological links between chronic stress and depression.* Progress in Neuro-Psychopharmacology and Biological Psychiatry, 2003. **27**(6): p. 893-903.

359. Burke, H.M., et al., *Depression and cortisol responses to psychological stress: a meta-analysis.* Psychoneuroendocrinology, 2005. **30**(9): p. 846-856.

360. Peña-Bautista, C., et al., *Stress and neurodegeneration.* Clinica Chimica Acta, 2020. **503**: p. 163-168.

361. Aguilera, O., et al., *Epigenetics and environment: a complex relationship.* Journal of applied physiology, 2010. **109**(1): p. 243-251.

362. Kaur, G., et al., *DNA Methylation: A Promising Approach in Management of Alzheimer's Disease and Other Neurodegenerative Disorders.* Biology (Basel), 2022. **11**(1).

363. Yao, B. and P. Jin, *Cytosine modifications in neurodevelopment and diseases.* Cell Mol Life Sci, 2014. **71**(3): p. 405-18.

364. Kuehner, J.N., et al., *5-hydroxymethylcytosine is dynamically regulated during forebrain organoid development and aberrantly altered in Alzheimer's disease.* Cell Rep, 2021. **35**(4): p. 109042.

365. Sterrenburg, L., et al., *Chronic stress induces sex-specific alterations in methylation and expression of corticotropin-releasing factor gene in the rat.* PLoS One, 2011. **6**(11): p. e28128.

366. Golden, S.A., et al., *A standardized protocol for repeated social defeat stress in mice.* Nature protocols, 2011. **6**(8): p. 1183-1191.

367. McEwen, B.S., *Protective and damaging effects of stress mediators.* New England journal of medicine, 1998. **338**(3): p. 171-179.

368. Arnsten, A.F., *Stress signalling pathways that impair prefrontal cortex structure and function.* Nature reviews neuroscience, 2009. **10**(6): p. 410-422.

369. Taiwo, O., et al., *Methylome analysis using MeDIP-seq with low DNA concentrations.* Nature protocols, 2012. **7**(4): p. 617-636.

370. Ball, M.P., et al., *Targeted and genome-scale methylomics reveals gene body signatures in human cell lines.* Nature biotechnology, 2009. **27**(4): p. 361.

371. Wu, H.J., et al., *Life extension factor klotho regulates behavioral responses to stress via modulation of GluN2B function in the nucleus accumbens.* Neuropsychopharmacology, 2022. **47**(9): p. 1710-1720.

372. Thaweethee-Sukjai, B., et al., *Parvalbumin Promoter Methylation Altered in Major Depressive Disorder.* Int J Med Sci, 2019. **16**(9): p. 1207-1214.

373. Chen, C.C., et al., *FoxOs inhibit mTORC1 and activate Akt by inducing the expression of Sestrin3 and Rictor.* Dev Cell, 2010. **18**(4): p. 592-604.

374. Lee, J.H., et al., *Maintenance of metabolic homeostasis by Sestrin2 and Sestrin3.* Cell Metab, 2012. **16**(3): p. 311-21.

375. Schwartz, M.W., et al., *Cooperation between brain and islet in glucose homeostasis and diabetes.* Nature, 2013. **503**(7474): p. 59-66.

376. Gammie, S.C., *Creation of a gene expression portrait of depression and its application for identifying potential treatments.* Sci Rep, 2021. **11**(1): p. 3829.

377. Ghosal, S., B. Myers, and J.P. Herman, *Role of central glucagon-like peptide-1 in stress regulation.* Physiology & behavior, 2013. **122**: p. 201-207.

378. Valverde, O., et al., *GPR3 receptor, a novel actor in the emotional-like responses.* PloS one, 2009. **4**(3): p. e4704.

379. Tsigos, C., et al., *Stress: endocrine physiology and pathophysiology.* Endotext [Internet], 2020.

380. Santisteban, M.M., et al., *Endothelium-macrophage crosstalk mediates blood-brain barrier dysfunction in hypertension.* Hypertension, 2020. **76**(3): p. 795-807.

381. Di Narzo, A.F., et al., *A unique gene expression signature associated with serotonin 2C receptor RNA editing in the prefrontal cortex and altered in suicide.* Human molecular genetics, 2014. **23**(18): p. 4801-4813.

382. Tomlinson, J.W., et al., *11β-Hydroxysteroid dehydrogenase type 1: a tissue-specific regulator of glucocorticoid response.* Endocrine reviews, 2004. **25**(5): p. 831-866.

383. Zaccaria, M., et al., *Dystroglycan distribution in adult mouse brain: a light and electron microscopy study.* Neuroscience, 2001. **104**(2): p. 311-324.

384. Ohlson, J., et al., *Editing modifies the GABAA receptor subunit a3.* Rna, 2007. **13**(5): p. 698-703.

385. Burns, C.M., et al., *Regulation of serotonin-2C receptor G-protein coupling by RNA editing.* Nature, 1997. **387**(6630): p. 303-308.

386. Wang, Y., et al., *Salt-inducible kinase 1-CREB-regulated transcription coactivator 1 signalling in the paraventricular nucleus of the hypothalamus plays a role in depression by regulating the hypothalamic–pituitary–adrenal axis.* Molecular Psychiatry, 2022: p. 1-11.

387. Machado, A., et al., *Chronic stress as a risk factor for Alzheimer's disease.* Reviews in the Neurosciences, 2014. **25**(6): p. 785-804.

388. Wang, W., et al., *Inhibiting Brd4 alleviated PTSD‐like behaviors and fear memory through regulating immediate early genes expression and neuroinflammation in rats.* Journal of Neurochemistry, 2021. **158**(4): p. 912-927.

389. Kim, E., et al., *GKAP, a novel synaptic protein that interacts with the guanylate kinase-like domain of the PSD-95/SAP90 family of channel clustering molecules.* The Journal of cell biology, 1997. **136**(3): p. 669-678.

390. Miyata, S., et al., *Blood transcriptomic markers in patients with late-onset major depressive disorder.* PLoS One, 2016. **11**(2): p. e0150262.

391. Dias, C., et al., *beta-catenin mediates stress resilience through Dicer1/microRNA regulation.* Nature, 2014. **516**(7529): p. 51-5.

392. Pepper, R.E., et al., *How do cells of the oligodendrocyte lineage affect neuronal circuits to influence motor function, memory and mood?* Frontiers in cellular neuroscience, 2018. **12**: p. 399.

393. Jones, K.L., M. Zhou, and D.J. Jhaveri, *Dissecting the role of adult hippocampal neurogenesis towards resilience versus susceptibility to stress-related mood disorders.* npj Science of Learning, 2022. **7**(1): p. 1-8.

394. Madden, K.S., V.M. Sanders, and D.L. Felten, *Catecholamine influences and sympathetic neural modulation of immune responsiveness.* Annual review of pharmacology and toxicology, 1995. **35**(1): p. 417-448.

395. Cheadle, L. and T. Biederer, *The novel synaptogenic protein Farp1 links postsynaptic cytoskeletal dynamics and transsynaptic organization.* Journal of Cell Biology, 2012. **199**(6): p. 985-1001.

396. Jiang, W., et al., *Identification of protein tyrosine phosphatase receptor type O (PTPRO) as a synaptic adhesion molecule that promotes synapse formation.* Journal of Neuroscience, 2017. **37**(41): p. 9828-9843.

397. Chung, W.-S., et al., *Astrocytes mediate synapse elimination through MEGF10 and MERTK pathways.* Nature, 2013. **504**(7480): p. 394-400.

398. Jenniches, I., et al., *Anxiety, stress, and fear response in mice with reduced endocannabinoid levels.* Biological psychiatry, 2016. **79**(10): p. 858-868.

399. Vivien, D. and C. Ali, *Transforming growth factor-β signalling in brain disorders.* Cytokine & growth factor reviews, 2006. **17**(1-2): p. 121-128.

400. Pandey, G.N., et al., *Dysregulation of protein kinase C in adult depression and suicide: evidence from postmortem brain studies.* International journal of neuropsychopharmacology, 2021. **24**(5): p. 400-408.

401. Sial, O.K., et al., *Vicarious social defeat stress: Bridging the gap between physical and emotional stress.* Journal of neuroscience methods, 2016. **258**: p. 94-103.

402. Warren, M.S., et al., *Comparative gene expression profiles of ABC transporters in brain microvessel endothelial cells and brain in five species including human.* Pharmacological research, 2009. **59**(6): p. 404-413.

403. Holz, A., et al., *Molecular and developmental characterization of novel cDNAs of the myelin-associated/oligodendrocytic basic protein.* Journal of Neuroscience, 1996. **16**(2): p. 467-477.

404. Wang, B., et al., *Zfp462 deficiency causes anxiety - like behaviors with excessive self - grooming in mice.* Genes, Brain and Behavior, 2017. **16**(2): p. 296-307.

405. Gallagher, D., et al., *Ankrd11 is a chromatin regulator involved in autism that is essential for neural development.* Developmental cell, 2015. **32**(1): p. 31-42.

406. Feng, W., et al., *The chromatin remodeler CHD7 regulates adult neurogenesis via activation of SoxC transcription factors.* Cell Stem Cell, 2013. **13**(1): p. 62-72.

407. Renault, V.M., et al., *FoxO3 regulates neural stem cell homeostasis.* Cell stem cell, 2009. **5**(5): p. 527-539.

408. De Gois, S., et al., *Ctr9, a protein in the transcription complex Paf1, regulates dopamine transporter activity at the plasma membrane.* Journal of Biological Chemistry, 2015. **290**(29): p. 17848-17862.

409. Schnaar, R.L., R. Gerardy-Schahn, and H. Hildebrandt, *Sialic acids in the brain: gangliosides and polysialic acid in nervous system development, stability, disease, and regeneration.* Physiological reviews, 2014.

410. Rawal, P. and L. Zhao, *Sialometabolism in brain health and Alzheimer's disease.* Frontiers in Neuroscience, 2021. **15**: p. 648617.

411. Jung, S., et al., *Autophagic death of neural stem cells mediates chronic stress-induced decline of adult hippocampal neurogenesis and cognitive deficits.* Autophagy, 2020. **16**(3): p. 512-530.

412. Primeaux, S.D., et al., *Central administration of the RFamide peptides, QRFP-26 and QRFP-43, increases high fat food intake in rats.* Peptides, 2008. **29**(11): p. 1994-2000.

413. Giri, R., et al., *β-Amyloid-induced migration of monocytes across human brain endothelial cells involves RAGE and PECAM-1.* American Journal of Physiology-Cell Physiology, 2000. **279**(6): p. C1772-C1781.

414. Taracha, A., G. Kotarba, and T. Wilanowski, *Neglected functions of TFCP2/TFCP2L1/UBP1 transcription factors may offer valuable insights into their mechanisms of action.* International journal of molecular sciences, 2018. **19**(10): p. 2852.

415. Wolozin, B. and P. Ivanov, *Stress granules and neurodegeneration.* Nature Reviews Neuroscience, 2019. **20**(11): p. 649-666.

416. Mahoney, E.R., et al., *Brain expression of the vascular endothelial growth factor gene family in cognitive aging and alzheimer's disease.* Molecular psychiatry, 2021. **26**(3): p. 888-896.

417. Gold, P.W., J. Licinio, and M. Pavlatou, *Pathological parainflammation and endoplasmic reticulum stress in depression: potential translational targets through the CNS insulin, klotho and PPAR-γ systems.* Molecular psychiatry, 2013. **18**(2): p. 154-165.

418. Wardas, J., *Neuroprotective role of adenosine in the CNS.* Polish journal of pharmacology, 2002. **54**(4): p. 313-326.

419. Yang, R., et al., *The role of heparin and glycocalyx in blood-brain barrier dysfunction.* Frontiers in Immunology, 2021: p. 5389.

420. Rempe, R.G., A.M. Hartz, and B. Bauer, *Matrix metalloproteinases in the brain and blood–brain barrier: versatile breakers and makers.* Journal of Cerebral Blood Flow & Metabolism, 2016. **36**(9): p. 1481-1507.

421. Kohli, R.M. and Y. Zhang, *TET enzymes, TDG and the dynamics of DNA demethylation.* Nature, 2013. **502**(7472): p. 472-479.

422. D'Urso, A. and J.H. Brickner, *Mechanisms of epigenetic memory.* Trends in genetics, 2014. **30**(6): p. 230-236.

423. Hill, A.S., A. Sahay, and R. Hen, *Increasing adult hippocampal neurogenesis is sufficient to reduce anxiety and depression-like behaviors.* Neuropsychopharmacology, 2015. **40**(10): p. 2368-2378.

424. Schloesser, R., et al., *Environmental enrichment requires adult neurogenesis to facilitate the recovery from psychosocial stress.* Molecular psychiatry, 2010. **15**(12): p. 1152-1163.

425. Niciu, M.J., et al., *Glutamate and its receptors in the pathophysiology and treatment of major depressive disorder.* Journal of neural transmission, 2014. **121**: p. 907-924.

426. Nutt, D.J., *Relationship of neurotransmitters to the symptoms of major depressive disorder.* J Clin psychiatry, 2008. **69**(Suppl E1): p. 4-7.

427. Popoli, M., et al., *The stressed synapse: the impact of stress and glucocorticoids on glutamate transmission.* Nature Reviews Neuroscience, 2012. **13**(1): p. 22-37.

428. Hardingham, G.E. and H. Bading, *Synaptic versus extrasynaptic NMDA receptor signalling: implications for neurodegenerative disorders.* Nature Reviews Neuroscience, 2010. **11**(10): p. 682-696.

429. Werner, F.-M. and R. Covenas, *Classical neurotransmitters and neuropeptides involved in major depression: a review.* International Journal of Neuroscience, 2010. **120**(7): p. 455-470.

430. Fraporti, T.T., et al., *Synergistic effects between ADORA2A and DRD2 genes on anxiety disorders in children with ADHD.* Progress in Neuro-Psychopharmacology and Biological Psychiatry, 2019. **93**: p. 214-220.

431. Canela, L., et al., *The neuronal Ca2+-binding protein 2 (NECAB2) interacts with the adenosine A2A receptor and modulates the cell surface expression and function of the receptor.* Molecular and Cellular Neuroscience, 2007. **36**(1): p. 1-12.

432. Ferre, S., et al., *Stimulation of high-affinity adenosine A2 receptors decreases the affinity of dopamine D2 receptors in rat striatal membranes.* Proceedings of the National Academy of Sciences, 1991. **88**(16): p. 7238-7241.

433. Bharadwaj, P. and R.N. Martins, *PRKAG2 Gene Expression Is Elevated and its Protein Levels Are Associated with Increased Amyloid-β Accumulation in the Alzheimer's Disease Brain.* Journal of Alzheimer's Disease, 2020. **74**(2): p. 441-448.

434. Kaether, C., et al., *Endoplasmic reticulum retention of the γ - secretase complex component Pen2 by Rer1.* EMBO reports, 2007. **8**(8): p. 743-748.

435. Sharoar, M.G., et al., *Dynactin 6 deficiency enhances aging-associated dystrophic neurite formation in mouse brains.* Neurobiology of Aging, 2021. **107**: p. 21-29.

436. Sturner, E. and C. Behl, *The Role of the Multifunctional BAG3 Protein in Cellular Protein Quality Control and in Disease.* Front Mol Neurosci, 2017. **10**: p. 177.

437. Tan, M.-S., et al., *Associations of Alzheimer's disease risk variants with gene expression, amyloidosis, tauopathy, and neurodegeneration.* Alzheimer's Research & Therapy, 2021. **13**(1): p. 1-11.

438. Zhang, Z., et al., *Cleavage of tau by asparagine endopeptidase mediates the neurofibrillary pathology in Alzheimer's disease.* Nature medicine, 2014. **20**(11): p. 1254-1262.

439. Jun, G.R., et al., *Protein phosphatase 2A and complement component 4 are linked to the protective effect of APOE ε2 for Alzheimer's disease.* Alzheimer's & Dementia, 2022.

440. Weber, M., et al., *Chromosome-wide and promoter-specific analyses identify sites of differential DNA methylation in normal and transformed human cells.* Nat Genet, 2005. **37**(8): p. 853-62.

441. Robinson, J.T., et al., *Integrative genomics viewer.* Nat Biotechnol, 2011. **29**(1): p. 24-6.

442. Szklarczyk, D., et al., *Correction to 'The STRING database in 2021: customizable protein-protein networks, and functional characterization of user-uploaded gene/measurement sets'.* Nucleic Acids Res, 2021. **49**(18): p. 10800.

443. Antunes, C., et al., *Tet3 ablation in adult brain neurons increases anxiety-like behavior and regulates cognitive function in mice.* Mol Psychiatry, 2021. **26**(5): p. 1445-1457.

444. Yu, H., et al., *Tet3 regulates synaptic transmission and homeostatic plasticity via DNA oxidation and repair.* Nature neuroscience, 2015. **18**(6): p. 836-843.

445. Dominissini, D., et al., *Topology of the human and mouse m6A RNA methylomes revealed by m6A-seq.* Nature, 2012. **485**(7397): p. 201-206.

446. Wion, D. and J. Casadesus, *N6-methyl-adenine: an epigenetic signal for DNA-protein interactions.* Nat Rev Microbiol, 2006. **4**(3): p. 183-92.

447. Koziol, M.J., et al., *Identification of methylated deoxyadenosines in vertebrates reveals diversity in DNA modifications.* Nat Struct Mol Biol, 2016. **23**(1): p. 24-30.

448. Zhang, G., et al., *N6-methyladenine DNA modification in Drosophila.* Cell, 2015. **161**(4): p. 893-906.

449. Xiao, C.-L., et al., *N6-methyladenine DNA modification in the human genome.* Molecular cell, 2018. **71**(2): p. 306-318. e7.

450. Hao, Z., et al., *N6-deoxyadenosine methylation in mammalian mitochondrial DNA.* Molecular cell, 2020. **78**(3): p. 382-395. e8.

451. Shafik, A.M., et al., *N6-methyladenosine dynamics in neurodevelopment and aging, and its potential role in Alzheimer's disease.* Genome Biol, 2021. **22**(1): p. 17.

452. Zeng, Y., et al., *Refined RIP-seq protocol for epitranscriptome analysis with low input materials.* PLoS Biol, 2018. **16**(9): p. e2006092.

453. Roth, T.L. and J.D. Sweatt, *Annual Research Review: Epigenetic mechanisms and environmental shaping of the brain during sensitive periods of development.* J Child Psychol Psychiatry, 2011. **52**(4): p. 398-408.

454. Feil, R. and M.F. Fraga, *Epigenetics and the environment: emerging patterns and implications.* Nat Rev Genet, 2012. **13**(2): p. 97-109.

455. Vineis, P., et al., *Epigenetic memory in response to environmental stressors.* FASEB J, 2017. **31**(6): p. 2241-2251.

456. Perl, D.P., *Neuropathology of Alzheimer's disease.* Mount Sinai Journal of Medicine: A Journal of Translational and Personalized Medicine: A Journal of Translational and Personalized Medicine, 2010. **77**(1): p. 32-42.

457. Scheuner, D., et al., *Secreted amyloid beta-protein similar to that in the senile plaques of Alzheimer's disease is increased in vivo by the presenilin 1 and 2 and APP mutations linked to familial Alzheimer's disease.* Nat Med, 1996. **2**(8): p. 864-70.

458. Vaz, M. and S. Silvestre, *Alzheimer's disease: Recent treatment strategies.* Eur J Pharmacol, 2020. **887**: p. 173554.

459. Brosseron, F., et al., *Body fluid cytokine levels in mild cognitive impairment and Alzheimer's disease: a comparative overview.* Mol Neurobiol, 2014. **50**(2): p. 534-44.

460. Heppner, F.L., R.M. Ransohoff, and B. Becher, *Immune attack: the role of inflammation in Alzheimer disease.* Nat Rev Neurosci, 2015. **16**(6): p. 358-72.

461. Tarkowski, E., et al., *Intrathecal inflammation precedes development of Alzheimer's disease.* J Neurol Neurosurg Psychiatry, 2003. **74**(9): p. 1200-5.

462. De Strooper, B. and E. Karran, *The Cellular Phase of Alzheimer's Disease.* Cell, 2016. **164**(4): p. 603-15.

463. Sweeney, M.D., et al., *Vascular dysfunction-The disregarded partner of Alzheimer's disease.* Alzheimers Dement, 2019. **15**(1): p. 158-167.

464. King, A., *The search for better animal models of Alzheimer's disease.* Nature, 2018. **559**(7715): p. S13-S15.

465. Onos, K.D., et al., *Enhancing face validity of mouse models of Alzheimer's disease with natural genetic variation.* PLoS Genet, 2019. **15**(5): p. e1008155.

466. Edler, M.K., et al., *Aged chimpanzees exhibit pathologic hallmarks of Alzheimer's disease.* Neurobiology of Aging, 2017. **59**: p. 107-120.

467. Paspalas, C.D., et al., *The aged rhesus macaque manifests Braak stage III/IV Alzheimer's-like pathology.* Alzheimer's & Dementia, 2018. **14**(5): p. 680-691.

468. Neff, E.P., *Animal models of Alzheimer's disease embrace diversity.* Lab Anim (NY), 2019. **48**(9): p. 255-259.

469. Zhang, Y., et al., *Purification and characterization of progenitor and mature human astrocytes reveals transcriptional and functional differences with mouse.* Neuron, 2016. **89**(1): p. 37-53.

470. Lancaster, M.A., et al., *Cerebral organoids model human brain development and microcephaly.* Nature, 2013. **501**(7467): p. 373-9.

471. Luo, C., et al., *Cerebral Organoids Recapitulate Epigenomic Signatures of the Human Fetal Brain.* Cell Rep, 2016. **17**(12): p. 3369-3384.

472. Cederquist, G.Y., et al., *Specification of positional identity in forebrain organoids.* Nat Biotechnol, 2019. **37**(4): p. 436-444.

473. Farrer, L.A., et al., *Effects of age, sex, and ethnicity on the association between apolipoprotein E genotype and Alzheimer disease: a meta-analysis.* Jama, 1997. **278**(16): p. 1349-1356.

474. Yu, L., et al., *TOMM40'523 variant and cognitive decline in older persons with APOE epsilon3/3 genotype.* Neurology, 2017. **88**(7): p. 661-668.

475. Yu, L., et al., *APOE epsilon4-TOMM40 '523 haplotypes and the risk of Alzheimer's disease in older Caucasian and African Americans.* PLoS One, 2017. **12**(7): p. e0180356.

476. Mayeda, E.R., et al., *Inequalities in dementia incidence between six racial and ethnic groups over 14 years.* Alzheimer's & Dementia, 2016. **12**(3): p. 216-224.

477. Tang, M.-X., et al., *Incidence of AD in African-Americans, Caribbean hispanics, and caucasians in northern Manhattan.* Neurology, 2001. **56**(1): p. 49-56.

478. Raman, R., et al., *Disparities by Race and Ethnicity Among Adults Recruited for a Preclinical Alzheimer Disease Trial.* JAMA Netw Open, 2021. **4**(7): p. e2114364.

479. Deters, K.D., et al., *Amyloid PET imaging in self-identified non-Hispanic Black participants of the Anti-Amyloid in Asymptomatic Alzheimer's Disease (A4) study.* Neurology, 2021. **96**(11): p. e1491-e1500.

480. Tombaugh, T.N. and N.J. McIntyre, *The mini - mental state examination: a comprehensive review.* Journal of the American Geriatrics Society, 1992. **40**(9): p. 922-935.

481. Barnes, L.L., *Biomarkers for Alzheimer dementia in diverse racial and ethnic minorities—a public health priority.* JAMA neurology, 2019. **76**(3): p. 251-253.

482. Manly, J.J., A. Gilmore-Bykovskyi, and K.D. Deters, *Inclusion of Underrepresented Groups in Preclinical Alzheimer Disease Trials-Opportunities Abound.* JAMA Netw Open, 2021. **4**(7): p. e2114606.

483. Lutz, M.W., et al., *Genetic variation at a single locus and age of onset for Alzheimer's disease.* Alzheimers Dement, 2010. **6**(2): p. 125-31.

484. Liu, Y., et al., *Bisulfite-free direct detection of 5-methylcytosine and 5-hydroxymethylcytosine at base resolution.* Nat Biotechnol, 2019. **37**(4): p. 424-429.

485. Liu, Y., et al., *Subtraction-free and bisulfite-free specific sequencing of 5-methylcytosine and its oxidized derivatives at base resolution.* Nat Commun, 2021. **12**(1): p. 618.

486. Grubman, A., et al., *A single-cell atlas of entorhinal cortex from individuals with Alzheimer's disease reveals cell-type-specific gene expression regulation.* Nat Neurosci, 2019. **22**(12): p. 2087-2097.

487. Davis, M., et al., *Estimating Alzheimer's disease progression rates from normal cognition through mild cognitive impairment and stages of dementia.* Current Alzheimer Research, 2018. **15**(8): p. 777-788.

488. Sloan, S.A., et al., *Human Astrocyte Maturation Captured in 3D Cerebral Cortical Spheroids Derived from Pluripotent Stem Cells.* Neuron, 2017. **95**(4): p. 779-790 e6.

489. Zhang, Y., et al., *Purification and Characterization of Progenitor and Mature Human Astrocytes Reveals Transcriptional and Functional Differences with Mouse.* Neuron, 2016. **89**(1): p. 37-53.

490. Charney, D.S., *Psychobiological mechanisms of resilience and vulnerability: implications for successful adaptation to extreme stress.* Am J Psychiatry, 2004. **161**(2): p. 195-216.

491. Yehuda, R., et al., *Developing an agenda for translational studies of resilience and vulnerability following trauma exposure.* Annals of the New York Academy of Sciences, 2006. **1071**(1): p. 379-396.

492. Maden, C.H., et al., *NRP1 and NRP2 cooperate to regulate gangliogenesis, axon guidance and target innervation in the sympathetic nervous system.* Developmental biology, 2012. **369**(2): p. 277-285.

493. Piaton, G., et al., *Class 3 semaphorins influence oligodendrocyte precursor recruitment and remyelination in adult central nervous system.* Brain, 2011. **134**(4): p. 1156-1167.

494. Wang, Y. and T.C. Südhof, *Genomic definition of RIM proteins: evolutionary amplification of a family of synaptic regulatory proteins.* Genomics, 2003. **81**(2): p. 126-137.

495. Gurnik, S., et al., *Angiopoietin-2-induced blood–brain barrier compromise and increased stroke size are rescued by VE-PTP-dependent restoration of Tie2 signaling.* Acta neuropathologica, 2016. **131**(5): p. 753-773.

496. Reul, J. and E.d. Kloet, *Two receptor systems for corticosterone in rat brain: microdistribution and differential occupation.* Endocrinology, 1985. **117**(6): p. 2505-2511.

497. Roozendaal, B., *Glucocorticoids and the regulation of memory consolidation.* Psychoneuroendocrinology, 2000. **25**(3): p. 213-238.

498. Bremner, J.D., *Does stress damage the brain?* Biol Psychiatry, 1999. **45**(7): p. 797-805.

499. Ma, Q., et al., *Altered cerebellar–cerebral resting-state functional connectivity reliably identifies major depressive disorder.* Brain research, 2013. **1495**: p. 86-94.

500. Fitzgerald, P.B., et al., *A meta - analytic study of changes in brain activation in depression.* Human brain mapping, 2008. **29**(6): p. 683-695.

501. Moreno-Rius, J., *The cerebellum under stress.* Frontiers in neuroendocrinology, 2019. **54**: p. 100774.

502. Han, D., et al., *A highly sensitive and robust method for genome-wide 5hmC profiling of rare cell populations.* Molecular cell, 2016. **63**(4): p. 711-719.

503. Brody, D.J., L.A. Pratt, and J.P. Hughes, *Prevalence of Depression Among Adults Aged 20 and Over: United States, 2013-2016.* NCHS Data Brief, 2018(303): p. 1-8.

504. Albert, P.R., *Why is depression more prevalent in women?* J Psychiatry Neurosci, 2015. **40**(4): p. 219-21.

505. Verma, R., Y.P. Balhara, and C.S. Gupta, *Gender differences in stress response: Role of developmental and biological determinants.* Ind Psychiatry J, 2011. **20**(1): p. 4-10.

506. Harris, A.Z., et al., *A Novel Method for Chronic Social Defeat Stress in Female Mice.* Neuropsychopharmacology, 2018. **43**(6): p. 1276-1283.

507. Sial, O.K., et al., *Vicarious social defeat stress: Bridging the gap between physical and emotional stress.* J Neurosci Methods, 2016. **258**: p. 94-103.

508. Iniguez, S.D., et al., *Vicarious Social Defeat Stress Induces Depression-Related Outcomes in Female Mice.* Biol Psychiatry, 2018. **83**(1): p. 9-17.

509. Warren, B.L., et al., *Can I get a witness? Using vicarious defeat stress to study mood-related illnesses in traditionally understudied populations.* Biological psychiatry, 2020. **88**(5): p. 381-391.

510. Perlman, S.E., et al., *Short-term and medium-term health effects of 9/11.* The Lancet, 2011. **378**(9794): p. 925-934.

511. Van Wingen, G.A., et al., *Perceived threat predicts the neural sequelae of combat stress.* Molecular psychiatry, 2011. **16**(6): p. 664-671.